MECHANISMS OF INHIBITION OF CELL PROLIFERATION BY 1-*O*-OCTADECYL-2-*O*-METHYL-*sn*-GLYCERO-3-PHOSPHOCHOLINE IN EPITHELIAL CANCER CELL LINES

By

Xi Zhou

A thesis submitted to the Faculty of Graduate Studies

in partial fulfillment of the requirements for the degree of

Doctor of Philosophy

Department of Biochemistry and Molecular Biology

University of Manitoba

1997

THE UNIVERSITY OF MANITOBA

FACULTY OF GRADUATE STUDIES

*****

COPYRIGHT PERMISSION PAGE

MECHANISMS OF INHIBITION OF CELL PROLIFERATION BY 1-O-OCTADECYL-2-O-METHYL-Sn-GLYCERO-3-PHOSPHOCHOLINE IN EPITHELIAL CANCER CELL LINES

by

XI ZHOU

A Thesis/Practicum submitted to the Faculty of Graduate Studies of The University of Manitoba in partial fulfillment of the requirements of the degree

DOCTOR of PHILOSOPHY

This thesis is affectionately dedicated

To

MY WIFE WEI

MY CHILDREN NINA & TONY

AND MY PARENTS

Without whose help, understanding, and support

this thesis would not have been possible

ACKNOWLEDGEMENTS

I would like to thank Dr. Gilbert Arthur for giving me the opportunity for graduate training in his laboratory. I would also like to thank him for all the advice and support throughout these years filled with all kinds of hardship. I will never forget that when I called him at 2:00 a.m. about problems I encountered in an on-going experiment, he came to help me without delay. I greatly appreciate his support in the critical moments I had never experienced before. I have become more prepared to endure adversity thanks to his edification and bolstering.

I wish to thank members of my Ph.D. committee, Drs. James R. Davie, Rajinder P. Bhullar and Steven N. Pind, for their excellent advice over the five years of my study and critical assessment of this thesis. I also would like to thank Dr. David L. Severson, the external examiner, for his constructive and informative evaluation of this thesis.

My heartfelt thanks to the chair and members of the second committee for my candidacy examination Drs. J. Davie, R. Bhullar, Grant Hatch, Frits C. Stevens and Barbara Triggs-Raine for their extra time, energy, and fair judgement, without which, this thesis would not be crowned with "A thesis ... for the degree of Doctor of Philosophy".

I am very grateful to all the people in my lab who helped me in the progression towards the completion of my Ph.D. program; they are Lorie, Ketan, Xiaoli, Pranati, Wei Yang, Christina and Anthony.

To Dr. Patrick C. Choy, who was always available, amiable and helpful whenever I needed his guidance and support.

Again, to Drs. B. Triggs-Raine and Hans K. Jacobs for their understanding and timely assistance which will be alive in the memory of my wife and mine forever.

To Dr. Julian N. Kanfer and people in his lab, I would thank them for allowing me to borrow materials for my experiments. The same thanks to the people in Dr. P. Choy's lab, Dr. K. Wrogemann's lab, Dr. B. Triggs-Raine's lab, and Dr. J. Davie's lab.

To Dr. Jianmin Sun for many valuable discussions which accelerated the progress of my research.

To Miss Deborah Chadee for her assistance in scanning which is highly appreciated.

To my family, who have shared my sadness and happiness, my failure and success. I am proud to be a member of the family.

LIST OF CONTENTS

LIST OF FIGURES

LIST OF TABLES

LIST OF ABBREVIATIONS

3pK	chromosome 3p kinase
AA	arachidonic acid
AAS	acetic acid (0.2 M, pH 2.5) containing 0.5 M NaCl
Ab	antibody
1(or 2)-acyl-lysoPL	1(or 2)-acyl-lysophospholipid
AdoHcy	*S*-adenosyl-homocysteine
AdoMet	*S*-adenosyl-methionine
AEBSF	aminoethylbenzenesulfonyl fluoride
AELs	antitumor ether lipids
ALP	alkyl lysophospholipid
AMP	adenosine 5'-monophosphate
aPKCs	atypical PKCs (ζ, λ, ι)
ASK1	apoptosis signal-regulating kinase 1
AT	acyltransferase
ATCC	American Type Culture Collection
ATF-2	activating transcription factor-2 (also designated CRE-BP-1)
ATP	adenosine 5'-triphosphate
BM 41.440	1-*S*-hexadecylthio-2-methoxymethyl-*sn*-glycero-3-phosphocholine (also known as ilmofosine)
BSA	bovine serum albumin

°C	degree Celsius
cAMP	cyclic adenosine 3',5'-monophosphate
CAPK	ceramide-activated protein kinase
CAPP	ceramide-activated protein phosphatase
CBP	CREB binding protein
cdc	cell division cycle
CDP	cytidine 5'-diphosphate
CDP-Cho	CDP-choline
CDP-Etn	CDP-ethanolamine
C/EBP	CCAAT/enhancer-binding protein
CGP	cholineglycerophospholipid
Cho	choline
CHOP	C/EBP-homologous protein
Ci	Curie
CK	choline kinase
CMP-PA	cytidine monophosphoryl phosphatidate
CoA	coenzyme A
cPKCs	conventional (or classical) PKCs (α, βI, βII, γ)
$cPLA_2$	cytosolic PLA_2
CPT	(CDP-choline:1,2-diacylglycerol) choline phosphotransferase
CRD	cysteine-rich domain
CRE	cyclic AMP response element

CREB	CRE-binding protein
CRE-BP1	cyclic AMP response element-binding protein 1
C-terminus	carboxyl terminus or COOH-terminus
CTP	cytidine 5'-triphosphate
DAG	diacylglycerol
DAG-1(or 2)-lipase	diacylglycerol-1(or 2)-lipase
DDW	distilled deionized water
DGAT	diacylglycerol acyltransferase
2-D	two-dimensional
DHAP	dihydroxyacetone phosphate
DiC_8	1,2-dioctanoyl-*sn*-glycerol
DMEM	Dulbecco's modified Eagle medium
DMEM/BSA	DMEM containing 0.5 mg/ml of bovine serum albumin
DMEM/FBS	DMEM supplemented with 10% fetal bovine serum
DNA	deoxyribonucleic acid
dpm	disintegrations per minute
DTT	dithiothreitol
EC	enzyme classification
ECL	enhanced chemiluminesence
EDTA	ethylene diaminetetraacetic acid
EGF	epidermal growth factor
EGFr	epidermal growth factor receptor

EGP	ethanolamineglycerophospholipid
EGTA	ethyleneglycol-bis-(β-amino-ethyl ether)N,N'-tetraacetic acid
EK	ethanolamine kinase
Elk-1	Ets-related transcriptional factor
EPT	(CDP-ethanolamine:1,2-diacylglycerol ethanolamine phosphotransferase
ER	endoplasmic reticulum
ERK1 or 2	extracellular signal-regulated protein kinase 1 or 2
ET18-OCH_3	1-*O*-octadecyl-2-*O*-methyl-*sn*-glycero-3-phosphocholine (also known as edelfosine or ET18-OMe)
Etn	ethanolamine
FBS	fetal bovine serum
FFA	free fatty acid
GADD153	growth arrest and DNA damage-inducible gene 153
GAP	GTPase-activating protein
GDP	guanosine 5'-diphosphate
GNEFs	guanine nucleotide exchange factors
GPAT	glycerophosphate acyltransferase
GP-base	glycerophosphoryl base
GPCR	G protein-coupled receptor
Grb2	growth factor receptor-bound protein 2
Gro	glycerol

Gro-3-*P*	glycero-3-phosphate
Gro*P*Cho	glycerophosphoryl choline
GTP	guanosine 5'-triphosphate
GTPase	guanosine 5'-triphosphatase
H+L	heavy and light chains of antibodies
HBSS	Hank's balanced saline solution (see **Section 2.7**)
HBSS/BSA	HBSS containing 0.5 mg/ml bovine serum albumin
HePC	hexadecylphosphocholine (also known as miltefosine)
HEPES	N-[2-hydroxyethyl]piperazine-N'-[2-ethanesulfonic acid]
h	hour
HRP-	horseradish peroxidase-conjugated
Hsp	heat shock protein
IFN-γ	γ-interferon
IgG	immunoglobulin G
IL-1	interleukin-1
Ins(1)*P*	inositol (1)phosphate
Ins(3)*P*	inositol (3)phosphate
Ins(4)*P*	inositol (4)phosphate
Ins(1,4)P_2	inositol (1,4)bisphosphate
Ins(3,4)P_2	inositol (3,4)bisphosphate
Ins(1,3,4)P_3	inositol (1,3,4)trisphosphate
Ins(1,4,5)P_3	inositol (1,4,5)trisphosphate

Ins(1,3,4,5)P_4	inositol (1,3,4,5)tetrakisphosphate
Ins(1,3,4,6)P_4	inositol (1,3,4,6)tetrakisphosphate
Ins(1,4,5,6)P_4	inositol (1,4,5,6)tetrakisphosphate
Ins(3,4,5,6)P_4	inositol (3,4,5,6)tetrakisphosphate
Ins(1,3,4,5,6)P_5	inositol (1,3,4,5,6)pentakisphosphate
InsP_6	inositol hexakisphosphate
InsP_5P	inositol tetrakisphosphate pyrophosphate
InsP_6P	inositol pentakisphosphate pyrophosphate
IP_3R	the receptor of inositol (1,4,5)trisphosphate
JAK-2	Janus kinase-2
JNK	Jun N-terminus kinase
JNKK	JNK kinase (i.e., MKK4)
kDa	kilodaltons
KSR	kinase suppressor of Ras
L	liter
LPAAT	lysophosphatidic acid acyltransferase
lyso-PAF	1-*O*-alkyl-2-lyso-*sn*-glycero-3-phosphocholine (i.e., lyso-platelet-activating factor)
lysoPL	lysophospholipid
lyso-PLD	lysophospholipase D
lysoPtdCho	lysophosphatidylcholine
lysoPtdEtn	lysophosphatidylethanolamine

lysoPtdOH	lysophosphatidic acid
M	molar
mAb	monoclonal antibody
MAG	monoacylglycerol
MAPs	microtubule-associated proteins
MAPK	mitogen-activated protein kinase
MAPKAP kinase-1	MAPK-activated protein kinase-1 (i.e., S6 kinase-II)
MAPKAP kinase-2	MAPK-activated protein kinase-2
MAPKK	MAPK kinase
MAPKKK	MAPK kinase kinase
MBP	myelin basic protein
MEK	mitogen-activated protein kinase/extracellular signal regulated protein kinase kinase
MEKK	MEK kinase
mg	milligram
min	minute
MKK	MAPK kinase
MKP-1	mitogen-activated protein kinase phosphatase 1
ml	milliliter
mM	millimolar
MPF	maturation-promoting factor
M_r	the effective molecular radius (approximates to molecular size)

mSos	mammalian homologues of the *Drosophila* Son of Sevenless
N	normal concentration
NF1	neurofibromin
NF 1	neurofibromatosis type 1 gene
NF-IL6	a nuclear factor binding to the interleukin 1 (IL-1) responsive element in IL-6 gene
NF-κB	nuclear factor-κB
NGF	nerve growth factor
NIH	National Institute of Health
nm	nanometer
nM	nanomolar
non-RTK	non-receptor protein tyrosine kinase
NP-40	Nonidet P-40
nPKCs	novel PKCs (δ, ϵ, η(L), θ, μ)
N-terminus	amino terminus or NH_2-terminus
OD	optical density
OMG	1-*O*-octadecyl-2-*O*-methylglycerol
P	statistical probability, or phosphate radical
PAC-1	phosphatase of activated cells
PAF	platelet-activating factor
PAGE	polyacrylamide gel electrophoresis
PAP	phosphatidic acid phosphohydrolase

PBS	phosphate buffered saline solution (see **Section 2.7**)
PCCT	(CTP:)phosphocholine cytidylyltransferase
*P*Cho	phosphocholine
PC-PLC	phosphatidylcholine-specific PLC
PDGF	platelet derived growth factor
PDPK	proline-directed protein kinase
PECT	(CTP:)phosphoethanolamine cytidylyltransferase
PEMT	phosphatidylethanolamine methyltransferase
*P*Etn	phosphoethanolamine
PHAS-I	insulin-stimulated phosphorylated heat- and acid-stable protein
P-headgroup	phosphoryl headgroup
PIC	phosphoinositidase C (also known as phosphoinositide-specific PLC)
PI3-kinase	phosphoinositide 3-kinase (it can phosphorylate any inositol lipid *in vitro*)
PI-PLC	phosphoinositide-specific PLC (also known as phosphoinositidase C)
PKA	protein kinase A
PKB	protein kinase B (a target for PI3-kinase, see **Section 1.4.2**)
PKC	protein kinase C
PKI	protein kinase A inhibitor peptide [a 77 amino acid (8 kDa) protein]
PKM	protein kinase M (see the legend of **Figure 3**)
PL	phospholipid
PLA_1 (or A_2)	phospholipase A_1 (or A_2)

PLB	phospholipase B
PLC	phospholipase C
PLD	phospholipase D
PMSF	phenylmethylsulfonyl fluoride
PP1	type-1 serine/threonine protein phosphatase
PP2A	type-2A serine/threonine protein phosphatase
PPi	pyrophosphate
p70 S6K	70-kD ribosomal protein S6 kinase
p90 S6K	90-kD ribosomal protein S6 kinase
PtdCho	phosphatidylcholine
PtdEtn	phosphatidylethanolamine
PtdIns	phosphatidylinositol
PtdIns 3-kinase	phosphatidylinositol 3-kinase (it is a PtdIns-specific 3-kinase)
PtdIns 4-kinase	phosphatidylinositol 4-kinase
PtdIns 5-kinase	phosphatidylinositol 5-kinase
PtdIns(3)*P*	phosphatidylinositol 3-phosphate
PtdIns(4)*P*	phosphatidylinositol 4-phosphate
PtdIns(3,4)P_2	phosphatidylinositol (3,4)bisphosphate
PtdIns(4,5)P_2	phosphatidylinositol (4,5)bisphosphate
PtdIns(3,4,5)P_3	phosphatidylinositol (3,4,5)trisphosphate
PtdOH	phosphatidic acid
PtdSer	phosphatidylserine

Pte·H_4	tetrahydropteridine
PTK	protein tyrosine kinase
PTPα	protein tyrosine phosphatase α
RBD	Ras-binding domain
Rb protein	retinoblastoma protein
RK	reactivating kinase
RSK	p90 ribosomal protein S6 kinase (also known as $p90^{rsk}$)
RTK	receptor protein tyrosine kinase
SAP-1	serum response factor accessory protein-1
SAPK	stress-activated protein kinase
SDS	sodium dodecyl sulfate
SDS/NaOH	1% SDS in 0.3 *N* NaOH
SDS-PAGE	sodium dodecyl sulfate-polyacrylamide gel electrophoresis
SEK	SAPK/ERK kinase
SH2 or SH3	Src homology 2 domain or Src homology 3 domain
Shc	Src homology 2/α-collagen-related
SM	sphingomyelin
SMase	sphingomyelinase
Sos	Son of Sevenless (a guanine nucleotide exchange factor)
SRE	serum response element
SRF	serum response factor
SRI 62-834	2-{hydroxy[tetrahydro-2-(octadecyloxy)methylfuran-2-1-methoxyl]

	phosphinyloxy}-*N*,*N*,*N*-trimethylethaniminium hydroxyde
STMR	seven-pass transmembrane receptor
Syp	SH2-containing protein-tyrosine phosphatase (also known as SH-PTP2)
TAB1	TAK1 binding protein
TAG	triacylglycerol
TAK1	TGF-β-activated kinase 1
TCA	trichloroacetic acid
TCF	ternary complex factors
TCR	T-cell receptor
TCR-CD3	T-cell-receptor-CD3 complex
TEMED	N,N,N',N'-tetramethyl ethylenediamine
TGF-α, or -β	tumor growth factor-α, or -β
TLC	thin-layer chromatography
TNF-α	tumor necrosis factor-α
TPA	12-*O*-tetradecanoyl phorbol-13-acetate (a phorbol ester)
4-α-TPA	4-α-12-*O*-tetradecanoyl phorbol-13-acetate (a biologically inactive TPA)
Tris-HCl	Tris[hydroxymethyl]aminomethane hydrochloride
UV	ultraviolet
μ	micron
μCi	microcurie

µl	microliter
µM	micromolar
µmol	micromole
v	volume
v/v	by volume
w	weight
#	catalog number

ABSTRACT

1-*O*-Octadecyl-2-*O*-methyl-*sn*-glycero-3-phosphocholine (ET18-OCH_3), a prototype of synthetic antitumor ether lipids (AEL), selectively inhibits the growth of a variety of cancer cells relative to normal cells. The mechanism of its antiproliferative action remains obscure. We have explored a number of hypotheses using five epithelial cancer cell lines (MCF-7, T84, A427, A549 and Malme 3M). Our studies have shown [1] that cellular ether lipid content or composition does not correlate with the sensitivity of the cells to the growth-inhibitory activity of ET18-OCH_3; [2] the observed effects of this ether compound on the cellular lipid metabolism do not underlie its antiproliferative action; [3] ET18-OCH_3, rather than its metabolite 1-*O*-octadecyl-2-*O*-methyl-*sn*-glycerol, is the main active compound responsible for the growth-inhibitory effect in sensitive cell lines (e.g., MCF-7); [4] ET18-OCH_3 inhibits the PKC-dependent phosphorylation of endogenous proteins following stimulation of quiescent MCF-7 cells with TPA or DAG; [5] ET18-OCH_3 truncates the EGF- or serum-induced activation of MAPK in quiescent MCF-7 cells via interference in the membrane association of Raf-1 that leads to inhibition of the Raf-1 kinase activity and of the phosphorylation of MEK as well as MAPK. A direct correlation between ET18-OCH_3 accumulation, inhibition of cell proliferation, Raf-1 association with the membrane, and MAPK activation has also been established. These results suggest that inhibition of the MAPK cascade as a result of its effect on Raf-1 activation, and inhibition of the PKC pathway may be important mechanisms by which ET18-OCH_3 inhibits cell proliferation.

1. INTRODUCTION

Cancer, one of the most vicious foes of human beings, accounted for one fifth of the total mortality in 1994 (data from the United States, Singh *et al.*, 1995); the overall incidence of cancer is still increasing, even though we have been waging a tireless struggle against this ancient disease since the Hippocratic epoch (Rubin and Farber, 1994). These facts strongly call on us to persevere in this sacred struggle unremittingly.

Cancers are malignant tumors with the ability to invade contiguous tissues and metastasize to distant sites. These malignant neoplasms are classified according to the tissue and cell type from which they arise. Cancers arising from epithelial cells are termed carcinomas; those arising from connective tissue or muscle cells are termed sarcomas. Cancers that do not fit in either of these two broad categories include those derived from hemopoietic cells, cells of the nervous system and other unspecified sites.

1.1 Uncontrolled Proliferation: A Cardinal Property of Cancer Cells

Normally, cell proliferation is precisely controlled and, in multicellular organisms, is securely coordinated with other replicating cells. However, the finely tuned mechanisms go awry in cancer, resulting in unbridled proliferation of cancer cells. This anomaly of malignant cells is characterized by loss of differentiation (Hartwell and Kastan, 1994), a lowered requirement for growth factors (Alberts *et al.*, 1994; Rubin and Farber, 1994), a much reduced calcium requirement for growth (Nicholson *et al.*, 1984), loss of anchorage dependence (Alberts *et al.*, 1994; Hynes, 1994; Stroker *et al.*, 1968), loss of contact-inhibition response (Fagotto and Gumbiner, 1994) or other surveillance mechanisms (Hamel

et al., 1992; Kamb, 1995; Sherr, 1996; Ullrich *et al.*, 1992), increased invasiveness (Hartwell and Kastan, 1994), a higher proportion of cycling cells (Rubin and Farber, 1994), and insensitivity to physiological apoptotic stimuli (Ashwell *et al.*, 1994).

The past two decades have witnessed remarkable progress in our understanding of the molecular basis of cancer and the cell cycle control in both normal and tumor cells. The discovery of cellular oncogenes (Krontiris and Cooper, 1981; Shih *et al.*, 1981), tumor suppressor genes (Dryja *et al.*, 1986; Friend *et al.*, 1986; Lamb and Crawford, 1986) and their encoded proteins, with research advances into cellular signaling systems and the cell cycle machinery, have now allowed us to appreciate the complexity of, and discrepancy between, the signaling networks that regulate normal and neoplastic cell proliferation. However, in many cases, it is not presently clear how cancer cells escape from the normal growth control.

1.2 The Mitogen-activated Protein Kinase Cascade: A Common Growth Signaling Pathway in Various Types of Cells

It is generally accepted that a number of signal transduction pathways exist, each contributing to the eventual mitogenic response (Posada and Cooper, 1992a; Ralph *et al.*, 1990; Rozengurt, 1986). Some of these pathways or components of these signaling apparatus may not be essential for transduction of growth signals (their presence fulfilling a regulatory role rather than an obligatory requirement), while others may play an indispensable role in the induction of cell growth and division. However, the role of a factor or pathway can vary in different situations. A perfect example is cyclic adenosine 3',5'-monophosphate (cAMP) which serves as a second messenger positively regulating proliferation in one cell line, but

negatively acting in another, or having no profound effect on cell growth in others (**Section 1.2.10**).

In a wide variety of cell types, the Ras/Raf-dependent mitogen-activated protein kinase (MAPK) cascade is a pivotal signaling pathway through which cells transduce myriads of growth signals (Blumer and Johnson, 1994; Nishida and Gotoh, 1993) from receptor protein tyrosine kinases (RTK), non-receptor protein tyrosine kinases (PTK) and G protein-coupled receptors (GPCR) (Inglese *et al.*, 1995; Lopez-Ilasaca *et al.*, 1997) to the nucleus (Davis, 1995; Hill and Treisman, 1995) (**Figure 1**).

1.2.1 Transduction of signals via the Ras-mediated MAPK cascade

The sequence of events that transduce extracellular growth signals from the cell surface to the nucleus via the Ras-directed MAPK cascade is depicted using the epidermal growth factor receptor (EGFr) as an example (**Figure 2**). Sequentially, the flow of signals is from the receptor → the Grb2-Sos complex → Ras protein → Raf kinase (a MAPK kinase kinase) → MEK (*M*APK/*E*RK *k*inases) → ERK (*e*xtracellular signal-*r*egulated protein *k*inase, the archetype of MAPKs). This MAPK in turn phosphorylates various cytosolic and nuclear substrates, eventually leading to cellular responses including cell proliferation (Pagès *et al.*, 1993; Troppmair *et al.*, 1994) or differentiation (Crompton, 1996; Ferrell Jr., 1996).

A central component in this signal transduction system is the Ras protein, a low molecular weight guanosine triphosphate (GTP)-binding protein. Ras converges various stimuli from the plasma membrane environment and transmits signals to a cytosolic serine/threonine protein kinase Raf beneath the membrane. The kinase Raf is another critical

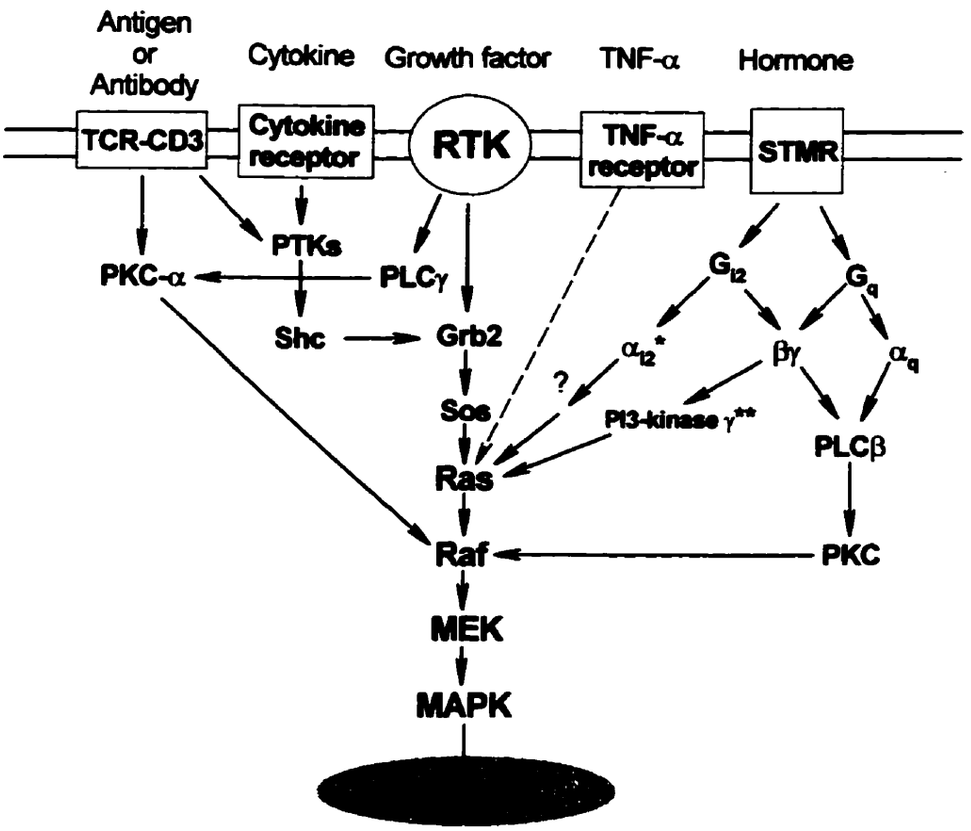

Figure 1. Activation of the Ras/Raf-dependent MAPK cascade. The Ras/Raf-dependent MAPK cascade can be activated by various extracellular signals such as growth factors, cytokines, antigens, antibodies against T-cell receptor (TCR) or CD3, tumor necrosis factor-α (TNF-α) and hormones via their respective receptors. PI3-kinase γ, phosphoinositide 3-kinase γ; RTK, receptor protein tyrosine kinase; STMR, seven-pass transmembrane receptor; and TCR-CD3, T-cell-receptor-CD3 complex. (* Alblas, *et al.*, 1993; Winitz, *et al.*, 1993. ** Lopez-Ilasaca, *et al.*, 1997)

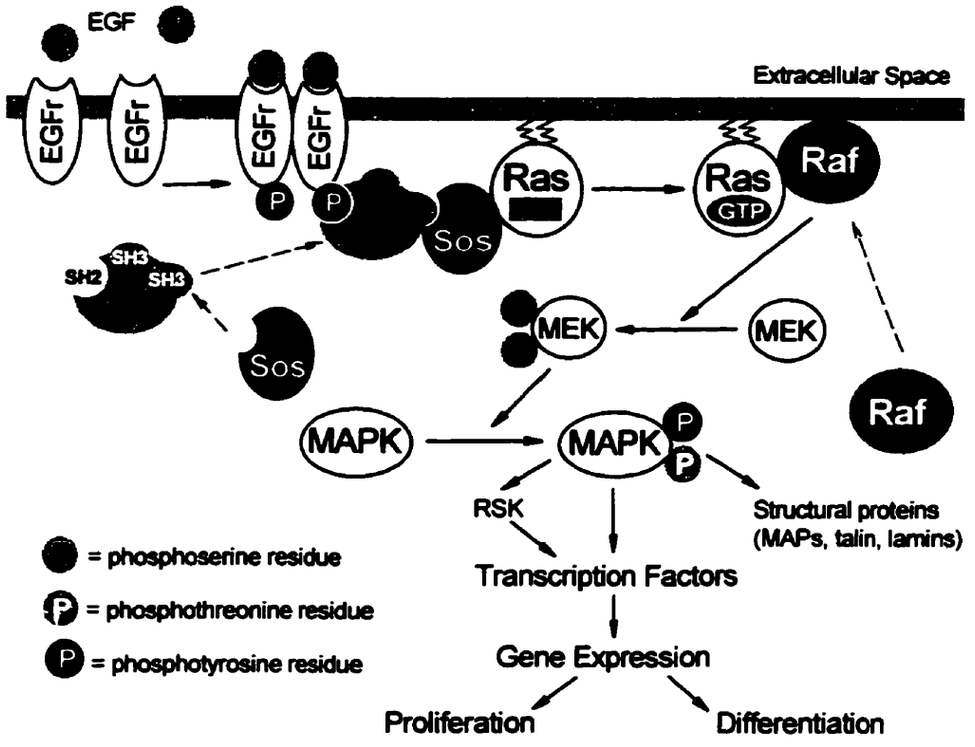

Figure 2. The Ras/Raf/MEK/ERK pathway. Upon EGF binding to receptors, the receptors undergo dimerization and tyrosine phosphorylation. An adaptor protein Grb2 binds to the phosphotyrosine residues via its SH2 domain. The SH3 domain of Grb2 binds to the C-terminal proline-rich sequence of Sos and recruits Sos to the plasma membrane. Subsequently, Sos activates Ras by unloading GDP from Ras followed by spontaneous association of GTP. The active GTP-bound Ras then interacts with Raf-1 and translocates Raf-1 to the membrane where it is activated by an unknown mechanism. After activation, Raf-1 phosphorylates and activates a dual-specificity kinase MEK, which in turn activates MAPK (ERK) by phosphorylating its adjacent threonine and tyrosine residues. Activated ERK phosphorylates cytosolic substrates, cytoskeletal elements, and enters the nucleus to phosphorylate nuclear transcription factors, ultimately leading to cell proliferation or differentiation.

intermediate, which further relays signals to MEK, a cytosolic element of the MAPK cascade, thereby linking the two cellular compartments (the plasma membrane and the cytosol) together. MAPK is also a key player. A wide range of molecules have been shown *in vitro* and/or *ex vivo* to be substrates of the kinase (Davis, 1993; 1995). These include receptors, protein kinases, cytoskeletal elements, nuclear transcription factors, and other cellular proteins (**Table 1**).

1.2.2 The EGF receptor tyrosine kinase

The EGF receptor is a 170-kDa polypeptide composed of an extracellular EGF-binding domain, a single hydrophobic transmembrane region and a cytoplasmic kinase domain (Cummings *et al.*, 1985). The binding of EGF to the extracellular domain induces receptor dimerization and activates the intrinsic tyrosine-specific protein kinase activity of EGF receptors. This activity results in autophosphorylation/transphosphorylation of several tyrosine (Tyr) residues on the EGF receptor (Panayotou and Waterfield, 1993) (see **Figure 2**). Specific phosphotyrosine residues serve as binding sites for cellular signaling molecules. These include Tyr1068 and Tyr1086 for Grb2 (Buday and Downward, 1993; Li *et al.*, 1993; Okutani *et al.*, 1994; Songyang *et al.*, 1993), Tyr1148 and Tyr1173 for Shc (Okabayashi *et al.*, 1994), and Tyr992 for PLCγ (Rotin *et al.*, 1992; Songyang *et al.*, 1993).

The activated EGF receptors are rapidly internalized into the endocytotic compartment and most of them do not recycle but are degraded in lysosomes (Alberts *et al.*, 1994). This ligand-induced endocytosis of the EGF-bound receptors utilizes mainly clathrin-coated pits mediated by adaptins (Nesterov *et al.*, 1995; Sorkin and Carpenter, 1993; Sorkin

Table 1. Summary of *in vitro* and/or *ex vivo* substrates of MAPK.

Substrates	References
Receptors	
EGF receptor	Northwood *et al.*, 1991; Takishima *et al.*, 1991
estrogen receptor	Kao *et al.*, 1995
Protein Kinases	
RSK	Blenis, 1993; Sturgill *et al.*, 1988; Sutherland *et al.*, 1993
MEK	Matsuda *et al.*, 1993
c-Raf-1	Anderson *et al.*, 1991; Lee RM *et al.*, 1992
MAPKAP kinase-2	Stokoe *et al.*, 1992
3pK	Ludwig *et al.*, 1996
Cytoskeletal Elements	
talin	Daum *et al.*, 1994
lamins	Peter *et al.*, 1992
MAPs (MAP2, MAP4)	Nishida and Gotoh, 1992
Transcription Factors	Davis, 1995; Hill and Treisman, 1995
TCFs (Elk-1, SAP-1)	Janknecht *et al.*, 1993; Kortenjann *et al.*, 1994; Marais *et al.*, 1993; Whitmarsh *et al.*, 1995
c-Jun	Binetruy *et al.*, 1991; Pulverer *et al.*, 1991; Smeal *et al.*, 1993
c-Fos	Thomas, 1992
c-Myc	Alvarez *et al.*, 1991; Seth *et al.*, 1991
NF-IL6	Nakajima *et al.*, 1993
ATF-2	Abdel-Hafiz *et al.*, 1992
Other Cellular Proteins	
PLA_2	Lin *et al.*, 1993; Nemenoff *et al.*, 1993
PHAS-I	Haystead *et al.*, 1994
RNA polymerase II	Dubois *et al.*, 1994

Abbreviations: ATF-2, activating transcription factor-2; Elk-1, Ets-related protein; MAPKAP kinase-2, MAPK-activated protein kinase-2; MAPs, microtubule-associated proteins; NF-IL6, a nuclear factor binding to the interleukin 1 (IL-1) responsive element in the IL-6 gene; PHAS-I, an insulin-stimulated phosphorylated heat- and acid-stable protein; 3pK, chromosome 3p kinase; PLA_2, phospholipase A_2; RSK, 90-kDa ribosomal protein S6 kinase; SAP-1, serum response factor accessory protein-1; TCFs, ternary complex factors.

and Waters, 1993). The receptor-adaptin association is tyrosine-phosphorylation-dependent (Nesterov *et al.*, 1995) and occurs in intact cells before coated pits are fully assembled (Sorkin and Carpenter, 1993). Recently, it was reported that the clathrin-mediated endocytosis of activated EGF receptors plays a critical role in attenuating EGFr signaling as well as in establishing and controlling specific signaling pathways (Vieira *et al.*, 1997). Internalization of EGF-receptor complexes is highly temperature dependent with a maximal rate at physiological temperatures and virtual blockage at 4°C (Sorkin and Waters, 1993).

1.2.3 The adaptor protein Grb2

The 25-kDa adaptor protein, growth factor receptor-bound protein 2 (Grb2, also known as Ash-1), contains one *src* homology 2 (SH2) domain and two SH3 domains. As a linker, its SH2 domain attaches to tyrosine-phosphorylated proteins (e.g., EGFr, Shc, Syp, PTPα), and its SH3 domain to a guanine nucleotide exchange factor, Sos. Therefore, Grb2 brings Sos to its target, the membrane-associated inactive Ras, leading to activation of the Ras signaling pathway. Grb2 can bind directly to either Tyr1068 or Tyr1086 on EGFr with high affinity, or associate with EGFr by binding to the phosphotyrosine (p-Tyr) residues on proteins that have already attached to EGFr via their own SH2 domains. These interactions include the binding of Grb2 to Tyr1148 on Shc (Okutani *et al.*, 1994), to Tyr542 on Syp (Bennett *et al.*, 1994; Li *et al.*, 1994), and to Tyr789 on protein tyrosine phosphatase α (PTPα) (den Hertog *et al.*, 1994). Interestingly, a very recent study demonstrates that Grb2 also mediates the internalization of EGFr through a specific interaction with dynamin (Wang and Moran, 1996), a guanosine 5'-triphosphatase (GTPase) that regulates endocytosis (Vallee

et al., 1993; Warnock and Schmid, 1996), indicating a novel mechanism by which EGFr is down-regulated.

Different isoforms or members of the growth factor receptor-bound protein family have been identified. Grb7 has been shown to bind to activated HER2/*neu*, a receptor with close similarity to the EGFr, and was found to be coamplified and overexpressed with HER2/*neu* in certain forms of breast cancer (Stein *et al.*, 1994). Grb10 specifically associates with Ret, a receptor protein tyrosine kinase implicated in the development of the enteric nervous, endocrine, and renal systems (Pandey *et al.*, 1995). Grb3-3, a Grb2 isoform that has a deletion in the SH2 domain, is expressed in high amounts in thymocytes that are destined to undergo negative selection (Fath *et al.*, 1994). Microinjection of Grb3-3 into Swiss 3T3 fibroblasts induced apoptosis, suggesting that Grb3-3 may trigger active programed cell death by suppressing proliferative signals as a result of competition with Grb2 for Sos (Fath *et al.*, 1994).

1.2.4 The Ras guanine nucleotide exchange factor Sos

The rate at which guanine nucleotides bind to and dissociate from purified Ras proteins is very slow (Downward, 1992). Specific Ras guanine nucleotide exchange factors (GNEFs) promote the release of guanosine diphosphate (GDP) from the inactive Ras-GDP complex. Consequently, an increase in GTP-bound Ras protein occurs as GTP is the predominant guanine nucleotide found in the cytosol (Downward, 1992). GNEFs are highly conserved in evolution. In *Drosophila*, the GNEF for Ras is encoded by the *son of sevenless* gene (*sos*). Mammalian cells contain two distinct homologues of *Drosophila* Sos protein

(mSos), Sos1 and Sos2 (Bowtell *et al.*, 1992; Chardin *et al.*, 1993). Both contain a proline-rich sequence at the carboxyl terminus that binds to the SH3 domain of Grb2 (Yang *et al.*, 1995). Membrane recruitment of Sos by the interaction between Grb2 and Sos appears to be the primary mechanism leading to Ras activation, since targeting of Sos to the plasma membrane by using Sos derivatives containing either farnesylation or myristoylation signals is sufficient for Ras activation (Aronheim *et al.*, 1994).

Interestingly, Ras activation can result in MEK-dependent phosphorylation of Sos and subsequent dissociation of the Grb2-Sos complex (Langlois *et al.*, 1995; Waters *et al.*, 1995). This feedback mechanism may account for, at least in part, the transient activation of Ras despite the continuous presence of stimuli.

1.2.5 The small GTPase Ras

ras genes

The *ras* genes were first discovered as retroviral oncogenes (Barbacid, 1987). In mammals, three closely related *ras* genes are now known, H-, K- and N-*ras*. The H-*ras* and K-*ras* genes gave rise to the v-H-*ras* gene of Harvey (Ha-*ras*) and the v-K-*ras* gene of Kirsten (Ki-*ras*) rat sarcoma viruses, respectively (Ellis *et al.*, 1981; Ruta *et al.*, 1986); hence the acronym ras is derived from ***ra***t ***s***arcoma. N-*ras* was found in a neuroblastoma cell line as a transforming gene with homology to the other *ras* genes (Shimizu *et al.*, 1983). Thus, Ras proteins are proto-oncogene or oncogene products in mammals.

Post-translational modification of Ras protein

The Ras protein ($p21^{ras}$) is synthesized in the cytoplasm on free ribosomes as pro-

p21. It undergoes a series of post-translational modifications at the C-terminus, increasing the hydrophobicity of the protein and resulting in its association with the inner face of the plasma membrane (Lowy and Willumsen, 1993). The attachment of the isoprenoid farnesol to the cysteine (Cys) residue of the C-terminal CAAX motif (C, Cys; A, aliphatic amino acid; X, another amino acid) of Ras is the critical modification required for Ras membrane association and transforming activity. The subsequent modifications—proteolytic cleavage of the AAX residues, carboxyl methylation of the farnesylated cysteine, and palmitoylation of cysteines upstream of the CAAX box—are not obligatory for Ras membrane association or cell-transforming activity, although they increase membrane affinity and biological activity (Gibbs *et al.*, 1994; Lowy and Willumsen, 1993).

GAP1 inactivates Ras by boosting its GTPase activity

Ras proteins are monomeric small G proteins distinct from heterotrimeric G proteins. Ras binds the magnesium/guanine nucleotide complexes with high affinity (10^{11}-10^{12} M^{-1} at 5°C) and shows remarkable selectivity against other nucleotides (John *et al.*, 1990). When bound to GTP, Ras assumes an active conformation; the Ras-GDP complex comprises an inactive form (Bourne *et al.*, 1990, 1991). Active Ras cannot be turned off by its very low intrinsic GTPase activity, the reaction rate of which is 0.028 min^{-1} (Mittal *et al.*, 1996). Ras inactivation is achieved by interaction with a GTPase-activating protein (GAP), which accelerates Ras GTPase activity by 10,000-fold (Marshall, 1993). GAP1, a 120-kDa cytosolic protein containing two SH2 and one SH3 domains, is highly specific for Ras (Trahey and McCormick, 1987). Formation of the GAP1-receptor complex through its SH2 domain and the phosphotyrosine residues on the receptor may increase its ease of interaction

with Ras, thereby inactivating the protein (Downward, 1992). It was also reported that membrane targeting of GAP1 by Ras C-terminal motifs (see below) enabled GAP1 to act as a potent suppressor of Ras function (Huang *et al.*, 1993).

The interaction of GAP1 with Ras may be controlled through Rap1, a 21-kDa protein closely related to Ras. Rap1 has an identical effector domain to Ras and an overall sequence identity of 50%; presumably it is able to compete with Ras for GAP1 (Bokoch, 1993; Noda, 1991). In fact, the affinity of Rap1:GTP for GAP1 (~50 nM) is much higher than that of Ras:GTP for GAP1 (~2 μM) (Downward, 1992). Even though GAP1 binds tightly to Rap1, it does not stimulate Rap1 GTPase. Whether Rap1 sequesters GAP1 to maintain Ras activation in the cell is at present unknown (see **Section 1.2.6**).

It is interesting that GAP1 may also function as a Ras effector for the germinal vesicle breakdown in *Xenopus oocytes* and its SH3 domain is essential for this signal transduction (Duchesne *et al.*, 1993). This finding begs the question of whether GAP1 is also a transmitter of Ras signaling in mammalian cells. Indeed, GAP1 plays a role in other effects of Ras, for instance, regulation of the actin cytoskeleton through p190, a protein that associates tightly with GAP1 and has Rho-GAP activity (Boguski and McCormick, 1993; Polakis and McCormick, 1993).

Is neurofibromin a Ras-specific GAP?

Another molecule with GAP activity is neurofibromin (NF1), a 235-kDa mammalian protein, encoded by the neurofibromatosis type 1 gene (*NF 1*) (Martin *et al.*, 1990). NF1 has a GAP-related catalytic domain but lacks SH2 and SH3 domains (Downward, 1992). Surprisingly, the full length protein has not yet been shown to possess GAP activity.

However, the NF1 catalytic domain, when expressed in non-mammalian systems, inactivated Ras, and intriguingly had a much higher affinity (~50 nM) for Ras than did GAP1 (~2 μM) (Martin *et al.*, 1990). Both GAP1 and the NF1 catalytic fragment are only able to promote the GTPase activity of the wild type Ras proteins, but fail to stimulate the activity of activated Ras mutants (Downward, 1992). The cellular function of NF1 is not yet clear. Complicating matters further, a study showed that NF1 inhibited Ras-dependent growth by a mechanism independent of its GAP activity (Johnson *et al.*, 1994).

Ras effectors

The best-characterized direct effector of Ras is the Raf protein kinase, which activates the MAPK, and possibly other (Kuo *et al.*, 1996), pathways (Marshall, 1994). The activated Ras interacts via its effector domain (**Figure 3**) with the N-terminal regulatory region of Raf-1 (**Figure 4**) (Chuang *et al.*, 1994; Ghosh and Bell, 1994; Hu *et al.*, 1995; Zhang *et al.*, 1993), resulting in Raf membrane association and activation. Other potential targets of Ras include PI-3 kinase (Rodriguez-Viciana *et al.*, 1994), GAP1 (Boguski and McCormick, 1993; Polakis and McCormick, 1993), and Jun N-terminal kinase (JNK) (Adler *et al.*, 1995). Little is known about what Ras-directed cell fates (e.g., transformation, mitogenesis, differentiation, apoptosis) are due to Ras-mediated activation of these effectors (Feig and Schaffhausen, 1994).

ras oncogenes and human cancers

ras oncogenes, often resulting from mutations in either the phosphoryl group- or the purine ring-binding sites of *ras* genes (**Figure 3**), exist in a variety of human cancers. They have been identified in carcinomas of the bladder, breast, colon, kidney, liver, lung, ovary,

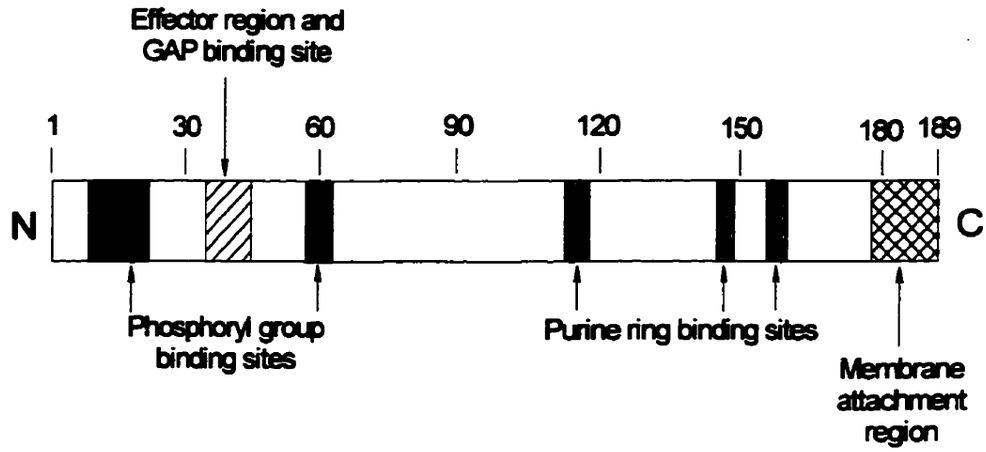

Figure 3. Structure of Ras protein. The functional regions shown here are known from crystallographic or mutagenesis studies. The numbers indicate positions of amino acid residues in Ras protein. The activating mutations have frequently been found in either the phosphoryl group- or the purine ring-binding sites of *ras* oncogenes.

pancreas and stomach, in hematopoietic tumors of various lymphomas and leukemias, and in sarcomas such as fibrosarcomas and rhabdomyosarcomas (Barbacid, 1987). Activated *ras* oncogenes are estimated to play a role in development of at least 30% of all human cancers (Marshall, 1993).

1.2.6 Raf: a serine/threonine protein kinase

raf genes and Raf proteins

Raf proteins are members of the MAPK kinase kinase (MAPKKK) family. These serine/threonine protein kinases are evolutionarily highly conserved, and are essential for growth and development in worms, flies, frogs and mammals (Daum *et al.*, 1994). Like Ras, Raf kinases are also proto-oncoproteins. They were first discovered as gain-of-function mutants with the ability to transform cells oncogenically (Rapp *et al.*, 1988). A single functional gene has been identified in *Drosophila* and *Caenorhabditis elegans*, which encodes D-Raf (Brunner *et al.*, 1994) and Ce-Raf (Han *et al.*, 1993), respectively. Three such genes were described in vertebrates that encode A-Raf, B-Raf and c-Raf-1 (Heidecker *et al.*, 1992) (**Figure 4**). They have been mapped to three different chromosomes and located at sites that are frequently altered in human tumors (Sithanaadam *et al.*, 1989; Storm *et al.*, 1990a, 1990b). These *raf* genes can be oncogenically activated *in vitro* (Heidecker *et al.*, 1990; Huleihel *et al.*, 1986; Sithanandam *et al.*, 1990). A-*raf* expression is most abundant in urogenital tissues; B-*raf* transcripts are most prominent in testis and cerebrum; and c-*raf*-1 is ubiquitously expressed although at variable levels (Storm *et al.*, 1990b). All Raf proteins share three highly conserved regions (CR1-3) (**Figure 4**). CR1 has a composite structure

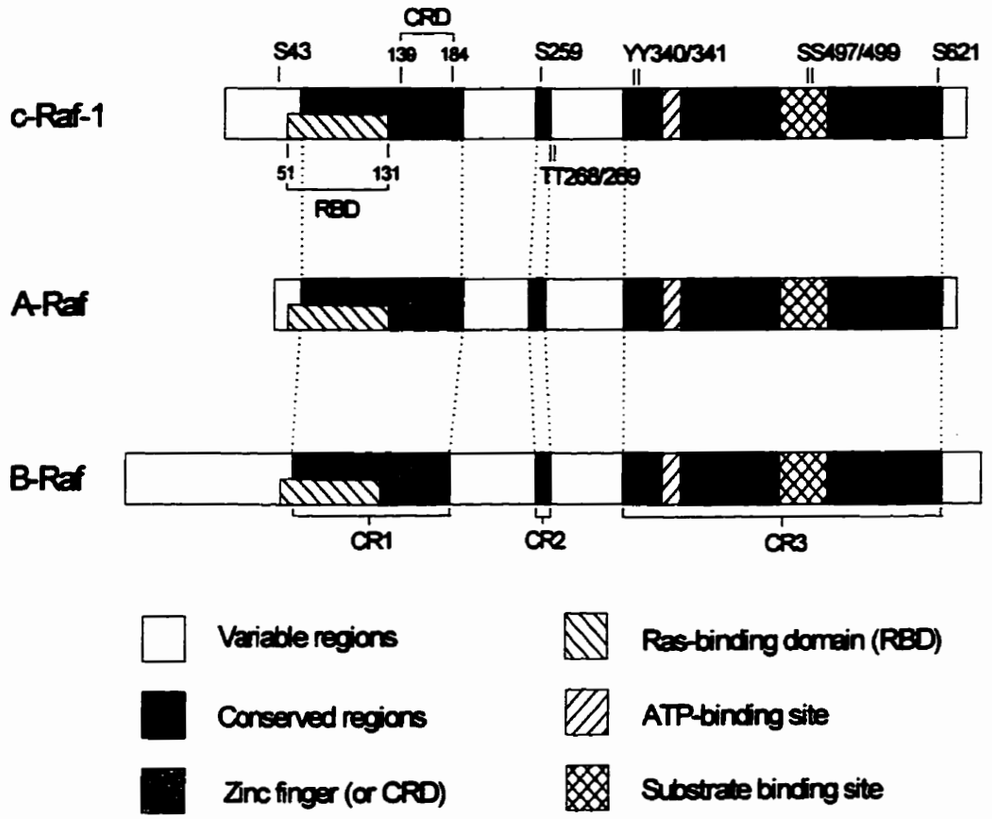

Figure 4. Structure of mammalian Raf protein kinases. Functional regions are indicated. Three conserved regions are CR1 (residues 62-196), CR2 (residues 255-268) and CR3 (residues 331-625). The conserved cysteine-rich domain (CRD) encompasses a zinc finger motif. Numbers refer to c-Raf-1. The serine (S), threonine (T) and tyrosine (Y) phosphorylation sites given for c-Raf-1 are not necessarily present on the other Raf isozymes. Effects of phosphorylation of these residues on activation of c-Raf-1 kinase are described in **Section 1.2.6**. (Modified from Daum *et al.*, 1994)

consisting of a Ras-binding domain (RBD) and a zinc-finger motif ($^{152}Cx_2Cx_9Cx_2Cx_7Cx_7C^{184}$) within a cystine-rich domain. CR2 is rich in serine and threonine residues, some of which are regulatory phosphorylation sites. CR3 harbors the catalytic domain of the Raf kinase with both ATP- and substrate-binding sites.

The activation of the kinase Raf is proving to be an intricate multistep process. Protein-protein/protein-lipid interactions and phosphorylation are essential for regulation of the Raf kinase activity.

Raf-Ras interaction

The role of the Raf kinase as a critical transformation effector of Ras has been firmly established (Avruch *et al.*, 1994; Bruder *et al.*, 1992; Hallberg *et al.*, 1994). Examination of Ras-Raf binding in the yeast two-hybrid system (Avruch *et al.*, 1994) and suppression of Ras-induced malignant phenotype by overexpression of Raf fragments (Fridman *et al.*, 1994) have revealed an 81 amino acid sequence (residues 51-131 of c-Raf-1) as a Ras-binding domain. The association of the RBD with the Ras effector domain is mediated primarily by residues Gln66, Lys84, and Arg89 of Raf-1 (Block *et al.*, 1996). However, mutational studies (e.g., C168S) showed that the zinc-finger structure, although not localized in the RBD, is also critical for Ras-Raf interaction (Bruder *et al.*, 1992). It has been shown that this cysteine-rich domain (CRD, residues 139-184 of c-Raf-1) serves as another Ras-binding site. The interaction between the RBD and Ras appears to allow for the CRD to contact Ras (Brtva *et al.*, 1995; Drugan *et al.*, 1996; Hu *et al.*, 1995). In addition to its contact with Ras, the CRD may mediate interactions of Raf with other molecules (Daum *et al.*, 1994; Mott *et al.*, 1996; and see below).

The N-terminal half of Raf functions as a dominant autoinhibitor (Daum *et al.*, 1994), suppressing the Raf catalytic domain in unstimulated cells. Substitutions, insertions or deletions in this region activate the transforming activity of Raf (Avruch *et al.*, 1994; Heidecker *et al.*, 1990). It has been shown that the N-terminal regulatory domain interacts with the active Ras after receptor stimulation. Although Ras:GTP is required for translocation and activation of the Raf kinase, attempts to activate purified Raf with Ras:GTP failed, indicating a need for additional factors (Daum *et al.*, 1994). Moreover, when a CAAX box (a signal for farnesylation) and a neighboring polybasic domain of six lysine residues were attached to the carboxyl terminus of Raf, the modified Raf (RafCAAX) was localized exclusively to the plasma membrane and stimulated the downstream kinase cascade without the requirement of Ras (Leevers *et al.*, 1994; Stokoe *et al.*, 1994). These data strongly imply that the only role for Ras:GTP in the MAPK cascade is to localize Raf to the plasma membrane and the activation of Raf may be fulfilled by other unknown Raf activator(s) (Hall, 1994).

Raf-14-3-3 interaction

The highly conserved 14-3-3 proteins, a family of 27- to 30-kDa acidic proteins, have been shown to participate in the Raf activation processes in yeast and mammalian cells (Fantl *et al.*, 1994; Freed *et al.*, 1994; Fu *et al.*, 1994; Irie *et al.*, 1994). The 14-3-3 proteins are specific phosphoserine-binding proteins (Muslin *et al.*, 1996), binding to Raf-1 on the phosphorylated Ser259 in the amino-terminal regulatory domain or Ser621 in the carboxy-terminal kinase domain (**Figure 4**). These two serine residues reside in the 14-3-3-binding motif of Raf-1: RxSxS*xP (single-letter code for amino acids; x represents any amino acid

and S* represents phosphorylated serine). However, this consensus binding motif may not account for all interactions between Raf-1 and 14-3-3. 14-3-3 isoforms (β and ζ) interact principally with the cysteine-rich domain of the Raf-1 protein (Freed *et al.*, 1994). Mutations introduced into the cysteine-rich domain prevent the stable interaction of Raf-1 with 14-3-3 (Michaud *et al.*, 1995).

Association with 14-3-3 proteins alone is not sufficient to activate the kinase activity of Raf (Freed *et al.*, 1994), reflecting the requirement for Ras-mediated Raf translocation from the cytosol to the plasma membrane. Synergistic activation of another MAPK kinase kinase (a Raf equivalent) by Ras and 14-3-3 has also been reported (Shimizu *et al.*, 1994). 14-3-3 may function in stabilization, rather than direct stimulation, of Raf association with the membrane and/or of the Raf kinase activity. This idea is consistent with the observations that the interaction of activated Raf-1 with 14-3-3 protects Raf-1 from being inactivated by phosphatase treatment (Dent *et al.*, 1995; Muslin *et al.*, 1996). In addition, 14-3-3 may play a critical role in the formation of higher-order protein complexes. Several proteins such as B cell antigen receptor (Braselmann and McCormick, 1995), cdc25 (Conklin *et al.*, 1995) and A20 (Vincenz and Dixit, 1996) have been reported to interact with Raf-1 in a 14-3-3-dependent manner.

Lipid activators may play a role in Raf activation

Michaud *et al.* (1995) reported that Raf-1 mutants that failed to stably interact with 14-3-3 could still be activated in a Ras-dependent manner, suggesting that this potential activator may not be a necessary factor for the activation of Raf-1. An unknown coactivator may be involved in Raf activation (Daum *et al.*, 1994; Hall, 1994). It was found that

membranes were the source of a factor that enabled the GTP-bound Ras, but not the GDP-bound Ras, to mediate Raf activation in *in vitro* reconstruction experiments, and the membrane-derived coactivator was detergent labile (Daum *et al.*, 1994). A convincing argument arising from these observations is that an intact lipid bilayer or a lipid activator is required for activation of Raf-1 kinase. Ceramide has been shown to specifically bind to and activate Raf-1, suggesting that ceramide may be an authentic lipid activator of Raf-1 (Huwiler *et al.*, 1996). It has also been demonstrated *in vitro* that the cysteine-rich N-terminal domain of Raf-1 interacts selectively with phosphatidylserine (Ghosh *et al.*, 1994), while a C-terminal region of Raf-1 (residues 295-648) interacted specifically and strongly with phosphatidic acid (Ghosh *et al.*, 1996). The interactions between Raf-1 and these acidic phospholipids are unlikely to be nonspecific because these agents interact with distinct regions of Raf-1. However, the role of lipid activators in regulation of Raf activation in the cell awaits further investigation.

Dimerization or oligomerization leads to Raf activation

Recent studies by Farrar *et al.* (1996) and Luo *et al.* (1996) advanced a provocative hypothesis that dimerization or oligomerization may provide a mechanism for Raf activation. They demonstrated that Raf-1 constructs containing binding domains for bivalent drugs (coumermycin or FK1012) were *in situ* dimerized/oligomerized and activated to levels equivalent to those achieved with known Raf-1 activators (e.g., EGF or phorbol esters). Interestingly, 14-3-3 proteins are dimers and different members of the 14-3-3 family can heterodimerize, so in cells, two Raf-1 molecules could be close enough to be activated by binding to each 14-3-3 dimer or heterodimer. Activation of Raf constructs induced by

bivalent drugs may (Luo *et al.*, 1996) or may not (Farrar *et al.*, 1996) require the Ras-Raf interaction. The reason for this difference is unknown. Dimerization/oligomerization activates Raf-1 presumably by changing its conformation and reducing the suppressive effect of the amino-terminal regulatory domain or through increased transphosphorylation of serine/threonine residues located in CR2 domain (see below). Whether the artificial dimerization/oligomerization of Raf-1 represents a real mechanism for Raf activation in cells remains uncertain.

Hsp90 stabilizes Raf protein and its association with Ras

Although activated Raf-1 is plasma membrane-associated, this 74-kDa protein is primarily cytosolic in location and exists in a high molecular weight complex with the heat shock protein Hsp90 (Stancato *et al.*, 1993) and Hsp50 (Morrison and Cutler Jr, 1997). Raf-1 binds to Hsp90 via its COOH-terminal catalytic domain (Stancato *et al.*, 1993) and remains complexed to Hsp90 even when bound to Ras at the plasma membrane (Wartmann and Davis, 1994). Disruption of the complex results in destabilization of Raf-1 and loss of Raf-Ras association, suggesting Hsp90 plays a critical role in stabilization of Raf-1 protein and its proper localization in the cell (Schulte *et al.*, 1995; 1996).

Raf phosphorylation has dual effects on its activation

Raf-1 activation is accompanied by its increased phosphorylation, often leading to a characteristic shift in apparent molecular weight, suggesting a causal relationship between phosphorylation and Raf-1 activation (Heidecker *et al.*, 1992). This is further supported by the observation that purified and membrane-associated protein phosphatases can inactivate Raf kinase activity (Dent *et al.*, 1995). Mechanisms of regulation of Raf-1 function by

phosphorylation include directly altering the intrinsic activity of Raf-1 and mediating critical protein interactions, such as with 14-3-3 (see above). The phosphorylation sites that lead to Raf-1 activation may be Ser497, Ser499, Ser621, Thr268, Thr269, Tyr 340 and Tyr341 (Daum *et al.*, 1994; Morrison *et al.*, 1993). The kinases implicated in phosphorylating Raf-1, and thereby enhancing its activity, include protein kinase C (Carroll and May, 1994; Kolch *et al.*, 1993; Ueda *et al.*, 1996), a ceramide-activated protein kinase (Yao *et al.*, 1995), the Src family of kinases (Fabian *et al.*, 1993; Marais *et al.*, 1995; Park *et al.*, 1996) and Janus kinase (JAK)-2 (Xia *et al.*, 1996). On the other hand, phosphorylation of Raf-1 on Ser43 by cAMP-dependent protein kinase (PKA) inhibits Ras-mediated Raf activation (Hafner *et al.*, 1994; Marx, 1993), but has no effect on previously activated Raf-1 activity (Morrison *et al.*, 1993). Thus, phosphorylation of Raf protein may result in stimulation or inhibition of its kinase activity depending on which site(s) is being phosphorylated.

Rap1 competes with Ras for Raf and suppresses Raf activation

As discussed in **Section 1.2.5**, Rap1 and Ras share complete identity in their effector domains. Since the RBD of Raf interacts with Ras at this effector domain for Raf activation, it raises the enticing possibility that Rap1 might function as a Ras antagonist to suppress Raf activation rather than as a Ras ally to sequester GAP1 and therefore maintain Ras activation. Several forms of evidence are in favor of this idea. [1] Rap1 was cloned as a protein capable of reverting transformation induced by the K-Ras oncogene (Kitayama *et al.*, 1989); [2] Conditional or constitutive expression of RapV12, a Rap1 mutant that is insensitive to the Rap-specific GAP, at physiological levels inhibited downstream signaling from Ras to ERKs *in vivo*, but did not interfere with mitogen-stimulated increase in Ras-GTP (Cook *et al.*,

1993); [3] The cAMP-mediated inhibition of Ras-dependent MAPK activation, which is well documented, resembles that caused by expression of RapV12, and elevation of $[cAMP]_i$ results in Rap1 phosphorylation and activation (Altschuler *et al.*, 1995); [4] The role for Rap1 in antagonizing Ras function is strongly supported in other model systems such as *Drosophila* (Hariharan *et al.*, 1991) and *Xenopus oocytes* (Campa *et al.*, 1991); and [5] The X-ray crystal structure of the RBD of Raf-1 with Rap1A and a GTP-analog has been solved and published (Nassar *et al.*, 1995).

A burning question is: why is the membrane-associated Rap1 (which also contains a C-terminal CAAX motif) unable to activate Raf-1 supposing recruitment of Raf-1 to the plasma membrane is sufficient for Raf-1 activation? Studies by Beranger *et al.* (1991) indicate that Rap1 is associated with a Golgi-like structure, while Ras is clearly detected in the plasma membrane. Thus, the Rap1-associated subcellular compartment may lack the putative indispensable activator(s) required for Raf activation.

Novel Raf activators

Two important findings have prompted a search for novel Raf-1 activators. First, an activator termed TAB1 (for TAK1 binding protein) was recently reported to activate TAK1 (for TGF-β-activated kinase 1) in TGF-β signal transduction (Shibuya *et al.*, 1996). TAK1 has been identified as being equivalent to Raf-1 for the phosphorylation and activation of the SEK1 subfamily of MAPKK, but not MEK1 (Yamaguchi *et al.*, 1995; see **Section 1.2.8** and **Figure 5**). In view of the existence of equivalent components in the multiple MAPK cascades (Cano and Mahadevan, 1995), one would expect that such an activator for Raf-1 activation must exist in the MEK/ERK signaling pathway (**Figure 5**). Second, three

research groups (Kornfeld *et al.*, 1995; Sundaram and Han, 1995; Therrien *et al.*, 1995) provided evidence that a novel protein KSR (for kinase suppressor of Ras) can function as an activator of the Raf-1 kinase activity in *C. elegans* and *Drosophila* (Downward, 1995a). As expected, the mammalian homologue of KSR has recently been cloned (Therrien *et al.*, 1996). KSR associates with Raf-1 at the plasma membrane in a Ras-dependent manner and facilitates signal propagation within the Raf-1/MEK/ERK cascade. Very recent studies demonstrated that KSR functions as a ceramide-activated protein kinase (CAPK), phosphorylating and activating Raf-1 in response to stimulation with TNF-α and ceramide analogs (Zhang *et al.* 1997). Determining whether KSR is functionally equivalent to TAB1 requires further investigation.

Substrates of c-Raf-1

The only known physiological substrates of c-Raf-1 are MEK1 and MEK2 (Dent *et al.*, 1992; Howe *et al.*, 1992; Kyriakis *et al.*, 1992; Daum *et al.*, 1994). The Raf-specific phosphorylation sites have been determined for MEK1 (Ser218 and Ser222), and either is sufficient for activation (Alessi, 1994). Raf acts as a bridge, interacting with MEK and Ras via its COOH- and NH_2-termini respectively (Crews and Erikson, 1993). More recently, it was reported that Cdc25, which dephosphorylates and activates $p34^{cdc2}$ (Lee *et al.*, 1992), could be an *in vivo* substrate of Raf-1 (Galaktionov *et al.*, 1995), suggesting the existence of a link between mitogenic signal transduction and the cell cycle machinery.

Other members of MAPKKK family

In addition to c-Raf-1, A-Raf and B-Raf, several other MEK kinases (MEKKs) have been identified in mammalian cells. MEKK1 is a 195-kDa protein homologous to the

MEKK of the yeast pheromone-response pathway (Xu *et al.*, 1996). The cDNAs encoding MEKK2 and MEKK3 were recently cloned (Blank *et al.*, 1996). TAK1 is distinct from other members of the MAPKKK family. Its kinase activity is stimulated in response to TGF-β and bone morphogenetic protein (Yamaguchi *et al.*, 1995). ASK1 has recently been identified as a novel MAPKKK (Ichijo *et al.*, 1997). When overexpressed, ASK1 can induce apoptotic cell death, and therefore is referred to as apoptosis signal-regulating kinase 1 (Ichijo *et al.*, 1997). The substrate specificity of these MAPKKKs will be described in **Section 1.2.8**.

1.2.7 MEKs are dual-specificity kinases that phosphorylate and activate MAPKs

MAPK/ERK kinases (MEKs) are members of the MAPK kinase (MAPKK) family with dual specificity for phosphorylation of both tyrosine and serine/threonine (Hanks and Hunter, 1995). Six MEK family members (MEK1-6) have been reported (Robinson and Cobb, 1997). Both MEK1 and MEK2 activate ERKs by catalyzing phosphorylation of the regulatory sites of ERKs, the TEY sequence (see **Section 1.2.8**), though the efficiency of the kinase action of two MEKs toward substrates may be different (Zheng *et al.*, 1993). So far, no alternative substrates to ERKs have yet been identified for MEKs (Nishida and Gotoh, 1993). In contrast, the 45-kDa MEK proteins can be phosphorylated by several different protein kinases including Raf, a 39-kDa germ-cell-specific serine/threonine kinase Mos (Posada *et al.*, 1993), MEKK (Lange-Carter *et al.*, 1993; Yan and Templeton, 1994), $p34^{cdc2}$ (Rossomando *et al.*, 1994), and ERKs (Matsuda *et al.*, 1993). Unlike most kinase-substrate interactions, which are transient, Raf stably associates with MEK *in vitro* and *in vivo* (Crews

and Erikson, 1993). MEK1 and MEK2 contain proline-rich inserts in their C-terminal domains that are absent from other MEK family members. Deletion of the insert from the MEK1 impairs its activation by Raf-1, suggesting this proline-rich sequence in MEK may couple it to Raf-1 (Catling *et al.*, 1995).

MEK3 (Dérijard *et al.*, 1995) and MEK6 (Han *et al.*, 1996) activate a MAPK termed p38; MEK4 acts on JNK/SAPK and p38 subgroups of MAPKs (Dérijard *et al.*, 1995; Lin *et al.*, 1995); and MEK5 has no proven substrates, but binds ERK5 in a yeast two-hybrid assay (Waskiewicz and Cooper, 1995; Zhou *et al.*, 1995). Each MEK appears to act in a single, or at most two, MAPK cascade (Brunet and Pouyssegur, 1996; Robinson *et al.*, 1996; see **Section 1.2.8** for details).

1.2.8 Mammalian MAPK subtypes

MAPKs are proline-directed protein kinases that phosphorylate substrates on serine or threonine adjacent to proline residues. The consensus recognition sequence for phosphorylation by MAPKs has been defined as PXS(or T)P where X is ideally a basic or neutral amino acid for ERK1 and ERK2 (Pelech and Sanghera, 1992). The MAPK cascade has been highly conserved through evolution (Marshall, 1994; Sprague Jr, 1992). The mammalian MAPKs are mainly grouped into three subfamilies based on their mode of activation and substrate phosphorylation (Cano and Mahadevan, 1995). Unlike multiple MAPK cascades in yeast, where different cascades are activated by distinct stimuli and regulate separate phenomena such as mating type, cell-wall biosynthesis and osmosensitivity (Ammerer, 1994), the mammalian MAPK subtypes have been shown in many instances to

be activated simultaneously, though to different extents, via distinct parallel cascades in response to the same stimuli (Cano and Mahadevan, 1995) (**Figure 5**).

The ERK subfamily of MAPKs

The extracellular signal-regulated kinases, the 44-kDa ERK1 (or $p44^{mapk}$) and the 42-kDa ERK2 (or $p42^{mapk}$), are the archetypal and best-studied members of the mammalian MAPK family. The upstream MEK1 or MEK2 specifically activates ERKs by phosphorylation on Thr183 and Tyr185 of ERK2 or Thr188 and Tyr190 of ERK1 within the motif TEY in domain VIII (Cano and Mahadevan, 1995; Posada and Cooper, 1992). This dual phosphorylation on TEY is the defining property of the ERK subfamily of MAPKs. ERKs have many potential cytosolic and nuclear substrates (see **Section 1.2.1**).

Activated ERKs phosphorylate and activate RSK in the cytosol (Ahn *et al.*, 1991; Blenis, 1993; Chung *et al.*, 1991; Grove *et al.*, 1993; Lavoinne *et al.*, 1991). These activated ERKs and RSK migrate from the cytosol to the nucleus and phosphorylate the C-terminal region of Elk-1, a ternary complex factor (TCF) (Hipskind *et al.*, 1994; Janknecht *et al.*, 1993; Marais *et al.*, 1993; Rao and Reddy, 1994; Zinck *et al.*, 1993) and serum response factor (SRF) at Ser103 (Rivera *et al.*, 1993), respectively. Elk-1 and SRF together bind to the serum response element (SRE) present in the promoters of many genes including c-*fos*, leading to gene expression (see **Figure 5**). Also, RSK phosphorylates and activates the transcription factor cAMP response element-binding protein (CREB) on Ser133 (Xing *et al.*, 1996), mediating expression of many genes including c-*fos* (Bonni *et al.*, 1995; Ginty *et al.*, 1994; Robertson *et al.*, 1995). Thus, ERKs and RSK relay signals arising at the plasma membrane to the c-*fos* gene in the nucleus. It is worth noting that repression of c-*fos* gene

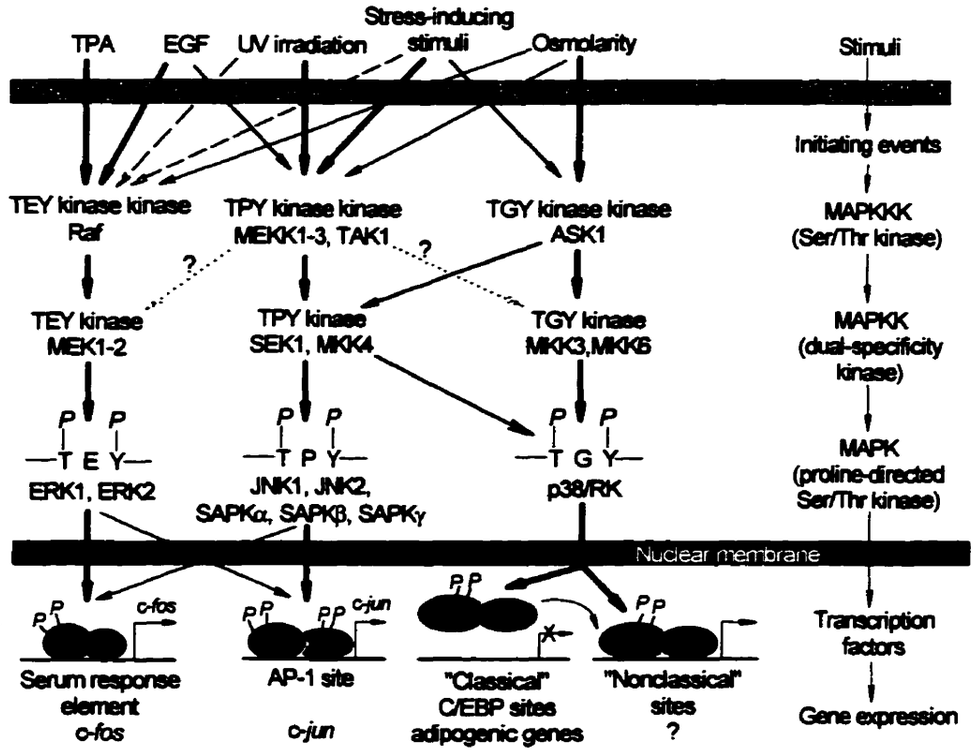

Figure 5. Parallel cascades of three MAPK subfamilies in mammalian cells. Three MAPK subclasses (ERKs, JNKs/SAPKs and p38/RK) are defined according to the dual-phosphorylation motifs TEY, TPY and TGY, respectively. Dual-specificity kinases for each of the MAPK subclasses and MAPKKKs that are specific for MEK1/MEK2, SEK/MKK4, or MKK3/MKK6 have been discovered. Thick arrows indicate strong responses to upstream signals; thinner arrows indicate weaker responses; and broken arrows indicate extremely poor stimulation. Stress-inducing stimuli include translational inhibitors, okadaic acid, heat shock, tumor necrosis factor-α and -β, pro-inflammatory cytokines, lipopolysaccharide. ASK1, apoptosis signal-regulating kinase 1; C/EBP, CCAAT/enhancer-binding protein; CHOP, C/EBP-homologous protein; RK, reactivating kinase; SRF, serum-response factor; TAK1, TGF-β-activated kinase 1; TCF, ternary complex factors. (Modified from Cano and Mahadevan, 1995)

expression following its activation is also mediated through phosphorylation of the newly synthesized c-Fos protein by ERKs and RSK. The sites for this phosphorylation have been identified as Ser374 (for ERKs) and Ser362 (for RSK) at the C-terminal transrepression domain (Chen *et al.*, 1993). All these indicate a role of ERKs in modulating the expression of c-*fcs* gene at multiple levels.

Cytoplasmic PLA_2 ($cPLA_2$) is another well-characterized ERK substrate. Phosphorylation of $cPLA_2$ by ERKs at Ser505 causes the activation of this enzyme, resulting in increased arachidonic acid release and formation of lysophospholipids (Lin *et al.*, 1993). ERKs can therefore trigger the generation of multiple secondary signaling molecules.

ERK1 and ERK2 are essential elements of mitogenic signaling. Prolonged activation and nuclear retention of ERKs is required for transcription of *cyclin D1*, indicating a connection between ERK activation and promotion of entry into the cell cycle (Lavoie *et al.*, 1996). Functions of ERKs outside the nucleus also contribute to proliferative responses. A substantial proportion of the ERKs in activated cells associate with the cytoskeleton, suggesting the involvement of ERKs in cytoskeletal reorganization (Reszka *et al.*, 1995).

The JNK/SAPK subfamily of MAPKs

This subfamily comprises c-Jun NH_2-terminal kinases (JNKs) and stress-activated protein kinases (SAPKs). They contain the sequence TPY in domain VIII (Cano and Mahadevan, 1995) and phosphorylation of threonine and tyrosine within this TPY motif are required for their activation (Dérijard *et al.*, 1994; Kyriakis *et al.*, 1994). A MAPK kinase called SEK1, which stands for SAPK/ERK kinase 1, is the kinase responsible for dual phosphorylation at the TPY site, while MEK1 and MEK2, which phosphorylate ERK1 or

ERK2 on TEY, do not recognize TPY on the JNK/SAPKs (Minden *et al.*, 1994; Sánchez *et al.*, 1994; Yan *et al.*, 1994). Another MAPK kinase, termed MKK4 or MEK4 or JNKK, is a human homologue of murine SEK1 (Sánchez et al., 1994). MKK4 appears to activate both JNK and another MAPK p38, but it is inactive toward ERK1 and ERK2 (Dérijard *et al.*, 1995; Lin *et al.*, 1995). Recent evidence suggests that SEK1 and MKK4, but not MEK1 or MEK2, may be the physiological targets for MEKKs (Dérijard *et al.*, 1995; Minden *et al.*, 1994; Yan *et al.*, 1994). MEKKs can phosphorylate MEK1 and MEK2 *in vitro* and was thought to be a MEK1/MEK2 kinase (Lange-Carter *et al.*, 1993; Yan and Templeton, 1994). Another MAPKKK for SEK1 (Yamaguchi *et al.*, 1995) and MKK4 (Robinson and Cobb, 1997) is TAK1, which is inert toward MEK1 and MEK2 (Yamaguchi *et al.*, 1995).

Five members of the JNK/SAPK subfamily have been described so far. The two kinases of 46 and 55 kDa were designated JNK1 and JNK2; they phosphorylate c-Jun protein on Ser63 and Ser73, respectively, upon the exposure of cells to ultraviolet (UV) radiation (Dérijard *et al.*, 1994; Hibi *et al.*, 1993). The phosphorylated c-Jun proteins form homodimers or heterodimers with newly synthesized c-Fos proteins that are phosphorylated by ERKs, and bind to AP-1 sites that are located within the promoters of many genes, leading to an increase in transcriptional activity (see **Figure 5**). Activating transcription factor-2 (ATF2), also designated cyclic AMP response element-binding protein 1 (CRE-BP1), can be phosphorylated by JNK on Thr69 and Thr71 within the NH_2-terminal activation domain either (Gupta *et al.*, 1995). This phosphorylation may increase transcriptional activity mediated by phosphorylation-dependent binding of ATF2 to CRE-like elements in the promoters of many genes as a heterodimer with partners such as the CREB binding protein

CBP (Chrivia *et al.*, 1993; Kwok *et al.*, 1994), or c-Jun (Banbrook *et al.*, 1990; Hai and Curran, 1991; Ivashkiv *et al.*, 1990; Macgregor *et al.*, 1990). The ATF2-c-Jun heterodimer is probably a physiologically relevant target of JNK. Interestingly, JNK can also phosphorylate Elk-1, leading to ternary complex formation and transcriptional activation, in cells treated with interleukin-1, suggesting that the SRE is a site of integration of signal transduction via the ERK and JNK pathways (Whitmarsh *et al.*, 1995).

Three rat isoforms were named stress-activated protein kinases (SAPKα, β, γ) because they were potently activated by stress-inducing stimuli such as translational inhibitors, heat shock and tumor necrosis factor (TNF), etc. (Kyriakis *et al.*, 1994). SAPKα and SAPKβ, similar in size to JNK2, have relative molecular masses of approximately 55 kDa, whereas SAPKγ is about 45 kDa, close to the size of JNK1 (Dérijard *et al.*, 1994; Kyriakis *et al.*, 1994).

The p38/RK subfamily of MAPKs

A third subfamily of mammalian MAPKs includes p38 (Han *et al.*, 1994) and reactivating kinase (RK) (Rouse *et al.*, 1994). This subfamily is distinguished from the other two by the TGY sequence of the dual phosphorylation motif. A human MAPK kinase, termed MKK3 or MEK3, has been cloned (Dérijard *et al.*, 1995). MKK3 activates p38 by dual phosphorylation on its TGY and thus functions as the p38 kinase (Dérijard *et al.*, 1995). Nevertheless, MKK3 failed to activate ERK1 and ERK2 (Dérijard *et al.*, 1995). MKK6 (or MEK6), a close relative of MKK3 identified by homology cloning, database searching and protein purification, also activates p38 (Han *et al.*, 1996). Recently, a MAPKKK termed ASK1 (apoptosis signal-regulating kinase 1) has been identified as a MKK3/MKK6 kinase

and a SEK1/MKK4 kinase (Ichijo *et al.*, 1997). ASK1 is activated in cells treated with TNF-α. The activated kinase stimulates the downstream kinases MKK3/MKK6 and SEK/MKK4, which in turn activate p38 and JNK/SAPKs, respectively (Ichijo *et al.*, 1997).

The p38 and JNK are activated in response to osmotic stress in mammalian cells (Han *et al.*, 1994; Galcheva-Gargova *et al.*, 1994), and both can complement mutant strains of the yeast *Saccaromyces cerevisiae* that lack the osmotic stress-activated HOG1 MAPK (Han *et al.*, 1994; Galcheva-Gargova *et al.*, 1994). Thus, it is not surprising that ASK1 (Ichijo *et al.*, 1997), MKK4 (Dérijard *et al.*, 1995), and perhaps TAK1 (Robinson and Cobb, 1997) are shared upstream activators for these two subtypes of MAPK. This finding, together with the observation that lipopolysaccharide, pro-inflammatory cytokines and environmental stress cause p38 activation, suggests that the p38 pathway may be even more closely related to the JNK/SAPK signaling pathway than to the ERK cascade.

Two potential substrates for p38 have recently been reported. $cPLA_2$ was shown to be phosphorylated by p38 in human platelets upon stimulation with thrombin (Kramer *et al.*, 1995). Transcription factor CHOP (*C*/EBP-*ho*mologous *p*rotein), also known as *g*rowth *a*rrest and *D*NA *d*amage-inducible gene 153 (GADD153), is a C/EBP (*C*CAAT/*e*nhancer-*b*inding *p*rotein)-like nuclear protein that lacks a functional DNA-binding domain (Ron and Habener, 1992). CHOP dimerizes avidly with other C/EBP proteins and the resulting heterodimers are directed away from classical C/EBP sites, leading to potent inhibition of adipocytic differentiation of 3T3-L1 cells (Batchvarova *et al.*, 1995). CHOP can also influence gene expression by directing CHOP-C/EBP heterodimers to unique "nonclassical" sites to activate gene expression (Barone *et al.*, 1994; Ubeda *et al.*, 1996). Stress-induced

phosphorylation of CHOP on Ser78 and Ser81 by p38 enhanced transcriptional activation by CHOP and was also required for the full inhibitory effect of CHOP on adipose cell differentiation (**Figure 5**). Thus, CHOP has two opposing effects on regulation of gene expression. Phosphorylation of CHOP inhibits expression of genes with the classical C/EBP site and stimulates expression of other genes. This finding links the p38 pathway to regulation of cellular growth and differentiation (Wang and Ron, 1996).

Recently, a new MAPK-activated protein kinase (MAPKAP-K), named 3pK, has been shown *in vitro* and *in vivo* to be activated through all three MAPK cascades (Ludwig *et al.*, 1996). 3pK, whose name is derived from its genetic locus on the short arm of chromosome 3 (chromosome 3p kinase) (Sithanandam *et al.*, 1996; Szeles *et al.*, 1996), contains a putative nuclear localization signal at the carboxyl terminus. 3pK is therefore a novel convergence point of different MAPK pathways, integrating signals elicited by both mitogen and stress stimulus, and presumably transmitting them into the nucleus.

Other MAPKs

Many other MAPKs have been discovered recently. A constitutively nuclear protein kinase ERK3, which lacks the dual phosphorylation motif, lies in an uncharacterized pathway (Cheng *et al.*, 1996a; 1996b). ERK5 (Zhou *et al.*, 1995) is another member of the MAPK family, presumably being activated by MEK5 (Robinson and Cobb, 1997). Four p38 homologues constitute the p38-like kinase subgroup, which includes Mxi2 (Zervos *et al.*, 1995), ERK6 (Lechner *et al.*, 1996), SAPK3 (Mertens *et al.*, 1996) and p38β (Jiang *et al.*, 1996). Mxi2 is truncated from kinase subdomain XI, and the other three are 63%, 60% and 74% identical to p38, respectively. These p38-like kinases may not be regulated like p38

itself, suggesting that they define novel MAPK modules (Robinson and Cobb, 1997).

1.2.9 Negative regulation by protein phosphatases

This appears to be currently one of the most enigmatic aspects of regulation of signaling via the MAPK pathway. Nevertheless, it is generally believed that signal transduction through the MAPK cascade can be inhibited by the action of a number of phosphatases on specific signaling elements (Hunter, 1995; Nebreda, 1994; Walter and Mumby, 1993). Raf-1 can be dephosphorylated and inhibited by type-1 serine/threonine protein phosphatase (PP1). PP2A is able to inactivate MEK, as well as ERKs in the cytosol. However, this inactivation can be suppressed by the interaction of SV40 small tumor antigen with PP2A (Sontag *et al.*, 1993). Both PP1 and PP2A are capable of attenuating RSK activity. Two dual-specificity phosphatases (MKP-1 and PAC-1) specifically act on ERKs in the nucleus (Hunter, 1995; Nebreda, 1994; Sun *et al.*, 1993, 1994; Ward *et al.*, 1994). Interestingly, the synthesis of these phosphatases is also induced by mitogens via the MAPK pathway (Nebreda, 1994). This feedback loop creates an elegant yin-yang regulation between kinases and phosphatases. This delicate input-and-output balance was challenged by a recent study that showed MKP-1 gene expression was induced via the SAPK pathway rather than the ERK cascade in NIH 3T3 fibroblasts (Bokemeyer *et al.*, 1996). It is not yet known whether the demonstrated crosstalk between the ERK and SAPK signaling pathways via the MKP-1 exists ubiquitously or what is the significance of the crosstalk. Moreover, the temporal relationship may argue against the role of the feedback loop in the negative regulation of the MAPK pathway since the activation of MAPK by many mitogens is

transient and is terminated before the mitogen-induced synthesis of these phosphatases.

1.2.10 Regulation by crosstalking with other signaling systems

Since the cell, in its natural environment, is awash in a sea of signals and the operation of the cell requires coordination of multiple signal pathways, a degree of crosstalk between different pathways is believed to exist. Raf is an integrator of various inputs. The Raf kinase activity may be stimulated via its phosphorylation by cPKCs (α, β and γ) (Burgering and Bos, 1995) and PKC-ϵ (Daum *et al.*, 1994), or by a myristoylation-anchored oncogenic tyrosine kinase $pp60^{src}$ (Marais *et al.*, 1995), or by ceramide-activated protein kinase (CAPK) (Yao *et al.*, 1995).

The inhibition of the transmission of growth messages through the Ras pathway by cyclic AMP has been established in many cell types including certain strains of fibroblasts (Rat-1, NIH 3T3, A14), adipocytes and smooth muscle cells (Burgering *et al.*, 1993; Cook and McCormick, 1993; Hordijk *et al.*, 1994; Marx, 1993; Wu *et al.*, 1993), but is not universal. The location of the blockage appears to be Raf-1 kinase. The mechanism underlying the inhibitory effect may involve phosphorylation of Raf-1 and phosphorylation of small GTP-binding proteins such as Rap1 by protein kinase A (PKA). These phosphorylations could result in altering the Raf-1 conformation or promoting the association of Raf-1 with Rap1, therefore interfering with Ras-Raf-1 interaction and Raf-1 activation (Bokoch, 1993; Wu *et al.*, 1993; Kikuchi and Williams, 1996; Vossler *et al.*, 1997). In contrast, it has been reported that cAMP is able to activate MAPK cascade in some cell lines such as PC12 (Frödin *et al.*, 1994; Pan *et al.*, 1995; Young *et al.*, 1994) and COS-7 (Faure

et al., 1994). The rational for the differential effects of cAMP on the MAPK cascade in different cell types is still a mystery.

Crosstalk between MAPK signaling and the cell cycle machinery occurs at multiple levels. Activation of p38 inhibited transcription of *cyclin D1*, while activation of ERK1 and ERK2 stimulated transcription of this gene (Lavoie *et al.*, 1996), indicating stress stimuli and mitogens have opposite effects on cell cycle progression. MEK1 contains a consensus sequence for phosphorylation by $p34^{cdc2}$. MEK1 can be phosphorylated (at Thr286 and Thr292) and inactivated *in vitro* by $p34^{cdc2}$. Phosphorylation of MEK1 on the same residues occurs *in vivo*, implying that $p34^{cdc2}$ could negatively regulate the signaling process via the ERK pathway (Rossomando *et al.*, 1994). As mentioned in **Section 1.2.6**, Raf-1 could phosphorylate and activate Cdc25, a specialized dual-specificity phosphatase capable of dephosphorylating and activating $p34^{cdc2}$ kinase. Hence, one could simplistically postulate a feedforward control from Raf-1 to Cdc25 to $p34^{cdc2}$ to MEK. The existence of such a control mechanism has yet to be fully explored.

1.3 Protein Kinase C and Cell Growth

Protein kinase C (PKC) is a widespread family of kinases responsible for many diverse and critical cellular functions including growth control. To date, at least eleven distinct PKC isozymes have been identified and classified into three groups based on their sequence homologies and cofactor requirements (**Figure 6**) (Dekker and Parker, 1994; Newton, 1995; Nishizuka, 1995). The conventional or classical isoforms (cPKCs: α, βI/βII, γ) meet the original definition of PKC as Ca^{2+}- and phospholipid-dependent protein kinase.

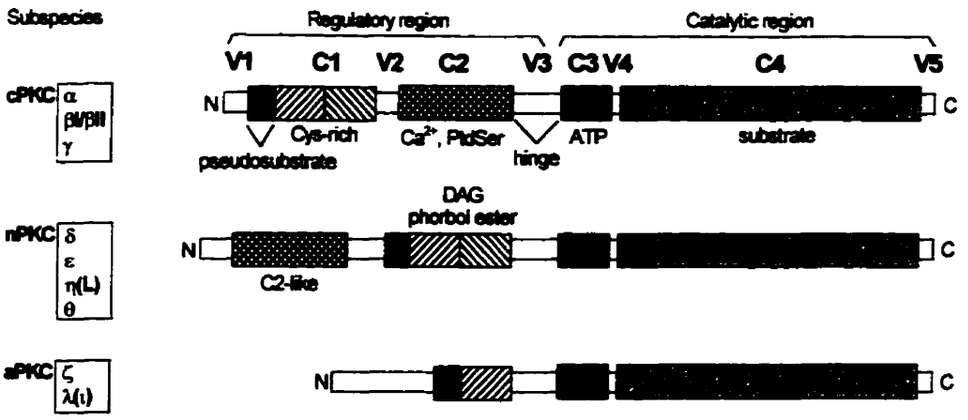

Figure 6. Domain structure of PKC subspecies. Four conserved (C1 to C4) and five variable (V1 to V5) regions of conventional PKCs (cPKC) are indicated. The C1 domain comprises one or two cysteine (Cys)-rich motifs that form the diacylglycerol (DAG)/phorbol ester binding site; this domain is immediately preceded by an autoinhibitory pseudosubstrate domain. The C2 domain contains the Ca^{2+}-binding site and the recognition site for phosphatidylserine (PtdSer). The C3 and C4 domains form the ATP- and substrate-binding lobes of the kinase core, respectively. The N-terminal regulatory and C-terminal catalytic halves are separated by the hinge region (V3). Proteolytic cleavage at V3, when the enzyme is membrane-bound, generates a constitutively active kinase domain (protein kinase M). The C2 domain of novel PKCs (nPKC) lacks the amino acids necessary for Ca^{2+} binding but has key conserved residues involved in maintaining the C2 fold (hence the name "C2-like"). Atypical PKCs (aPKC) have only one Cys-rich motif, and phorbol ester binding has not been detected. The βI and βII subspecies are derived from a single gene by alternative splicing.

The novel isoforms (nPKCs: δ, ϵ, η(L), θ) are not dependent on Ca^{2+}. Both cPKCs and nPKCs can be activated by either diacylglycerol (DAG) or phorbol esters. The third group, or atypical isoforms, (aPKCs: ζ, λ, ι) are not affected by Ca^{2+}, DAG, or phorbol esters. The human PKC-μ isozyme (also known as protein kinase μ) and its murine homologue, protein kinase D, form a distinct class. These isozymes have no pseudosubstrate motif and their kinase domains are actually more similar to that of calmodulin-dependent kinases (Newton, 1997). The expression of PKC isoforms varies between tissues and cell types (Asaoka *et al.*, 1992; Hug and Sarre, 1993; Nishizuka, 1995), suggesting that individual isoforms may differ in their cellular functions, or in tissue- and cell-type-specificity.

Considerable evidence suggests that PKC occupies a pivotal role in growth control. The direct activation of cPKCs and nPKCs by tumor-promoting phorbol esters in almost all cell types examined so far strongly supports this notion. PKCs may mediate cell proliferation in several ways. Alessandrini *et al.* (1992) showed that stimulation of PKC with phorbol ester resulted in phosphorylation and activation of MEK and MAPK, probably through activation of Raf-1. It was further shown that PKC activates Raf-1 by direct phosphorylation *in vitro* (Sözeri *et al.*, 1992) and *in vivo* (Kolch *et al.*, 1993; Carrol *et al.*, 1994). In T- and B-lymphocytes, PKC may link with MAPKs at the point of Ras activation (Downward *et al.*, 1990; Harwood *et al.*, 1993). Several studies demonstrated that the activation of MAPKs by G protein-coupled receptors is through the PKC signaling pathway (Blenis, 1993; Lange-Carter *et al.*, 1993; Malarkey *et al.*, 1995; Seuwen *et al.*, 1992). A research group led by Lefkowitz presented recent data that the G_o protein α-subunit activated MAPK via a nPKC-dependent mechanism (van Biesen *et al.*, 1996). The inactive transcription factor, NF-κB

(nuclear factor-κB), a heterodimer consisting of p50/p65, is retained in the cytoplasm through interaction with the inhibitor protein Iκ-B. Phosphorylation of Iκ-B by PKC and other kinases (Baeurle and Baltimore, 1988; Liou and Baltimore, 1993; Lozano *et al.*, 1994) triggers Iκ-B degradation through the ubiquitin-proteasome pathway (Thanos and Maniatis, 1995). This results in release of NF-κB and its translocation to the nucleus where it is transcriptionally active. Takuwa *et al.* (1992) reported that activation of PKC (α, δ, ϵ) causes $p34^{cdc2}$ histone H1 kinase activation and mitogenesis in swiss 3T3 fibroblasts. There is compelling evidence for the involvement of PKC in lamin B phosphorylation (Buchner, 1995), which is required for induction of nuclear envelope breakdown. Recent data (Goss *et al.*, 1994) confirmed that lamin B is a true physiological substrate of PKC by identifying the phosphorylation sites, although lamin B may also be phosphorylated by $p34^{cdc2}$ (Nigg, 1992). A number of other nuclear proteins phosphorylated by PKC are summarized by Buchner (1995); they include proteins implicated in maintaining chromatin structure, in replication, transcription or repair of DNA.

Some PKC isoforms appear to be essential for cell growth in certain cell types. Murray *et al.* (1993) demonstrated that PKC-βII is required for human erythroleukemia (K562) cell proliferation. Several lines of evidence including the specific inhibition of PKC-ζ by pseudosubstrate peptides, the depletion of PKC-ζ with antisense probes, and overexpression of a wild-type PKC-ζ or a dominant kinase-defective mutant of this isotype demonstrated that activation of PKC-ζ is necessary and sufficient by itself for mitogenic activation in oocytes and NIH 3T3 fibroblasts (Berra *et al.*, 1993; Dominguez *et al.*, 1992).

On the other hand, PKC activation can lead to cell differentiation (Mischak *et al.*,

1993). Interestingly, PKC may also function as a cellular guardian to prevent overstimulation by mitogenic signals through feedback inhibition of the activity of growth factor receptors, as well as inhibition of phospholipid hydrolysis and Ca^{2+} mobilization.

1.4 Phospholipids: Structural Components of Cellular Membranes and Source of Secondary Messengers

Lipid molecules constitute about 50% of the mass of most animal cell membranes, with phosphatidylcholine (PtdCho) and phosphatidylethanolamine (PtdEtn) being the two major phospholipid components (Alberts *et al.*, 1994). Membrane phospholipid synthesis is coordinated with the cell cycle (Jackowski, 1994). Net phospholipid accumulation starts in cells in late G_1 and increases dramatically as cells enter S phase (Jackowski 1994), strongly implying that cells have to synthesize sufficient phospholipids to make cellular membranes for their growth and division.

1.4.1 Many cellular events occur at the plasma membrane

The plasma membrane is the microenvironment for many cellular events such as cell-cell and cell-matrix interactions, binding of free ligands to their receptors, anchorage of a host of cytosolic signaling proteins through protein-protein interactions (Cohen *et al.*, 1995; Panayotou and Waterfield, 1993; Pawson, 1995) or protein lipidation (Casey, 1995; McLaughlin and Aderem, 1995; Milligan *et al.*, 1995), endocytosis and exocytosis (Alberts *et al.*, 1994), subcellular location of ion channels, transporters, G proteins, ATPase, protein kinases and phosphatases, and adenylyl cyclases to name but a few. Evidently, its

multifunctional nature implies that changes in lipid metabolism and/or lipid composition of the plasma membrane would affect related cellular functions.

1.4.2 Phospholipids as a source of lipid or lipid-derived signaling molecules

Phospholipids also serve as a source of secondary messengers for cell signaling (Divecha and Irvine, 1995; Liscovitch and Cantley, 1994) (**Figure 7**). Messengers produced from phospholipids include DAG, inositol(1,4,5)-trisphosphate (InsP_3), 3-phosphorylated inositide lipids, lysophosphatidylcholine (lysoPtdOH), platelet-activating factor (PAF), fatty acids (such as arachidonic acid), ceramide and sphingosine. These molecules participate in a variety of cellular signaling processes.

Inositol lipids and inositol phosphates

Inositol lipids have been intensively studied as second messengers *per se* or precursors and storage forms for various messenger molecules since the 1980s (Michell, 1992a). The metabolism of inositol lipids and inositol phosphates is delineated in **Figure 8** based on *in vitro* and *in vivo* studies. Some metabolites such as InsP_3 and DAG are well-defined second messengers, while others are putative secondary messengers or messenger precursors.

Many stimuli (e.g., neurotransmitters, hormones and growth factors) that stimulate G protein-coupled receptors, receptor tyrosine kinases, or non-receptor tyrosine kinases (for example, members of the *src* family, *fyn* and *lck*) induce formation of both InsP_3 and DAG by hydrolysis of phosphatidylinositol(4,5)bisphosphate (PtdIns(4,5)P_2) by the action of phosphoinositidase C (PIC), also known as phosphoinositide-specific phospholipase C (PI-

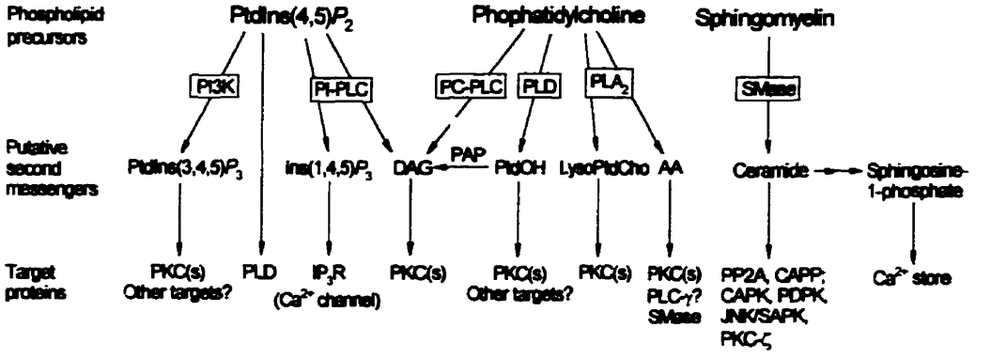

Figure 7. Lipid and lipid-derived signaling molecules and their signaling pathways. Three phospholipids: phosphatidylinositol (4,5)bisphosphate (PtdIns(4,5)P_2), phosphatidylcholine and sphingomyelin, function as major precursors of well-known and putative second messengers. These signaling molecules then induce diverse cellular responses by mediating functions of their target proteins. AA, arachidonic acid; CAPK, ceramide-activated protein kinase; CAPP, ceramide-activated protein phosphatase; DAG, diacylglycerol; Ins(1,4,5)P_3, inositol (1,4,5)trisphosphate; IP_3R, the receptor of Ins(1,4,5)P_3; JNK/SAPK, c-Jun NH_2-terminal kinase/stress-activated protein kinase; lysoPtdCho, lysophosphatidylcholine; PAP, phosphatidic acid phosphohydrolase; PC-PLC, phosphatidylcholine-specific PLC; PDPK, proline-directed protein kinase; PI3-kinase, phosphoinositide 3-kinase; PI-PLC, phosphoinositide-specific PLC; PLA_2, phospholipase A_2; PLCγ, phospholipase C γ isoform; PLD, phospholipase D; PP2A, type-2A protein phosphatase; PtdIns(3,4,5)P_3, phosphatidylinositol (3,4,5)trisphosphate; PtdOH, phosphatidic acid; SM, sphingomyelin; SMase, sphingomyelinase. (Modified from Liscovitch and Cantley, 1994)

PLC) (Berridge, 1993).

Phospholipase C (PLC) can be classified into three major groups (β, γ and δ), and each group consists of more than one isoform (Cockcroft and Thomas, 1992; Rhee and Choi, 1992). All PLC isoforms thus far isolated from mammalian tissues hydrolyze phosphatidylinositol (PtdIns), phosphatidylinositol(4)phosphate [PtdIns(4)*P*], and PtdIns(4,5)P_2, but not 3-phosphorylated inositol phospholipids (Nishizuka, 1995), generating diacylglycerol and corresponding inositol mono(bis, or tri)phosphate (see **Figure 8** and **Figure 9**). The activation of PLCβ_1, β_2 or β_3 is mediated by the $\beta\gamma$ subunits of G_i or by the α subunit of G_q. They are responsible for the pertussis toxin-sensitive or -insensitive activation of PtdIns(4,5)P_2 hydrolysis, respectively. The PLCγ isozymes (γ_1 and γ_2) are activated via direct phosphorylation on their tyrosine residues by receptor tyrosine kinases or receptor-associated tyrosine kinases. How the PLCδ isozymes are activated remains unknown (Liscovitch and Cantley, 1994), but they exhibit enzymatic activity in response to Ca^{2+} signals (Nishizuka, 1995).

InsP_3 (a calcium-mobilizing second messenger) and DAG (a PKC activator) together with other inositol-containing messenger molecules (Irvine, 1991; Irvine and Cullen, 1993; Menniti *et al.*, 1993) may regulate many cellular processes including gametogenesis, fertilization, cell growth, transformation, secretion, smooth muscle contraction, sensory perception and neuronal signaling in a typical cell (Bansal and Majerus, 1990; Berridge, 1993; Divecha and Irvine, 1995; Downes and Macphee, 1990).

PtdIns(4,5)P_2 hydrolysis is essential in yeast cell proliferation (Uno *et al.*, 1988). The association of embryonic cell mitosis with InsP_3-triggered calcium oscillation in

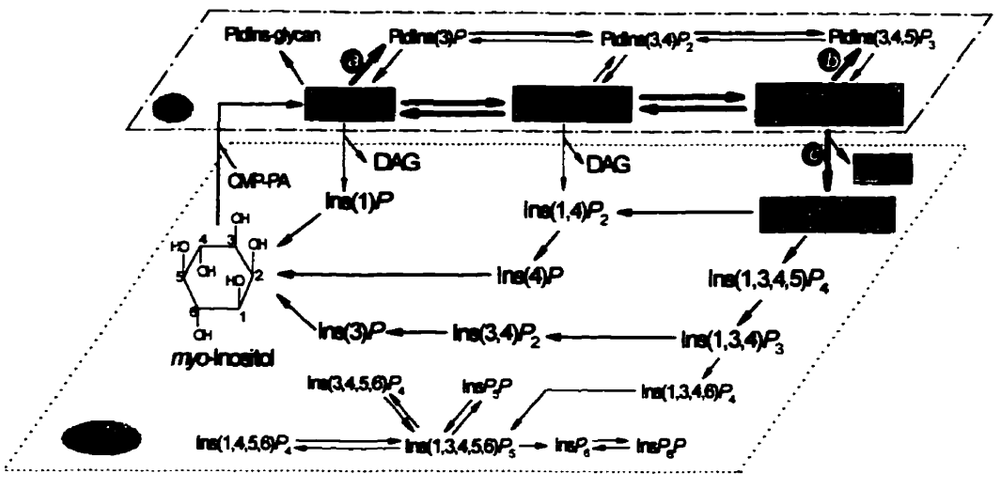

Figure 8. Metabolism of inositol lipids and inositol phosphates. The interconversions among the known inositol lipids are illustrated at the *top* (Note: All these have been documented *in vitro* but not all have been established *in vivo* yet). The interconversions among water-soluble inositol phosphates are presented at the *bottom*. The 3-phosphorylation of PtdIns (***a***) and of PtdIns(4,5)P_2 (***b***), and the hydrolysis of PtdIns(4,5)P_2 by phosphinositide-specific phospholipase C (PIC) (***c***) are believed to be rate limiting or receptor controlled. It is worth noting that a PtdIns-specific 3-kinase (PtdIns 3-kinase) specifically catalyzes reaction ***a***, while a phosphoinositide 3-kinase (PI3-kinase) can phosphorylate any inositol lipids. PtdIns(4,5)P_2, the major source of DAG generated from inositol lipids, is formed by the sequential actions of PtdIns 4-kinase and PtdIns(4)*P* 5-kinase. Arrow thickness indicates the relative importance in cells. CMP-PA, cytidine monophosphoryl phosphatidate; InsP_5P or InsP_6P, inositol tetrakis(or pentakis)phosphate pyrophosphate. For simplicity, inositol cyclic phosphates have been omitted in the figure.

Xenopus embryos is also well documented (Berridge, 1993). It has been known that PtdIns(4,5)P_2 hydrolysis generates DAG and InsP_3 (which mobilizes intracellular Ca^{2+}), and that both DAG and Ca^{2+} synergistically activate PKC. What remains to be answered is how this signaling pathway interacts with the cell cycle machinery resulting the G_1-S transition in yeast, and how it interacts with maturation-promoting factor (MPF), a protein complex containing a mitotic cyclin and a cyclin-dependent kinase, to orchestrate an orderly entry into mitosis in *Xenopus* embryos. In addition, there are several lines of evidence that suggest PtdIns(4,5)P_2 hydrolysis is not required for mitogenesis in some cells (Cuadrado and Molloy, 1990; Margolis *et al.*, 1990; Mohanmmadi *et al.*, 1992; Peters *et al.*, 1992).

Activation of receptors with intrinsic or associated tyrosine kinase activity (Schlessinger and Ullrich, 1992), or G protein-coupled receptors (Stephens *et al.*, 1993, 1994; Stoyanov *et al.*, 1995) leads to the activation of phosphoinositide 3-kinase (PI3-kinase), an enzyme that phosphorylates the hydroxyl group at position 3 on the inositol ring of phosphoinositides (**Figure 8**) (Downes and Carter, 1991). It is very likely that the PI3-kinases will show a similar type of grouping (Divecha and Irvine, 1995). PI3-kinase has an 85-kDa subunit (p85) and a 110-kDa subunit (p110). The p85 mediates the enzyme association through its SH2 domain with a variety of tyrosine kinases (including activated growth factor receptors) or with other signaling proteins such as insulin receptor substrate-1 (IRS-1). The p110 has the catalytic activity. Interestingly, the enzyme also possesses an intrinsic protein kinase activity and is able to phosphorylate the p85 subunit on Ser608 (Dhand *et al.*, 1994) and IRS-1 on serine residues (Lam *et al.*, 1994). Studies from several laboratories have revealed a signaling pathway that links PI3-kinase to cell proliferation.

PI3-kinase has been positioned both immediately downstream (Rodriguez-Viciana *et al.*, 1994) and upstream (Hu *et al.*, 1995; Yamauchi *et al.*, 1993) of Ras. Recently, protein kinase B (PKB), a target for PI3-kinase, was identified independently by two groups (Burgering and Coffer, 1995; Franke *et al.*, 1995; Didchenko *et al.*, 1996), and a series of conceivable linkages between a signaling pathway from Ras to PI3-kinase to PKB to $p70^{S6k}$ and cell proliferation has emerged (Cheatham *et al.*, 1994; Downward, 1995). Direct activation of PKC isoforms (δ, ϵ, ζ, η) by 3-phosphorylated inositol lipids was also reported (Nakanishi *et al.*, 1993; Toker *et al.*, 1994). The role of this action in regulation of cell proliferation remains obscure.

The existence of a nuclear inositide cycle (Divecha *et al.*, 1993; Mechell, 1992b), the nuclear localization of the β-isozyme of PI-PLC (Martelli *et al.*, 1992), the dramatic increase in the level of nuclear calcium following mitogenic stimulation (Stricker *et al.*, 1992; Yamada *et al.*, 1991), the cell-cycle-associated transient changes in intracellular calcium (Ciapa *et al.*, 1994; Hepler, 1992; Wahl *et al.*, 1993), and the ability of calcium to activate MAPK (Chao *et al.*, 1992) all indicate possible functions of inositol lipids-derived messengers in cell proliferation. The decrease in nuclear phosphatidylinositols during S-phase of cell cycle in HeLa cells (York and Majerus, 1994) and changes in the cellular mass of highly phosphorylated inositol lipids during cell cycle progression in rat thymocytes (Guse *et al.*, 1993) suggest a role for these lipids in cell growth.

The key unknowns are what are the specific and essential roles of inositol lipid-derived messengers in mammalian cell growth. Also, there is a great deal of conflicting evidence on regulation of cell growth by inositol lipid-derived signals (Berridge, 1993 and

refs therein); this discrepancy may be due to the cell-specific effect of the signaling system.

Diacylglycerol

Another important second messenger DAG can be generated in response to various extracellular signals either directly by activation of phospholipase C or by the sequential actions of phospholipase D (PLD) and phosphatidic acid phosphohydrolase (PAP) (**Figure 9**) (Nishizuka, 1992; 1995). Current evidence suggests that receptor-coupled PLD is activated via multiple mechanisms: in a PKC-dependent manner, in a Ca^{2+}-dependent manner, through interactions with a GTP-binding protein, and via phosphorylation by a receptor tyrosine kinase and/or a receptor-associated tyrosine kinase (Dennis *et al.*, 1991; Thompson *et al.*, 1993). Elevation of DAG resulting from hydrolysis of inositol phospholipids via PI-PLC activation is rapid and transient. A slow and sustained DAG production is often observed following the transient DAG elevation in response to long-acting signals such as growth factors, cytokines, and phorbol esters (Exton, 1990; 1994). Sometimes, sustained DAG production occurs alone in response to mitogenic signals (Nishizuka, 1995). The sustained wave of DAG production appears to be due to hydrolysis of PtdCho via the sequential action of PLD and PAP (Nishizuka, 1992; 1995) or via activation of PtdCho-specific PLC (PC-PLC) (Exton, 1990; 1994). It is believed to be important for long-term cellular responses such as growth and differentiation (Nishizuka, 1995). There is evidence that PC-PLC functions downstream of Ras but upstream of Raf-1 (Cai *et al.*, 1993) generating signals to both Raf-1 and PKC-ζ for the mitogenic/oncogenic responses (Bjørkøy *et al.*, 1995). Some experiments have demonstrated that phosphatidylethanolamine (PtdEtn) (Kiss and Anderson, 1989; 1990) and other phospholipids (Liscovitch, 1992) may also serve as a

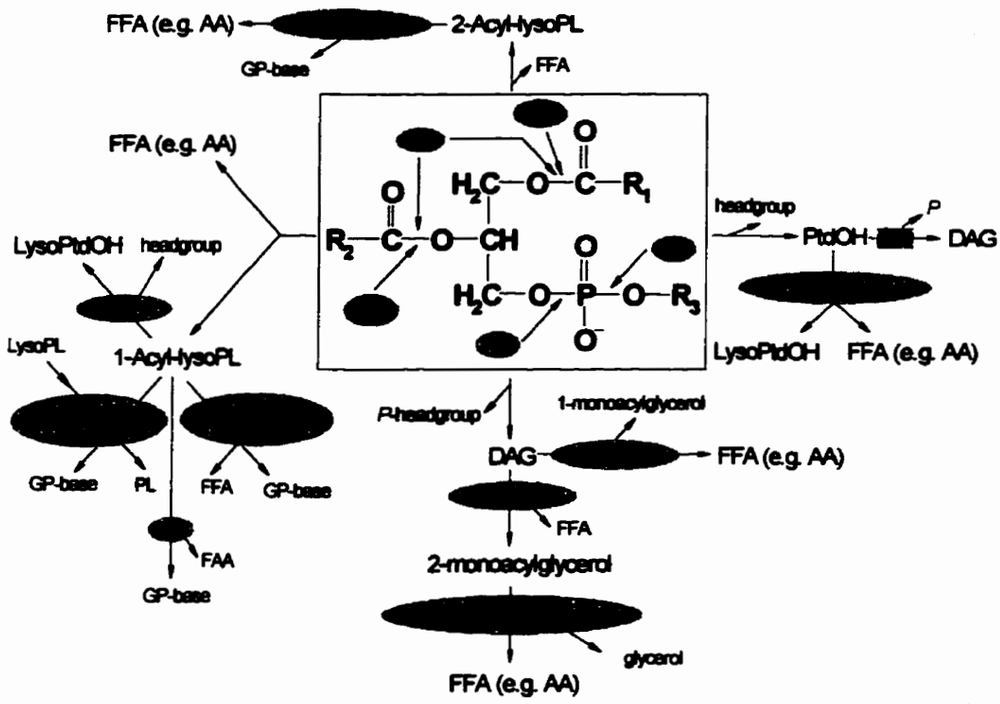

Figure 9. Specificities of (phospho)lipases. Substrate- and bond-specificities of (phospho)lipases are depicted. All (phospho)lipases are highlighted in grey ellipsoids. Three well-known signal-activated phospholipases (PLA_2, PLC, PLD), together with PLA_1 as well as PLB, and their sites of action are shown in the central box. Other lipases and reactions they catalyze are presented outside the box. Enzymes with a ? tag require further confirmation. Headgroups (or bases) in phospholipids include inositol, choline, ethanolamine, and serine. AA, arachidonic acid, 1(or 2)-acyl-lysoPL, 1(or 2)-acyl-lysophospholipid; DAG-1(or 2)-lipase, diacylglycerol-1(or 2)-lipase; FFA, free fatty acid; GP-base, glycerophosphoryl base; (lyso)PL, (lyso)phospholipid; lyso-PLD, lysophospholipase D; (lyso)PtdOH, (lyso)phosphatidate; *P*, phosphate; PAP, phosphatidic acid phosphohydrolase; *P*-headgroup, phosphoryl headgroup; R_1 (often saturated) and R_2 (often unsaturated) are hydrocarbon chains of long chain fatty acids.

source for DAG production; however, the physiological role of DAG produced from PtdEtn and other phospholipids are currently undefined.

Unsaturated fatty acids, lysoPtdCho, lysoPtdOH and PtdSer

Various *cis*-unsaturated fatty acids such as oleic (18:1), linoleic (18:2), linolenic (18:3), arachidonic (20:4), and docosahexaenoic (22:6) released from the *sn*-2 position of phospholipids by phospholipase A_2 (PLA_2) activation (**Figure 9**) greatly enhance the activation of cPKC and nPKC in the presence of DAG or phorbol ester (Nishizuka, 1995). Hydrolysis of PtdCho by PLA_2 also leads to generation of lysoPtdCho (**Figure 9**). LysoPtdCho significantly potentiates cellular responses, such as T-lymphocyte activation and HL-60 cell differentiation, when added to intact cells together with a membrane-permeant DAG or phorbol ester (Nishizuka, 1995), suggesting that lysoPtdCho interacts with the PKC pathway. Another product, lysophosphatidic acid (lysoPtdOH), is formed through PLA_2-mediated deacylation of newly generated phosphatidic acid (PtdOH) (**Figure 9**). The mitogenic activities of lysoPtdOH have been demonstrated in various cell types through an undefined receptor, G protein, and the Ras-directed MAPK cascade (Moolenaar, 1995).

In addition, phosphatidylserine (PtdSer), an acidic lipid located exclusively on the cytoplasmic face of membrane, is required for optimal activity of almost all PKC isozymes (Mosior and Epand, 1993; Nishizuka, 1995; Orr and Newton, 1992a; 1992b). As mentioned in **Section 1.2.6**, PtdSer as well as PtdOH may interact with Raf-1 and regulate its kinase activity (Ghosh *et al.*, 1994, 1996).

Ceramide

In analogy with the central role of DAG in glycerolipid metabolism, ceramide

occupies an equally critical role in the biosynthesis and breakdown of sphingolipids (**Figure 10**) (Hannun, 1994; Hannun and Obeid, 1995). Ceramide is generated from the hydrolysis of sphingomyelin (SM), a lipid that is preferentially concentrated in the plasma membrane (Kolesnick, 1991), by the action of sphingomyelinase (SMase). Ceramide serves as a pleiotropic biological activator capable of inducing differentiation (Pushkareva *et al.*, 1995), apoptosis (Hannun and Obeid, 1995), growth arrest (Jayadev *et al.*, 1995; Obeid and Hannun, 1995), or mitogenesis (Boucher *et al.*, 1995). Ceramide signaling may occur through the Ras pathway (Gulbins *et al.*, 1995), a ceramide-activated protein kinase (CAPK) (Kolesnick *et al.*, 1994; Wright and Kolesnick, 1995; Yao *et al.*, 1995), a cytosolic ceramide-activated protein phosphatase (CAPP) (Dobrowsky and Hannun, 1992; Wolff *et al.*, 1994), PKC-ζ (Lozano *et al.*, 1994), or the JNK/SAPK pathway (Verheij *et al.*, 1996; Westwick *et al.*, 1995). Events underlying the specificity of cellular responses to ceramide are currently unknown.

1.5 Biosynthesis of Phosphatidylcholine and Phosphatidylethanolamine and Signaling Through Phosphatidylcholine Breakdown

1.5.1 Phosphatidylcholine biosynthesis

The principal route of phosphatidylcholine (PtdCho) synthesis is by the CDP-choline pathway (**Figure 11**) which was first described by Eugene Kennedy and coworkers (Kennedy *et al.*, 1989). Choline (Cho) is phosphorylated to phosphocholine (*P*Cho) by a cytosolic enzyme choline kinase (CK) using ATP as a donor of the phosphate group (Ishidate, 1989). *P*Cho then reacts with cytosine triphosphate (CTP) to form CDP-choline (CDP-Cho), catalyzed by the rate-limiting enzyme phosphocholine cytidylyltransferase (PCCT). The

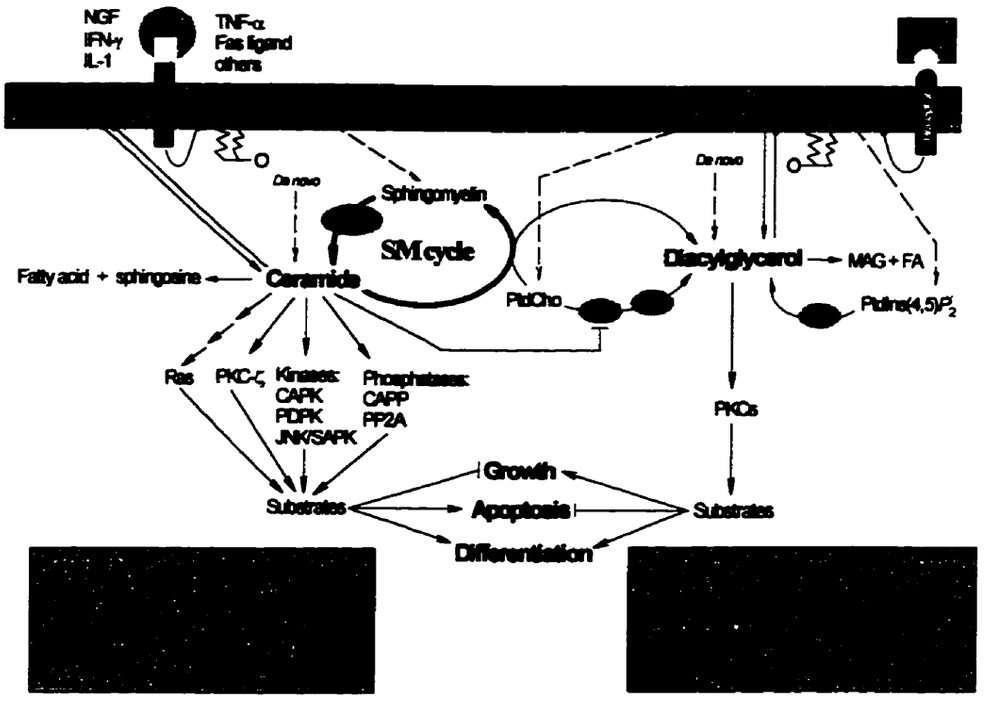

Figure 10. Functions of ceramide in sphingolipid metabolism and cellular signaling. Ceramide plays a central role in sphingolipid biosynthesis and catabolism as does DAG in glycerophospholipids. The hydrolysis of sphingomyelin (SM) by a sphingomyelinase (SMase) to produce ceramide is a signal-inducible process. The resynthesis of SM occurs, presumably by the transfer of phosphocholine headgroup from PtdCho to ceramide; this together with SM hydrolysis form the SM cycle. Ceramide has been shown to activate a number of protein kinases, phosphatases and Ras signaling, and thereby couples ceramide production to downstream events such as activation of NF-κB, downregulation of c-Myc, activation of Rb protein and induction of cyclooxygenase. Ceramide antagonizes the action of DAG not only by the putative ultimate effects such as induction of apoptosis, cell-cycle arrest and differentiation, but also by decreasing the production of DAG via inhibition of PLD. All abbreviations used are the same as in text.

phosphorylcholine unit of CDP-Cho is then transferred to a DAG to form PtdCho by choline phosphotransferase (CPT). Choline phosphotransferase is an integral membrane protein of the endoplasmic reticulum (ER) and Golgi (Cornell, 1989), while *P*Cho cytidylyltransferase is found both in the cytosol as an inactive enzyme and on the membrane of the ER where it is active (Vance, 1991). An increase in the concentration of fatty acids, especially oleic acid, and DAG in cell cultures promotes the association of PCCT with membranes, thereby boosting its activity (Vance, 1989; 1990). However, the subcellular localization of PCCT has been questioned by a series of studies from Dr. Kent's laboratory (Wang *et al.*, 1993a, 1993b; Watkins and Kent, 1992). They demonstrated that PCCT is predominantly an intranuclear enzyme, activated by dephosphorylation and translocation to the nuclear envelope. The nuclear membrane may therefore be a site of *de novo* PtdCho biosynthesis.

Phosphatidylcholine can also be synthesized via the methylation of PtdEtn catalyzed by a methyltransferase with a M_r of approximately 18 kDa (Ridgway, 1989; Vance, 1990). This enzyme is expressed at a high level only in liver; its expression is 1% or less in nonhepatic cells and tissues (Ridgway, 1989). The major function of this transmethylation reaction, together with the subsequent hydrolysis of the formed PtdCho, appears to be the *de novo* formation of choline (Vance, 1991).

1.5.2 Phosphatidylethanolamine biosynthesis

Phosphatidylethanolamine can be synthesized *de novo* in eucaryotes from ethanolamine (Etn) by the CDP-ethanolamine (CDP-Etn) pathway through analogous reactions to those described above for PtdCho (**Figure 11**). In animal tissues examined, the

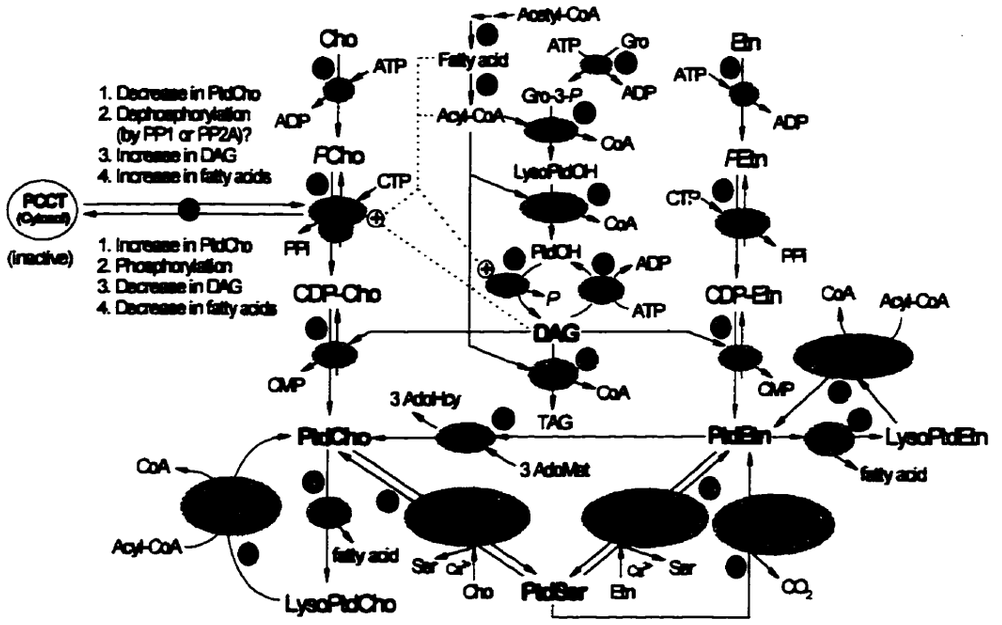

Figure 11. Biosynthesis of PtdCho and PtdEtn. Reactions **1-3** represent the principal route of PtdCho synthesis (i.e., the CDP-Cho pathway). The rate-limiting step (**2**) of this pathway is catalyzed by CTP:*P*Cho cytidylyltransferase (PCCT), which is active when bound to membrane or inactive when free in the cytosol. Many cellular events listed above regulate the process (**23**) of PCCT translocation between the cytosol and membranes. PtdCho can also be synthesized by lysoPtdCho acylation (**5**), PtdEtn methylation (**6**) and base exchange (**7**). Similarly, reaction **8-10** represent the CDP-Etn pathway for PtdEtn synthesis. CTP:*P*Etn cytidylyltransferase (PECT) catalyzes the rate-limiting step (**9**) for PtdEtn biosynthesis. The enzyme has recently been found in the rough ER, and is therefore not localized exclusively in the cytosol as previously thought. However, it has no lipid requirement for activity. Etn kinase (EK) (**8**) appears to be identical to Cho kinase (CK) (**1**) in animals. LysoPtdEtn acylation (**12**), PtdSer decarboxylation (**13**) and base exchange (**14**) also play a role for PtdEtn biosynthesis. DAG is a common precursor for biosynthesis of PtdCho, PtdEtn and triacylglycerol (TAG). AdoHcy, *S*-adenosyl-homocysteine; AdoMet, *S*-adenosyl-methionine; AT, acyltransferase; CPT, CDP-Cho:DAG cholinephosphotransferase; DGAT, DAG acyltransferase; DGK, DAG kinase; EPT, CDP-Etn:DAG ethanolaminephosphotransferase; GK, glycerol kinase; GPAT, glycerophosphate acyltransferase; Gro, glycerol; Gro-3-*P*, glycero-3-phosphate; LPAAT, lysoPtdOH acyltransferase; *P*, phosphate; PAP, phosphatidate phosphohydrolase; PEMT, PtdEtn methyltransferase. Other standard abbreviations are as in text.

ethanolamine kinase (EK) and the choline kinase appear to be the same enzyme since the purified choline kinase (a dimer of 42 kDa subunits) phosphorylates ethanolamine equally well (Ishidate, 1989). Similar to PCCT, phosphoethanolamine cytidylyltransferase (PECT) catalyzes the rate-limiting step, the formation of CDP-Etn by the reaction between phosphoethanolamine (*P*Etn) and CTP, for PtdEtn biosynthesis. The enzyme was thought to exclusively exist in the cytosol (Vance, 1991). However, recent immunogold electron microscopy studies showed that the PECT label was concentrated in the rough ER cisternae and was in close contact with the rough ER membrane (Van Hellemond *et al.*, 1994). Little is known about the regulation of the PECT reaction. It has no lipid requirement for activity, but the rate of PtdEtn biosynthesis, however, can be regulated by either the supply of DAG or CTP (Vance, 1991). The third enzyme in the CDP-Etn pathway is ethanolaminephosphotransferase (EPT), which is also found as an intrinsic membrane protein on the ER and the Golgi but is different from CPT (Vance, 1991). A comparison of the CDP-Cho and CDP-Etn pathways (see **Figure 11**) indicates that the use of radiolabeled choline or ethanolamine as the precursor of biosynthesis will specifically produce the labeled PtdCho or PtdEtn respectively, while both PtdCho and PtdEtn (as well as other glycerolipids) will be labeled by using labeled glycerol as the precursor.

Three other routes for PtdEtn synthesis (**Figure 11**) arise as a result of the modification of pre-existing phospholipids (Vance, 1991).

1.5.3 Signaling through phosphatidylcholine breakdown

Accumulated evidence supports the current view that PtdCho (and perhaps PtdEtn)

is more than just a structural membrane lipid. Phosphatidylcholine breakdown generates a number of lipid signaling molecules (Divecha and Irvine, 1995; Exon, 1990; 1994; Liscovitch and Cantley, 1994; Pelech and Vance, 1989) (**Figure 12**). Hydrolysis of PtdCho by PLA_2 is an important source of arachidonic acid, which can either act as a messenger in its own right or be subsequently metabolized to a variety of bioactive eicosanoids. LysoPtdCho, the other product of PtdCho hydrolysis by PLA_2, exhibits a number of biological activities, including potentiation of the DAG- or TPA-induced PKC activation (Nishizuka, 1995), but lysoPtdCho alone is inert toward PKC.

Hydrolysis of PtdCho by PLC or by the sequential action of PLD and PAP generates DAG. Cook and Wakelam (1992) reported that EGF stimulated the PLC hydrolysis of PtdCho to produce DAG, tetradecanoyl phorbol acetate induced an increase in DAG generation from PtdCho through the PLD pathway, and bombesin (which interacts with a G protein-coupled receptor) enhanced the hydrolysis of PtdCho via both the PLC and PLD activities to yield DAG. The differential effects of these stimuli suggest multiple functions of PtdCho hydrolysis in cellular signaling. *P*Cho, the other product of PtdCho hydrolysis by PLC, may serve as a second messenger for mitogenicity of growth factors (Cuadrado *et al.*, 1993).

LysoPtdOH has been proposed to be mitogenic in various cell types (van Corven *et al.*, 1989), presumably acting by stimulating tyrosine kinases and by Ras activation through stimulation of its own cell surface G protein-coupled receptor (Hordijk *et al.*, 1994; van Corven *et al.*, 1989; van der Bend *et al.*, 1992). LysoPtdOH also mediates the assembly of focal adhesions and actin filaments through the action of a small G protein Rho (Ridley and

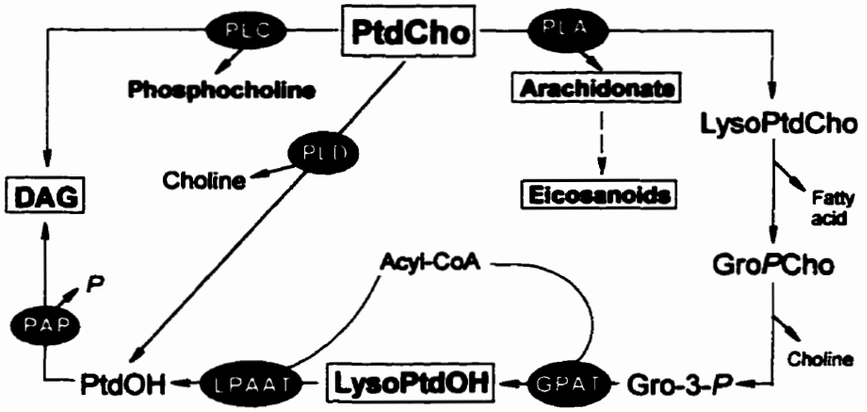

Figure 12. Signaling molecules generated from phosphatidylcholine breakdown. Signaling molecules produced from phosphatidylcholine (PtdCho) degradation include 1,2-diacylglycerol (DAG), lysophosphatidic acid (lysoPtdOH) and arachidonic acid, an immediate precursor of eicosanoids that have a wide variety of biological activities and act in an autocrine mode. Lysophosphatidylcholine (lysoPtdCho) and phosphocholine have also been shown to function as signaling molecules in some studies. GPAT, glycerophosphate acyltransferase; Gro-3-*P*, glycero-3-phosphate; Gro*P*Cho, glycerophosphocholine; LPAAT, lysophosphatidate acyltransferase; *P*, phosphate; PAP, phosphatidate phosphohydrolase; PLA_2, phospholipase A_2; PLC, phospholipase C; PLD, phospholipase D; PtdOH, phosphatidate.

Hall, 1992).

1.6 Cellular Metabolism of Ether Glycerolipids

Much of the current interest in ether-linked glycerolipids arose from the discovery in 1979 of the chemical structure of platelet activating factor (PAF, 1-*O*-alkyl-2-acetyl-*sn*-glycerol-3-phosphocholine, **Figure 15, e**), an endogenous ether phospholipid mediator of inflammation with a wide range of biological activities. Ether linkages associated with glycerolipids occur in nature primarily as *O*-alkyl and *O*-alk-1-enyl moieties (Snyder, 1991). In mammals, both types of ether chains are located predominantly at the *sn*-1 position of glycerolipids. Lipids with *O*-alk-1-enyl moiety are often referred to as 'plasmalogens'. In general, the alkyl groupings are primarily associated with the choline glycerophospholipids, while the alk-1-enyl species are almost exclusively found in the ethanolamine-containing phospholipids (Snyder, 1991). The terms *plasmanyl* and *plasmenyl* are used for the 1-alkyl-2-acyl-*sn*-glycero-3-phospho-moiety and 1-alk-1-enyl-2-acyl-*sn*-glycero-3-phospho-moiety, respectively. They are equivalents of '*phosphatidyl*' that can only be used to designate the diacylglycerophospho-moiety in glycerophospholipids.

1.6.1 Biosynthesis

Fatty alcohol precursors in ether lipid biosynthesis are derived from acyl-CoAs in a reaction sequence catalyzed by a membrane-associated NADPH-dependent acyl-CoA reductase (**Figure 13**). The enzyme prefers saturated over unsaturated acyl-CoA. Ether glycerophospholipids are synthesized starting with dihydroxyacetone phosphate

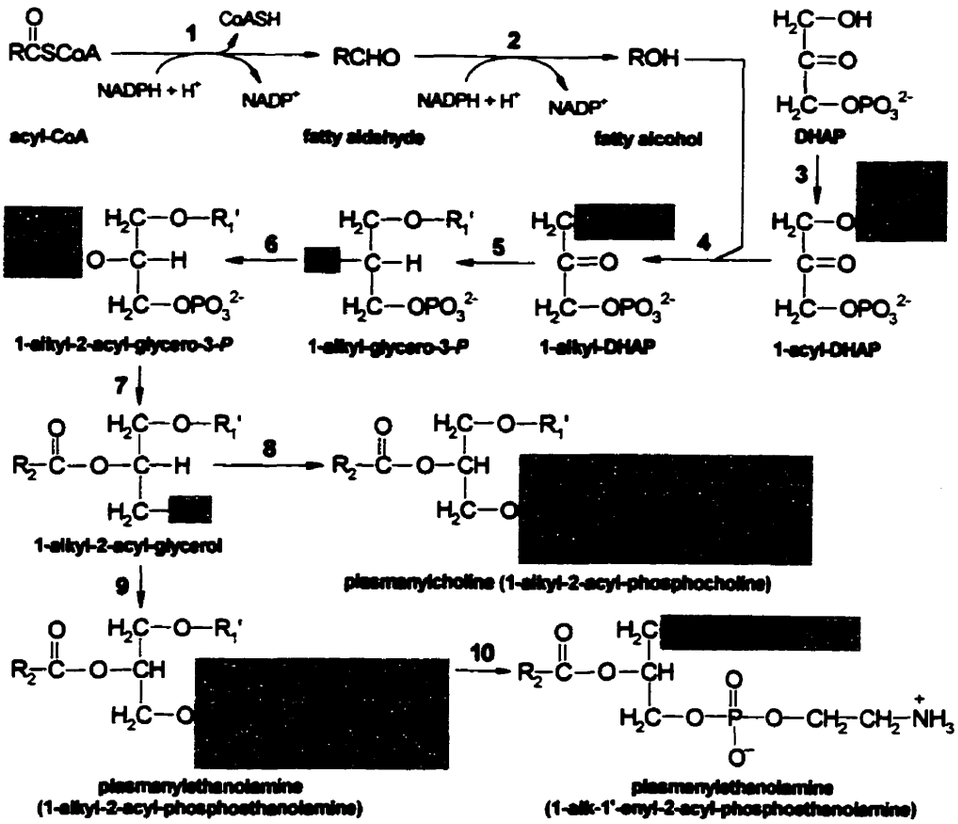

Figure 13. Ether glycerophospholipid biosynthesis. Enzymes responsible for catalyzing the reactions shown in this figure are: acyl-CoA reductase (**1** and **2**), dihydroxyacetone phosphate (DHAP) acyltransferase (**3**), alkyl-DHAP synthase (**4**), NADPH:alkyl-DHAP oxidoreductase (**5**), acyl-CoA:1-alkyl-2-lyso-*sn*-glycero-3-phosphate acyltransferase (**6**), 1-alkyl-2-acyl-*sn*-glycero-3-phosphate phosphohydrolase (**7**), 1-alkyl-2-acyl-*sn*-glycerol:CDP-choline (or CDP-ethanolamine) choline(ethanolamine)phosphotransferase (**8** and **9**), and 1-alkyl-2-acyl-*sn*-glycero-3-phosphoethanolamine Δ'-desaturase (**10**). R_1, R_1', R_1'' (two CH_2 shorter than R_1') and R_2 are hydrocarbon chains of long chain fatty acids. The conversion by each reaction is highlighted in a grey box. Please see **Section 1.6.1** for other details.

(dihydroxyacetone-*P* or DHAP) (**Figure 13**). Acylation by acyl-CoA via dihydroxyacetone-*P* acyltransferase yields 1-acyldihydroxyacetone-phosphate (1-acyldihyroxyacetone-*P* or 1-acyl-DHAP). The initial formation of the alkyl ether bond in glycerolipids is catalyzed by alkyldihydroxyacetone-*P* synthase, whereby a fatty alcohol is substituted for an acyl moiety at the *sn*-1 position. The keto group at the *sn*-2 position is reduced by NADPH via NADPH:alkyldihydroxyacetone-*P* oxidoreductase, and the resultant alcohol at the *sn*-2 position is acylated by a long-chain CoA via acyl-CoA:1-alkyl-2-lyso-*sn*-glycero-3-phosphate acyltransferase. Removal of the 3-phosphate group by 1-alkyl-2-acyl-*sn*-glycero-3-phosphate phosphohydrolase yields 1-alkyl-2-acyl-*sn*-glycerol, which reacts with CDP-Cho or CDP-Etn to form an ether analogue of PtdCho or PtdEtn (Snyder 1991). 1-Alk-1-enyl species are formed from 1-alkyl groupings by the Δ^1-alkyl desaturase; the reverse of this reaction has never been demonstrated (Snyder, 1991).

1.6.2 Catabolism

The metabolic removal of ether lipid precursors is one of the important control points for maintaining the cellular levels of ether lipids. Long-chain fatty alcohols are oxidized to fatty acids via an NAD^+:fatty alcohol oxidoreductase. Dihydroxyacetone-*P* can be converted into *sn*-glycerol-3-phosphate by NADH:glycerol-3-phosphate dehydrogenase. Acyldihydroxyacetone-*P* can be reduced by the NADPH-dependent oxidoreductase to 1-acyl-2-lyso-*sn*-glycerol-3-phosphate, which is then directed into diacylglycerolipids.

The *O*-alkyl linkage in glycerolipids is oxidatively cleaved in membranes by a microsomal tetrahydropteridine ($Pte{\cdot}H_4$)-dependent alkyl monooxygenase (**Figure 14**). Fatty

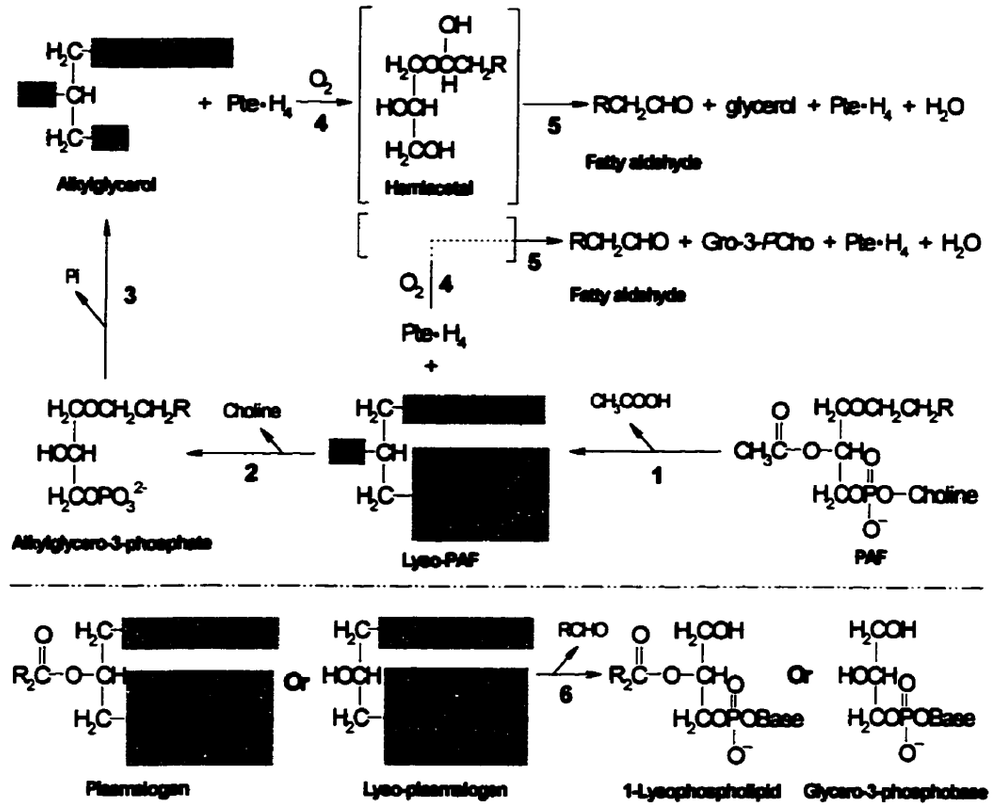

Figure 14. Cleavage of ether bonds in glycerolipids and inactivation of PAF. Alkyl and alkenyl linkages in glycerolipids are cleaved by tetrahydropteridine ($Pte{\cdot}H_4$)-dependent alkyl monooxygenase (**4** and **5**) and plasmalogenase (**6**), respectively. The structural requirements of the substrates for each enzyme are highlighted in grey boxes. Inactivation of platelet-activating factor (PAF) by hydrolysis of the acetate moiety is catalyzed by an acetylhydrolase (**1**). Lyso-PAF can be further degraded by (lyso-)PLD (**2**) plus phosphohydrolase (**3**) or by PLC alone, generating alkylglycerol. Both lyso-PAF and alkylglycerol can be eliminated from the ether lipid pool by reactions **4** and **5**.

aldehydes produced in this cleavage reaction can be either oxidized to the corresponding acid or reduced to an alcohol. Structural requirements of glycerolipid substrates utilized by the alkyl cleavage enzyme are [1] an *O*-alkyl moiety at the *sn*-1 position, [2] a free hydroxyl group at the *sn*-2 position, and [3] a free hydroxyl or a phosphobase group at the *sn*-3 position (Snyder, 1991). Thus, both alkylglycerols and 1-alkyl-2-lysophospholipids (e.g., lyso-PAF, see **Figure 14**) are substrates for this cleavage enzyme. In contrast, microsomal plasmalogenase activities hydrolyze the alk-1-enyl bond in both plasmalogens and lyso-plasmalogens in membranes, producing a fatty aldehyde and either 1-lyso-2-acyl-*sn*-glycero-3-phosphobase or *sn*-glycero-3-phosphobase depending on the type of substrate used (Snyder, 1991).

Inactivation of platelet-activating factor (PAF) is achieved via a specific phospholipase A_2 termed PAF acetylhydrolases. The enzyme activity is present in cell cytosol and serum, producing the inactive 2-lyso form of PAF. Lyso-PAF can be either reacylated to the membrane precursor (alkylarachidonoylglycerophosphocholine) of PAF, or utilized by a lyso-phospholipase D or PLD to form an alkylglycero-phosphate that can be further degraded to alkylglycerols by a phosphohydrolase. Both lyso-PAF and alkylglycerols can be completely eliminated from the ether lipid pool by the Pte·H_4-dependent alkyl monooxygenase action (see above) (Snyder, 1991).

1.7 ET18-OCH_3: A Prototype of a Novel Class of Antitumor Agents

Currently, successful therapy for solid tumors relies on an early diagnosis and surgical resection. However, a surgical operation is not suitable for the high-incidence blood

cancers or for tumors located in parts of the body not easily accessible to surgeons such as brain and hilus pulmonis. Besides, despite significant improvements in diagnosis and surgical techniques, most deaths from solid tumors are due to metastases that often make surgical therapy impossible (Fidler *et al.*, 1987). Naturally, another therapeutic strategy, chemotherapy, is attracting more and more interest and attention. Antitumor ether lipids are one branch of a great many promising chemotherapeutic armamentaria. They, in striking contrast to essentially all other conventional chemotherapeutic drugs, do not appear to directly interact with cellular DNA or to be mutagenic (Bauchinger *et al.*, 1983; King *et al.*, 1981), thus representing a novel class of antitumor agents. This may open up entirely new avenues to cancer therapy.

1-*O*-Octadecyl-2-*O*-methyl-*sn*-glycero-3-phosphocholine (ET18-OCH_3) is one of the most efficient and widely used antitumor ether lipids (AELs). To explore mechanisms of antitumor activity by these ether compounds, ET18-OCH_3 has been chosen as a probe for our studies.

1.7.1 Historical recollections

The discovery of the antitumor activity of ether lipids stems from studies by Drs. Herber Fischer, Paul Gerhard Munder and their coworkers at Max-Planck-Institut für Immunbiologie in Freiburg, Germany in the 1960s. They observed that lysoPtdCho (**Figure 15, f**) strongly enhanced the phagocytic activity of peritoneal macrophages *in vitro* and *in vivo* (Burdzy *et al.*, 1964; Fischer 1964; Munder *et al.*, 1966). This inspired an extensive investigation on the potential role of lysoPtdCho in immune responses.

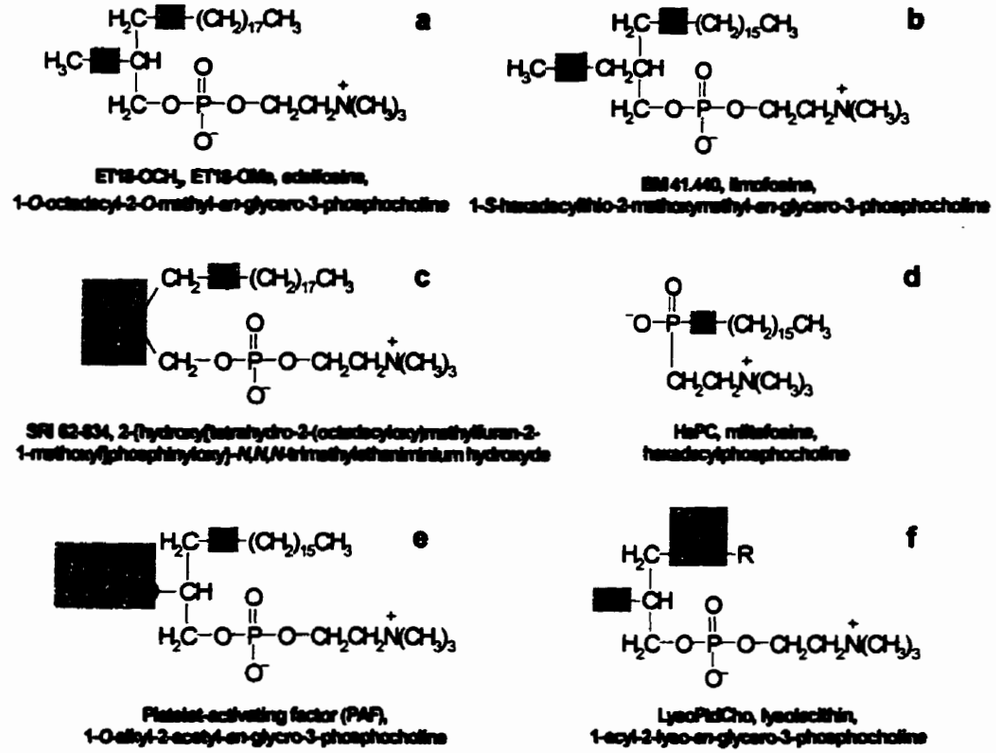

Figure 15. Structures of ether phospholipids and lysophosphatidylcholine.

The chemical structures of four types of synthetic antitumor ether phospholipids are shown. ET18-OCH_3 (**a**) is referred as the "leader molecule" of antitumor ether lipids (AELs); BM 41.440 (**b**) is the representative of thioether phospholipids; SRI 62-834 (**c**) represents a cyclic ether analog of ET18-OCH_3, in which the oxygen atom at the *sn*-2 position of the glycerol backbone has been incorporated into a five-membered heterocycle; HePC (**d**), the simplest AEL, is the prototype of a group of alkylphosphocholines. For comparison, the structures of naturally-occurring ether phospholipid PAF (**e**) and lysoPtdCho (**f**) are also shown.

Naturally-occurring lysoPtdCho is liable to be hydrolyzed by lysophospholipase at the fatty ester bond to yield glycerophosphocholine or metabolized by an acyltransferase at the hydroxyl group to PtdCho. Either of these transformations leads to biological inactivation of lysoPtdCho. This led to the synthesis of structurally defined ether analogues of lysoPtdChos because of their higher metabolic stability and longer half life. In 1967, Arnold and Weltzien synthesized ET18-OCH_3 (**Figure 15, a**) (Arnold *et al.*, 1967). With this and many other highly purified synthetic lysoPtdCho analogues, a series of *in vivo* and *in vitro* biological screenings was initiated in 1967. Munder and his colleagues were first to report the selective action of these compounds on various tumor cells (Andreesen *et al.*, 1978; Modolell *et al.*, 1979; Tarnowski *et al.*, 1978) and define some of the structural requirements for optimal antitumor activity (Munder *et al.*, 1977).

In addition, a number of the ether compounds including ET18-OCH_3 were fully active when given orally (Munder *et al.*, 1981). This greatly facilitated the start-up of clinical trials. Currently, many AELs are being tested in different stages of clinical trials. After phase I studies in various groups of patients suffering from advanced solid tumors and leukemias refractory to standard therapy, ET18-OCH_3 is currently under a large phase II/III study in Germany and USA (Houlihan *et al.*, 1995). Hexadecylphosphocholine (HePC, the prototype of another class of AEL—the alkylphosphocholine, **Figure 15, d**) is now on the market in Germany for topical applications in cutaneous breast cancer and also in phase I/II studies in USA, France and Netherlands (Houlihan *et al.*, 1995; Lohmeyer and Bittman, 1994). Other AELs that are under clinical phase I/II studies include ilmofosine (a thioether phospholipid, **Figure 15, b**) (Winkelmann *et al.*, 1992) and cytarabine ocfosfate (Ueda *et al.*, 1990).

Cytarabine ocfosfate has recently been approved for market in Japan (Houlihan *et al.*, 1995). Substantial evidence shows that the utility of AELs as purging agents in autologous bone marrow transplantation is an effective treatment for patients with leukemia (Houlihan *et al.*, 1995). The selective cytotoxic effect against neoplastic cells while sparing non-tumor cells is the basis for this treatment. Monoclonal antibodies have not been helpful in purging myeloid leukemia cells because of the phenotypic similarities between normal and leukemic stem cells (Vogler *et al.*, 1990). The preliminary results from the AEL clinical trials are encouraging and promising.

1.7.2 Structural features of ET18-OCH_3 and related compounds

ET18-OCH_3 is a synthetic alkyl lysophospholipid (ALP) (**Figure 15, a**). It contains a glycerol backbone, an ether (alkyl) bond rather than ester bond linking C_{18} fatty acid chain at the *sn*-1 position, a methoxyl group instead of hydroxyl group at the *sn*-2 position, and a *P*Cho headgroup at the *sn*-3 position. Both ether linkages render this synthetic LPC analogue resistant to the action of either lysophospholipase (**Figure 9**) or acyltransferase (**Figure 11**), therefore increasing the biological half life of this compound (Westphal, 1987). The $C_{16\text{-}18}$ fatty acid chain is necessary for efficient antitumor activity; shortening or elongation of this chain impairs the antitumor activities toward most tested tumor cell lines and animal tumors (Houlihan *et al.*, 1995; Kudo *et al.*, 1987). The choline moiety is important, since stepwise replacement of the methyl groups by hydrogen in this moiety (Honma *et al.*, 1981; Kudo *et al.*, 1987) or replacement of the choline moiety with inositol (Noseda *et al.*, 1987) did not yield potent compounds. To meet the minimal structural requirements discussed above for

the antitumor activity, a simple molecule, hexadecylphosphocholine, was therefore synthesized. As expected, the absence of the glycerol structure does not hamper the antitumor activity of the alkylphosphocholine (Houlihan *et al.*, 1995; Uger and Eibl, 1991).

1.7.3 Proposed hypotheses on the mechanisms of antitumor action

Antitumor ether lipids are active *in vitro* and *in vivo* against a wide variety of cancer cells (Berdel, 1991; Houlihan *et al.*, 1995; Lohmeyer and Bittman, 1994). The sensitivity to AELs varies from cell to cell. Interestingly, normal cell lines and non-transformed cells appear to be more resistant to the AELs than cancer cells (Berdel, 1991; Lohmeyer and Bittman, 1994). The basis of this selectivity is currently unknown because there is still a profound lack of knowledge on the mechanism of the antiproliferative action of AELs. A number of hypotheses have been proposed to explain their antiproliferative effects.

AEL uptake

It was reported that AELs localized preferentially to tumor tissues *in vivo* (Plotzke *et al.*, 1992; Diomede *et al.*, 1993). The uptake of these compounds was suggested to be a major determinant of tumor cell sensitivity (Bazill and Dexter, 1990). However, studies with a number of different cell lines revealed that rates of uptake were similar among cells regardless of sensitivity (Fleer *et al.*, 1992). Moreover, no correlation between AELs uptake and resistance was observed by our laboratory (Lu and Arthur, 1992) and other investigators (Diomede *et al.*, 1991; Fleer *et al.*, 1992). These suggest that the uptake of AEL is unlikely to be a determinant of tumor cell sensitivity to the compound.

Detergent lysis

Lysophospholipids are maintained at a relatively constant concentration in cell membranes; their potent surface-active properties, otherwise, can destroy cell membranes at critical micellar concentrations (CMC) of approximately 20 mole% of cell membrane phospholipids (Weltzien, 1979). Due to the structural similarity to lysophospholipids, AELs are able to act as membrane-active detergent molecules. The membrane-lytic effects were, therefore, surmised to be the mechanism underlying antitumor activity (Dive *et al.*, 1991; Workman, 1990). However, perturbation of membrane structure occurs only when moderate and relatively high concentrations of AELs are applied (Houlihan *et al.*, 1995; Lohmeyer and Bittman, 1994). Direct lysis is certainly not an important mechanism of growth-inhibitory action at low concentrations that have been used in many studies by various researchers, provided that cells are maintained in normal serum- or BSA-supplemented medium (Houlihan *et al.*, 1995; Lohmeyer *et al.*, 1992; 1993; Lohmeyer and Bittman, 1994). On the other hand, AELs are known to be quite selective toward cells (Berdel, 1991) and the ester analogues and natural ether lipids are much less potent compared to AELs (Moriboto *et al.*, 1991; Noseda *et al.*, 1989). Obviously, these agent and cell line selectivity would not be expected if the mechanism of action was solely dependent on the detergent properties of these lipids.

Nutrient starvation

One interesting hypothesis is that the inhibition of membrane transport processes by AELs is one of the prime reasons for their antitumor toxicity (Vallari *et al.*, 1988). Consistent with this is their ability to inhibit the uptake of various nutrients such as glucose, choline, *myo*-inositols, amino acids and fatty acids in sensitive cells (Berkovic *et al.*, 1992, Hoffman *et al.*, 1992, Melchior *et al.*, 1990). However, it is not known yet whether this inhibition is

a consequence, rather than the cause, of suppressing cell proliferation.

Induction of differentiation

It has been known that AELs can induce differentiation in a number of leukemia cell lines (Honma *et al.*, 1981, 1991; Maurer and Hilgard, 1992). However, this is unlikely to be the general mechanism underlying the antitumor activity of AELs as differentiation induced by AELs only occurred in leukemic cells already predisposed to differentiation (Lohmeyer and Bittman, 1994).

Induction of apoptosis

Another important aspect of antitumor activities of AELs is their ability to induce apoptosis or programed cell death. After ET18-OCH_3 exposure, cells underwent morphological changes resembling those seen in apoptosis (Vagnetti *et al.*, 1990); flow cytometric analysis (Fujiwara *et al.*, 1992; 1993) and DNA fragmentation analysis (Diomede *et al.*, 1992) suggested that ET18-OCH_3 was able to induce apoptosis in AEL-sensitive cells, but not in AEL-resistant cells (Diomede *et al.*, 1992; Mollinedo *et al.*, 1993). However, the induction of apoptosis by AELs has not been observed in a large panel of cell lines by other investigators (Houlihan *et al.*, 1995).

Perturbation of cellular lipid composition and metabolism

As AELs are lipids, it is not surprising to envisage that AELs, once taken up into the cell, would interrupt normal phospholipid metabolism, leading to inhibition of cell growth as a consequence of the lack of newly synthesized phospholipids. It has been known for some time that neoplastic cells contain larger proportion of ether phospholipids than their normal counterparts (Snyder *et al.*, 1968; 1969) and the levels of ether lipids are progressively lower

in the less rapidly growing and more highly differentiated tumors (Howard *et al.*, 1972). This led to a hypothesis that the higher susceptibility of malignant cells to AELs might be due to the higher content of cellular ether lipids because of higher levels of ether lipid synthesis enzyme activities (Chabot *et al.*, 1989), but not of lower levels of ether cleavage enzyme activities (Hoffman *et al.*, 1986). Another hypothesis was that the inhibition of cell growth resulted from an interference of AEL in the cellular processes by which cells maintain a required complement of unsaturated fatty acids in their membrane phospholipids (Modolell *et al.*, 1979). Studies in our laboratory have demonstrated that perturbations of these acylation processes by ET18-OCH_3 do not correlate with the differential sensitivity of cells to the growth-inhibitory effects of this compound in four epithelial cancer cell lines (Lu and Arthur, 1992a, 1992b). It was also postulated that cell growth was arrested as a consequence of inhibition of phospholipid synthesis (Modolell *et al.*, 1979), particularly that of phosphatidylcholine (Vogler *et al.*, 1985). The effect of ET18-OCH_3 on lipid metabolism has been studied with radiolabeled lysoPtdCho (Vogler *et al.*, 1985), choline (Modolell *et al.*, 1979; Vogler *et al.*, 1985), methionine (Vogler *et al.*, 1985), and fatty acids (Herrmann, 1985; Herrmann and Neumann, 1986; Modolell *et al.*, 1979; Vogler *et al.*, 1985) as precursors. With the exception of choline, incorporation of the other precursors is not necessarily via *de novo* synthesis and, other than fatty acids, these precursors are specific for PtdCho and do not reveal the effect of ET18-OCH_3 on the metabolism of other lipids.

With all these thoughts in mind, we initiated studies to examine if there was a relationship between the sensitivity of cells to AELs and their cellular content and composition of ether phospholipids, the metabolism of ET18-OCH_3, and effects of ET18-

OCH_3 on phospholipid metabolism with emphasis on the *de novo* synthesis of phospholipids by using radiolabeled glycerol, choline and ethanolamine as precursors in sensitive and relatively resistant cells.

Interference with cellular signal transduction

An alternative hypothesis can be advanced that AELs may inhibit cell growth by interfering in cellular signal transduction processes. Being structurally similar to the natural lipid mediator platelet-activating factor (PAF, **Figure 15, e**), ET18-OCH_3 may antagonize PAF binding to its receptor. However, ET18-OCH_3, albeit considerably more cytotoxic to a variety of tumor cell lines than PAF, is 100 times less effective than PAF in inducing serotonin release and 1000 times weaker in promoting aggregation in rabbit platelets (Hanahan *et al.*, 1981; Söling *et al.*, 1987). No correlation was found between modulation of PAF receptor binding and biological effects of ET18-OCH_3, other AELs and PAF (Berdel *et al.*, 1987). Furthermore, the biological activities of PAF are largely restricted to inflammatory and allergic responses. AELs are therefore unlikely to act against tumor cells through the interaction with the PAF receptor.

Reduction of EGF binding to its receptors by ET18-OCH_3 was proposed to be the mechanism by which this compound inhibited the growth of hormone-dependent breast cancer cell lines (MCF-7 and ZR-75-1) (Kosano and Takatani, 1988). This hypothesis was modified by their later studies that demonstrated that ET18-OCH_3 inhibited the internalization of occupied EGF receptors in the above lines but had little effect on the binding of EGF to the receptor. Therefore, the authors suggested that the inhibition of the internalization process might be one of the modes of antitumoral action of this AEL (Kosano and Takatani, 1989).

However, this suggestion can be questioned: Is the internalization of EGF-bound receptors essential for cell growth or does this process transmit growth signals into inner cellular machineries? Currently, there is no evidence for positive answers to these issues.

The effect of AELs on the calcium signaling is controversial. It has been reported that AELs induced elevations of $[Ca^{2+}]_i$ in human neutrophils and a number of human and murine leukemia cell lines that are either sensitive (e.g., HL-60) or resistant (e.g., K-562) to AEL cytotoxicity (Lazenby *et al.*, 1990; Lohmeyer and Workman, 1993). The calcium response in murine EMT6 mammary carcinoma cells was not universal, with a sizeable population of non-responding cells when flow cytometry with quin2 as the reporter fluorophore was used (Watson *et al.*, 1990). In contrast, preincubation of ET18-OCH_3 or HePC was shown to strongly inhibit the neurotensin-induced calcium signal in HT-29 cells (Houlihan *et al.*, 1995). The significance of these differential calcium responses induced by AELs remains unknown, but it does not appear to be directly related to the antiproliferative activity of AELs.

Inhibition of PKC has been proposed as the mechanism by which AELs inhibit cell proliferation (Powis, 1991), but it is contentious since inhibition (Grunicke *et al.*, 1989; Helfman *et al.*, 1983), activation (Heesbeen *et al.*, 1991) and lack of a pronounced effect (van Blitterswijk *et al.*, 1987) on PKC, largely based on results from *in vitro* assays, have all been reported. The effect of AELs on *in vivo* PCK activation is not very clear yet. Moreover, a number of studies have revealed that no correlation exists between inhibition of cell proliferation and inhibition of PKC activity (Berkovic *et al.*, 1994; Houlihan *et al.*, 1995; Salari *et al.*, 1992). In fact, there have been suggestions that the inhibitory effect of AELs on

cellular PKC might be mediated primarily by inhibition of phosphoinositide-specific phospholipase C (PI-PLC), resulting in reduced cellular DAG levels (Powis *et al.*, 1992b; Überall *et al.*, 1991).

AELs are among the most potent known inhibitors of PI-PLC (Pawelczyk *et al.*, 1993; Powis *et al.*, 1992a; 1992b; Überall *et al.*, 1991). The inhibitory effect of AELs on PI-PLC is believed to be responsible for a decrease in the production of InsP_3 (Powis *et al.*, 1992a; Seewald *et al.*, 1990). However, inhibition of PI-PLC may not be the critical cellular lesion, since lyso-PAF (**Figure 14**), which is at least 10 to 15 times less cytotoxic than ET18-OCH_3, was of similar potency to ET18-OCH_3 in inhibition of PI-PLC (Powis *et al.*, 1992b). ET18-OCH_3 inhibited PI-3 kinase in purified preparations and cell lysates, and reduced the production of 3-phosphorylated inositol lipids after platelet-derived growth factor (PDGF) stimulation of NIH 3T3 cells (Berggren *et al.*, 1993). Inasmuch as PI-3 kinase activation alone may not be sufficient to initiate cell proliferation (Parker and Waterfield, 1992), it is not known what role any inhibition of PI-3K activation by AELs plays in their antiproliferative activity.

The mechanisms by which AELs disrupt cellular signaling processes and their contributions to the inhibitory effect on cell proliferation are currently unclear. However, it appears that AELs could act at a number of key stages in perhaps more than one signaling pathway. These include receptor activation, secondary messenger generation, interaction between signaling mediators, and protein phosphorylation. A long-unresolved puzzle is what are the primary target(s) for AELs' antitumor action—which signaling pathway and what step, providing interference in signal transduction by AELs may be the principal mechanism

underlying their antitumor activities as currently suggested.

1.7.4 Hypotheses

Initially, we hypothesized [1] the cellular ether lipid content and/or composition determined cell susceptibility to ET18-OCH_3; [2] the rate of ET18-OCH_3 metabolism in cells accounted for its antitumor activity; and [3] the perturbation of cellular phospholipid metabolism by ET18-OCH_3 underlay the mechanism of its antiproliferative action.

After examining the above hypotheses and questioning the relationship between cellular ether glycerophospholipid content/composition and sensitivity of cancer cells to ET18-OCH_3, the relationship between cell sensitivity and cellular metabolism of this AEL, and the relationship between the sensitivity and modulation of cellular phospholipids by this ether compound, we further hypothesized that ET18-OCH_3 is likely to interfere with a widely used signal transduction mechanism that initiates proliferation since this AEL inhibits proliferation of a wide range of cancer cells. Two such pathways that may be involved are the Ras/Raf/MEK/ERK cascade and the PKC-dependent signaling pathway.

1.8 Research Aims

The overall objective of this research is to study mechanisms by which ET18-OCH_3 inhibits the proliferation of cancer cells. To achieve this general objective, I have divided our research into two sections and specifically investigated the following issues.

Section A: Lipid Composition, Content and Metabolism

[1] Does the content or composition of cellular ether phospholipids correlate with the

susceptibility of the cell to ET18-OCH_3?

[2] Is there any difference in the metabolism of ET18-OCH_3 between sensitive and resistant cell lines? If there is, do the differences correlate with the cell sensitivity to ET18-OCH_3?

[3] Does ET18-OCH_3 disturb the metabolism of cellular phospholipids? And, could the observed disturbance account for the growth-inhibitory action by this antitumor ether lipid?

Section B: Signal Transduction

[4] Does ET18-OCH_3 interfere in cellular signal transduction? And could the interference, if any, be responsible for the inhibition of cell proliferation? The studies on these issues have specifically been focused on the effect of ET18-OCH_3 on the Ras/Raf/MEK/ERK cascade and PKC-dependent phosphorylation of endogenous proteins in cultured MCF-7 cells.

2 MATERIALS

2.1 Cell Lines, Media and Other Tissue Cultures Materials

MCF-7 (human breast adenocarcinoma), A549 and A427 (human lung carcinoma), T84 (human colon carcinoma), and Malme 3M (human malignant melanoma) cell lines were grown from frozen stocks originally obtained from **American Type Culture Collection** (ATCC) (Rockville, Maryland).

Fetal bovine serum (FBS) (Cellect Gold, # 29-167-54) was from **ICN**

Pharmaceuticals (Montreal, Quebec, Canada).

Bovine serum albumin (BSA) (# A-9418) was purchased from **Sigma Chemical Co.** (St. Louis, Missouri).

All tissue culture media and subculturing reagents were obtained from **Gibco BRL** (Burlington, Ontario, Canada).

Tissue culture ware (Falcon) was purchased from **Baxter Canlab Diagnostics Incorporation** (Winnipeg, Manitoba, Canada).

2.2 Antibodies and Related Reagents

Anti-Raf-1 antiserum (SP63) was generously provided by Dr. **U. Rapp** (National Cancer Institute, NIH).

Horseradish peroxidase (HRP)-conjugated goat anti-mouse IgG (H+L) (# 170-6516) and HRP-goat anti-rabbit IgG (H+L) (# 170-6515) was obtained from **BioRad Laboratories** (Hercules, California).

Rabbit polyclonal anti-ERK1 [ERK1 (c-16), # sc-93 AC], rabbit polyclonal anti-ERK2 [ERK2 (c-14), # sc-154 AC], rabbit polyclonal anti-MEK [MEK (c-18), # sc-219], rabbit polyclonal anti-MEK1 [MEK-1 (12-B), # sc-436], mouse anti-PKC monoclonal IgG_{2a} [PKC (MC5), # sc-80], rabbit polyclonal anti-Raf-1 [Raf-1 (c-12), # sc-133], rat anti-Ras monoclonal IgG_1 [v-H-ras (259), # sc-35 AC], rabbit polyclonal anti-14-3-3 proteins [14-3-3β (K-19), # sc-629], protein A-agarose (# sc-2001) and protein G plus-agarose (# sc-2002) was purchased from **Santa Cruz Biotechnology, Inc.** (La Jolla, California).

Rabbit anti-PKC-δ anti-peptide Ab (# 3197SA) was a product of **Gibco BRL**

(Burlington, Ontario, Canada). All other anti-PKC isoform Abs (# S85080) were purchased from **Transduction Laboratories** (Lexington, Kentucky).

Sheep polyclonal anti-EGF receptor (α-h EGFr, # 06-129), mouse anti-phosphotyrosine monoclonal $IgG_{2b\kappa}$ (# 05-321) and rabbit polyclonal anti-Ras (# 06-226) were from **Upstate Biotechnology Inc.** (Lake Placid, New York).

Mouse anti-ERK1+2 monoclonal IgG_1 (anti-MAPK, # 03-6600), goat anti-rabbit IgG (H+L) (# 62-6100), rabbit anti-mouse IgG (H+L) (# 61-6500), protein A Sepharose 4B (# 10-1141), rec-protein G Sepharose 4B (# 10-1241) and HRP-rabbit anti-sheep IgG (H+L) (# 61-8620) were obtained from **Zymed Laboratories, Inc.** (South San Francisco, CA).

2.3 Radiochemicals and Related Reagents

CDP-[*methyl*-^{14}C]choline (# CFA 528), [*methyl*-^{3}H]choline chloride (# TRK 593), [5-^{3}H]cytidine 5'-triphosphate (# TRK 339), [1-^{3}H]ethan-1-ol-2-amine hydrochloride (# TRK 462), 1-*O*-[^{3}H]octadecyl-2-*O*-methyl-*sn*-glycero-3-phosphocholine (# TRQ 5643), phosphoryl[*methyl*-^{14}C]choline (# CFA 525), [1-^{14}C]oleoyl-CoA (# CFA 634), 1-stearoyl-2-[1-^{14}C]arachidonoyl-glycerophosphocholine, the enhanced chemiluminesence (ECL) solutions (# RPN 2109) and the cAMP[^{3}H] assay kit (# TRK 432) were purchased from **Amersham International** (Oakville, Ontario, Canada).

Cytidine diphosphocholine[*methyl*-^{14}C] (# NEC-575), [1,2,3-^{3}H]glycerol (# NET-848) and [1-^{14}C]oleoyl CoA (# NEC-651) were obtained from **Du Pont** (Mississauga, Ontario, Canada).

Adenosine 5'-[γ-^{32}P]triphosphate (# 35001x), CDP-[1,2-^{14}C]ethanolamine (# 17150),

[1,2-^{14}C]ethanolamine HCl (# 17202), [^{32}P]orthophosphate (# 64014RT) and Ecolite scintillation solution (# 882475) were products of **ICN Biomedicals** (St. Laurent, Quebec, Canada).

Kodak GBX developer + replenisher (# 252320) was purchased from **Picker** (Ontario, Canada).

2.4 Enzymes, Substrates and Inhibitor Peptides

Active recombinant ERK2 was generously provided by **Dr. N. Ahn** (University of Colorado, Boulder).

PKI (# H-3234) and Kemptide (# M-1510) were obtained from **Bachem** (Torrance, California).

Phospholipase C (# 691 950) and D (# 430 331) were purchased from **Boehringer Mannheim** (St. Laval, Quebec, Canada).

Full length MEK-1 [MEK (FL), a 55-kDa polyhistidine fusion protein, # sc-4025] was obtained from **Santa Cruz Biotechnology, Inc.** (La Jolla, California).

Choline kinase (from *Saccharomyces cerevisae*, EC 2.7.1.32, # C-7635)was a product of **Sigma Chemical Co.** (St. Louis, Missouri).

2.5 Chemicals

Bio-Lyte 3/10 (# 163-1112), Bio-Lyte 6/8 (# 163-1162), Bio-Lyte 5/7 (# 163-1152) were purchased from **BioRad Laboratories** (Mississauga, Ontario). Pharmalyte 4/6.5 (# 1818-116) was obtained from **Pharmacia Biotech Inc.** (Baie D'Urfé, Quebec).

Acrylamide (Serva, # 10675), ammonium persulfate (Serva, # 13375), N,N'-methylene bisacrylamide (Serva, # 29195), sodium dodecyl sulfate (SDS) (Serva, # 20760), N,N,N',N'-tetramethyl ethylenediamine (TEMED) (Serva, # 35925) were obtained from **Crescent Chemical Co., Inc.** (New York).

Ammonium molybdate (# A674-500), benzene (# B-245), hydrogen chloride (HCl) and 70% perchloric acid ($HClO_4$) were from **Fisher Scientific Company** (Fair Lawn, New Jersey).

Diethyl ether (# 31700) and ethyl acetate (# 45760) were obtained from **Fluka** (CH-9470 Buchs, Switzerland).

12-*O*-tetradecanoylphorbol 13-acetate (TPA, # P-1680) and 4-α-TPA (# P-8880) were from **LC Laboratories** (Woburn, Massachusetts).

Phenol (AR, loose crystals, # 2000) and n-Propyl alcohol (AR, # 7169) were obtained from **Mallinckrodt** (Parts, Kentucky).

ET18-OCH_3 was a product of **MedMark Pharmaceuticals** (Gruenwald, Germany).

Oleic acid was obtained from **Nu Chek Prep** (Elysian, Minnesota).

Vitride reducing reagent [sodium bis(2-methoxyethoxy)aluminum hydride, $NaAlH_2(OCH_2CH_2OCH_3)_2$] was from **Eastman Kodak** (Rochester, New York).

Ro 31-8220 was a gift from **Roche** (Welwyn, Herts, United Kingdom).

CDP-choline, 1,2-dioctanoyl-*sn*-glycerol (DiC_8), other neutral lipids and purified phospholipids were obtained from **Serdary Research Laboratories** (St. Catherines, Ontario, Canada).

ATP (# A 6144), calmidazolium (# C 3930), CDP-ethanolamine (# C 0456), choline

chloride (# C 7017), CTP (# C 1506), dansyl chloride (# D 2625), 1,2-dichlorofluorescein (# D 6665), dimethyldichlorosilane (# D 3879), EGF (# E 1264), ethanolamine (# E 9508), N-[2-hydroxyethyl]piperazine-N'-[2-ethanesulfonic acid] (HEPES, # H 089), 1-*O*-hexadecyl-2-*O*-methylglycerol (# H 3144), malachite green base (# M-8635), myelin basic protein (MBP, # M 1891), ninhydrin (# N 4876), nonidet P-40 (NP-40, # N 6507), oleyl alcohol (# O 8880), phosphorylcholine chloride (# P 0378), phosphorylethanolamine (# P 0503), sodium orthovanadate (Na_3VO_4, # S 6508), Trizma base (# T 1503), Trizma hydrochloride (Tris-HCl, # T 3253), Trypan Blue (# T 6146), Triton X-100, Tween 20, Tween 40 and all protease inhibitors such as aminoethylbenzenesulfonyl fluoride (AEBSF, # A 8456), aprotinin (# A 1153), benzamidine (# B 6506), leupeptin (# L 2023), phenylmethylsulfonyl fluoride (PMSF, # P 7626) were purchased from **Sigma Chemical Co.** (St. Louis, Missouri).

All other reagents were from **Baxter Canlab Diagnostics Incorporation** (Winnipeg, Manitoba, Canada).

2.6 Equipment

Model ZM Coulter Counter (Coulter Electronics Inc.), Model TMS-F Microscope (Nikon, Japan), L-80 Ultracentrifuge (Beckman), J2-HS centrifuge (Beckman), LS3801 Liquid Scintillation System (Beckman), 1271 Riagamma Automatic Gamma Counter (LKB), U-2000 Double-beam Spectrophotometer (Hitachi, Tokyo), Cell Sorter EPICS 753 and the PARA 1 analysis software (Coulter Electronics Inc.), and Model PDI 325oe High Resolution Color Scanner (Protein + DNA Imageware Systems, Huntigton Station, New York) were utilized for this thesis research.

2.7 Water and Buffers

Distilled deionized water (DDW) (conductance ≤-18 μΩ) from a Mili Q Plus water purification system was used throughout these studies.

Buffer A: 20 mM Tris-HCl (pH 7.4), 150 mM NaCl, 2 mM EGTA, 100 mM β-glycerophosphate, 1 mM Na_3VO_4, 0.1 mM PMSF, 0.2 mM AEBSF, 0.2 mM benzamidine, 10 μg/ml aprotinin, and 10 μg/ml leupeptin.

Buffer B: **(For MAPK assay)** Buffer A plus 1 mM dithiothreitol (DTT) and minus NaCl.

Buffer C: **(For MAPK and MEK immunoprecipitation)** Buffer A plus 1% (w/v) Triton X-100 and 0.5% (w/v) NP-40.

Buffer D: **(Lysate buffer for Ras studies)** 20 mM Tris-HCl (pH 7.4), 5 mM $MgCl_2$, 150 mM NaCl, 0.5% (w/v) NP-40, 1% (w/v) Triton X-100, 0.1 mM PMSF, 0.2 mM benzamidine, and 10 μg/ml each of aprotinin and leupeptin (Li *et al.*, 1992).

Buffer E: **(Washing buffer for Ras studies)** 50 mM Tris-HCl (pH 7.4), 5 mM $MgCl_2$, 150 mM NaCl, and 0.1% (w/v) Triton X-100 (Downward *et al.*, 1990; Satoh *et al.*, 1990a).

Buffer F: **(Eluting buffer for Ras studies)** 20 mM Tris-HCl (pH 7.4), 20 mM EDTA, 2% SDS, and 0.5 mM each of GDP and GTP (Satoh *et al.*, 1990b).

Buffer G: **(For EGFr studies)** 10 mM HEPES (pH 7.5), 10 mM NaCl, 1 mM EGTA, 0.5 mM Na_3VO_4, 100 mM β-glycerophosphate, 0.1 mM PMSF, and 10 μg/ml each of aprotinin and leupeptin **(hypotonic HNG buffer)**.

Buffer H: **(For EGFr studies)** 50 mM HEPES (pH 7.5), 125 mM NaCl, 1 mM

EGTA, 0.5 mM Na_3VO_4, 100 mM β-glycerophosphate, 1% (w/v) Triton X-100, 0.1 mM PMSF, and 10 μg/ml each of aprotinin and leupeptin (**HNG buffer**).

Buffer I: **(For Raf translocation studies)** 25 mM HEPES (pH 7.4), 100 mM β-glycerophosphate, 2 mM EDTA, 0.1 mM PMSF, 0.1 mM AEBSF, 0.2 mM benzamidine, and 10 μg/ml each of aprotinin and leupeptin (Wartmann *et al.*, 1994).

Buffer J: **(For Raf translocation studies)** Buffer I plus 1% Triton X-100 (Wartmann *et al.*, 1994).

Buffer K: **(For Raf kinase assay)** 20 mM Tris-HCl (pH 7.4), 2 mM EDTA, 50 mM β-glycerophosphate, 1 mM Na_3VO_4, 1% Triton X-100, 10% glycerol, 1 mM PMSF, and 10 μg/ml each of aprotinin and leupeptin (Kharbanda *et al.*, 1994).

Buffer L: **(For Raf kinase assay)** 20 mM Tris-HCl (pH 7.4), 50 mM β-glycerophosphate, 1.5 mM EGTA, 1 mM DTT, and 0.03% Brij-35 (Kharbanda *et al.*, 1994).

Buffer M: **(For PKC studies)** Buffer A plus 0.5% NP-40 and minus NaCl.

Buffer N: **(For PKC translocation studies)** Buffer M without NP-40.

Buffer O: **(For PKC translocation studies)** Buffer N plus 1% Triton X-100 and 0.5% NP-40.

Hanks' balanced saline solution (HBSS): 0.04% KCl, 0.8% NaCl, 0.006% KH_2PO_4, 0.009% $Na_2HPO_4 \cdot 7H_2O$, and 1% D-glucose (all were w/v).

Homogenization buffer: 0.25 M sucrose, 10 mM Tris-HCl (pH 7.4) and 1 mM EDTA.

Kreb's buffer: 10 mM HEPES (pH 7.5), 25 mM $NaHCO_3$, 4.7 mM KCl, 118 mM NaCl, 1.2 mM $MgSO_4$, 1.4 mM $CaCl_2$ and 25 mM glucose. [Note: The order of addition of

chemicals to prepare the Kreb's buffer is important, i.e. add HEPES, $NaHCO_3$, KCl, NaCl, $MgSO_4$, $CaCl_2$ and glucose sequentially while vigorously stirring, then adjust pH to 7.35 followed by filtering through 0.2 μm filter; the pH will increase to ~7.5].

LiCl buffer: (**For Raf kinase assay**) 0.5 M LiCl, 100 mM Tris-HCl, pH 7.4 (Kharbanda *et al.*, 1994).

$MgCl_2$ buffer: (**For Raf kinase assay**) 20 mM Tris-HCl (pH 7.4), 10 mM $MgCl_2$ (Kharbanda *et al.*, 1994).

PBS: 8 g NaCl, 0.2 g KCl, 1.15 g $Na_2HPO_4 \cdot 7H_2O$, 0.2 g KH_2PO_4 in one liter.

PBS-EDTA buffer : PBS containing 2 mM EDTA (Edelmann *et al.*, 1996).

2.8 Miscellaneous

Cellulose coated plates (Avicel, 250 microns, # 05011) were from **Analtech, INC.** (Newark, Delaware).

Silica gel K6 thin-layer chromatography (TLC) plates (# 4860 820) was purchased from **Baxter Canlab Diagnostics Incorporation** (Winnipeg. Manitoba, Canada).

Analytical grade anion exchange resin (AG 1-X4 Resin, 200-400 mesh, chloride form, # 140-1351), low and high molecular weight protein standards (# 161-0304 and 161-0303), 0.2 μm nitrocellulose membrane (# 162-0097) and cellophane membrane (# 165-0963) were obtained from **BioRad Laboratories** (Richmond, California).

PEI cellulose TLC plates (# 22023849) were purchased from **E. Merck** (Darmstedt, Germany).

Coomassie protein assay solution (# 23200) was from **Pierce** (Rockford, Illinois).

Jurkat and HeLa cell lysates were obtained from **Transduction Laboratories** (Lexington, Kentucky).

Whatman P81 filter paper (# 3698-021) was purchased from **Mandel Scientific Company Ltd.** (Guelph, Ontario)

Macroporous filter (41 μm mesh) was generously provided by Dr. E. Rector.

3 EXPERIMENTAL METHODS

3.1 Cell Culture

Cells were cultured in the appropriate media supplemented with 10% fetal bovine serum, penicillin (50 U/ml), streptomycin (50 μg/ml) and fungizone (0.3 μg/ml) at 37°C in 5% CO_2/95% humidified air atmosphere as previously described (Lu and Arthur, 1992a; 1992b). A427 cells were cultured in Eagle's minimum essential medium with nonessential amino acids and pyruvate as recommended by ATCC, A549 cells in Ham's F-12 medium, Malme 3M cells in McCoy's 5a medium, MCF-7 cells in Dulbecco's modified Eagle medium (DMEM), and T84 cells in a 1:1 mixture of DMEM and Ham's F-12 medium.

3.2 Cellular Ether Glycerophospholipid and Sensitivity of the Cells to ET18-OCH_3

To explore a putative relationship between cellular ether glycerophospholipid content/composition and sensitivity of cancer cells to ET18-OCH_3, we determined the cellular ether glycerophospholipid content and composition in five epithelial cancer cell lines (A427,

A549, Malme 3M, MCF-7 and T84) with differential susceptibility to ET18-OCH_3.

3.2.1 Determination of cell sensitivity to the growth-inhibitory activity of ET18-OCH_3 (contribution by Xiaoli Lu)

Stock solutions of ET18-OCH_3 (2 mg/ml) were prepared in DMEM containing 0.5 mg/ml BSA (DMEM/BSA) and stored at -20°C. Working solutions of growth media supplemented with the required concentrations of ET18-OCH_3 were prepared fresh.

Cells were seeded in 24-well plates and grown to log phase. At 0 time, the cell number was determined with a Model ZM Coulter Counter after cell detachment with 0.25% trypsin and 1 mM EDTA·4Na in HBSS for approximately 2 min. Cells in parallel plates were continuously cultured in growth media containing 0-15 μg/ml ET18-OCH_3 for 24 h, followed by determination of the cell number as described above. Increases in cell number of cultures at different concentrations of ET18-OCH_3 were plotted against the reference value (100%) of control cells (no ET18-OCH_3) (**Figure 17**).

3.2.2 Determination of cellular phospholipid composition

Extraction of lipids from cells

Cells were detached with trypsin (see **Section 3.2.1**) and pelleted by centrifugation (1000 rpm for 5 min). After two washes with HBSS and resuspension in a known volume of HBSS, the cells were dispersed with a 21-gauge needle and aliquots were taken for determination of cell number. Lipids were extracted from the remainder of cells (Lu and Arthur, 1992a) as described below. Cells were extracted once with 5 ml chloroform/methanol

(1:1, v/v) and twice with chloroform/methanol (2:1, v/v). The extracts were combined in silated tubes and dried under a stream of nitrogen. Chloroform, methanol and 0.9% KCl were added to give a biphasic system of chloroform/methanol/0.9% KCl (4:2:3, v/v). After thorough mixing and centrifugation, the upper phase was removed and the lower phase was stored at -20°C for lipid analysis.

Separation of phospholipids on TLC

Phospholipids were separated by thin-layer chromatography (TLC) on Whatman K6 plates activated at 110°C for 1 h with a solvent system of chloroform/methanol/water/acetic acid (50:37.5:2:3.5, v/v) (Arthur *et al.*, 1991). The plates were sprayed with 0.25% 1,2-dichlorofluorescein in ethanol and phospholipid bands visualized under UV light. Individual phospholipids were identified by spotting authentic phospholipid markers as references in a parallel lane on the TLC plates.

Extraction of lipids from TLC plates

The phospholipids were extracted from silica gel by the method of Arvidson (1968). Briefly, lipid bands were scraped into tubes and extracted with 4 ml of chloroform/methanol/water/acetic acid (50:39:10:1, v/v) three times. One third volume of 4 M NH_4OH was added to the combined extract. After thorough mixing and phase separation, the upper phase was removed. Half the volume of methanol/water (1:1, v/v) was added to the lower phase followed by thorough mixing and phase separation by centrifugation. After removal of the upper phase by suction, the extract (lower phase) was dried under a stream of nitrogen and resuspended in a known volume of chloroform/methanol (2:1, v/v).

Phospholipid determination

Phospholipids were quantitated by determination of the released phosphate from phospholipids. The lipid phosphate content was measured by a modification of the malachite green method (Zhou and Arthur, 1992a). Briefly, phospholipids extracted from silica gel were completely digested with perchloric acid (0.5-1.0 ml) at 160°C. Tubes containing perchloric acid alone were subjected to digestion and used as blanks. Aliquots of the digests were transferred into tubes and distilled deionized water (DDW) was added to bring the volume to 0.4 ml. After mixing, 2 ml of freshly-prepared 0.4% malachite green working solution was added to each tube followed by immediate vortexing. The tubes were allowed to stand for 20 min at room temperature. The absorbance (OD) was read at 660 nm in a Hitachi U-2000 double-beam spectrophotometer with DDW as reference using 1-cm glass cuvettes. ΔOD was obtained by subtracting the blank from sample OD values. Quantities of phospholipids were calculated from standard curves plotted for each experiment.

3.2.3 Determination of subclass composition of cholineglycerophospholipids (CGP) and ethanolamineglycerophospholipids (EGP)

To quantitate proportions of diacyl, alkylacyl and alkenylacyl subclasses of CGP and of EGP, we employed alkaline hydrolysis or sequential hydrolyses by 0.11 *N* NaOH and 0.01 *N* HCl to lipid extracts. Mild alkaline hydrolysis destroys all ester bonds and leaves the ether (alkyl and alkenyl) linkages intact. Therefore, we could convert ether (alkylacyl and alkenylacyl) phospholipids to lysophospholipids and extract them into the organic phase. The difference between the remainder of phospholipids after this hydrolysis and the initial

quantities represented the amount of diacyl (i.e., ester) phospholipids. Acid hydrolysis destroys the alkenyl bond but leaves the ester and alkyl bonds intact. Thus the remainder of phospholipids after the double hydrolyses represented the alkylacyl proportion in phospholipids, whereas the difference between the single and double hydrolyses represented the alkenylacyl component in the phospholipids.

These selective hydrolytic procedures were modifications (Zhou *et al.*, 1992b) of those described by Wells and Dittmer (1966). For alkaline hydrolysis, aliquots of the individual phospholipids extracted from TLC plates were dried under nitrogen and dissolved in 1 ml of chloroform/methanol (1:4, v/v). One hundred microliters of 1.2 *N* NaOH in methanol/water (1:1, v/v) were added. After mixing, the tubes were covered with Teflon and incubated for 30 min at 37°C in a shaking water bath. In control tubes, NaOH was replaced with 1.2 M NaCl. The hydrolytic mixture was neutralized with 150 µl 1 *N* acetic acid. The lysophospholipids produced were extracted with 2 ml chloroform/methanol (9:1, v/v). After mixing, 2 ml chloroform and 2.8 ml 0.9% KCl were added. The two phases were clarified by centrifugation and the upper layer was aspirated. The phospholipid in aliquots of the lower phase was quantitated by the malachite green method (see **Secetion 3.2.2**). Alternatively, aliquots of the lower layer after alkaline hydrolysis were subjected to acid hydrolysis. The lipids were dried under a stream of nitrogen and dissolved in 1.6 ml of chloroform/methanol (5:11, v/v). 0.4 ml of 25 mM $HgCl_2$ in 50 mM HCl was added and subsequently incubated for 30 min at 37°C in a shaking water bath. In control experiments lipids were incubated with 0.4 ml of 0.9% NaCl. Lipids were extracted with 3.5 ml chloroform and 0.9 ml methanol. After mixing, 2.6 ml of 0.9% KCl were added. Upon mixing, the two phases were clarified

by centrifugation. The upper phase was removed by suction and aliquots of the lower phase were used for determination of lipid phosphate by the malachite green method (see **Section 3.2.2**). The values obtained from control experiments for both hydrolyses were used to correct for losses during manipulations.

3.3 Metabolism of ET18-OCH_3 and Inhibition of Cell Proliferation

(contribution in part by Xiaoli Lu and Dawn Kardash)

To test whether the inhibition of cell growth was due to ET18-OCH_3 *per se* or its metabolites, we examined the metabolism of ET18-OCH_3 in three epithelial cancer cell lines (A427, A549 and MCF-7) and the inhibition of cell proliferation by either ET18-OCH_3 or its major metabolite 1-*O*-octadecyl-2-*O*-methylglycerol (OMG).

3.3.1 Determination of the distribution of radiolabel from [^{3}H]ET18-OCH_3 to other lipid products

Log-phase cells growing in 100-mm dishes were incubated with [^{3}H]ET18-OCH_3 (25 μCi/dish) for 3, 6 or 12 h. At the end of the incubation, the cells were washed twice with medium and detached with trypsin. Aliquots were taken for determination of the cell number. Lipids were extracted from the remainder of cells and the phospholipids were separated by TLC using chloroform/methanol/water/acetic acid (50:37.5:2:3.5, v/v) as described in **Section 3.2.2**. In this system the ET18-OCH_3 band overlapped with the lysophosphatidylcholine and sphingomyelin bands. These three phospholipids were extracted from the gel and separated with chloroform/methanol/water/acetic acid (50:30:8:6, v/v). Neutral lipids were resolved

with hexane/ether/methanol/acetic acid (70:30:5:1, v/v). Authentic lipid markers, if necessary, were added to samples prior to loading. Lipid classes were extracted from the gel (Arvidson, 1968) and stored at -20°C. In all experiments, [^{3}H]ET18-OCH$_3$ was mixed with markers and applied to the blank lanes. The bands appearing on these lanes were treated in an identical manner as the samples and used to correct for background and radiopurity.

3.3.2 Preparation of 1-O-[^{3}H]octadecyl-2-O-methylglycerol (OMG)

[^{3}H]ET18-OCH$_3$ (0.25 μCi/μg) was subjected to Vitride reduction (**Box 1**) according to the protocol of Snyder *et al.* (1971). All the tubes used in the reaction were coated with dimethyldichlorosilane. Half a milliliter of Vitride reagent [$NaAlH_2(OCH_2CH_2OCH_3)_2$, 70% in benzene] was added to the labeled ET18-OCH$_3$ sample that was dissolved in 2.5 ml of diethyl ether containing 20% (v/v) benzene. The reaction mixture was then incubated in a closed tube placed in a shaking water bath at 37°C for 30 min. Products were extracted with

Box 1. Vitride reduction

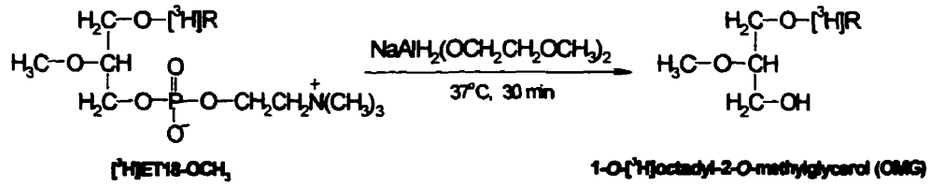

[^{3}H]ET18-OCH$_3$ 1-O-[^{3}H]octadecyl-2-O-methylglycerol (OMG)

diethyl ether after the addition of 6 ml of 4% acetic acid. Lipid extracts were fractionated by TLC with hexane/diethyl ether/methanol/acetic acid (70:30:5:1, v/v). OMG was extracted (Arvidson, 1968) and dried under a stream of nitrogen. The lipid was dissolved in chloroform and stored at -20°C.

3.3.3 OMG incorporation into and metabolism in cells and its effect on cell proliferation

Log-phase cells growing in six-well plates were incubated in media with 1 or 5 μg/ml of [^{3}H]OMG (0.25 μCi/μg) dissolved in ethanol. The final concentration of ethanol in media was less than 0.05% (v/v). Cells in control wells received media with the same amount of ethanol, but without OMG. At selected intervals, the cells were washed twice with HBSS and detached with trypsin. Aliquots were taken for determination of cell number. The remainder of cells were pelleted and dissolved in 1% SDS in 0.3 *N* NaOH (Lu and Arthur, 1992a). The associated radioactivity was determined by scintillation counting with Ecolite as the scintillant.

The metabolism of OMG in cells was studied using a similar method as described in **Section 3.3.1** except that the lipids extracted from cells were separated on TLC with a solvent system of hexane/ether/methanol/acetic acid (70:30:5:1, v/v).

3.4 Relationship Between Effects of ET18-OCH_3 on Phospholipid Metabolism and Cell Proliferation

We investigated the effect of ET18-OCH_3 on the metabolism of cellular

phospholipids and its possible contribution to inhibition of cell proliferation. A sensitive cell line (MCF-7) and a relatively resistant cell line (A549) were used for these studies.

3.4.1 Determination of [^{3}H]glycerol incorporation into glycerolipids in ET18-OCH_3-treated and untreated cells

Log-phase cells growing in six-well plates were labeled with [1,2,3-^{3}H]glycerol (20 μCi/well) in the presence or absence of 5 μg/ml ET18-OCH_3. At selected intervals, the cells were washed three times with HBSS and harvested with trypsin. Aliquots were taken for determination of the cell number. The remainder of the cells were pelleted and cellular lipids were extracted and separated by TLC as described in **Section 3.2.2.** To determine the effect of ET18-OCH_3 on the uptake of glycerol, cells were incubated with 2 μCi/ml of [^{3}H]glycerol in the presence or absence of 5 μg/ml of ET18-OCH_3 for 6 h, washed three times with HBSS, and lysed with 1% SDS in 0.3 *N* NaOH. The radioactivity in the lysates was determined by scintillation counting.

3.4.2 Determination of incorporation of [^{3}H]choline or [^{3}H]ethanolamine into PtdCho or PtdEtn and their water-soluble metabolites in the ET18-OCH_3-treated and untreated cells

Log-phase cells growing in six-well plates were incubated with [^{3}H]choline (10 μCi/well for A549 cells and 5 μCi/well for MCF-7 cells), or with [^{3}H]ethanolamine (5 μCi/well) for 30 min. The cells were washed three times with HBSS and incubated in fresh media in the presence or absence of 5 μg/ml ET18-OCH_3. At selected times, the cells were

harvested with trypsin and aliquots were used for determination of cell number. The remainder of cells were pelleted and extracted into a biphasic system. Phospholipids in the organic phase were separated as described in **Section 3.2.2.** The metabolites in the aqueous phase were resolved using the method of Weinhold *et al.* (1991). Briefly, aliquots of the aqueous phase were dried and redissolved in water; after the addition of authentic standards, the metabolites were separated on TLC plates with a solvent system of methanol/0.15 M NaCl/28% NH_4 (10:10:1, v/v). The lipid (PtdCho and PtdEtn) and their metabolite bands were visualized in an iodine chamber. The associated radioactivity was determined by scintillation counting.

3.4.3 Quantitation of the mass of water-soluble choline and ethanolamine metabolites in the ET18-OCH_3-treated and untreated cells

Extraction of water-soluble metabolites from cells

Log-phase cells in 150-mm dishes were incubated in the presence or absence of 5 μg/ml ET18-OCH_3. At selected times, the cells were washed, harvested, pelleted and extracted with chloroform/methanol (2:1, v/v) as described in **Section 3.2.2.** The cell pellet obtained after the last extraction was extracted three times with 20% ethanol (Tijburg *et al.*, 1988). The chloroform/methanol extracts were dried under nitrogen and resuspended in a biphasic system of chloroform/methanol/water (4:2:3, v/v). The upper phase was removed and combined with the ethanol extract. The lower phase was washed with an equal volume of water/methanol (1:1, v/v, pH 9.0, adjusted with 1 *N* NaOH). The combined upper phases were dried under reduced pressure and redissolved in 4 ml DDW. The pH was adjusted to

8.5 with 1 *N* KOH.

Conversion of AG 1-X4 resin from Cl^- form to formate form

Conversion of AG 1-X4 resin from the Cl^- to formate form was conducted according to the instructions of the manufacturer (BioRad). First, the resin was converted from the Cl^- form to the OH^- form using 20 bed volumes of 1 *N* NaOH followed by rinsing with at least 4 bed volumes of DDW until the pH of the eluate was less than 9.0. Next, the OH^- form was converted to the formate form by running 2 bed volumes of 1 *N* formic acid at a flow rate of 2 cm bed per min until the pH was less than 2. Subsequently, the column was rinsed with 4 bed volumes of DDW until the pH was greater than 4.8. The resin was then packaged into small columns (1 x 23 cm). The columns were flushed with DDW until the base line was stable as monitored by UV absorbance at 340 nm.

Fractionation of water-soluble metabolites

The extracts containing water-soluble metabolites were chromatographically separated on the formate form of AG1-X4 resin into three fractions: choline (Cho) + ethanolamine (Etn), phosphocholine (*P*Cho) + phosphoethanolamine (*P*Etn), and CDP-Cho + CDP-Etn (Sundler, 1973). After loading the samples on the resin, the column was eluted with a linear gradient of 0-0.02 M formic acid in a total volume of 300 ml at a flow rate of 35 drops/min (~2.1 ml/min). The UV absorbance of the eluate was monitored at 340 nm. The eluate was collected in tubes (5 ml each). Five microliters (~1-4 x 10^6 dpm/μl) of each of [*methyl*-^{3}H]choline chloride, phosphoryl[*methyl*-^{14}C]choline and CDP-[*methyl*-^{14}C]choline, or [1,2-^{14}C]ethanolamine HCl, CDP-[1,2-^{14}C]ethanolamine were added to samples prior to loading to monitor the patterns of elution and to assay recoveries. Aliquots were taken for

determination of the radioactivity associated with each fraction by scintillation counting. Tubes 2-8, 15-33, and 37-50 represented Cho + Etn, *P*Cho + *P*Etn, and CDP-Cho + CDP-Etn fractions, respectively. Eluates in each fraction were pooled and evaporated under reduced pressure to dryness and resuspended in 1 ml DDW.

Release of choline and ethanolamine

Choline and ethanolamine were released from the phosphobase and CDP-base by acid digestion (Tijburg *et al.*, 1988). Aliquots of each sample were transferred to screw-capped tubes. HCl was added to each tube to make the final concentration of HCl 6 *N* and the tubes were left at 110°C for 18 h. This treatment resulted in complete hydrolysis of all the phosphate esters and released the free choline and ethanolamine (Tijburg *et al.*, 1988). The acid was removed under a stream of nitrogen. One hundred microliters of DDW were added to each tube. The hydrolysates were used for determination of choline or ethanolamine.

Determination of choline

Quantitation of choline in aliquots was achieved after conversion to [^{32}P]*P*Cho according to Porter and Kent (1992). A 5x concentrated cocktail was prepared which contained 335 mM Tris-HCl (pH 8.5), 55 mM $MgCl_2$, 6.5 mM DTT, and 50 mM ATP (0.2 mCi/ml of [γ-^{32}P]ATP). The reaction mixture contained 30 µl samples or standards, 12 µl 5x cocktail and 18 µl (0.1 unit) reconstituted choline kinase solution. Standards for the calibration line were prepared as follows (Hildebrand, 1974): 0.014 g choline chloride was dissolved in DDW in a final volume of 10 ml. Before use, a series of dilutions were made to obtain a range of choline standards from 0.5 to 50 nmol. The reaction was started by the addition of the enzyme solution. The reaction mixtures were incubated at 37°C in a shaking

water bath for 30 min. The reaction was terminated by boiling for 2 min. After centrifugation, 5 µl of the supernatant and authentic phosphorylcholine were applied to cellulose TLC plates and developed in a solvent system of *n*-propanol/acetic acid/water-saturated phenol/water (2:1:1:1, v/v). The phosphocholine was visualized by using Dittmer spray[1]. The phosphocholine band was scraped and the associated radioactivity was determined by Cerenkov counting. The calibration line for quantitation of the [^{32}P]phosphocholine produced by choline kinase at various concentrations of choline in the presence of [γ-^{32}P]ATP is shown in **Figure 16a.**

Determination of ethanolamine

Ethanolamine was quantitated spectrofluorimetrically after conversion to dansyl-ethanolamine (Sundler *et al.*, 1975). Forty microliters of ethanolamine standards (0, 10, 50, 100, 250, 500, 1000 nmol), or samples containing free or liberated ethanolamine were transferred to screw-capped test tubes and dried under a stream of nitrogen. One milliliter of dansyl chloride in acetone (1 mg/ml) and an excess of solid Na_2CO_3 were added (i.e., Na_2CO_3 was added until a sediment appeared at the bottom of tubes). The reaction with dansyl chloride was allowed to proceed for at least 10 h in the dark at room temperature. After dansylation, acetone was evaporated under a stream of nitrogen, and nonpolar dansyl-

---

[1] Dittmer spray: The Dittmer spray was prepared as follows: One litre of 25 *N* sulphuric acid (70%, v/v) was added to 40.11 g MoO_3 followed by boiling till the MoO_3 was dissolved (**Solution A**). 1.78 g molybdenum was added to 500 ml of solution A which was gently boiled for 15 min. This solution was cooled at room temperature and decanted from any residue remaining (**Solution B**). To prepare the working spray, equal volumes of solution A and B were mixed with 2 volumes of DDW. If the solution was too blue, DDW was added, if too yellow, more of mixed solution A and B was added. A greenish-blue solution is ideal.

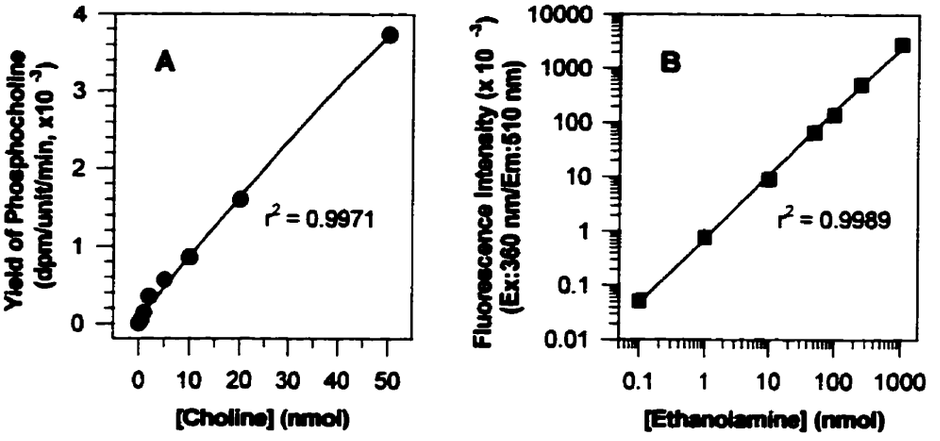

Figure 16. Standard curves. (*A*) The calibration line for quantitation of [^{32}P]*P*Cho produced by choline kinase (CK). A range (0.5 to 50 nmol) of Cho standards was used in the reaction catalyzed by CK (from *Saccharomyces cerevisae*) to convert Cho into [^{32}P]*P*Cho in the presence of [γ-^{32}P]ATP. The radioactivity associated with the *P*Cho band was determined after separation from [γ-^{32}P]ATP. The yield of [^{32}P]*P*Cho was plotted against the concentrations of Cho used in the reaction. The correlation index (r^2) of the calibration line was 0.9971. (*B*) The calibration line for quantitation of dansyl-Etn. A range (0.1-1000 nmol) of Etn standards was used for dansylation. The dansyl-Etn formed was separated by TLC, visualized under UV light, eluted from gel, and quantitated by spectrofluorometer with excitation at 360 nm and emission at 510 nm. The fluorescence density of the dansyl-Etn generated was plotted against the concentrations of Etn used in the reaction in the double log scales. The correlation index (r^2) of the calibration line was 0.9989.

derivatives were extracted into 1 ml of ethyl acetate. Dansyl-ethanolamine was then separated from dansyl chloride and other fluorescent products by TLC on silica gel K6 plates with a solvent system of ethylacetate/benzene (70:30, v/v), and visualized under UV light. Dansyl-ethanolamine was eluted from gel with benzene/methanol (90:10, v/v) and quantitated by spectrofluorimeter with excitation at 360 nm and emission at 510 nm. The calibration line for quantification of the produced dansyl-ethanolamine at various concentrations of ethanolamine in the dansylation reaction is shown in **Figure 16b**.

3.4.4 Determination of PtdCho and PtdEtn content in the ET18-OCH_3-treated and untreated cells

Cells were grown to the log phase in 150-mm dishes. On the day of the experiment, the cells were cultured in fresh media in the presence or absence of 5 μg/ml ET18-OCH_3. At selected times, the cells were washed and harvested with trypsin. Aliquots were taken for determination of the cell number. The remainder of cells were pelleted, lipids were extracted and fractionated by TLC, and the contents of PtdCho and PtdEtn were determined by the malachite green method (see **Section 3.2.2**).

3.4.5 Effect of oleic acid on ET18-OCH_3-induced inhibition of PtdCho synthesis and cell proliferation

To examine the effect of oleic acid on PtdCho synthesis and cell proliferation, log-phase MCF-7 cells in six-well plates were pre-labeled with [^{3}H]choline (10 μCi/ml/well) for 30 min followed by three washes with HBSS and incubation with various concentrations (0-

350 μM) of oleic acid in DMEM/FBS for 0.5-3 h. The cells were then washed and harvested with trypsin. The cell number and the radioactivity associated with each of *P*Cho, CDP-Cho and PtdCho fractions were determined as described in **Section 3.2.1** and **3.4.2**, respectively.

The oleic acid salt solution was prepared immediately prior to use. The required quantity of oleic acid (MW: 282.48) was weighed and dissolved in chloroform to yield an oleic acid solution of known concentration. A volume of oleic acid in chloroform containing the required quantity was transferred into a screw-capped tube and dried under a stream of nitrogen; 52 μl of 0.12 *N* KOH/95% ethanol was added to 6.25 μmol of oleic acid. This solution was mixed immediately and thoroughly, and dried under a stream of nitrogen. Then a known volume of a culture medium (e.g., 0.3-1.0 ml) was added to obtain the desired concentration of oleic acid solution by sonication and vigorous shaking; this oleic acid salt solution was ready to use.

The experiments were conducted using 75 μM oleic acid after preliminary studies indicated that this concentration of oleic acid did not affect cell growth. Log-phase MCF-7 cells in six-well plates were incubated with [^{3}H]choline (4 μCi/ml/well) for 3 h followed by three washes with HBSS. The cell number in parallel cultures was determined to obtain the initial cell number. The rest of the cells were incubated with either growth medium (control), growth medium with 75 μM of oleic acid, growth medium with 5 μg/ml of ET18-OCH_3, or growth medium with both oleic acid and ET18-OCH_3. After 12-h incubation, the cells were washed and harvested using trypsin. The cell number and the quantity of ^{3}H in PtdCho were determined as described in **Section 3.2.1** and **3.4.2**, respectively.

3.4.6 Preparation of subcellular fractions

Cells growing in 150-mm dishes were detached with trypsin, washed and dispersed in homogenization buffer (0.25 M sucrose, 10 mM Tris-HCl, 1 mM EDTA, pH 7.4). Aliquots were taken for the determination of cell number. The remainder of the cells were lysed by N_2 cavitation (Vallari *et al.*, 1989). Cells were placed in the Mini-Bomb cell disruption chamber. Tubes were rinsed with the homogenization buffer which was loaded to the chamber to bring the final volume to 14 ml. The cells were disrupted under 700 pounds (500 KPa) for 20 min. The mixture was centrifuged at 1,600 *g* (4,000 rpm in a JA 21 rotor, Bechman J2-HS centrifuge) for 10 min at 4°C to pellet nuclei, cell debris and unbroken cells. The supernatant was decanted into a tube and the pellet was disrupted once more followed by centrifugation as described above. This supernatant was combined with the first one. Subcellular fractions were isolated by differential centrifugation (Arthur *et al.*, 1985). The combined supernatant was centrifuged at 20,000 *g* (13,000 rpm in a Sorvall SS34/SS1) for 10 min at 4°C. The pellet was homogenized with 10 mM Tris-HCl (pH 7.4) and 0.25 M sucrose (**mitochondrial fraction**) and stored at -20°C. The supernatant was then centrifuged at 100,000 *g* (37,000 rpm in a Ti 70 rotor) for 1 h at 4°C. The resultant supernatant (**cytosol fraction**) was stored at -20°C. The pellet (**microsome fraction**) was homogenized and stored as described above.

The protein content of each fraction was determined by the method of Lowry *et al.* (1951) using BSA as standard. The samples or standards (0-100 μg) were pipetted into tubes, 0.1 ml of 5% sodium deoxycholate was added to each tube followed by the addition of DDW to bring the volume to 1 ml and mixing. After mixing equal volumes of 1% copper

sulphate and 2% potassium sodium tartarate, the solution was mixed with 2% sodium carbonate in 0.1 *N* NaOH at the ratio of 1:50 (v/v). Four milliliters of this mixed solution were added to each tube and mixed immediately. The tubes were left at room temperature for 10 min and 0.5 ml of the fresh diluted Folin Ciocalteau (phenol) reagent was added to each tube followed by instantaneous mixing. To stabilize the color, tubes were heated at 60°C for 10 min and then cooled. The absorbance was read at 730 nm.

3.4.7 Lipid metabolic enzyme assays

In all the following *in vitro* enzyme assays, aliquots of stock solutions of ET18-OCH_3 in DDW (50 or 250 μM) were added to yield the required final concentrations. The compound was preincubated with the assay mixture for 5 min prior to initiation of the reaction by the addition of radiolabeled substrates. Control assays did not have any ET18-OCH_3. Tubes without protein were used to correct for any non-enzymic reactions.

CDP-choline:1,2-diacylglycerol cholinephosphotransferase (EC 2.7.8.2) assay

The cholinephosphotransferase (CPT) activity was assayed as previously described (Arthur *et al.*, 1984). The reaction mixture (500 μl) contained 0-20 μM ET18-OCH_3, 100 mM Tris-HCl (pH 8.5), 5 mM DTT, 0.4 mM 1,2-diacylglycerol, 4 mM $MgCl_2$, 50 μg microsomal protein and 0.6 mM CDP[*methyl*-^{14}C]choline (0.12 μCi/μmol). The mixture was incubated in a shaking water bath at 37°C for 30 min. The reaction was terminated by the addition of 3 ml chloroform/methanol (2:1, v/v) and mixing. One milliliter of 0.9% KCl was added to the mixture followed by mixing and centrifugation at 2000 rpm for 5 min. The upper phase was removed by suction. The lower phase was washed twice with 2 ml of

methanol/0.3% KCl (2:5, v/v). The radioactivity in aliquots of the lower phase was determined by scintillation counting.

CDP-ethanolamine:1,2-diacylglycerol ethanolaminephosphotransferase (EC 2.7.8.1) assay

The ethanolaminephosphotransferase (EPT) activity was assayed in a similar fashion to CPT with 0.6 mM CDP[1,2-^{14}C]ethanolamine (0.13 μCi/μmol) instead of CDP-choline and with the inclusion of 2 mM Mn^{2+} in the reaction mixture. It is important to add $MnCl_2$ after the addition of DDW to the reaction mixture.

CTP:phosphocholine cytidylyltransferase (EC 2.7.7.15) assay

The *P*Cho cytidylyltransferase (PCCT) activity was assayed according to Tercé *et al.* (1988). The reaction mixture (250 μl) contained 0-20 μM ET18-OCH_3, 20 mM Tris-HCl (pH 7.8), 6 mM $MgCl_2$, 8 mM CTP, 50 μg microsomal protein and 4 mM phospho[*methyl*-^{14}C]choline (0.085 μCi/μmol). The mixture was incubated in a shaking water bath at 37°C for 30 min. The reaction was terminated by boiling for 3 min. CDP-Cho was separated from *P*Cho on silica gel K6 TLC plates with a developing solvent system of methanol/0.15 M NaCl/28% NH_4OH (10:10:1, v/v) (Weinhold *et al.*, 1991), and visualized by the Dittmer's spray. The radioactivity associated with CDP-Cho was determined by scintillation counting.

CTP:phosphoethanolamine cytidylyltransferase (EC 2.7.7.14) assay

The *P*Etn cytidylyltransferase (PECT) activity was assayed according to the method of Sundler (1975). The reaction mixture (300 μl) contained 0-20 μM ET18-OCH_3, 20 mM Tris-HCl (pH 7.8), 10 mM $MgCl_2$, 1 mM *P*Etn, 5 mM DTT, 50 μg cytosolic protein and 2 mM [5-^{3}H]CTP (0.0965 μCi/μmol). The mixture was incubated in a shaking water bath at 37°C for 30 min. The reaction was stopped by boiling for 3 min. CTP (R_f 0.165) and CDP-

ethanolamine (R_f 0.494) were separated on silica gel K6 TLC plates with 1 M ammonium acetate, 0.01 M EDTA/90% ethanol (30:70, v/v). CDP-ethanolamine was identified with 0.25% ninhydrin in acetone and the associated radioactivity was quantitated by scintillation counting.

*Acyl-CoA:1,2-diacyl-sn-glycerol O-acyltransferase (DAG acyltransferase, EC 2.3.1.20) and acyl-CoA:1-acyl-sn-glycero-3-phospha*e O-acyltransferase (or lysoPtdOH acyltransferase, EC 2.3.1.51) assays*

The methods used to measure the DAG acyltransferase (DGAT) and lysoPtdOH acyltransferase (LPAAT) activities were modified from those of Yamashita *et al.* (1981a). A stock solution of 20 mM 1,2-diacyl-*sn*-glycerol emulsified in 0.2% Tween 20 containing 1 mM DTT and a stock solution of 1 mM 1-acyl-*sn*-glycero-3-phosphate in 10 mM Tris-HCl (pH 7.4) containing 0.25 M sucrose and 1 mM EDTA were prepared separately. The reaction mixtures (500 µl) for DGAT assay consisted of 0-20 µM ET18-OCH_3, 40 mM Tris-HCl (pH 7.4), 6 mM $MgCl_2$, 8 mM emulsified DAG, 4.4 mM DTT, 50 µg microsomal protein and 0.2 mM [1-^{14}C]oleoyl-CoA (0.097 µCi/µmol); the reaction mixture (500 µl) for LPAAT assay consisted of 0-20 µM ET18-OCH_3, 50 mM Tris-HCl (pH 7.4), 20 µM lysoPtdOH, 50 µg microsomal protein and 20 µM [1-^{14}C]oleoyl-CoA (0.097 µCi/µmol). The mixtures were incubated in a shaking water bath at 37°C for 10 min. The reactions were terminated by the addition of 3 ml chloroform/methanol (2:1, v/v) and 1 ml of 0.9% KCl followed by mixing, centrifugation and removal of the upper phase. The radioactivities associated with triacylglycerol and PtdOH were determined after separation on silica gel K6 TLC plates with developing solvent systems of hexane/ethyl ether/methanol/acetic acid (70:30:5:1, v/v) or

chloroform/methanol/acetic acid/water (50:37.5:3.5:2, v/v), respectively and visualized in an iodine chamber.

Acyl-CoA:glycero-3-phosphate O-acyltransferase (EC 2.3.1.15) assay

Gro-3-*P* acyltransferase (GPAT) activity was measured by a modification of the procedure described by Yamashita *et al.* (1981b). The reaction mixture (350 µl) consisted of 0-20 µM ET18-OCH_3, 57.1 mM Tris-HCl (pH 7.6), 0.71 mM *sn*-glycero-3-phosphate, 50 µg microsomal protein and 28.6 µM [1-^{14}C]oleoyl-CoA (0.1 µCi/µmol). The mixture was incubated in a shaking water bath at 22°C for 10 min. Termination of the reaction, extraction of lysoPtdOH, separation of lysoPtdOH from oleoyl-CoA, and determination of the radioactivity associated with lysoPtdOH were as described above for the LPAAT assay.

Diacylglycerol kinase (EC 2.7.1.107) assay

The DAG kinase (DGK) activity was assayed according to the procedure of Schaap *et al.* (1990). The 10x reaction buffer which contained 0.5 M Tris-HCl (pH 7.5), 5 mM DTT, 0.1 M NaF and 0.1 M $MgCl_2$ was prepared fresh from stock solutions of the individual component solutions. The 2.5x DAG/deoxycholate mixture (2.5 mM) was prepared as follows. DAG solution (621 µl, 10 mg/ml) was dried under a stream of nitrogen and re-dissolved in 1 ml DDW by thorough sonication. Three microliters of deoxycholate (1.382 mg/ml) was added to DAG solution followed by thorough mixing and sonication. The reaction mixture (200 µl) contained 0-20 µM ET18-OCH_3, 50 mM Tris-HCl (pH 7.5), 0.5 mM DTT, 10 mM NaF, 10 mM $MgCl_2$, 2 mM phosphatidylserine, 1 mM DAG/deoxycholate, 50 µg cytosolic protein and 2 mM [γ-^{32}P]ATP. The mixture was incubated in a shaking water bath at 30°C for 10 min. Termination of the reaction, extraction and separation of

PtdOH, and determination of the associated radioactivity were as described above for the LPAAT assay.

Phosphatidic acid phosphatase (EC 3.1.3.4) assay

The PtdOH phosphatase (PAP) activity was measured by the method of Sleight and Kent (1980). 1-Stearoyl-2-[1-^{14}C]arachidonoyl-glycerophosphatidate was prepared by PLD hydrolysis of 1-stearoyl-2-[1-^{14}C]arachidonoyl-glycerophosphocholine (Comfurius *et al.*, 1977). The reaction mixture (500 µl) was composed of 0-20 µM ET18-OCH_3, 80 mM Tris-maleate (pH 6.5), 50 µg microsomal protein and 2 mM [^{14}C]phosphatidate (0.084 µCi/µmol). The mixture was incubated in a shaking water bath at 37°C for 20 min. Termination of the reaction, extraction of DAG, separation of DAG from PtdOH, and determination of the radioactivity associated with DAG were as described for the DGAT assay.

3.5 Effect of ET18-OCH_3 on Cellular Signal Transduction

3.5.1 Determination of effect of ET18-OCH_3 on serum-induced cell proliferation in quiescent MCF-7 cells (contribution by Wei Xiong and Xiaoli Lu)

Quiescent MCF-7 cells were obtained by seeding cells in tissue culture dishes overnight in DMEM supplemented with 10% FBS (DMEM/FBS), followed by washing and incubation in DMEM containing 0.5 mg/ml BSA (DMEM/BSA) for 4-6 days. The cells were considered quiescent when the 24-h increase in cell number of the parallel culture was 15% or less.

Stock solutions of ET18-OCH_3 (2 mg/ml) were prepared in DMEM/BSA and stored at -20°C. Working solutions of ET18-OCH_3 in media at the concentrations indicated

elsewhere were prepared fresh. Quiescent cells were incubated in DMEM/BSA in the presence or absence of 10 μg/ml ET18-OCH_3 for selected periods. At the end of incubation, cells were washed and incubated with DMEM/FBS for 4 days. The cell number was determined every 24 h up to 96 h. Cell viability at each time point was also determined using the Trypan Blue dye assay as described by the manufacturer (Sigma). Briefly, 0.5 ml of cell suspension (~2-5 x 10^6 cells per ml of HBSS) was mixed thoroughly with an equal volume of 0.08% Trypan Blue diluted with HBSS. The trypan blue-cell suspension was allowed to stand for 5 to 15 min. The cells were transferred into chambers of a hemocytometer and counted under a microscope. The percentage of cell viability was calculated based on at least 100 counted cells.

$$\% \text{ Cell Viability} =$$

$$\text{total viable cells (unstained)} \div \text{total cells (unstained and stained blue)} \times 100\%$$

3.5.2 [^{3}H]Thymidine incorporation into MCF-7 cells

Quiescent MCF-7 cells in six-well plates were preincubated with or without ET18-OCH_3 (10 μg/ml) for selected periods. After washing, the cells were incubated with DMEM/BSA or DMEM/FBS for 20 h followed by the addition of [^{3}H]thymidine (0.5 μCi/well) for an additional 4 h. The medium was then aspirated and the wells were washed three times with HBSS. One milliliter of ice-cold 10% trichloroacetic acid (TCA) was added to each well. After incubating for 15 min at 4°C, the TCA was aspirated and each well was washed twice with 10% ice-cold TCA. The wells were then air dried for 10 min, followed

by solubilization by the addition of 2 x 1 ml 0.2 *N* NaOH. [^{3}H]Thymidine incorporation was measured by scintillation counting (Piazza *et al.*, 1995).

3.5.3 Incorporation of ET18-OCH_3 into quiescent MCF-7 cells

Serum-deprived quiescent MCF-7 cells cultured in 24-well plates were incubated with 1-*O*-[^{3}H]octadecyl-2-*O*-methyl-*sn*-glycero-3-phosphocholine (10 μg/ml, 0.5 μCi/well) for 1, 2, or 3 h, and subsequently washed three times with HBSS/BSA. The cells were detached with trypsin, transferred to 15-ml polypropylene tubes, and dispersed with a 21-gauge needle. Aliquots were taken for determination of the cell number. The remainder of the cells were pelleted by centrifugation. After the removal of the supernatant, the pellet was dissolved in 1% SDS in 0.3 *N* NaOH. The radioactivity associated with the cells was determined by scintillation counting.

3.5.4 In-gel MAPK assay

Stock solutions

The stock solutions were (*a*) 1 M Tris-HCl (pH 8.0), (*b*) 1 M β-mercaptoethanol, (*c*) 1 M $MgCl_2$, (*d*) 100 mM EGTA, (*e*) 1 M HEPES (pH 8.0), (*f*) 10 mM ATP, (*g*) 50% TCA, (*h*) 10% Tween 40, (*i*) 5% Na pyrophosphate, and (*j*) 1 mM PKI.

Preparation of working solutions

(*A*) Washing Buffer I (50 mM Tris-HCl, 20% 2-propanol, pH 8.0) was prepared by mixing 50 ml (*a*) with 200 ml 2-propanol and bringing the final volume to 1 L with DDW.

(*B*) Denaturing Buffer (50 mM Tris-HCl, 5 mM β-mercaptoethanol, 6 M guanidine

HCl, pH 8.0) was prepared by dissolving 114.6 g guanidine HCl (added slowly and mixed vigorously) to the mixture of 10 ml (*a*) and 50 ml DDW, adjusting the pH to 8.0, adding 1 ml (*b*) and DDW to a final volume of 200 ml.

(*C*) Renaturing Buffer (50 mM Tris-HCl, 5 mM β-mercaptoethanol, 0.04% Tween 40, pH 8.0) was prepared by mixing 25 ml (*a*), 2.5 ml (*b*), and 2 ml (*h*), and adding DDW to a final volume of 500 ml.

(*D*) Washing Buffer II (40 mM HEPES, pH 8.0, 2 mM DTT, 0.5 mM EGTA, 10 mM $MgCl_2$) was prepared by dissolving 61.704 mg DTT (**FRESH**) in the mixture of 8 ml (*e*), 1 ml (*d*), 2 ml (*c*) and 180 ml DDW, and bringing the final volume to 200 ml with DDW.

(*E*) Kinase Buffer [*D* + 40 μM ATP (20 μCi/ml), 2 μM PKI] was prepared by dissolving 6.17 mg DTT (**FRESH**) in the mixture of 0.8 ml (*e*), 0.1 ml (*d*), 0.2 ml (*c*), 40 μl (*j*), 80 μl (*f*) and 15 ml DDW, then adding 40 μl (≈ 400 μCi) [γ-^{32}P]ATP (i.e. 20 μCi/ml) and bringing the final volume to 20 ml with DDW.

(*F*) Stopping Solution (5% TCA, 1% sodium pyrophosphate) was prepared by mixing 100 ml (*g*) and 200 ml (*i*). and adding DDW to 1 L.

Procedure

One volume of 4x SDS sample buffer was added to 3 volumes of cell lysates, followed by boiling for 5 min and centrifugation for 1 min at 14,000 rpm in a microfuge. Samples (10-20 μg) were run on a 10% SDS gel containing myelin basic protein (MBP, 0.5 mg/ml). The gel was washed with Washing Buffer I (*A*) for at least 1 h at room temperature with 3 buffer changes. Proteins in the gel were denatured by washing the gel with Denaturing Buffer (*B*) for 1 h at room temperature. The renaturing of proteins was achieved by placing

the gel in Renaturing Buffer (*C*) for at least 16 h at 4°C with several buffer changes. The gel was washed with Washing Buffer II (*D*) for 30 min at room temperature. Kinase reaction was carried out by incubation of the gel in Kinase Buffer (*E*) at room temperature for 4 h followed by extensive gel washing with Stopping Solution (*F*) for at least 2 h. The gel was dried after being covered on both sides by a cellophane membrane (Matsudaira et al., 1978) and then subjected to autoradiography.

3.5.5 MAPK assay with P81 paper

Cells were scraped into Buffer B and disrupted by ultrasonication. Cytosol was prepared as described above and stored at -70°C. MAPK activity was measured as the phosphorylation of MBP (Ahn *et al.*, 1990; Ahn and Krebs, 1990). The reaction mixture (30 µl) contained 2 µM protein kinase A inhibitor (PKI) peptide, 10 µM calmidazolium, 8 µg of MBP, 20 mM $MgCl_2$, 0.1 mg/ml BSA, 40 mM β-glycerophosphate, 0.15 mM Na_3VO_4 and 0.15 mM ATP (3×10^6 cpm/nmol). The reaction was initiated by the addition of 1 µg of cytosolic protein and the mixture was incubated at 30°C for 10 min. The reaction was terminated by spotting 20 µl of the mixture on P81 paper and washing several times with 150 mM phosphoric acid. After drying the paper, the amount of bound ^{32}P on the paper was quantitated and the values were corrected for blanks (assay without MBP).

3.5.6 Immunoprecipitation, phosphorylation and Western blotting of MAPK

Quiescent MCF-7 cells in 150-mm dishes were washed with Kreb's buffer (2 x 15 ml) and incubated with [^{32}P]orthophosphate (300 µCi/ml) in 12 ml phosphate-free DMEM/BSA

for 3 h. After three washes with Kreb's buffer and incubation in 10 ml phosphate-free DMEM/BSA with or without ET18-OCH_3 (10 μg/ml, 3 h), the cells were washed with Kreb's buffer (2 x 15 ml), incubated in 10 ml fresh phosphate-free DMEM/BSA, and stimulated with EGF (10 ng/ml) for selected periods. The cells were then quickly rinsed three times with ice-cold Kreb's buffer, scraped into 0.75 ml Buffer C, and mixed immediately. Lysates were centrifuged at 200,000 *g* for 30 min at 4°C. Supernatants (soluble cell lysates) were transferred to microfuge tubes and stored at -70°C until use.

Pre-clearance of samples was achieved by mixing in the presence of protein A-agarose (Zymed, # 10-1041) in a rotator for 0.5 h at 4°C and centrifugation. The supernatants were used for MAPK immunoprecipitation. MAPKs ($p42^{mapk}$ and $p44^{mapk}$) were immunoprecipitated from 0.75 mg of cell lysate protein (0.8 ml) in Buffer C with 3 μg each of agarose-conjugated polyclonal Abs to ERK1 (C-16) and ERK2 (C-14) by mixing overnight in a rotator at 4°C. Protein A-agarose alone without Abs was used as a negative control. Pellets were washed with Buffer C (8 x 0.8 ml) by centrifugation. The immunoprecipitates were heated at 100°C in 40 μl of SDS sample buffer for 5 min.

Proteins in 20 μl SDS sample buffer were resolved on 10% SDS-PAGE gels. Phosphorylated bands were visualized by autoradiography. Proteins separated on a parallel gel were transferred to nitrocellulose membrane, probed with 0.2 μg/ml of mouse anti-MAP kinase (ERK1+2) mAbs (Zymed, # 03-6600), and detected using HRP-goat anti-mouse IgG (H+L) and the ECL immunodetection system.

3.5.7 Immunoprecipitation, phosphorylation and Western blotting of MEK

Quiescent MCF-7 cells in 150-mm dishes were washed, labeled with ^{32}P, treated with or without ET18-OCH_3, stimulated with EGF, and soluble cell lysates were prepared and stored as described in **Section 3.5.6**.

Samples were pre-cleared as described above. MEK was immunoprecipitated from 0.8 mg of cell lysate protein (0.8 ml) in Buffer C with 3 μg of anti-MEK-1 Abs (Santa Crutz, # sc-436). After mixing in a rotator overnight at 4°C, 40 μl of protein A-agarose were added to each sample. The samples were rotated for another hour at 4°C. Protein A-agarose alone without Abs was used for negative control. Pellets were washed with Buffer C (8 x 0.8 ml) by centrifugation. The immunoprecipitates were boiled in 40 μl SDS sample buffer for 5 min.

Proteins separation by SDS-PAGE, autoradiography and immunoblotting were as described in **Section 3.5.6**, except the use of 0.5 μg/ml of affinity-purified rabbit polyclonal Abs to MEK (Santa Crutz, # sc-219) and HRP-goat anti-rabbit IgG (H+L) as probes.

3.5.8 EGF binding

Time course

Since the internalization of ligand-bound receptors is halted at low temperatures (Wiley *et al.*, 1981), the time course experiments were conducted at 4°C to determine the total EGF binding. For these experiments, all buffers and media used were pre-cooled to 4°C and procedures were conducted on ice. Experiments to determine the surface binding of EGF and internalization of EGF-bound receptors were conducted at 37°C.

To determine the total surface binding of EGF at 4°C, quiescent MCF-7 cells in six-well plates were pre-cooled on ice for at least 20 min and washed with 1 ml ice-cold HBSS

containing 0.5 mg/ml BSA (HBSS/BSA). The ice-cold binding medium (DMEM/BSA with 10 ng/ml EGF, 120,000 cpm/ml, 0.7 ml) was added to each well at selected times. Cells were incubated in the binding medium on ice for 0-120 min, followed by the removal of the binding medium and three washes with 1 ml of ice-cold HBSS/BSA. The cells were then lysed in 0.8 ml of 1% SDS in 0.3 *N* NaOH (SDS/NaOH) at 37°C for 1 h. The radioactivity in aliquots of cell lysates was determined by a gamma counter.

For experiments at 37° C, quiescent MCF-7 cells in six-well plates were washed with 1 ml HBSS/BSA and incubated with 0.7 ml binding medium for 0-120 min. After the removal of the binding medium and three washes with ice-cold HBSS/BSA, ice-cold acetic acid (0.2 M, pH 2.5) containing 0.5 M NaCl (AAS) was added to each well and left on ice for 6 min. The cells were rinsed with another 0.5 ml of ice-cold AAS and combined with the initial wash. The radioactivity in the combined AAS that represents the surface binding of EGF was determined with a gamma counter. To determine the internalization of ligand-bound EGF receptors, the AAS-washed cells were then lysed in 0.8 ml of SDS/NaOH at 37°C for 1 h. The radioactivity was determined as described above.

To determine the nonspecific binding, 100-fold concentration of cold EGF was used for competition. The nonspecific binding was < 25% of the total radioactivity associated with the cells.

EGF binding as a function of EGF concentration

Similar procedures to those for the *time course* studies were used except that the EGF concentrations tested ranged from 0 to 20 ng/ml (159,400 cpm/ml) and the stimulation time was 30 min.

Effect of ET18-OCH_3 on EGF binding and EGF receptor internalization in quiescent MCF-7 cells at 37 °C

Quiescent MCF-7 cells in six-well plates were pre-incubated with or without 10 μg/ml ET18-OCH_3 for 3 h followed by washing with 1 ml HBSS/BSA once. The cells were then incubated with 0.7 ml of the binding medium, consisting of DMEM/BSA containing 0-10.2 nM EGF (566.9 μCi/nmol), at 37°C for 30 min. At the end of incubation, the binding medium was removed and the cells were washed three times with ice-cold HBSS/BSA. Determination of EGF surface binding and internalization was as described above for the *time course* studies. Nonspecific binding (<10%) was determined in the presence of 400-fold concentration of cold EGF.

Effect of ET18-OCH_3 on EGF binding and EGF receptor internalization in quiescent MCF-7 cells at 4 °C

Quiescent MCF-7 cells in six-well plates were pre-incubated with or without 10 μg/ml ET18-OCH_3 for 3 h. The cells were washed twice with 1 ml ice-cold HBSS/BSA and incubated in ice-cold medium on ice for 20 min. All subsequent procedures were as described for the above experiment conducted at 37°C with the exception that this experiment was carried out on ice. The EGF concentrations used for this experiment ranged from 0 to 3.12 nM with EGF specific radioactivity of 93,870 cpm/ng.

3.5.9 Immunoprecipitation and tyrosine phosphorylation of EGF receptors

Quiescent MCF-7 cells in 150-mm dishes were incubated in 10 ml DMEM/BSA with or without 10 μg/ml ET18-OCH_3 for 3 h. After two washes with 15 ml PBS, 10 ml fresh

DMEM/BSA was added to each well. The cells were stimulated with 10 ng/ml EGF for 0, 2, 5, or 10 min, and then washed with ice-cold PBS (3 x 15 ml) [All the subsequent steps were carried out on ice]. The cells were scraped in 2 ml Buffer G, sonicated (3 x 10 seconds) and rapidly mixed. Lysates were centrifuged at 20,000 *g* (16,000 rpm in a 70.1 Ti rotor in a Beckman L-80 centrifuge) for 10 min to remove nuclei, cell debris and mitochondria. Supernatants were centrifuged at 200,000 *g* (50,000 rpm in a 70.1 Ti rotator) for 30 min. Pellets were resuspended in 0.5 ml Buffer H to give a protein concentration of 2-5 mg/ml. Samples were quickly frozen by ethanol/dry ice and stored at -70°C until use.

Samples containing 1.7 mg protein in a final volume of 0.68 ml Buffer H were pre-cleared for 0.5 h with rec-protein G Sepharose 4B (Zymed, # 10-1241). Samples containing 1.5 mg protein in a final volume of 0.6 ml Buffer H were used for immunoprecipitation. Fourteen micrograms of sheep polyclonal Ab against human EGFr (UBI, # 06-129) were added to each sample and rotated overnight at 4°C. Forty microliters of rec-protein G Sepharose 4B were added to each sample and rotated for another 2 h at 4°C. Protein G alone without anti-EGFr Ab in immunoprecipitation was used for the negative control. Immunecomplexes were pelleted and washed four times with Buffer H. After the final wash, immunecomplexes were spun down and boiled in 50 µl of 2 x SDS sample buffer for 5 min.

Proteins were resolved on 8% SDS-PAGE gels, transferred to 0.2 µm nitrocellulose membranes, and probed with sheep anti-human EGFr (UBI, # 06-129) or mouse anti-phosphotyrosine mAb (UBI, # 05-321). The EGFr and tyrosine phosphorylated EGFr bands were detected using the ECL system with HRP-rabbit anti-sheep IgG (H+L) Ab (Zymed, # 61-8620) or HRP-goat anti-mouse IgG (H+L) Ab (BioRad, # 170-6516), respectively.

3.5.10 Ras activation

Quiescent MCF-7 cells in 100-mm dishes were washed with Kreb's buffer (2 x 10 ml), labeled with 300 μCi/ml [^{32}P]orthophosphate in 5 ml phosphate-free DMEM/BSA for 4 h, and washed with Kreb's buffer (3 x 10 ml). The cells were then incubated in 6 ml DMEM/BSA without or with 10 μg/ml ET18-OCH_3 for 3 h and washed again with Kreb's buffer (2 x 10 ml). Fresh DMEM/BSA (6 ml) was added to each dish. The cells were stimulated with 10 ng/ml EGF for 0, 2, 4, 7 or 10 min, washed with PBS (3 x 15 ml), scraped into 0.5 ml Buffer D, and mixed briefly. Lysates were centrifuged at 14,000 *g* for 10 min at 4°C to remove nuclei and cell debris. Supernatants were quickly frozen in ethanol/dry ice and stored at -70°C until use.

Lysates were pre-cleared for 1 h as described in **Section 3.5.6**. $p21^{ras}$ was immunoprecipitated from 0.5 mg of cell lysate protein (0.8 ml in Buffer D) using 3 μg of anti-Ras (259) (Santa Cruz, # sc-35). The sample-antibody mixtures were mixed at 4°C overnight with a rotator. Protein G-Sepharose 4B (15 μl) was then added and the mixtures were rotated for another hour at 4°C. Immunoprecipitates were washed with Buffer E (8 x 0.8 ml). Nucleotides were eluted with 20 μl of Buffer F at 68°C for 20 min. Ten microliters of the eluate were loaded on PEI-cellulose plates. The free nucleotides were resolved in 0.75 M KH_2PO_4, pH 3.5 (Li *et al.*, 1992; Downward *et al.*, 1990; Koide *et al.*, 1993). The radiolabeled nucleotides were visualized by autoradiography; the corresponding areas of phosphorylated bands were excised and the associated radioactivity was determined by Cerenkov counting. The molar ratio of $p21^{ras}$-bound GTP was calculated as follows (Satoh *et al.*, 1990a):

$$GTP\ (\%) = \{GTP(cpm)/[1.5 \times GDP\ (cpm) + GTP\ (cpm)]\} \times 100$$

The remainder (10 µl) of the eluate was boiled in SDS sample buffer (2.5 µl, 5x) for 5 min. An aliquot (10 µl) was subjected to SDS-PAGE on a 12% gel. Proteins were transferred to nitrocellulose membrane, probed with 1.5 µg/ml of rabbit polyclonal IgG against Ras protein (UBI, # 06-226) and detected using HRP-goat anti-rabbit IgG (H+L) (BioRad, # 170-6515) and the ECL immunodetection system.

3.5.11 Translocation of Raf-1 to membrane

MCF-7 cells in 150-mm dishes were incubated in 10 ml DMEM/BSA without or with 10 µg/ml ET18-OCH_3 for 3 h. The media were then replaced with 10 ml of fresh DMEM/BSA. The cells were stimulated with 10 ng/ml EGF for 0, 2, 4, 7 or 10 min, or with DMEM/FBS for 0, 5, 10, 15 or 30 min, washed with PBS (3 x 15 ml), scraped off in 0.5 ml Buffer I, and disrupted by sonication (3 x 10 seconds). Lysates were centrifuged at 1,600 *g* (4,000 rpm in a JA 21 rotor) for 15 min at 4°C to remove unbroken cells, nuclei and cell debris. Supernatants were centrifuged at 200,000 *g* (50,000 rpm in a Ti 70 rotor) for 30 min at 4°C to separate the cytosol (the supernatant) and membrane (the pellet) fractions. The pellets were resuspended in 0.5 ml Buffer J, sonicated (3 x 10 seconds), and re-centrifuged at 200,000 *g* for 20 min at 4°C to obtain a clarified membrane extract (Wartmann *et al.*, 1994). Samples (= 40 µg membrane protein) were loaded on 10% SDS-PAGE gels and transferred to nitrocellulose membranes. The Raf-1 protein was probed with 0.5 µg/ml of non-conjugated rabbit anti-Raf-1 Ab (Santa Crutz, # sc-133) and detected using HRP-goat

anti-rabbit IgG (H+L) and the ECL immunodetection system. To determine Raf-1 content in MCF-7 cells, the cells were lysed in Buffer L and 10 μg cell lysate protein was loaded in each lane for Western blot analysis as described above.

3.5.12 Raf-1 kinase assay

Membranes were obtained from control and ET18-OCH_3-treated cells, solubilized and pre-cleared as described in **Section 3.5.11**. Immunoprecipitation from 300 μg membrane protein was achieved using anti-Raf-1 antiserum (SP63) and protein A Sepharose. Three micrograms of the antiserum and 20 μl of protein A-Sepharose were added to each sample followed by 16-h incubation at 4°C. The immunoprecipitates were washed three times with Buffer K, three times with LiCl buffer (0.5 M LiCl, 100 mM Tris-HCl, pH 7.4) and once with Buffer L. The immunecomplexes were then suspended in 20 μl of $MgCl_2$ buffer (20 mM Tris-HCl, pH 7.4, 10 mM $MgCl_2$). Raf-1 kinase activity was assayed by using 10 μg of histone H1 or 2.5 μg of MEK (FL) as substrates. The reaction was started by the addition of 50 μM ATP with 10 μCi of [γ-^{32}P]ATP and allowed to proceed for 10 min at 30°C. The reaction was terminated by boiling in SDS sample buffer for 5 min. The proteins were separated by electrophoresis on 12% SDS gels. The phosphorylated bands were visualized by autoradiography (Kharbanda *et al.*, 1994).

3.5.13 PKA assay

PKA activity was measured with Kemptide as substrate (Corbin *et al.*, 1974) and was taken as the difference in phosphorylation of the peptide in the absence and presence of 2 μM

PKI. The reaction mixture (30 µl) contained 12 mM KCl (pH6.8), 7.14 mg/ml Kemptide, 4.29 mM magnesium acetate, 0.24 mM ATP (specific activity: ~100 cpm/pmol), 10 µl lysate (enzyme source = 1 µg protein) with or without 2 µM PKI. The reactions were initiated by the addition of 10 µl of lysate into the mixtures, mixing, and placing the reaction tubes in a water bath at 30°C. After incubation for 10 min, the reaction was stopped by spotting 20 µl of the reaction mixture on Whatman P81 filter paper followed by four washes with 150 mM phosphoric acid. The amount of ^{32}P-bound Kemptide on the P81 paper was quantitated by Cerenkov counting and the values were corrected for blanks (assay without Kemptide).

3.5.14 Determination of cellular cAMP levels

Cyclic AMP levels were measured with a cAMP[^{3}H] assay kit from Amersham. Briefly, quiescent MCF-7 cells were incubated in DMEM/BSA media containing 0 or 10 µg/ml ET18-OCH_3 for 3 h followed by stimulation with 10 ng/ml EGF for 0-10 min. The cells were harvested in extraction buffer containing 2 mM EGTA and sonicated. Cytosolic fractions were prepared by centrifugation (100,000 *g*, 30 min, 4°C). Cytosolic samples were boiled for 5 min followed by centrifugation. Supernatants (50 µl) were used for cAMP assay. The cAMP assay was performed as described in the instruction enclosed with the Cyclic AMP [^{3}H] Assay System (Amersham).

3.5.15 Flow cytometry

Quiescent MCF-7 cells in 100-mm dishes were processed for flow cytometry analysis according to the method of Edelmann *et al.* (1996). After appropriate treatments, the cells

were harvested with trypsin, pelleted by centrifugation at 1200 rpm for 3 min, and washed with ice-cold PBS containing 2 mM EDTA (PBS-EDTA buffer, 3 x 3 ml). The cells were resuspended in 0.75 ml ice-cold PBS-EDTA buffer by gentle pipetteman action. While mixing, 2 ml of ice-cold ethanol (95%) was added drop-wise to each tube to fix cells and permeablize the cell membrane. The samples were stored at 4°C overnight. The fixed cells were then pelleted and washed twice with 3 ml ice-cold PBS-EDTA buffer and subsequently resuspended in 0.8 ml RNase-PI staining solution to a cell density of approximately 1.25 x 10^6 cells/ml. The cells were incubated for at least 1 h in the dark at 4°C. Then, the cells were filtered through a 41-μm mesh macroporous filter and processed for flow cytometry analysis by Dr. Edward Rector. Data were collected and analyzed with a cell sorter EPICS 753 and the PARA 1 analysis software.

3.5.16 Analysis of phosphorylated proteins by SDS-PAGE

Quiescent MCF-7 cells in 60-mm dishes were labeled with [^{32}P]orthophosphate (150-300 μCi/ml) in phosphate-free DMEM/BSA for 3 h followed by washing. Unless otherwise stated, the cells were incubated with ET18-OCH_3 (10 μg/ml, 3 h) or Ro 31-8220 (5 μM, 20 min), and subsequently stimulated with TPA (1 μM, 10 min) or a cell-permeable DAG—DiC_8 (20 μM, 10 min). Thereafter, the cells were quickly washed with ice-cold PBS, harvested in Buffer M by scraping, and sonicated (3 x 10 seconds). Aliquots of the lysate were taken for determination of protein content using the Coomassie protein assay with BSA as the standard. Lysates were boiled in the SDS sample buffer for 5 min and centrifuged at 20,000 *g* for 1 min. Proteins were resolved on 10% SDS gels followed by Coomassie blue staining and

autoradiography.

In initial experiments, conditions (time and concentration) that resulted in the optimal stimulation of PKC by TPA or DiC_8 were determined. ^{32}P-labeled quiescent MCF-7 cells were incubated with TPA (0.02-1 μM for 2-20 min) or DiC_8 (10-40 μM for 1-10 min) followed by analysis of protein phosphorylation as described above.

To determine conditions for inhibition of PKC by Ro 31-8220, the effects of Ro 31-8220 on cell proliferation and on PKC-induced phosphorylation were studied. MCF-7 cells growing in six-well plates were incubated with Ro 31-8220 at concentrations from 0.5-10 μM for up to 72 h. The cell numbers were determined at the time of the addition of Ro 31-8220 (0 h) and every 24 h thereafter as described in **Section 3.2.1**. In studies on the effect of Ro 31-8220 on PKC phosphorylation, the pre-labeled quiescent MCF-7 cells were treated with the PKC inhibitor (5 μM) for selected periods (0.5-2 h), followed by stimulation of the cells with TPA and analysis of protein phosphorylation as described above.

3.5.17 Analysis of phosphorylated proteins by two-dimensional (2-D) gel electrophoresis

Solutions

1. Acrylamide Stock Solution (T = 30%, C = 5.4%): stored at 4°C in the dark (30 days maximum).
2. 10% NP-40.
3. 0.05% (w/v) Bromophenol Blue.
4. First Dimension Sample Buffer: The following compounds, 5.7g urea (9.5 M), 2 ml

10% NP-40 (2%), 0.5 ml β-mercaptoethanol (5%), 100 µl Bio-Lytes 3/10 and 5/7 (0.4% each), 150 µl Bio-Lyte 6/8 and Pharmalyte 4/6.5 (0.6% each), were dissolved in DDW in a final volume of 10 ml. The final concentration of each component is indicated in parenthesis. To dissolve urea, the mixture was warmed in a water bath to a temperature no greater than 45°C with stirring. The buffer was aliquoted in 0.5 ml volumes into microfuge tubes and stored at -70°C.

5. First Dimension Sample Overlay Buffer: The following compounds, 5.41g urea (9 M), 50 µl Bio-Lytes 3/10 and 5/7 (0.2% each), 75 µl Bio-Lyte 6/8 and Pharmalyte 4/6.5 (0.3% each) and 0.5 ml 0.05% bromophenol blue (0.0025%), were dissolved in DDW in a final volume of 10 ml. The final concentration of each component is indicated in parenthesis. Urea was dissolved and the buffer was stored as described above.

6. Upper Chamber Buffer for IEF (20 mM NaOH): The buffer was degassed thoroughly (for at least 30 min) before use.

7. Lower Chamber Buffer for IEF (10 mM H_3PO_4): The buffer was degassed thoroughly (for at least 30 min) before use.

8. SDS Sample Equilibration Buffer: This buffer was prepared by dissolving 12.5 ml 0.5 M Tris-HCl, pH 6.8 (0.0625 M), 23 ml 10% SDS (2.3%), 5 ml β-mercaptoethanol (5.0%, v/v), 8 ml glycerol (10%, w/v), and 2.5 ml 0.05% bromophenol blue (0.00125%, w/v) in 49 ml DDW. The final volume is 100 ml and the final concentration of each component is indicated in parenthesis.

Preparation of solid molecular weight standard

1. 1% Agarose in SDS Sample Buffer: The following compounds, 10 mg agarose (1%), 0.2 ml 5x SDS sample buffer without β-mercaptoethanol (1x), and 50 µl 1% bromophenol blue (0.05%) were mixed with 0.65 ml DDW at 70-80°C until clear. Then 50 µl β-mercaptoethanol (5%) was added and the agarose solution was quickly swirled.

2. Solid Molecular Weight Standards: Immediately after the addition of β-mercaptoethanol to the agarose solution (see above), 0.45 ml of the agarose solution was mixed with 25 µl each of the low and high molecular weight standards followed by casting the standard agarose gel into mini 2-D gel tubes. The gels were left at room temperature until solid, extruded onto a parafilm film, cut into 3-4 mm lengths and stored in an eppendorf tube at -20°C.

Preparation of first dimensional tube gels for IEF

Two milliliters of IEF gel solution (4% gel, 9.2 M urea, 2% NP-40, 0.4% of each of Bio-Lytes 3/10 and 5/7, 0.6% of each of Bio-Lyte 6/8 and Pharmalyte, 0.01% ammonium persulfate and 0.1% TEMED): 1.375 g urea, 0.3325 ml 30% acrylamide stock solution, 0.5 ml 10% NP-40, 25 µl each of Bio-Lytes 3/10 and 5/7, 37.5 µl each of Bio-Lyte 6/8 and Pharmalyte 4/6.5 and 492.5 µl DDW were mixed by swirling in a warm water bath (≤ 45°C) to dissolve the urea. The solution was degassed carefully for 15 min. Two and a half microliters of 10% ammonium persulfate and 10 µl TEMED were added. The gel solution was gently mixed and immediately casted in mini 2-D gel tubes.

Preparation of second dimensional slab gels for SDS-PAGE

Slab gels (8%, 10%, or 12%) were preparated as previously described (Laemmli,

1970) with a single well for loading the tube gel.

Analysis of phosphorylated proteins

Labeling and treatments of quiescent MCF-7 cells and cell lysate preparation were as described in **Section 3.5.15**. Protein denaturing was achieved by the addition of the urea sample buffer to the lysates to a final urea concentration of 6 M and incubation at room temperature for 30 min. After centrifugation, proteins in the supernatants (5-10 µl) were resolved on two dimensional gels under the following conditions:

Dimension	Condition
First (IEF)	*Pre-run*: 200 V for 10 min + 300 V for 15 min + 400 V 15 min; *Sample-run*: 500 V for 8 h. (The chamber was surrounded by ice in the cold room for both runs)
Second (SDS-PAGE)	150 V for approximate 1 h.

3.5.18 PKC translocation

Quiescent MCF-7 cells were pre-incubated with or without ET18-OCH_3 (10 µg/ml, 3 hr) followed by stimulation with TPA (1 µM, 10 min). The cells were harvested in ice-cold Buffer N by scraping and sonicated briefly (3 x 10 seconds). Lysates were centrifuged at 1,600 *g* (4,000 rpm in a JA 21 rotor) for 15 min at 4°C to remove unbroken cells, nuclei and cell debris. Cytosolic fractions were obtained by centrifugation at 200,000 *g* (50,000 rpm in a Ti 70 rotor) for 30 min at 4°C. The pellets were dissolved in ice-cold Buffer N plus 1% Triton X-100 and 0.5% NP-40 (Buffer O) by ultrasonication. The soluble membrane extracts

were obtained by re-centrifugation. Samples were stored at -70°C until required. The protein content of each fraction was determined by the Coomassie protein assay (**Section 3.5.19**). Twenty micrograms of proteins of membrane fractions were separated on 8% SDS-PAGE followed by immunoblotting with monoclonal mouse anti-PKC α (IgG_{2b}), γ (IgG_1), or ε (IgG_{2b}). The specific bands of PKC species were visualized with ECL detection system. Lysates from HeLa cells served as positive controls for α and ε isoforms while Jurkat cell lysates were used as positive control for the γ isoform.

3.5.19 Quantitation of cellular proteins

Quantitation of cellular proteins was conducted primarily by the Coomassie protein assay as described by the manufacture (Pierce).

3.5.20 Quantitation of the band density on gel, membrane and film

Quantitation of immunoblots and autoradiographs was achieved by densitometric analysis with a high resolution color scanner model PDI 325oe using the ImageMaster scanning program (Pharmacia).

3.6 Statistical Analysis

The Student's *t* test was applied to all data analyses whenever necessary. The lowest level of significance was at $P < 0.05$.

4. RESULTS

4.1 Studies on Phospholipid Content, Composition and Metabolism

Since a higher content of cellular ether lipids has been reported in the AEL-sensitive HL-60 cells compared to the AEL-resistant K562 cells (Chabot *et al.*, 1989), and net phospholipid biosynthesis is required for cell growth (Jackowski, 1994), we screened five epithelial cancer cell lines with differential sensitivity to ET18-OCH_3, and specifically addressed the following questions. [1] Were there any differences in the content and composition of cellular ether phospholipids among these cells? [2] Were there any differences in the metabolism of ET18-OCH_3 among these cells? [3] Did ET18-OCH_3 differentially affect cellular phospholipid metabolism in these cells? [4] Did a relationship exist between cell susceptibility to ET18-OCH_3 and any of the observed differences mentioned above?

4.1.1 ET18-OCH_3 has differential inhibitory effects on five epithelial cancer cell lines

To investigate the relationships between cellular ether glycerophospholipid content, composition or phospholipid metabolism and sensitivity of cancer cells to ET18-OCH_3, we screened five epithelial cancer cell lines that had different susceptibility to this ether compound. **Figure 17** shows the effect of a 24-h incubation with ET18-OCH_3 (0-15 μg/ml) on the proliferation of A427, A549, Malme 3M, MCF-7 and T84 cell lines growing in the log phase. The concentrations that inhibited an increase in cell number by 50% (IC_{50}) in 24 h were estimated to be 2.08 μg/ml for MCF-7, 2.23 μg/ml for T84, 4.10 μg/ml for Malme 3M, 8.91 μg/ml for A427, and 10.31 μg/ml for A549 (**Figure 17**). These results were consistent

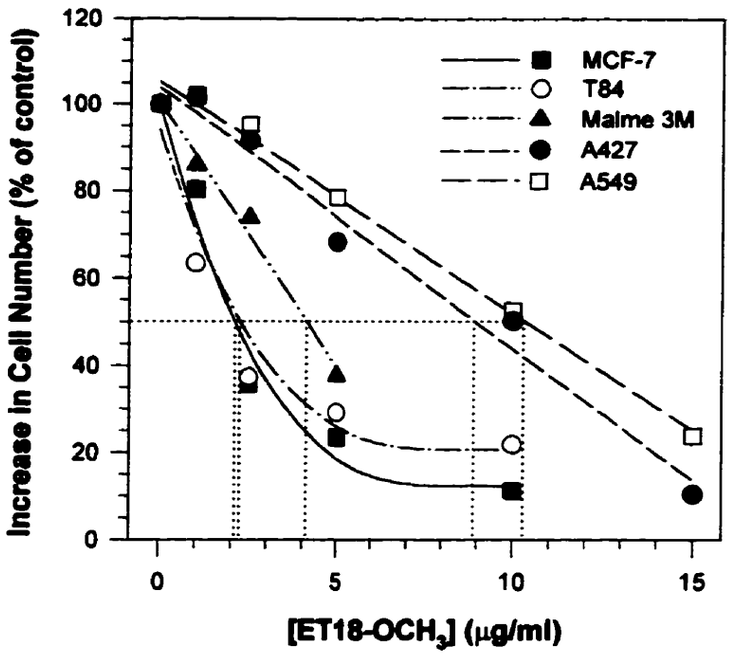

Figure 17. Differential sensitivities of epithelial cells to ET18-OCH_3. Five human epithelial cancer cell lines, MCF-7 (breast cancer cell line), T84 (colon cancer cell line), Malme 3M (skin cancer cell line), A427 and A549 (lung cancer cell lines) growing in 24-well plates were incubated with 0-15 μg/ml of ET18-OCH_3. After 24 h, the increase in cell number was determined and expressed as a percentage of controls (no ET18-OCH_3). The results are the means of eight separate determinations with standard deviation ≤ 12%. The concentrations that inhibited increase in cell number by 50% (IC_{50}) in 24 h are displayed by vertical dotted lines (·····) in the figure.

with previous studies from our laboratory (Lu and Arthur, 1992a; 1992b) which showed that MCF-7 and T84 were very sensitive to the antiproliferative effects of ET18-OCH_3, whereas A427 and A549 were relatively resistant, requiring significantly higher concentrations to affect cell growth. The effect on proliferation of Malme 3M was intermediate between the two groups.

4.1.2 Cellular phospholipid content and composition

The phospholipid content and composition of the five cell lines are displayed in **Table 2**. Malme 3M had the highest phospholipid content (98 nmol/10^6 cells), followed by A549 (65 nmol/10^6 cells). The other three cell lines had a similar cellular content of phospholipids of around 50 nmol/10^6 cells. The phospholipid composition was relatively similar in all the cells. Cholineglycerophospholipids (CGP) accounted for about 50% of the total phospholipid content in all the cell lines except in A427 where it was around 58%. Ethanolamineglycero-phospholipids (EGP) was next with around 25% of the total phospholipid content in all the cell lines except in A427 where it was approximately 19%.

4.1.3 Comparison of the subclass composition of cholineglycerophospholipids (CGP) and ethanolamineglycerophospholipids (EGP)

Analysis of the CGP and EGP subclass composition of the lipid extracts from the cells revealed very significant differences in the subclass composition of the five cell lines (**Table 3**). In CGP, the proportion of the ether subclass (alkylacyl + alkenylacyl) was 45% in T84, 23% in A427, 10% in A549, 9% in Malme 3M and only 3% in MCF-7. The

Table 2. Phospholipid composition and content in five epithelial cancer cell lines. Log-phase T84, MCF-7, A427, A549 and Malme 3M cells growing in 150-mm dishes were harvested. Aliquots were taken to determine the cell number. Lipids were extracted and the lipid classes were separated by TLC. Lipid-associated phosphate in each fraction was quantitated by an improved malachite green method as described in **Section 3.2.2**. The values represent the means ± S.D. of five experiments.

Phospholipid	Cell line				
	T84	MCF-7	A427	A549	Malme 3M
LysoPtdCho [a]	0.48 ± 0.05	0.36 ± 0.06	0.40 ± 0.04	0.35 ± 0.03	0.56 ± 0.05
SM [a]	5.80 ± 0.74	3.55 ± 0.36	4.92 ± 1.27	7.84 ± 0.42	4.90 ± 1.17
CGP [a]	51.30 ± 0.38	50.55 ± 1.34	58.11 ± 1.43	49.75 ± 0.75	49.88 ± 2.87
LysoPtdEtn + PtdSer [a]	7.40 ± 0.65	7.20 ± 1.12	6.19 ± 0.28	6.62 ± 0.62	8.39 ± 1.11
PtdIns [a]	6.87 ± 0.58	6.87 ± 0.19	6.81 ± 0.36	5.98 ± 3.41	6.36 ± 0.44
EGP [a]	24.25 ± 1.10	25.00 ± 0.94	18.77 ± 0.27	25.94 ± 0.73	26.55 ± 0.39
PtdOH [a]	3.91 ± 0.05	6.46 ± 0.31	4.80 ± 0.24	3.52 ± 0.21	3.36 ± 0.18
Phospholipid content [b]	48.51 ± 3.84	53.28 ± 6.47	55.27 ± 3.60	64.71 ± 5.20	97.99 ± 11.32

[a] % of total lipid phosphate; [b] nmol/10^6 cells.

Table 3. Subclass composition of cholineglycerophospholipid (CGP) and ethanolaminoglycerophospholipid (EGP) in five epithelial cancer cell lines. Log-phase T84, MCF-7, A427, A549, and Malme 3M cells growing in 150-mm dishes were harvested. Lipids were extracted. CGP and EGP fractions were purified by TLC. Analysis of subclasses of CGP and EGP has been described in **Section 3.2.3**. The values represent % of lipid phosphate in CGP or EGP and are the means ± S.D. of four experiments.

Cell line	CGP			EGP		
	Diacyl (%)	Alkylacyl (%)	Alkenylacyl (%)	Diacyl (%)	Alkylacyl (%)	Alkenylacyl (%)
T84	54.96 ± 2.74	36.75 ± 3.58	8.29 ± 0.87	43.43 ± 5.99	11.83 ± 0.68	44.74 ± 5.67
MCF-7	97.34 ± 0.73	1.98 ± 0.87	0.69 ± 0.17	96.15 ± 0.45	1.69 ± 0.79	2.16 ± 0.44
A427	77.48 ± 0.42	12.39 ± 0.48	10.13 ± 0.29	58.59 ± 1.38	5.58 ± 0.09	35.84 ± 1.34
A549	90.26 ± 1.06	5.26 ± 1.09	4.48 ± 0.12	42.25 ± 0.39	5.17 ± 0.56	52.57 ± 0.20
Malme 3M	90.87 ± 0.48	7.62 ± 0.44	1.51 ± 0.49	43.69 ± 7.29	3.84 ± 1.40	52.48 ± 8.64

proportion of the alkylacyl subclass was higher than that of the alkenylacyl subclass in all the five cell lines. This is consistent with the previous report by Horrocks (1972) on the distribution of ether bonds in CGP.

Analysis of the EGP fraction revealed that A549 (58%), T84 (57%) and Malme 3M (56%) contained the highest proportion of ether EGP followed by A427 (41%), whereas a much lower proportion (4%) of ether EGP was found in MCF-7. In contrast to CGP, the alkenylacyl subclass of EGP was much greater than the alkylacyl subclass in all the five cell lines.

The content of the total ether CGP and EGP and its percentage of the total phospholipid in each of the five cell lines are displayed in **Table 4**. The highest proportion of ether lipids was found in T84 (37%), followed by A427, A549 and Malme 3M with similar values of around 20%. In MCF-7 cells, the ether varieties accounted for less than 2% of the total phospholipids.

4.1.4 Metabolism of ET18-OCH_3 in MCF-7, A427 and A549 cells

Studies in our laboratory had previously demonstrated that incubation of MCF-7 cells for 12 h with 2.75 μg/ml of ET18-OCH_3 significantly decreased cell proliferation, while 12-h incubation of A427 and A549 with 5 μg/ml of this compound had moderate or little effect on cell growth, respectively (Lu and Arthur 1992a; 1992b). To determine if there were any differences in cellular metabolism of ET18-OCH_3 between these sensitive and relatively resistant cancer cells that might account for the differential effect of this ether lipid on cell proliferation, we investigated its metabolism in these cell lines. Cells were incubated with

Table 4. Ether-phospholipid content in T84, MCF-7, A427, A549 and Malme 3M cells. The values were calculated from the data in **Tables 2** and **3**.

Cell line	Alkylacyl + alkenylacyl (nmol/10^6 cells)	Alkylacyl + alkenylacyl (% of total phospholipids)
T84	17.87	36.83
MCF-7	0.96	1.79
A427	11.53	20.86
A549	12.53	19.36
Malme 3M	19.12	19.51

5 μg/ml [^{3}H]ET18-OCH_3 (specific radioactivity of 0.25 μCi/μg) for 3-12 h. In each experiment, all the bands corresponding to the known markers, as well as the areas between them, were analyzed. The molecular identity of 1-*O*-alkyl-2-*O*-methyl-*sn*-glycerol (OMG) was established by co-chromatography with the authentic standard, Vitride reduction, and alkali hydrolysis of extracted compound (see below). **Table 5** shows the distribution of radiolabel into cellular lipids extracted from the cells after 12-h incubation with [^{3}H]ET18-OCH_3. The distribution of radiolabel in each lipid fraction among all the cell lines was qualitatively similar with the exception of no detectable label in the PtdOH fraction in MCF-7 cells. In all the cell lines, more than 95% of radioactivity was still associated with ET18-OCH_3 after 12-h incubation; the rest of the label was found in the phospholipid fractions: PtdCho, PtdEtn, PtdSer, PtdIns, PtdOH and OMG. No labeling was detected in the fatty acid or fatty alcohol fractions. The extracted compound from the putative OMG band, which co-chromatographed with authentic standards, was subjected to Vitride reduction, and alkali hydrolysis. After either treatment, the radiolabel in the hydrolytic product co-chromatographed with authentic OMG, indicating that the compound was indeed OMG. The qualitative distribution of the radiolabel in lipids after incubation with ET18-OCH_3 for 3 and 6 h was similar to those obtained after 12-h incubation. A comparison of the quantitative distribution after incubations for 3, 6, and 12 h showed a gradual decrease in the label of ET18-OCH_3 and increases in the proportion of the label incorporated into OMG and the phospholipids.

The extracted phospholipids were subjected to alkali hydrolysis to hydrolyze all ester linkages. Subsequent analysis of the distribution of the radiolabel in the reaction products

Table 5. Distribution of ^3H label in lipids extracted from cells incubated with [^3H]ET18-OCH_3. Log-phase MCF-7, A427, and A549 cells were incubated with [^3H]ET18-OCH_3 for 12 h and then harvested. Lipids were extracted and the lipid classes were separated by TLC. The radioactivity associated with each lipid fraction was quantitated by scintillation counting. The values are the means ± S.D. of three different experiments.

Lipid fraction	% distribution		
	MCF-7	A427	A549
PtdCho	0.35 ± 0.04	0.94 ● 0.02	1.74 ± 0.05
PtdSer	0.14 ● 0.01	0.28 ● 0.02	0.25 ± 0.02
PtdIns	0.15 ± 0.02	0.55 ● 0.03	0.35 ± 0.02
PtdEtn	0.34 ● 0.05	0.28 ● 0.01	0.71 ● 0.09
PtdOH	0	0.10 ● 0.01	0.50 ± 0.02
ET18-OCH_3	98.39 ± 0.16	96.57 ± 0.97	96.30 ± 0.31
OMG	0.63 ± 0.10	1.27 ± 0.05	0.60 ± 0.01

revealed that all the radioactivity was associated with the fatty acid fraction. This indicates that the label was attached to the glycerol moiety of the lipids by ester bonds. Confirmation was obtained by subjecting aliquots of the extracted lipids to Vitride reduction. The label was found in the fatty alcohol band. These results suggest that the label in the compounds comigrating with the phospholipids was attached by an ester bond and make it very likely that they are indeed the phospholipids.

4.1.5 Role of endogenously produced OMG in the inhibition of cell growth by ET18-OCH_3

Since phospholipids are normal cellular constituents, the major cellular metabolite of ET18-OCH_3 in the three cell lines that could contribute to the inhibition of cell growth other than the parent compound *per se* would be OMG. To investigate whether OMG, rather than ET18-OCH_3, was responsible for the observed inhibition of cell proliferation, cells were incubated with 1 or 5 μg/ml (2.8 or 13.9 μM) of [^{3}H]OMG (specific radioactivity of 0.25 μCi/μg). The compound was synthesized as described in **Section 3.3.2**. The quantities incorporated into the cells were determined (**Figure 18**). The accumulation of radioactivity into cells peaked after 6 h at both concentrations. The order of increasing accumulation of the radiolabel was A427 < MCF-7 ≤ A549. To investigate how much of the incorporated label was associated with OMG, the distribution of the radiolabel in OMG and possible metabolites following a 12-h incubation of cells with OMG was determined. The results showed that 95-97% of the radiolabel was associated with the OMG fraction in all cells, around 3% with the phospholipid fraction, and less than 0.1% with the fatty acid or fatty

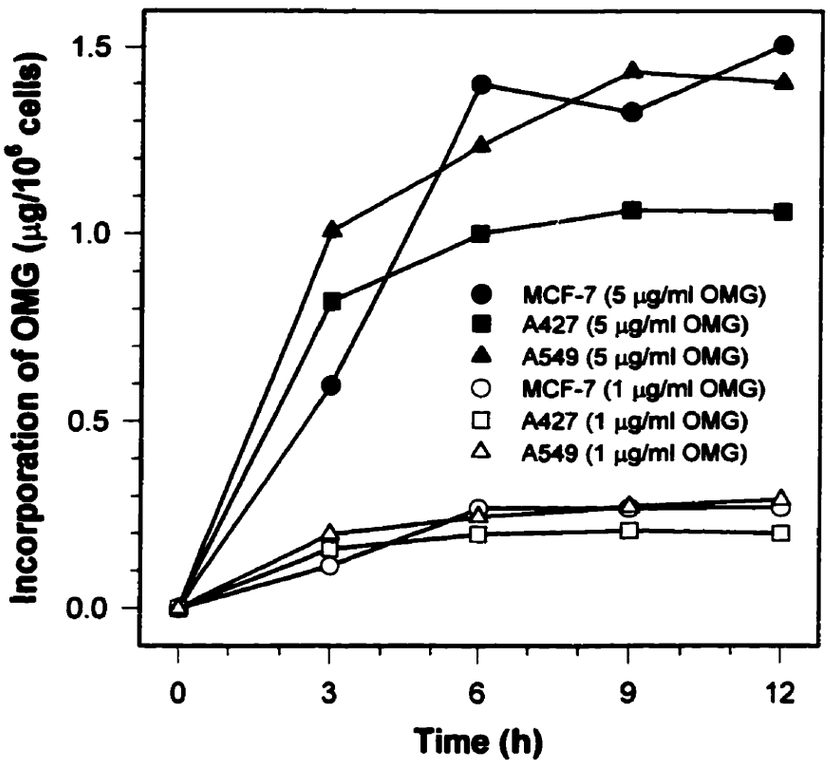

Figure 18. Incorporation of 1-*O*-octadecyl-2-*O*-methyl-*sn*-glycerol into cells. Log-phase MCF-7 (*circles*), A549 (*squares*) and A427 (*triangles*) growing in six-well plates were incubated with 1 µg/ml (*open symbols*) or 5 µg/ml (*closed symbols*) of [^{3}H]1-*O*-octadecyl-2-*O*-methyl-*sn*-glycerol (OMG). At selected times, the cells were washed and harvested. Cellular lipids were extracted and separated by TLC. The quantity of OMG incorporated in the cells was determined by scintillation counting. The values are the means of four independent determinations with standard deviations less than 9%.

alcohol fraction.

To further examine whether a correlation existed between quantities of OMG produced from ET18-OCH_3 and the inhibition of cell proliferation, we compared the quantity of OMG in cells incubated with OMG at 1 μg/ml (2.8 μM) with the quantity of OMG present in cells incubated with 5 μg/ml (9.6 μM) of ET18-OCH_3 (**Table 6**) and also compared their effects on cell proliferation (**Figure 19**). The amount of OMG present in the cells incubated with 1 μg OMG/ml for 12 h was 5- to 25-fold greater than the quantities present in cells incubated with 5 μg ET18-OCH_3/ml for 12 h. However, this OMG treatment resulted in slight decreases (< 12%) in cell proliferation and it was only statistically significant ($P < 0.01$) in A549 cells and not in MCF-7 or A427 cells, whereas the incubation with ET18-OCH_3 revealed a 90% inhibition in growth of MCF-7 cells, about 15% in A427 cells, and no significant effect on the growth of A549 cells. Interestingly, the 5 μg/ml OMG treatment resulted in significant decreases in cell proliferation in all three cell lines (A549 > MCF7 > A427). Thus, OMG more effectively inhibited proliferation of A549 cells that were insensitive to ET18-OCH_3 (**Figure 19**).

4.1.6 Effect of ET18-OCH_3 on [^{3}H]glycerol uptake and incorporation into cellular glycerolipids in MCF-7 and A549 cells

The uptake of glycerol into cells was not affected when MCF-7 or A549 cells were incubated with [^{3}H]glycerol for up to 6 h in the presence of 5 μg/ml ET18-OCH_3 (**Figure 20**). However, the compound affected the incorporation of [^{3}H]glycerol into cellular phospholipids in both cell lines (**Table 7**). In MCF-7 cells, a decrease in the quantity of

Table 6. OMG content in cells incubated with ET18-OCH_3 or OMG. Log-phase MCF-7, A427, and A549 cells were incubated with 5 μg [^{3}H]ET18-OCH_3/ml (†) or 1 μg [^{3}H]OMG/ml (‡) for 12 h. The specific radioactivity of both agents was 0.25 μCi/μg. The cells were harvested and aliquots were taken to determine the cell number. Lipids were extracted from the remainder of the cells and the quantities of OMG were determined after separation by TLC. The results in columns A and B are the means ± S.D. of four different determinations.

Cell line	OMG content (μg/10^6 cells)		
	A†	B‡	B/A
MCF-7	0.032 ± 0.002	0.259 ± 0.011	8.1
A427	0.037 ± 0.001	0.191 ± 0.013	5.2
A549	0.011 ± 0.001	0.276 ± 0.017	25.1

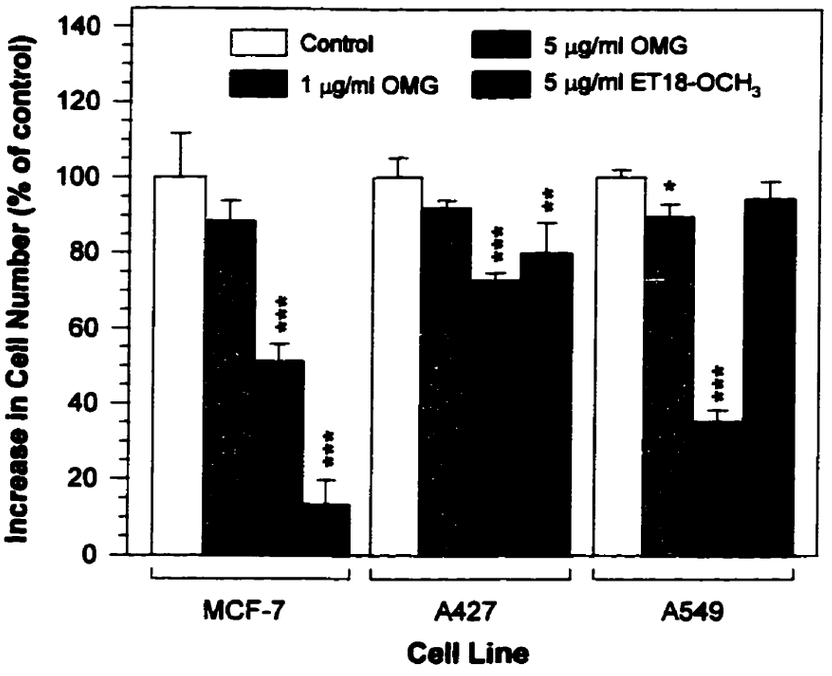

Figure 19. Effect of OMG and ET18-OCH_3 on proliferation of MCF-7, A427 and A549 cell lines. Log-phase cells growing in six-well plates were incubated for 12 h with 1 µg OMG/ml, 5 µg OMG/ml, or 5 µg ET18-OCH_3/ml, or left untreated as controls. The increase in cell number relative to controls was determined. The results represent the means ± S.D. of four independent determinations. * $P < 0.05$, ** $P < 0.01$, and *** $P < 0.001$ compared with controls by Student's *t* test.

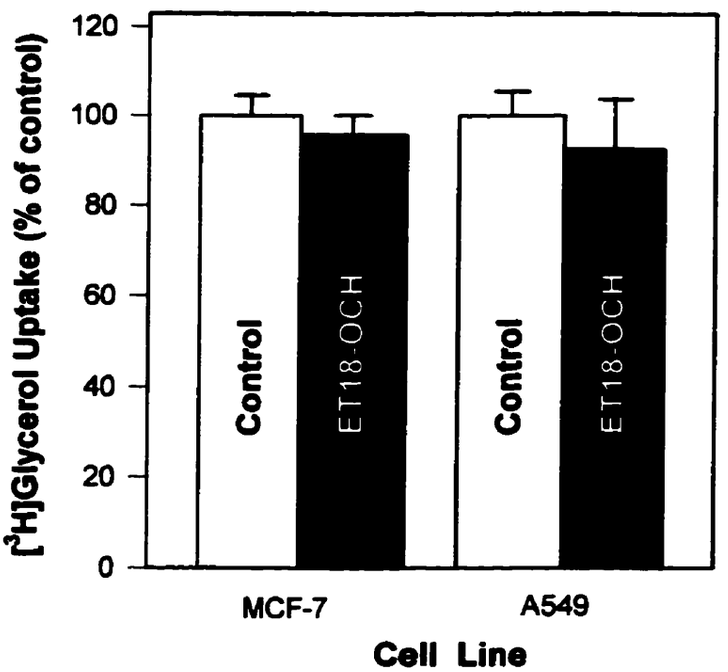

Figure 20. Uptake of [^{3}H]glycerol into MCF-7 and A549 cells. Cells growing in the log phase were incubated with [^{3}H]glycerol (20 μCi/well) in the absence or presence of ET18-OCH_3 (5μg/ml) for up to 6 h. The cells were then washed, lysed with 1% SDS in 0.3 *N* NaOH and the radioactivity in the lysates was determined by scintillation counting. The results represent the average percentages ± S.D. of the corresponding controls of six independent determinations.

Table 7. Effect of incubation with ET18-OCH_3 (5 µg/ml, 6 h) on incorporation of [^{3}H]glycerol into MCF-7 and A549 cellular lipids. MCF-7 and A549 cells growing in the log phase were incubated with [^{3}H]glycerol in the absence or presence of 5 µg/ml ET18-OCH_3. Cells were harvested after 6 h and the cell number was determined. Lipids were extracted and the lipid classes were separated by TLC. The radioactivity associated with each lipid fraction was quantitated by scintillation counting. The results represent the means ± S.D. of six indcpendent determinations. Asterisks indicate results significantly different from control at * $P < 0.05$, ** $P < 0.01$, or *** $P < 0.001$ level by Student's *t* test.

Lipid	MCF-7		A549	
	Control	ET18-OCH_3	Control	ET18-OCH_3
	dpm/10^6 cells (% distribution of [^{3}H]glycerol)			
LysoPtdCho	962 ± 118 (0.44)	812 ± 44 * (0.35)	565 ± 34 (0.40)	512 ± 18 ** (0.35)
SM	755 ± 105 (0.35)	569 ± 32 ** (0.25)	661 ± 72 (0.47)	480 ± 12 ** (0.33)
PtdCho	126361 ± 4756 (57.98)	92439 ± 5335 *** (40.06)	80384 ± 4619 (56.66)	69686 ± 3075 *** (47.45)
LysoPtdEtn	4817 ± 333 (2.21)	2476 ± 476 *** (1.07)	659 ± 58 (0.46)	634 ± 75 (0.43)
PtdSer	8087 ± 991 (3.71)	5293 ± 472 *** (2.29)	2687 ± 165 (1.89)	2589 ± 156 (1.76)
PtdIns	10985 ± 789 (5.04)	12760 ± 1431 * (5.53)	12007 ± 935 (8.46)	11908 ± 638 (8.11)
PtdEtn	41636 ± 1211 (19.11)	71332 ± 5876 *** (30.91)	15023 ± 864 (10.56)	16496 ± 969 * (11.23)
PtdOH	13701 ± 1350 (6.29)	25484 ± 1228 *** (11.04)	10139 ± 1062 (7.15)	12296 ± 785 ** (8.37)
MAG	481 ± 79 (0.22)	672 ± 55 ** (0.29)	407 ± 49 (0.29)	647 ± 282 (0.44)
DAG	1814 ± 64 (0.83)	3661 ± 268 *** (1.59)	1821 ± 117 (1.28)	2408 ± 222 *** (1.64)
TAG	8319 ± 393 (3.82)	15247 ± 1257 *** (6.61)	17508 ± 1169 (12.34)	29202 ± 1613 *** (19.88)
Phospholipids	207304 ± 7867 (95.13)	211165 ± 11123 (91.51)	122125 ± 5088 (86.09)	114601 ± 4781 * (78.04)

[^{3}H]glycerol incorporated into lysoPtdCho (-16%), SM (-25%), PtdCho (-27%), lysoPtdEtn (-49%) and PtdSer (-35%), and an increase into PtdIns (+16%), PtdEtn (+71%), PtdOH (+86%), MAG (+40%), DAG (+102%) and TAG (+83%) were observed after a 6-h incubation with 5 μg/ml ET18-OCH_3. When the distribution of the radiolabel in each lipid class was expressed as a percentage of the label in the total lipid fraction, the major changes caused by this AEL were an 18% decrease into PtdCho and a 12% and 5% increase into PtdEtn and PtdOH, respectively. Although the quantities in DAG and TAG were minor, the changes in the label incorporation into these fractions in cells incubated with ET18-OCH_3 were significant relative to those in control cells.

In similar experiments with A549 cells, ET18-OCH_3 decreased the amount of the label in PtdCho (-13%), lysoPtdCho (-9%) and SM (-27%), and increased the quantities incorporated into PtdEtn (+10%), PtdOH (+21%), DAG (+32%) and TAG (+67%). When the values were expressed as a function of the total amount of the label in the total lipid fraction, the major differences observed were a 9% decrease in PtdCho and a 7% increase in TAG.

In both MCF-7 and A549 cells, the relative changes caused by ET18-OCH_3 described above were also observed after a 12-h incubation of cells with the compound (**Table 8**).

4.1.7 Effect of ET18-OCH_3 on [^{3}H]choline incorporation and the pool sizes of water-soluble choline metabolites

To investigate the mechanism underlying the observed inhibition of PtdCho synthesis by ET18-OCH_3 in both MCF-7 and A549 cells, these cells were labeled with

Table 8. Effect of incubation with ET18-OCH_3 (5 µg/ml, 12 h) on incorporation of [^{3}H]glycerol into MCF-7 and A549 cellular lipids. MCF-7 and A549 cells growing in the log phase were incubated with [^{3}H]glycerol in the absence or presence of 5 µg/ml ET18-OCH_3. Cells were harvested after 12 h and the cell number was determined. Lipids were extracted and the lipid classes were separated by TLC. The radioactivity associated with each lipid fraction was quantitated by scintillation counting. The results represent the means ± S.D. of six independent determinations. Asterisks indicate results significantly different from control at * $P < 0.05$, ** $P < 0.01$, or *** $P < 0.001$ level by Student's t test.

Lipid	MCF-7		A549	
	Control	ET18-OCH_3	Control	ET18-OCH_3
	dpm/10^6 cells (% distribution of [^{3}H]glycerol)			
LysoPtdCho	565 ± 48 (0.17)	1747 ± 119 *** (0.36)	853 ± 23 (0.34)	786 ± 25 *** (0.32)
SM	899 ± 39 (0.27)	1073 ± 71 *** (0.22)	1359 ± 26 (0.54)	766 ± 84 *** (0.31)
PtdCho	193303 ± 10013 (57.62)	213706 ± 10123 ** (44.26)	146388 ± 4521 (58.67)	123678 ± 3349 *** (50.22)
LysoPtdEtn	6913 ± 614 (2.06)	6482 ± 618 (1.34)	1743 ± 237 (0.70)	1781 ± 362 (0.72)
PtdSer	11060 ± 706 (3.30)	11210 ± 1152 (2.32)	7523 ± 728 (3.01)	5765 ± 356 *** (2.34)
PtdIns	16466 ± 667 (4.91)	20709 ± 2914 ** (4.29)	18692 ± 1145 (7.50)	16982 ± 1690 (6.90)
PtdEtn	68853 ± 2676 (20.52)	144527 ± 11037 *** (29.93)	24015 ± 1108 (9.62)	25798 ± 942 * (10.47)
PtdOH	22267 ± 996 (6.64)	48639 ± 3546 *** (10.07)	19598 ± 793 (7.85)	23163 ± 862 *** (9.40)
MAG	946 ± 111 (0.28)	1317 ± 281 ** (0.27)	868 ± 41 (0.35)	882 ± 109 (0.34)
DAG	3253 ± 266 (0.97)	8805 ± 437 *** (1.82)	4883 ± 389 (1.96)	4985 ± 333 (2.02)
TAG	10962 ± 1313 (3.27)	24664 ± 1237 *** (5.11)	23601 ± 1397 (9.46)	41702 ± 1285 *** (16.93)
Phospholipid	320326 ± 17807 (95.48)	448093 ± 23043 *** (92.80)	220171 ± 9051 (88.24)	198719 ± 3749 *** (80.69)

[^{3}H]choline for 30 min followed by washing and incubation with ET18-OCH_3 for varying times (0-3 h). This approach was used to eliminate any effects the AELs might have on the uptake of choline into the cell (Hoffman *et al.*, 1992). In MCF-7 cells, ET18-OCH_3 caused a significant decrease in the incorporation of [^{3}H]choline into CDP-Cho ($P < 0.05$) and PtdCho ($P < 0.01$) as early as 30 min after incubation with the compound (the upper panel of **Figure 21**). The loss of the label from the choline fraction was reduced by the AEL but this was only significantly different from controls ($P < 0.05$) after 3-h incubation. No effect was observed on the incorporation of the label into the phosphocholine fraction.

In A549 cells (the lower panel of **Figure 21**), ET18-OCH_3 increased the incorporation of [^{3}H]choline into *P*Cho but had no significant effect on the incorporation of the label into CDP-Cho. The incorporation of [^{3}H]choline into PtdCho decreased by 14% ($P < 0.001$) after a 3-h incubation with the AEL.

To investigate if the inhibition of [^{3}H]choline incorporation into PtdCho was due to the possibility that ET18-OCH_3 might affect the pool sizes of the precursors for PtdCho synthesis, we determined the mass of choline, *P*Cho and CDP-Cho in MCF-7 and A549 cells. **Figure 22** shows, in both cell lines, no significant differences in the pool sizes of water-soluble choline metabolites between cells treated without or with ET18-OCH_3 for 1.5, 3, or 6 h.

4.1.8 Effect of ET18-OCH_3 on [^{3}H]ethanolamine incorporation and the pool sizes of water-soluble ethanolamine metabolites

To investigate the mechanism underlying the observed increase in PtdEtn synthesis

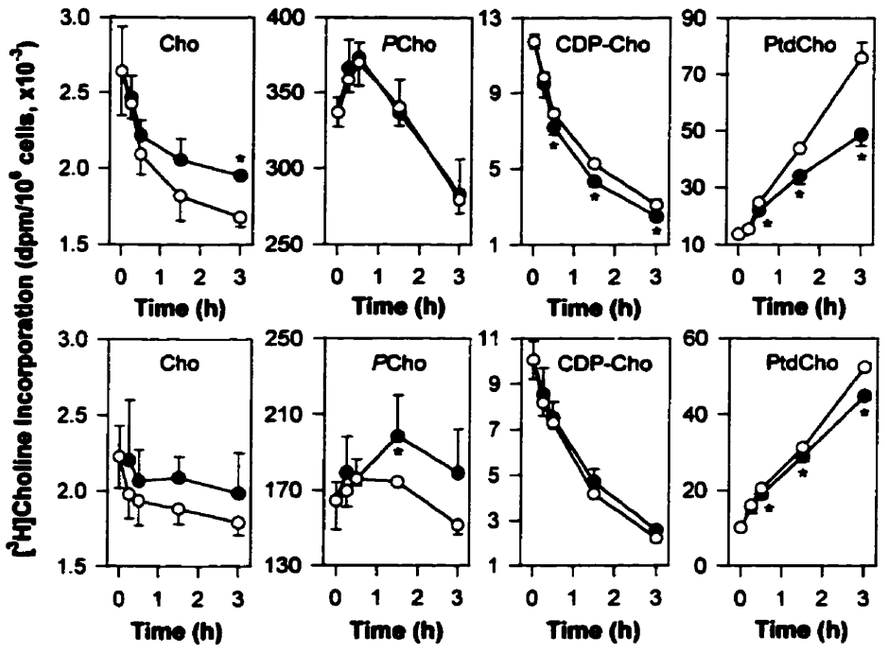

Figure 21. Effect of ET18-OCH_3 on incorporation of [^{3}H]choline into cellular choline metabolites. MCF-7 (*upper panel*) or A549 (*lower panel*) cells growing in the log phase in six-well plates were incubated with [^{3}H]choline (5 μCi/well for MCF-7 or 10 μCi/well for A549) for 30 min, washed and then incubated with growth medium in the absence (○) or presence (●) of ET18-OCH_3 (5 μg/ml) for the indicated periods. The quantity of ^{3}H label in choline (Cho), phosphocholine (*P*Cho), CDP-choline (CDP-Cho) and phosphatidylcholine (PtdCho) was determined using procedures described in **Section 3.4.2.** The values represent the means ● S.D. of four independent determinations. An asterisk indicates significant differences between values obtained from ET18-OCH_3-treated and untreated cells at a level of at least $P < 0.05$ by Student's *t* test.

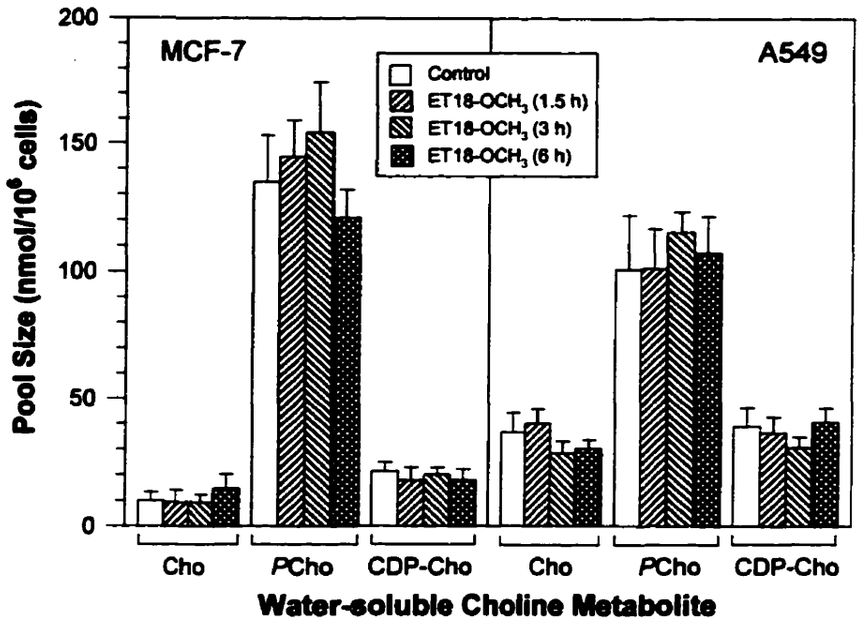

Figure 22. Effect of ET18-OCH_3 on the pool size of water-soluble choline metabolites. Log-phase MCF-7 (*left panel*) and A549 (*right panel*) cells growing in 150-mm dishes were treated with ET18-OCH_3 (5 μg/ml) for 0 (control), 1.5, 3, or 6 h. The cells were then harvested and washed. The cell number was determined and the mass of choline (Cho), phosphocholine (*P*Cho) and CDP-choline (CDP-Cho) in each cell line was quantitated as described in **Section 3.4.3**. The results represent the means ± S.D. of three independent determinations.

in MCF-7 cells, a similar approach to that described above for PtdCho was used by labeling the cell with [^{3}H]ethanolamine (instead of [^{3}H]choline) for 30 min, followed by washing and incubation with ET18-OCH_3 for different times (0-3 h). The distributions of the radiolabel in water-soluble and lipid ethanolamine metabolites extracted from MCF-7 cells are shown in the upper panel of **Figure 23**. ET18-OCH_3 caused significant increases in the incorporation of [^{3}H]ethanolamine into the CDP-Etn ($P < 0.02$) and PtdEtn ($P < 0.02$) fractions after a 30-min or 1-h incubation with the AEL, respectively. The incorporation of the label into the *P*Etn fraction first increased significantly ($P < 0.01$) after incubation with ET18-OCH_3 for 0.5 and 1 h and gradually declined reaching statistically significant levels ($P < 0.01$) after 6-h incubation with the AEL. No significant difference was observed in the incorporation of the label into the ethanolamine fraction between the control and ET18-OCH_3-treated cells. Similar experiments were also conducted with A549 cells for comparison. The lower panel of **Figure 23** shows the incorporation of [^{3}H]ethanolamine into the water-soluble and lipid ethanolamine metabolites extracted from A549 cells. The only significant difference ($P < 0.02$) observed between the ET18-OCH_3-treated and untreated cells was a 15% increase in the label in CDP-Etn fraction after 6-h incubation with the AEL.

We also determined the mass of ethanolamine, *P*Etn and CDP-Etn in both MCF-7 and A549 cells. The data showed that, in cells incubated with ET18-CH_3 for 1, 1.5, 3, or 6 h, the pool sizes of these precursors for PtdEtn synthesis were the same as those in control cells (**Figure 24**).

4.1.9 Effect of ET18-OCH_3 on phospholipid biosynthetic enzymes

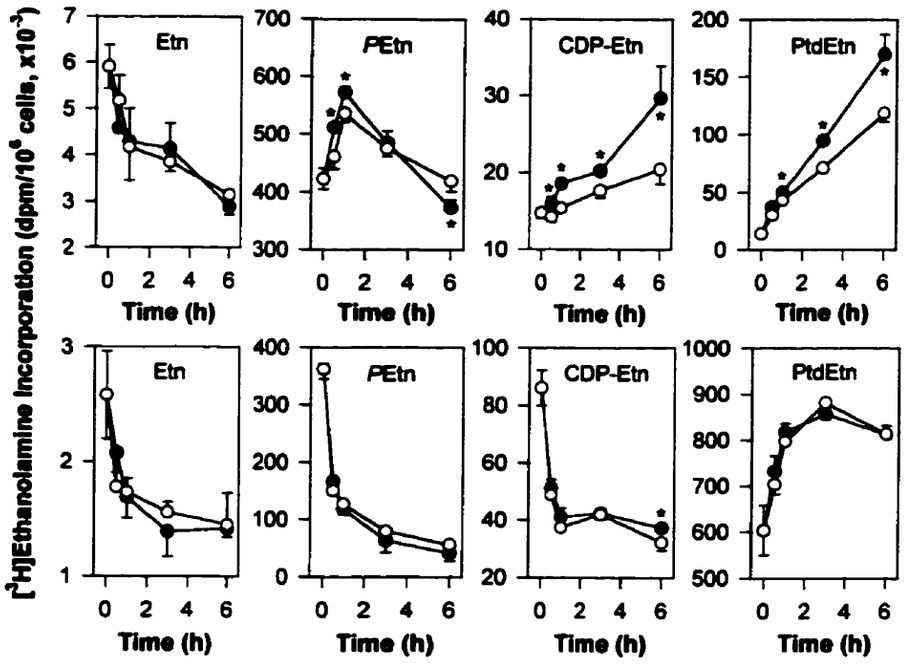

Figure 23. Effect of ET18-OCH$_3$ on incorporation of [^{3}H]ethanolamine into cellular ethanolamine metabolites. MCF-7 (*upper panel*) or A549 (*lower panel*) cells growing in the log phase in six-well plates were incubated with [^{3}H]ethanolamine (5 μCi/well) for 30 min, washed and then incubated with growth medium in the absence (○) or presence (●) of ET18-OCH$_3$ (5 μg/ml) for the indicated periods. The quantity of ^{3}H labeling in ethanolamine (Etn), phosphoethanolamine (*P*Etn), CDP-ethanolamine (CDP-Etn) and phosphatidylethanolamine (PtdEtn) was determined using procedures described in **Section 3.4.2.** The values represent the means ± S.D. of four independent determinations. An asterisk indicates significant differences between values obtained from ET18-OCH$_3$-treated and untreated cells at a level of at least $P < 0.05$ by Student's *t* test.

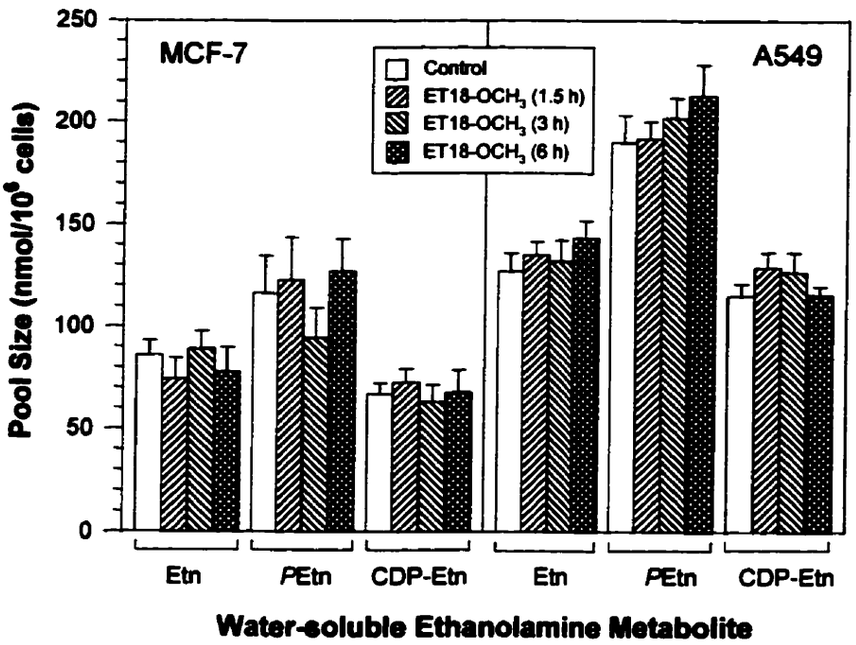

Figure 24. Effect of ET18-OCH_3 on the pool sizes of water-soluble ethanolamine metabolites. Log-phase MCF-7 (*left panel*) and A549 (*right panel*) cells growing in 150-mm dishes were treated with ET18-OCH_3 (5 μg/ml) for 0 (control), 1.5, 3, or 6 h. The cells were then harvested and washed. The cell number was determined and the mass of ethanolamine (Etn), phosphoethanolamine (*P*Etn) and CDP-ethanolamine (CDP-Etn) in each cell line was quantitated as described in **Section 3.4.3**. The results represent the means ● S.D. of three independent determinations.

The observations that ET18-OCH_3 caused changes in radiolabeling of soluble choline and ethanolamine metabolites but had little effect on the pool sizes of these precursors reflect perturbations in the rate of synthesis of PtdCho and PtdEtn by the AEL, implying that ET18-OCH_3 could be affecting the activity of some of the enzymes in the biosynthetic pathways for PtdCho and PtdEtn. To test this, we examined the effects of increasing concentrations of ET18-OCH_3 (0-20 μM) on several enzyme activities of the PtdCho and PtdEtn biosynthetic pathways in *in vitro* assays. The activities of the enzymes tested in assays without ET18-OCH_3 are shown in **Table 9**, using microsomal and cytosolic fractions from MCF-7 and A549 cells.

The effect of the AEL on the cytidylytransferases and phosphotransferases in subcellular fractions of MCF-7 and A549 cells is displayed in the upper panel of **Figure 25**. *P*Etn cytidylyltransferase (PECT) in MCF-7 cytosol was activated at all ET18-OCH_3 concentrations examined except at 20 μM, with a maximum increase of 90% obtained at 5 μM of the AEL. In A549 cytosol, a slight activation of 20% was observed with 1 μM ET18-OCH_3 while a 20% of inhibition was seen with 20 μM. The ethanolaminephosphotransferase (EPT) activity was progressively enhanced by ET18-OCH_3 to produce 100% and 44% increased activity in microsomes derived from MCF-7 and A549, respectively, with 20 μM of the alkyllysophospholipid. ET18-OCH_3 was inhibitory to the microsomal *P*Cho cytidylytransferase (PCCT), with a maximum inhibition of around 50-60% in both MCF-7 and A549 cells at 20 μM of the agent. Cholinephosphotransferases (CPT) in microsomes derived from both cells were either slightly inhibited or not significantly affected by ET18-OCH_3.

The effect of ET18-OCH_3 on enzymes producing PtdOH, DAG, triacylglycerol

Table 9. Activities of enzymes for lipid biosynthesis in subcellular fractions of MCF-7 or A549 cells. Subcellular fractions were prepared from MCF-7 or A549 cells by differential centrifugation as described in **Section 3.4.6**. The appropriate fractions were used in *in vitro* assays, as described in **Section 3.4.7**, of phosphocholine cytidylyltransferase (PCCT), cholinephosphotransferase (CPT), phosphoethanolamine cytidylyltransferase (PECT), ethanolaminephosphotransferase (EPT), diacylglycerol acyltransferase (DGAT), diacylglycerol kinase (DGK), glycero-3-phosphate acyltransferase (GPAT), lysophosphatidic acid acyltransferase (LPAAT), and phosphatidic acid phosphatase (PAP) in the absence of ET18-OCH_3. The results are the means ± S.D. of three separate determinations.

Enzyme (Subcellular fraction)	Activity (nmol · h^{-1} · mg $protein^{-1}$)	
	MCF-7	A549
PCCT (microsome)	240 ± 4	89 ± 9
CPT (microsome)	96 ± 13	70 ± 7
PECT (cytosol)	286 ± 9	378 ± 18
EPT (microsome)	72 ± 4	47 ± 3
DGAT (microsome)	18 ± 2	24 ± 2
DGK (cytosol)	38 ± 4	10 ± 1
GPAT (microsome)	188 ± 18	220 ± 34
LPAAT (microsome)	2812 ± 25	3105 ± 18
PAP (microsome)	27 ± 8	162 ± 19

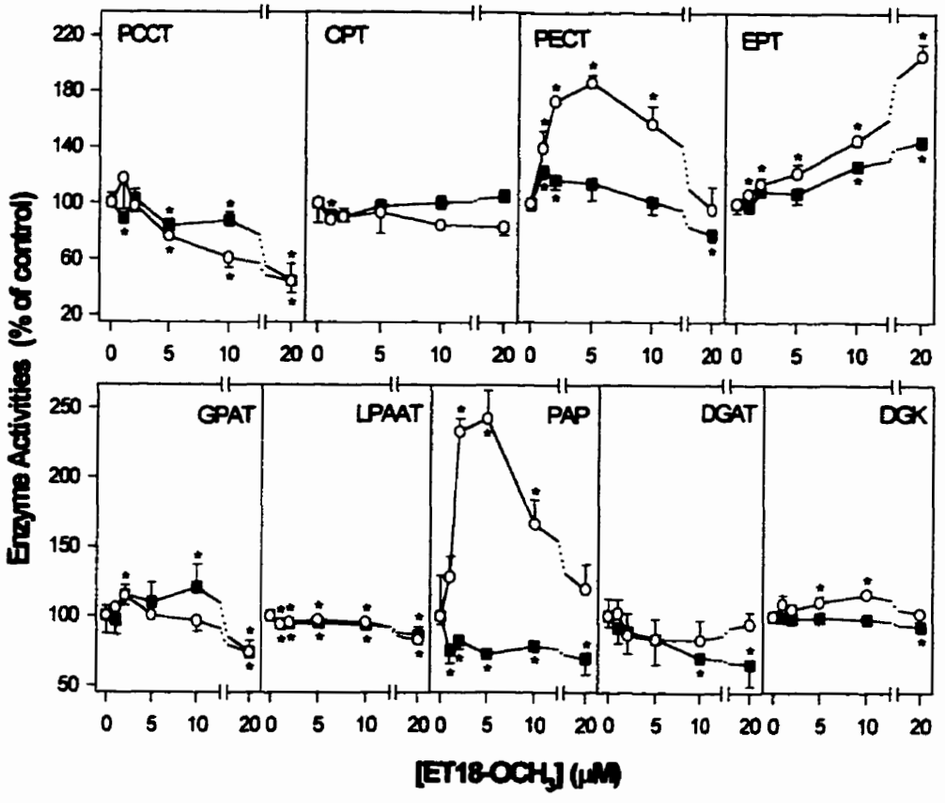

Figure 25. Effect of ET18-OCH_3 on the activities of enzymes for biosynthesis of PtdCho, PtdEtn, PtdOH, DAG and TAG in MCF-7 and A549 cells. Subcellular fractions were obtained from MCF-7 (○) and A549 (■) cells by differential centrifugation. The appropriate fractions were used in assays of (*top: from left to right*) *P*Cho cytidylyltransferase (PCCT), cholinephosphotransferase (CPT), *P*Etn cytidylyltransferase (PECT) and ethanolaminephosphotransferase (EPT), or of (*bottom: from left to right*) Gro-3-*P* acyltransferase (GPAT), lysoPtdOH acyltransferase (LPAAT), PtdOH phosphatase (PAP), DAG acyltransferase (DGAT) and DAG kinase (DGK) as described in **Section 3.4.7**. Effect of ET18-OCH_3 was determined by including the required quantity in assays. The results are expressed as the percentage of the specific activities obtained in its absence. The values represent the means ± S.D. of three separate determinations. * Significantly different from controls (without addition of ET18-OCH_3) at a level of at least $P < 0.05$ by Student's *t* test.

(TAG) was also investigated (the lower panel of **Figure 25**) to determine if any observed effects could account for the level and pattern of incorporation of glycerol into these lipids. The microsomal glycero-3-phosphate acyltransferase (GPAT) activity in A549 moderately increased (15-21%, $P < 0.05$) with 2 or 10 μM of ET18-OCH_3, but it dropped by 26% ($P < 0.02$) in both cell lines with 20 μM of the AEL. Lysophosphatidic acid acyltransferase (LPAAT) activity in both MCF-7 and A549 microsomes was slightly, but significantly ($P < 0.01$) inhibited at all tested concentrations of ET18-OCH_3, reaching about 14-17% inhibition at 20 μM of the AEL. Phosphatidic acid phosphatases (PAP) in A549 microsomes were significantly ($P < 0.02$) inhibited by 20-30% throughout. In contrast, the activity in MCF-7 microsome was dramatically stimulated by 133-143% at 2-5 μM ET18-OCH_3 ($P < 0.01$), but declined to a level of 20% increase ($P > 0.05$) at 20 μM of the agent. The diacylglycerol acyltransferase (DGAT) activity in MCF-7 microsomes was not significantly affected, but the activity in A549 microsomes was inhibited by 30-35% ($P < 0.001$) in assays with 10-20 μM ET18-OCH_3. A slight (10-16%), but significant ($P < 0.02$) activation of diacylglycerol kinase (DGK) activity by ET18-OCH_3 in MCF-7 cytosol was observed, but in A549 cytosol it was either unaffected or slightly inhibited (7%) at a concentration of 20 μM ($P < 0.01$).

4.1.10 Effect of oleic acid on the ET18-OCH_3-induced inhibition of PtdCho synthesis and inhibition of cell growth.

Oleic acid stimulates PtdCho synthesis in a number of cells and tissues (Van Hellemond *et al.*, 1994). Incubation of MCF-7 cells for 1.5 h with 100-350 μM oleic acid accelerated the loss of the label from the *P*Cho by 6-39% and enhanced the incorporation of

[^{3}H]choline into CDP-Cho by 40-712% and PtdCho by 72-212% (**Figure 26**). We reasoned that the stimulative action of oleic acid could overcome the inhibitory effect of ET18-OCH_3 on PtdCho synthesis. This prompted an investigation into whether a causative relationship existed between the reduction of PtdCho synthesis and inhibition of MCF-7 cell growth by ET18-OCH_3. The experiments were conducted with 75 μM oleic acid after preliminary studies indicated that this concentration of oleic acid had no effect on cell growth for up to 24 h incubation. The results of experiments on the effects of oleic acid, ET18-OCH_3 and the combination on PtdCho synthesis and cell proliferation are shown in **Figure 27**. The presence of 75 μM oleic acid effectively nullified the inhibitory effect of ET18-OCH_3 on PtdCho synthesis in MCF-7 cells. In spite of this, there was no significant difference in the growth rate of the cells incubated with ET18-OCH_3 alone or with ET18-OCH_3 plus oleic acid.

4.1.11 Effect of ET18-OCH_3 on PtdCho and PtdEtn content in MCF-7 and A549 cells

To investigate whether the effect of ET18-OCH_3 on incorporation of Etn and Cho into cellular glycerophospholipids affected the content of these major phospholipids, cells were incubated with ET18-OCH_3 (5 μg/ml) for up to 12 h followed by extraction and quantitative analysis of the PtdCho and PtdEtn content. The results are displayed in **Figure 28**. Incubation of either cell line for up to 12 h with ET18-OCH_3 did not affect the PtdEtn content. A significant decrease in PtdCho content, 17% and 21% in MCF-7 and A549 cells respectively, was observed only 12 h after incubation of the cells with the AEL.

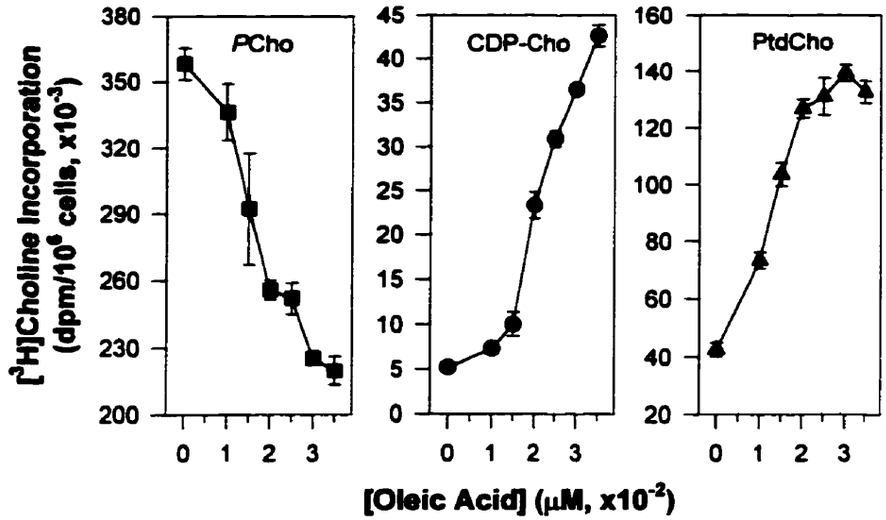

Figure 26. Stimulation of PtdCho synthesis by oleic acid in MCF-7 cells. Log-phase MCF-7 cells growing in six-well plates were pre-labeled with [^{3}H]choline (10 μCi/ml) for 30 min, washed and incubated with various concentrations (0-350 μM) of oleic acid for 1.5 h. The cells were washed and harvested. The cell number was determined and the radioactivity associated with each of *P*Cho, CDP-Cho and PtdCho fractions was quantitated after separation as described in **Section 3.4.2**. The results represent the means ± S.D. of four independent determinations.

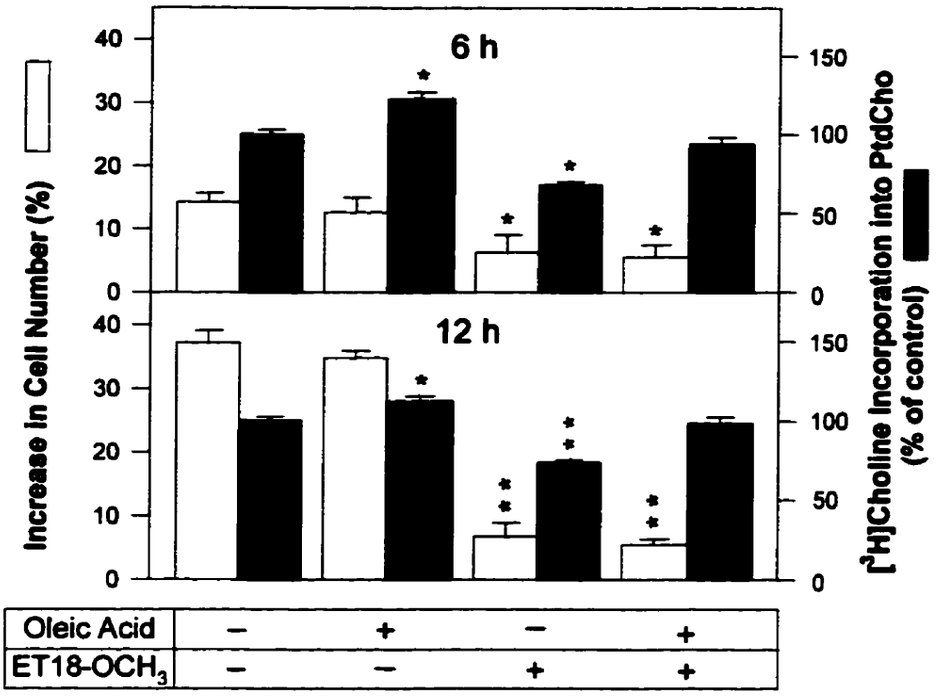

Figure 27. Effect of oleic acid on ET18-OCH_3-induced inhibition of PtdCho synthesis and MCF-7 cell proliferation. Log-phase MCF-7 cells growing in six-well plates were incubated with [^{3}H]choline (4 μCi/ml/well) for 3 h, washed and incubated with medium (control), or medium containing either oleic acid (75 μM), ET18-OCH_3 (5 μg/ml) or both. After 6 h (*upper panel*) or 12 h (*lower panel*), the cells were washed, the cell number was determined, and the radioactivity associated with the PtdCho fraction was quantitated as described in **Section 3.4.2**. The results represent the means ± S.D. of three independent determinations. Asterisks indicate results significantly different from control cells (without oleic acid or ET18-OCH_3) at $P < 0.05$ (*) or $P < 0.001$ (**) levels by Student's *t* test.

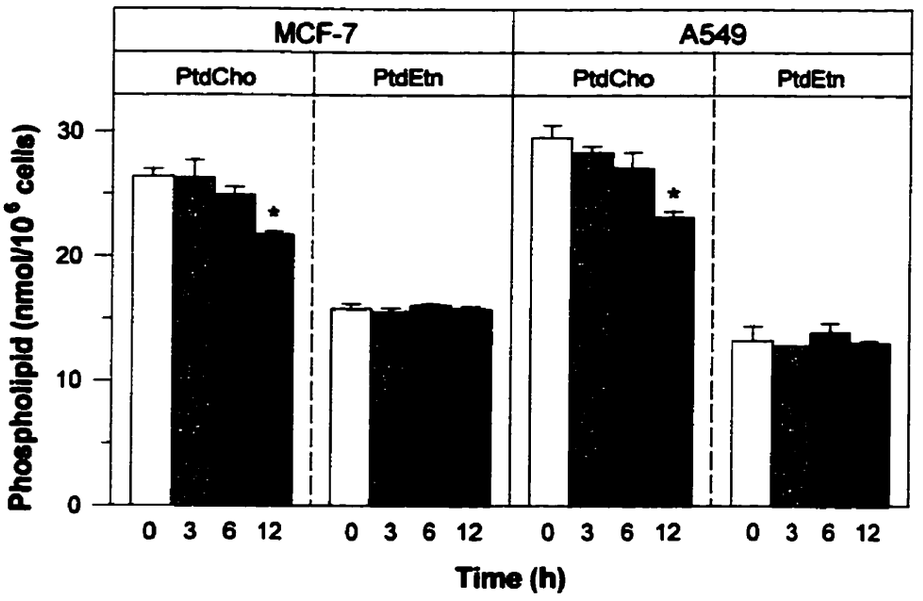

Figure 28. Effect of ET18-OCH_3 on PtdCho and PtdEtn content in MCF-7 and A549 cells. Log-phase MCF-7 and A549 cells growing in 150-mm dishes were incubated without or with 5 μg/ml ET18-OCH_3 for the indicated times. The cells were then harvested and the lipids were extracted. PtdCho and PtdEtn were separated by TLC and the cellular content of each phospholipid was determined by the improved malachite green methods (see **Section 3.2.2**). The values represent the means ± S.D. of triplicate determinations from two separate cell preparations. An asterisk indicates values significantly different from those obtained in cells incubated without ET18-OCH_3 at a level of $P < 0.01$ by Student t test.

4.2 Effect of ET18-OCH_3 on the PKC-dependent Phosphorylation of Endogenous Proteins in MCF-7 cells

PKC plays a pivotal role in regulation of cell growth in many cell types (see **Section 1.3**). In MCF-7 cells, PKC may also be a key element that participates in regulation of cell proliferation since a specific PKC inhibitor Ro 31-8220 inhibited MCF-7 cell growth in a dose-dependent manner (**Figure 32**). The effect of AEL on PKC has yet to be established as differential effects of AEL on PKC have been reported by different laboratories (see **Section 1.7.3**). To explore this issue, we examined the effect of ET18-OCH_3 on the PKC-dependent phosphorylation of cellular proteins in MCF-7 cells.

4.2.1 Accumulation of [^{3}H]ET18-OCH_3 by quiescent MCF-7 cells

To investigate the effect of ET18-OCH_3 on cellular signal transduction that may account for its inhibition of cell proliferation, quiescent MCF-7 cells were used for these studies. The accumulation of [^{3}H]ET18-OCH_3 as a function of time in serum-deprived quiescent MCF-7 cells was determined. After incubation for 1, 2, and 3 h with 10 μg/ml of ET18-OCH_3, the quantities of the AEL incorporated into the quiescent cells were 0.44, 0.63 and 0.74 μg/ml/10^6 cells, respectively.

4.2.2 ET18-OCH_3 inhibited serum-induced cell proliferation and [^{3}H]thymidine incorporation

To correlate any observed cellular perturbations with the inhibition of cell proliferation, incubation conditions were established whereby quiescent MCF-7 cells

accumulated sufficient ET18-OCH_3 to inhibit cell proliferation following the readdition of DMEM/FBS without loss of cell viability. As expected, the addition of serum-containing medium to quiescent MCF-7 cells by serum starvation stimulated proliferation, while continued deprivation of serum did not (**Figure 29A**). Preincubation of the quiescent cells with ET18-OCH_3 (10 μg/ml) for 1 h and subsequent incubation with DMEM/FBS decreased their rate of proliferation relative to controls while preincubation for 2 h or more completely inhibited cell proliferation.

In cells preincubated with ET18-OCH_3 for 3 h prior to incubation in DMEM/FBS for up to 4 days, the proportion of cells excluding trypan blue dye (> 90%) was similar to that of controls, indicating that the viability of the cells had not been compromised.

Preincubation of quiescent MCF-7 cells with ET18-OCH_3 followed by stimulation with serum also inhibited the incorporation of [^{3}H]thymidine into the cells (**Figure 29B**), indicating that progression of the cells into S phase had been inhibited.

4.2.3 Identification of proteins phosphorylated in response to PKC activation

The criteria used to identify cellular proteins whose phosphorylation was PKC-dependent were [1] the increase in their phosphorylation in response to stimulation with PKC agonists (phorbol esters or diacylglycerol) and [2] the inhibition of the induced phosphorylation by a specific PKC inhibitor Ro 31-8220 (Simpson *et al.*, 1993; Standaert *et al.*, 1996; Sullivan *et al.*, 1994).

Analysis of phosphorylation of proteins by one-dimensional polyacrylamide gel electrophoresis (PAGE) revealed that the most prominent phosphorylation occurred on a

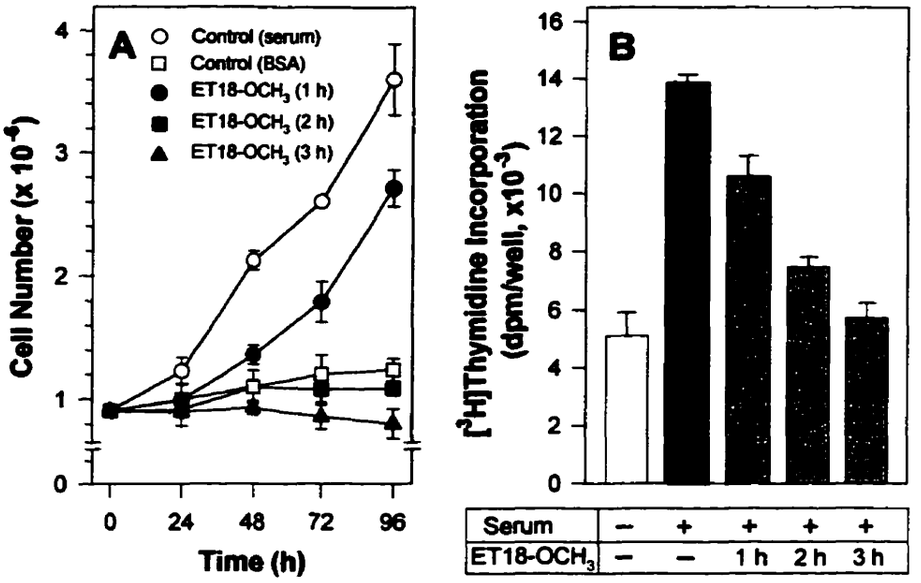

Figure 29. Preincubation of quiescent MCF-7 cells with ET18-OCH_3 inhibits cell proliferation and thymidine incorporation. (*A*) Quiescent MCF-7 cells were incubated with 10 μg/ml ET18-OCH_3 for 1 h (●), 2 h (■), or 3 h (▲). The cells were washed and incubated with DMEM/FBS and the cell numbers were determined at 24-h intervals. Control cells without ET18-OCH_3 pretreatment were incubated with DMEM/FBS (○) or DMEM/BSA (□). (*B*) Quiescent MCF-7 cells were treated with or without ET18-OCH_3 as described in (*A*). After washing, the cells were incubated with DMEM/FBS or DMEM/BSA for 20 h followed by the addition of [^{3}H]thymidine for an additional 4 h. [^{3}H]Thymidine incorporation in cells was determined as described in **Section 3.5.2**. The results of both studies are the means of six separate determinations.

protein(s) with a M_r of about 31 kDa (p31) in quiescent MCF-7 cells upon TPA stimulation (**Figure 30A**). This phosphorylation of p31 was also observed when the cells were stimulated with DiC_8, and both TPA- and DiC_8-induced phosphorylations of p31 were abolished by pre-incubation of the cells with Ro 31-8220 (**Figure 30B**). These results suggest that the induced phosphorylation of p31 by TPA or DiC_8 appeared to be due to PKC activation in MCF-7 cells. The inactive phorbol ester 4-α-TPA failed to cause the phosphorylation of p31 (**Figure 33A**) further strengthening the above argument.

A series of experiments was conducted to select concentrations and incubation times for PKC activators and inhibitor. The TPA-induced phosphorylation of p31 was observed at all tested concentrations and was most obvious with 1 μM TPA (**Figure 31A**). The optimal time for stimulation with 1 μM TPA was 10 min (**Figure 30A**). The phosphorylation of p31 was apparent in cells stimulated by DiC_8 at all tested concentrations for 5 or 10 min (**Figure 31B**). This TPA-induced phosphorylation of p31 was completely inhibited by incubation of the cells with 5 μM Ro 31-8220 for 20 min prior to TPA stimulation (**Figure 31C**). Incubation of MCF-7 cells with Ro 31-8220 also caused inhibition of cell proliferation with complete inhibition at 5 μM or more (**Figure 32**).

4.2.4 Effect of ET18-OCH_3 on phosphorylation of p31

In contrast to Ro 31-8220, preincubation of the labeled quiescent MCF-7 cells with ET18-OCH_3 (10 μg/ml) for 3 h prior to stimulation with TPA did not inhibit but rather appeared to enhance the phosphorylation of p31; ET18-OCH_3 alone also stimulated p31 phosphorylation (**Figure 33A**). This ET18-OCH_3-enhanced phosphorylation of p31 in

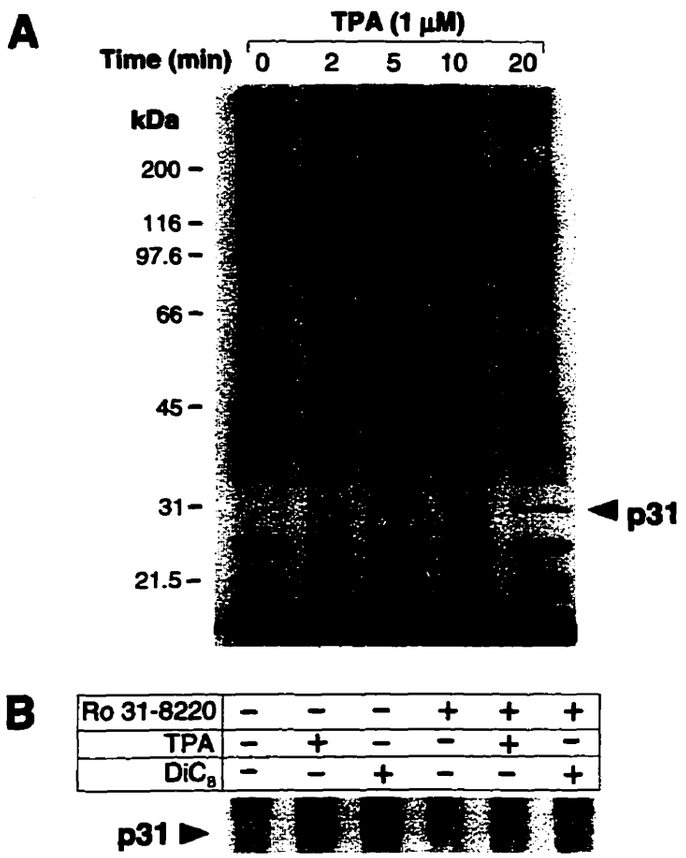

Figure 30. The PKC-dependent phosphorylation of p31. (*A*) Time course for TPA stimulation. Quiescent MCF-7 cells prelabeled with [^{32}P]orthophosphate were challenged with 1 μM TPA for 2-20 min or left unstimulated as control. Proteins in cell lysates were resolved on an 8% SDS gel and subjected to autoradiography. The cell treatments are indicated on the top of each lane. The M_r are displayed at the left side. The most prominent phosphorylation band (p31) is indicated by the arrow. (*B*) Effect of Ro 31-8220 (a specific PKC inhibitor) on TPA- or DiC_8-induced phosphorylation of p31. [^{32}P]Orthophosphate-labeled quiescent MCF-7 cells were incubated in fresh DMEM/BSA without or with 5 μM Ro 31-8220 for 20 min. The cells were washed and stimulated with TPA (1 μM, 10 min) or DiC_8 (20 μM, 10 min), or left untreated as control. Protein phosphorylation was determined by autoradiography after separation on a 10% SDS gel. The cell treatments and the p31 band are indicated in the figure.

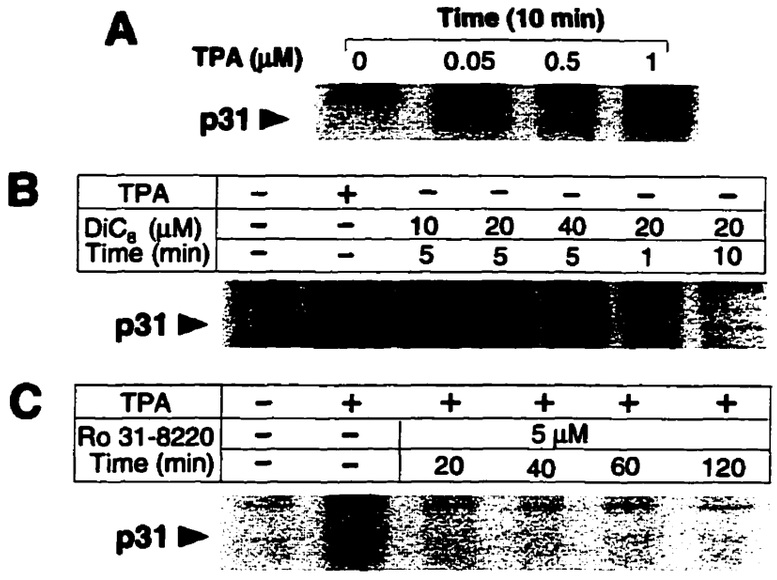

Figure 31. Characterization of p31 phosphorylation. (*A*) Dose-dependent TPA-induced p31 phosphorylation. Quiescent MCF-7 cells prelabeled with [^{32}P]orthophosphate were challenged with TPA for 10 min at concentrations from 0-1 μM. Proteins in cell lysates were resolved on a 10% SDS gel and subjected to autoradiography. (*B*) Time- and dose-dependent DiC_8-induced p31 phosphorylation. Experiments were conducted as described in (*A*), except stimulation of cells with DiC_8 as indicated. (*C*) Time course of the inhibitory effect of Ro 31-8220. [^{32}P]Orthophosphate-prelabeled quiescent MCF-7 cells were incubated in DMEM/BSA in the presence or absence of 5 μM Ro 31-8220 for 20-120 min. The cells were washed, and stimulated with TPA (1 μM, 10 min), or left untreated as control. Phosphorylation of cellular proteins was determined by autoradiography upon separation on a 10% SDS gel. In all three figures, the cell treatments are indicated on the top of each lane and the phosphorylated p31 band is indicated by the arrow.

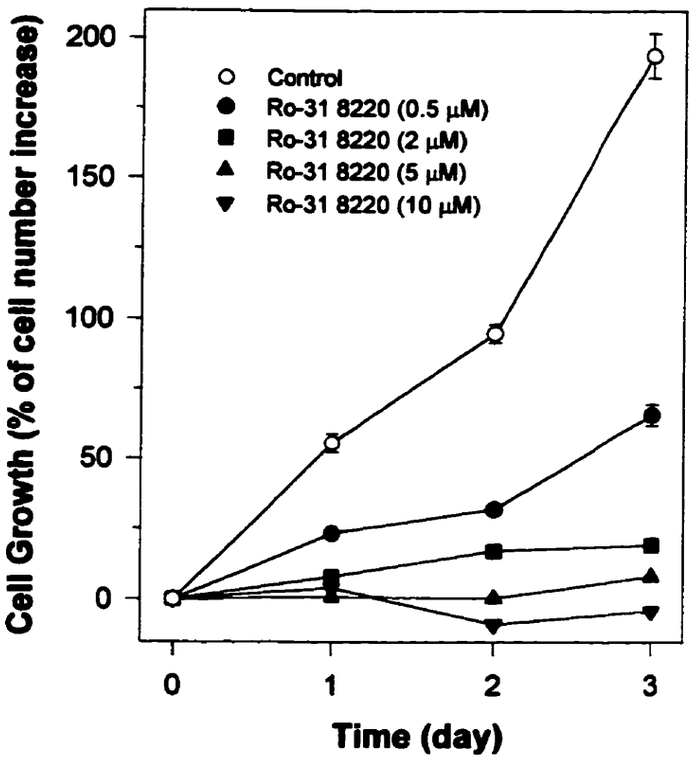

Figure 32. Inhibition of MCF-7 cell proliferation by Ro 31-8220. Log-phase MCF-7 cells growing in six-well plates were incubated with Ro 31-8220 at concentrations of 0.5, 2, 5, or 10 μM or left untreated as control. The cell number was determined at every 24-h interval. The percentages of the increase in the cell number over the initial cell number (at 0 time) were plotted against incubation time. The results represent the means ± S.D. of three independent determinations.

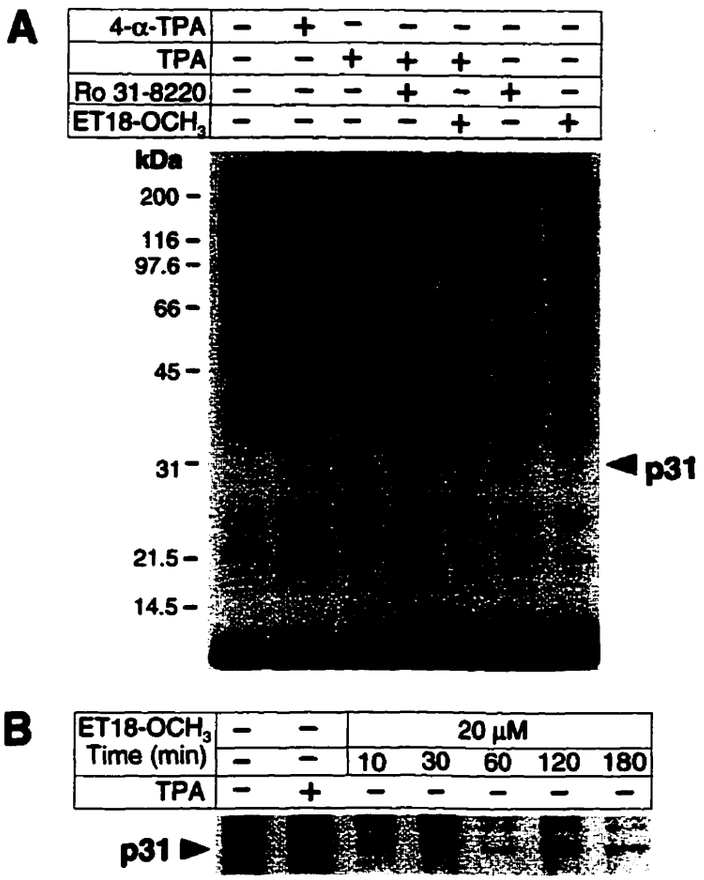

Figure 33. Enhanced phosphorylation of p31 in MCF-7 cells by ET18-OCH_3. (*A*) Quiescent MCF-7 cells prelabeled with [^{32}P]orthophosphate were incubated with or without ET18-OCH_3 (10 μg/ml, 3 h) or Ro 31-8220 (5 μM, 20 min) followed by stimulation with 1 μM TPA or 4-α-TPA for 10 min, or left untreated as control. Proteins in cell lysates were separated on a 10% SDS gel and subjected to autoradiography. Markings are as specified in **Figure 30A**. Three independent experiments with different cell preparations showed similar results. (*B*) Time-dependent ET18-OCH_3-induced phosphorylation of p31. Quiescent MCF-7 cells prelabeled with [^{32}P]orthophosphate were incubated with 20 μM (10.4 μg/ml) of ET18-OCH_3 for 10-180 min, or stimulated with TPA (1 μM, 10 min) or left untreated as control. Proteins in cell lysates were resolved on a 10% SDS gel and subjected to autoradiography. The phosphorylated p31 band is indicated by the arrow.

quiescent MCF-7 cells was a time-dependent event that was visible as early as 30 min after treatment with the maximum phosphorylation at 2 h (**Figure 33B**). Nevertheless, this ET18-OCH_3-enhanced phosphorylation of p31 was not inhibited by coincubation of the cells with Ro 31-8220 (**Figure 34G**), indicative of a PKC-independent phosphorylation.

4.2.5 Effect of ET18-OCH_3 on phosphorylation of endogenous proteins in MCF-7 cells

To investigate whether the protein(s) with a M_r of 31 kDa that were phosphorylated upon ET18-OCH_3- or TPA-treatment were identical, and whether phosphorylation of endogenous proteins other than p31 were also enhanced by incubation of the cells with ET18-OCH_3, phosphorylated proteins were analyzed by two-dimensional gel electrophoresis (2-D gel) (**Figure 34A-34G**).

Relative to unstimulated controls (**Figure 34A**), stimulation of quiescent MCF-7 cells with TPA resulted in increased phosphorylation of a number of proteins identified as spots **a**, **d-l** (**Figure 34B**). A series of spots (**b-g**) with M_r around 31 kDa were phosphorylated with spots **d-g** being the most prominent. These spots could be different phosphorylated forms of the same protein, since we observed an apparent shift of the phosphorylation pattern to the positive side (right) following TPA stimulation. Thus, phosphorylation of spots **b** and **c** in the controls disappeared in TPA-stimulated cells while phosphorylation of spots **d**, **e**, **f** and **g** were increased. Incubation of the cells with 5 μM Ro 31-8220 for 20 min (**Figure 34C**) resulted in decreased phosphorylation of spots **a-e**, **k**, **l** and many other unlabeled spots, reflecting that the compound had decreased basal phosphorylation levels. Preincubation of

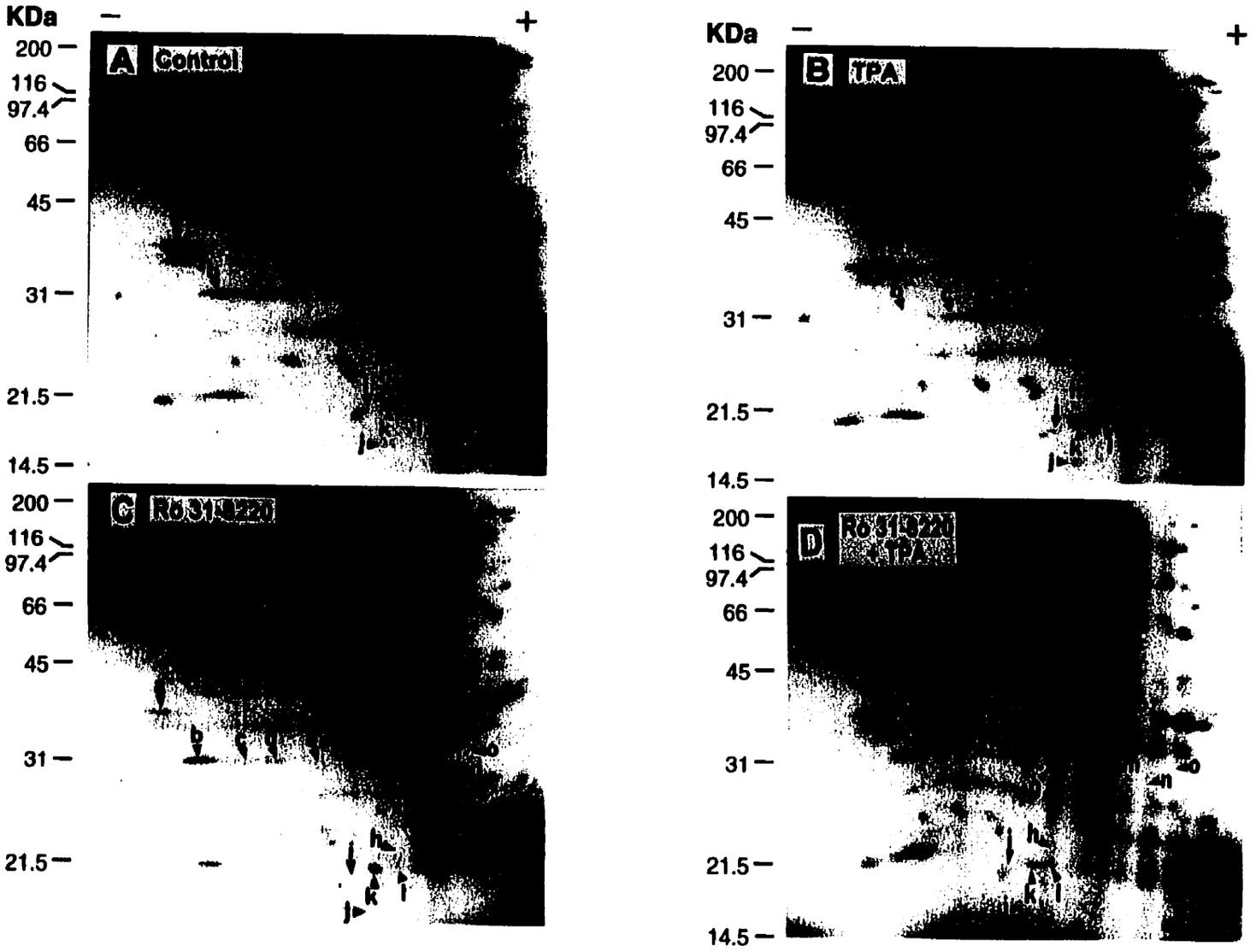
KDa
–
+
200
116
97.4
66
45
31
21.5
14.5
A Control
B TPA
C Rö 31-8220
D Rö 31-8220 + TPA

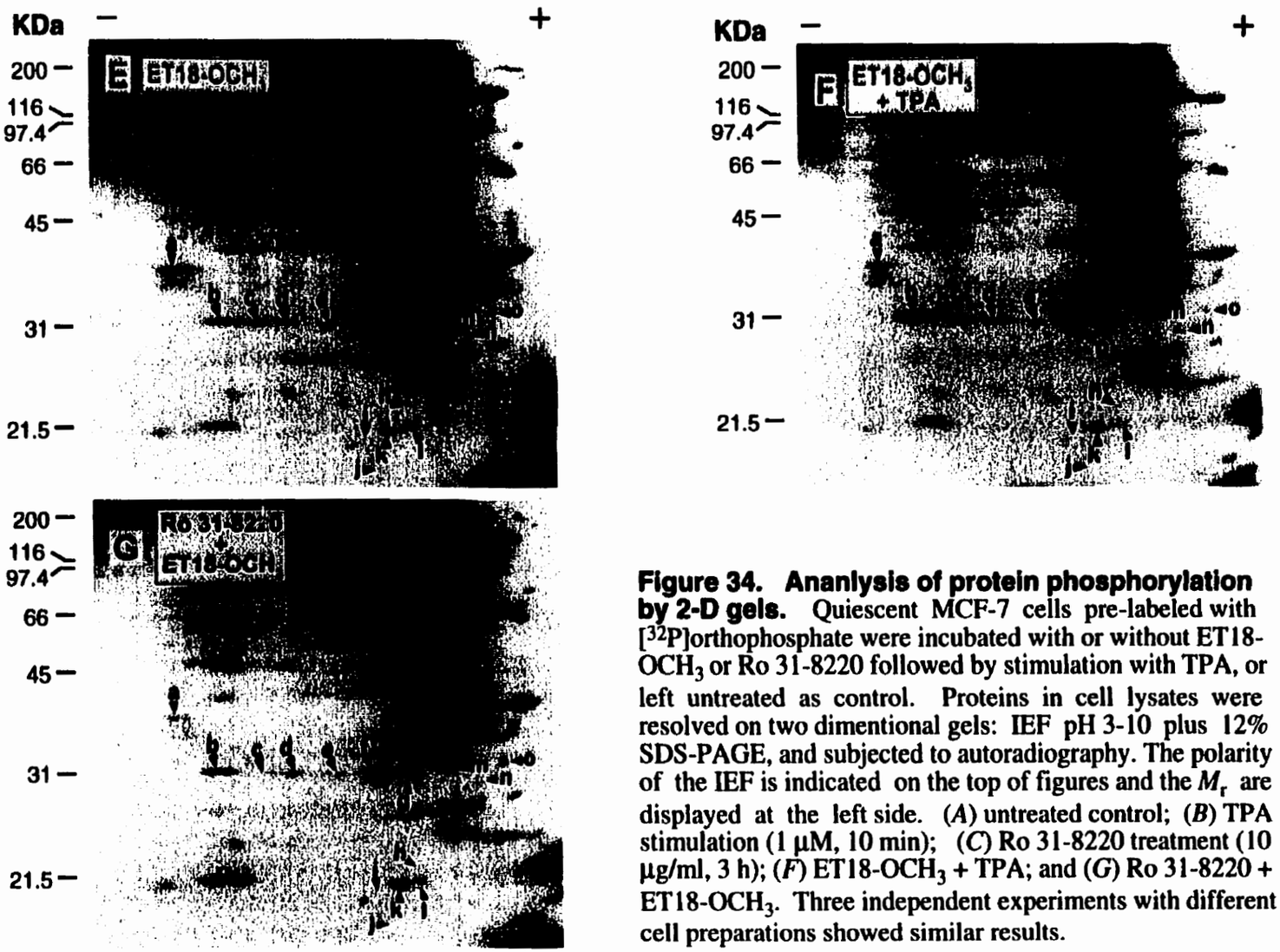

Figure 34. Ananlysis of protein phosphorylation by 2-D gels. Quiescent MCF-7 cells pre-labeled with [^{32}P]orthophosphate were incubated with or without ET18-OCH_3 or Ro 31-8220 followed by stimulation with TPA, or left untreated as control. Proteins in cell lysates were resolved on two dimentional gels: IEF pH 3-10 plus 12% SDS-PAGE, and subjected to autoradiography. The polarity of the IEF is indicated on the top of figures and the M_r are displayed at the left side. (*A*) untreated control; (*B*) TPA stimulation (1 μM, 10 min); (*C*) Ro 31-8220 treatment (10 μg/ml, 3 h); (*F*) ET18-OCH_3 + TPA; and (*G*) Ro 31-8220 + ET18-OCH_3. Three independent experiments with different cell preparations showed similar results.

cells with Ro 31-8220 (5 μM, 20 min) inhibited the phosphorylation of the spots that would otherwise be observed in response to the subsequent stimulation by TPA (1 μM, 10 min), i.e. spots **a** and **d-l** (**Figure 34D**). The ability of Ro 31-8220 to inhibit the phosphorylation of these spots identified the phosphorylation of these spots as being PKC-dependent.

The results obtained from the cells pretreated with ET18-OCH_3 (10 μg/ml, 3 h) prior to stimulation with TPA are shown in **Figure 34F**. ET18-OCH_3 was equally effective as Ro 31-8220 in inhibiting the TPA-induced phosphorylation of spots **a**, **d**, **e**, **h**, **i**, **j**, **k**, and **l**. ET18-OCH_3 alone (**Figure 34E**) decreased the phosphorylation of spot **l** down to the unstimulated control level (**Figure 34A**) but not to the level observed with Ro 31-8220 (**Figure 34D**). These suggested that pre-incubation of quiescent MCF-7 cells with ET18-OCH_3 inhibited PKC-dependent phosphorylation of endogenous proteins. In addition to the above inhibition of phosphorylation, ET18-OCH_3 also enhanced the incorporation of ^{32}P in spots **f**, **g**, **m**, **n**, and **o**. In fact, an enhanced phosphorylation of these spots was observed when the cells were preincubated with ET18-OCH_3 alone (**Figure 34E**), an indication that the enhanced phosphorylations were a consequence of incubation with the AEL. Phosphorylations of these spots were not abolished by the presence of Ro 31-8220 during incubation with ET18-OCH_3 (**Figure 34G**) and spots **m**, **n**, and **o** were not present in controls (**Figure 34A**) or TPA-treated cells (**Figure 34B**), suggesting that they were PKC-independent phosphorylations.

4.2.6 Effect of ET18-OCH_3 on translocation of PKC isoforms

To investigate what effect, if any, ET18-OCH_3 had on the translocation of selected

PKC species, quiescent MCF-7 cells were incubated with the AEL under identical conditions to those used for the phosphorylation studies, and stimulated with TPA followed by rapid washing and separation of membrane fractions from the cytosol as described in **Section 3.5.18**. The association of α, γ and ϵ PKC species with membranes was assessed by Western blot analysis with isotype-specific antibodies. The results obtained are displayed in **Figure 35A**. In unstimulated control cells, PKC-α, -γ, and -ϵ were not associated with membrane, but they became membrane-associated following stimulation with TPA. The membrane-association of PKC-α and -ϵ was evident after 1-min stimulation with TPA while the association of γ species with membrane appeared at 5 min following TPA stimulation. Pre-treatment of cells with ET18-OCH_3 alone resulted in the redistribution of PKC-α, but not the γ or ϵ isoforms, to the membrane. After correcting for any ET18-OCH_3-induced increase in PKC membrane association, the plot (**Figure 35B**) of the densitometric analysis of the Western blots revealed a moderate inhibition by ET18-OCH_3 of TPA-induced translocation of PKC-α. It is worth noting that there was no difference in the total amount of membrane-associated PKC-α in the ALP-treated and control cells after 10 min stimulation with TPA. Slight differences were observed in the kinetics of TPA-induced translocation of PKC-γ and PKC-ϵ to the membrane between the control and ET18-OCH_3-treated cells. After 10 min stimulation with TPA, the amount of membrane-associated PKC-γ was similar in control and ALP-treated cells while a slight inhibition of PKC-ϵ was observed in the drug-treated cells relative to controls.

4.3 Effect of ET18-OCH_3 on Signal Transduction via the MAPK Cascade

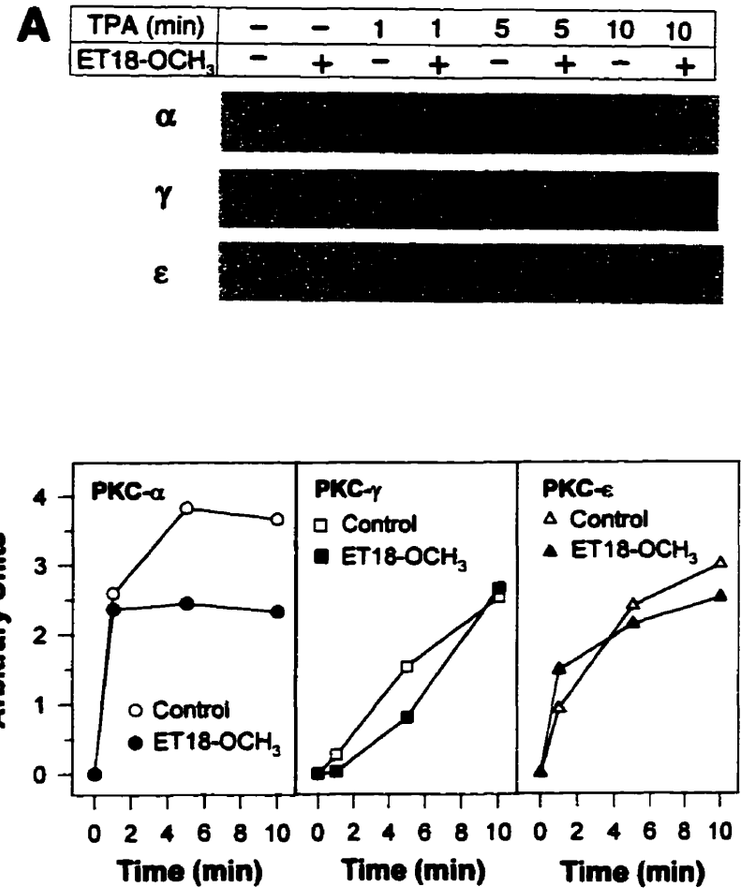

Figure 35. Translocation of PKC isoforms from cytosol to membrane. (*A*) Quiescent MCF-7 cells were incubated with or without ET18-OCH_3 (10 μg/ml, 3 h) followed by stimulation with 1 μM TPA for 1, 5, or 10 min, or left untreated as control. Proteins in membrane fraction were resolved on 8% SDS gels, transferred to nitrocellulose membranes, probed with monoclonal Abs specific to PKC isoforms, and visualized by the ECL detection system. Two separate experiments showed similar results. (*B*) Densitometric analysis of the blots shown in (*A*).

Since ET18-OCH_3 inhibited the serum-induced cell proliferation and [^{3}H]thymidine incorporation in MCF-7 cells (see **Section 4.2.2**), and the activation of MAPK (ERK) is crucial for cell proliferation after stimulation by extracellular ligands such as EGF or mitogens that exist in serum, we investigated whether the inhibitory locus of ET18-OCH_3 could be somewhere in the Ras/Raf/MEK/ERK pathway.

4.3.1 ET18-OCH_3 inhibited MAPK activation in MCF-7 cells

The objective of the initial studies was to determine if ET18-OCH_3 affected the MAPK activity or its activation. Quiescent MCF-7 cells were preincubated with or without ET18-OCH_3 (10 μg/ml) for 3 h, stimulated with EGF, and MAPK activity in the cytosolic fractions was measured. The results displayed in **Figure 36A** show that in control cells, MAPK activity peaked at 642 pmol/min per mg protein after 10-min stimulation, whereas in cells preincubated with ET18-OCH_3, a peak activity of 395 pmol/min per mg protein was observed after 5 min. At 10 min, MAPK activity was 2.5 times higher in the controls compared with the cells preincubated with ET18-OCH_3.

The in-gel assay revealed a similar inhibitory effect of preincubation of the cells with ET18-OCH_3 on MBP phosphorylation by MAPK in response to EGF stimulation (**Figure 36B**). There was little differences in MBP phosphorylation between the controls and ET18-OCH_3-treated cells 4 min after EGF stimulation. However, at 10 min, phosphorylation of MBP by $p42^{mapk}$ and $p44^{mapk}$ in the controls was still evident whereas that in the ET18-OCH_3-treated cells had declined considerably.

A similar inhibitory effect of ET18-OCH_3 on MAPK activation in cells stimulated

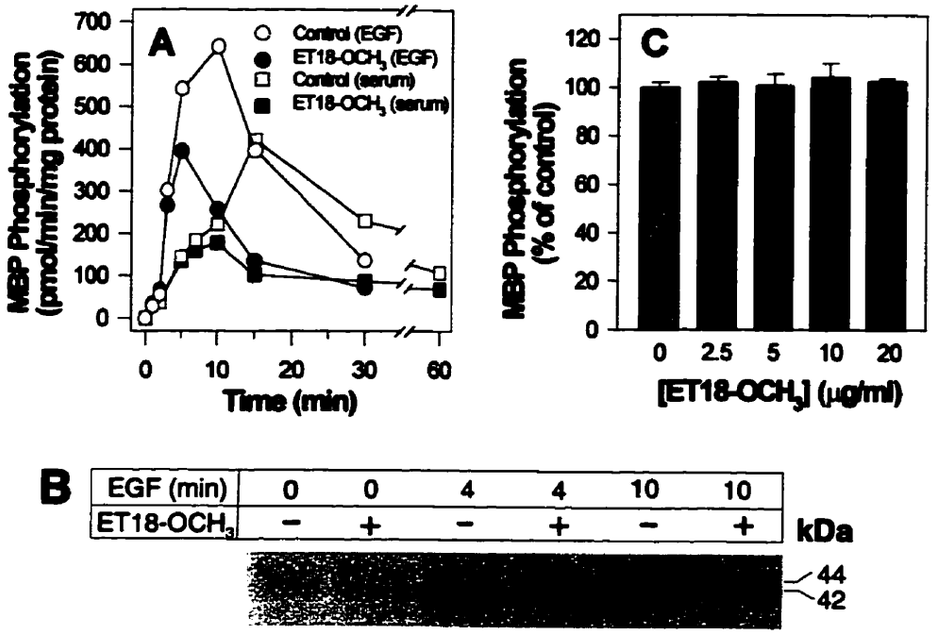

Figure 36. ET18-OCH_3 attenuates activation of MAPK in MCF-7 cells. (*A*) Quiescent cells were incubated without (*open symbols*) or with (*closed symbols*) ET18-OCH_3 (10 μg/ml) for 3 h, washed and stimulated with EGF (*circles*) or DMEM/FBS (*squares*). Cytosolic MAPK activity was measured as the phosphorylation of MBP as described in **Section 3.5.5.** The results are the means of triplicate incubations from a single experiment that is representative of four separate experiments. (*B*) Assessment of MAPK activity by the in-gel assay. Quiescent MCF-7 cells were preincubated with or without ET18-OCH_3 and stimulated with EGF. Cytosolic fractions were used for the in-gel MAPK assay as described in **Section 3.5.4.** The results are from a single experiment that is representative of two identical experiments. (*C*) Effect of the addition of ET18-OCH_3 on MAPK activity in *in vitro* assays. Cytosolic fractions were prepared from quiescent MCF-7 cells stimulated with EGF (10 ng/ml, 7 min). The *in vitro* MAPK assays that contained exogenous ET18-OCH_3 at final concentrations of 0-20 μg/ml were conducted as described in **Section 3.5.5.** The results represent the means ± S.D. of three separate determinations.

with serum was also observed (**Figure 36A**). Peak phosphorylation of MBP in control cell cytosol occurred 15 min after serum stimulation while preincubation of the cells with ET18-OCH_3 before serum stimulation yielded a peak activity at 10 min that was twofold lower than the peak activity in controls. The MAPK activity in the ET18-OCH_3-treated cell cytosol declined to one fourth of that in controls 15 min after serum stimulation.

To determine if the effect of ET18-OCH_3 on MAPK was due to a direct inhibition of the enzyme activity *per se* or interruption of upstream events that are essential for MAPK activation, the MAPK activity in the cytosolic fractions from stimulated cells were examined *in vitro* with ET18-OCH_3 added in the assays. The results revealed there was no impairment of the enzyme activity by the addition of up to 20 μg/ml of exogenous ET18-OCH_3 in assays (**Figure 36C**).

4.3.2 ET18-OCH_3 decreased EGF-induced phosphorylation of $p42^{mapk}$ and $p44^{mapk}$

As phosphorylation of MAPK is required for its activation (Anderson *et al.*, 1990), the effect of ET18-OCH_3 on this event was examined. $p42^{mapk}$ and $p44^{mapk}$ were immunoprecipitated from [^{32}P]orthophosphate-labeled cells incubated with or without ET18-OCH_3 and stimulated with EGF. Phosphorylated $p42^{mapk}$ and $p44^{mapk}$ bands were visualized by autoradiography after separation on 10% SDS gel (**Figure 37A**). Four minutes after EGF stimulation, there was little difference in the phosphorylation of the MAPK immunoprecipitated from the control and experimental cells. However, the phosphorylation significantly declined after 10 min in MAPK immunoprecipitates from cells incubated with

the ALP compared with controls (3.2- and 3.7-fold decrease in $p42^{mapk}$ and $p44^{mapk}$ by densitometric analysis, respectively). Western blot analysis of the cytosolic enzyme revealed no differences in the MAPK protein content.

Taken together, the effect of the preincubation of MCF-7 cells with ET18-OCH_3 under conditions that inhibit cell proliferation was a decrease in both the intensity and duration of MAPK activation in response to serum or EGF. This observed inhibition of MAPK activation in cells preincubated with ET18-OCH_3 is not due to a direct inhibition of the enzyme activity by the compound. The above results indicated that the upstream event(s) that are crucial for MAPK activation could be a potential target(s) for the ET18-OCH_3 action.

4.3.3 ET18-OCH_3 reduced EGF-induced phosphorylation of MEK

The activation of MEK is the immediate event upstream from MAPK activation and the phosphorylation of MEK by its kinase such as Raf-1 is required for MEK activation. To investigate if the inhibition of MAPK activation by ET18-OCH_3 resulted from perturbation of upstream events by this compound, phosphorylation of MEK in response to EGF in cells pretreated without or with ET18-OCH_3 was examined. MEK was immunoprecipitated from [^{32}P]orthophosphate-labeled cells incubated with or without ET18-OCH_3 and stimulated with EGF. Phosphorylation of MEK was visualized by autoradiography after PAGE on 10% SDS gels (**Figure 37B**). The results showed that the EGF-induced phosphorylation of MEK in quiescent MCF-7 cells was substantially reduced by pretreatment with ET18-OCH_3. This is consistent with the idea that ET18-OCH_3 inhibits MAPK activation via interference in upstream events.

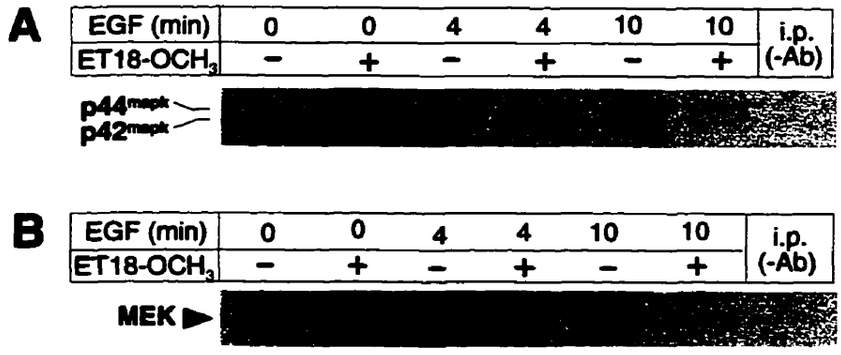

Figure 37. Effect of ET18-OCH_3 on phosphorylation of MAP kinases and MEK in MCF-7 cells. Quiescent MCF-7 cells prelabeled with [^{32}P]orthophosphate were incubated with or without ET18-OCH_3 (10 μg/ml, 3 h) followed by stimulation with 10 ng/ml EGF for 4 or 10 min, or left untreated as control. Proteins in cytosolic fraction were resolved on 10% SDS gels and subjected to autoradiography. The phosphorylation bands of $p42^{mapk}$ and $p44^{mapk}$ (*A*), and MEK (*B*) are indicated. Three independent experiments with different cell preparations showed similar results.

4.3.4 ET18-OCH_3 did not affect the activation of the EGF receptor

EGF binding to its receptors is the first event leading to MAPK activation following cell stimulation with EGF. Studies on the binding of [^{125}I]EGF to its receptors in cells incubated with or without ET18-OCH_3 at 4 and 37°C were conducted therefore. The results revealed no significant differences in the quantity of EGF bound or affinity of EGF binding for the receptors (**Figure 38A**). Decreased internalization of EGF in cells preincubated with ET18-OCH_3 relative to controls was observed at 37°C, but this was only apparent after 20 min incubation with the ligand (**Figure 38B**). The effect of ET18-OCH_3 on EGF receptor activation was assessed by monitoring the tyrosine phosphorylation of EGFr (Panayotou and Waterfield, 1993). Immunoblotting of the immunoprecipitated EGFr with anti-EGF receptor (αEGFr) Abs showed that similar amounts of the receptor were present in cells incubated with or without ET18-OCH_3 (**Figure 39**, *the upper panel*). Immunoblotting with antiphosphotyrosine (αP-Tyr) Abs revealed that the extent and kinetics of EGFr phosphorylation were similar in both groups (**Figure 39**, *the lower panel*). This was confirmed by densitometric analysis.

4.3.5 ET18-OCH_3 did not affect Ras activation

Activation of EGF receptor leads to the formation of a complex with Grb2/mSos that triggers the activation of $p21^{ras}$ by converting Ras:GDP to Ras:GTP (Egan *et al.*, 1993). The active Ras:GTP in turn induces Raf-1 activation and subsequently initiates the cytosolic kinase cascade. To investigate if the suppression of MAPK activation was due to inhibition of $p21^{ras}$ activity, we examined the effect of ET18-OCH_3 on Ras activation by quantitative

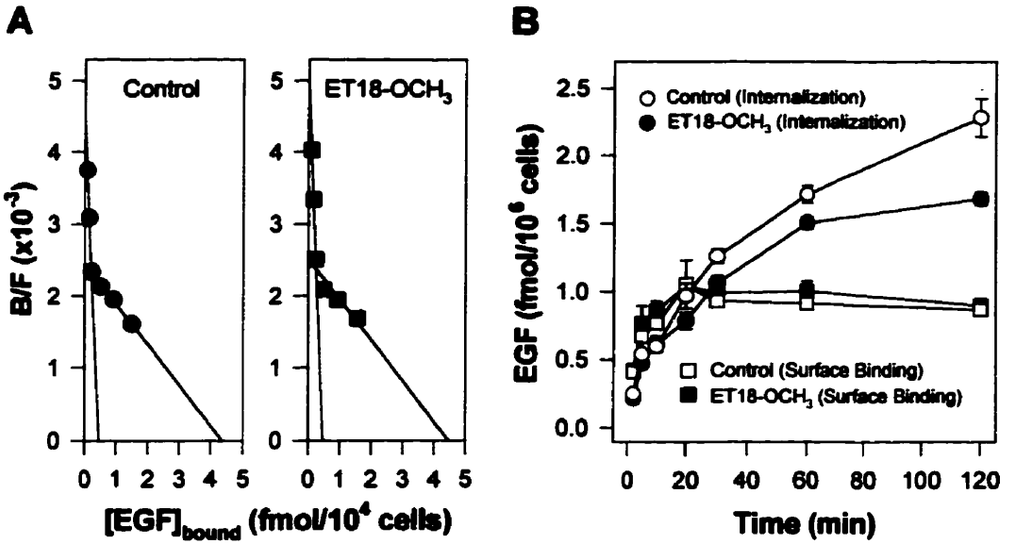

Figure 38. Effect of ET18-OCH_3 on the binding of EGF to EGFr and the internalization of EGF-bound receptors. (*A*) Scatchard plot of the EGF binding to receptors. After cooling the culture plates on ice, quiescent MCF-7 cells pretreated with or without ET18-OCH_3 (10 μg/ml, 3 h) were incubated with [^{125}I]EGF (0-3.12 nM, ~94000 cpm/ng) for 30 min. Determination of the radioactivity associated with the EGF receptors was as described in **Section 3.5.8**. The binding data were displayed after Scatchard analysis. The results are the means of triplicates from a single experiment that is representative of two similar experiments. (*B*) Time course of EGF binding on the surface and EGFr internalization. Quiescent MCF-7 cells pretreated as described in (*A*) were incubated with [^{125}I]EGF (10 ng/ml, ~120000 cpm/ml) for 0-120 min. The radioactivities associated with EGFr on the cell surface or internalized were determined as described in **Section 3.5.8**. The results are the means ± S.D. of triplicates from a single experiment that is representative of two separate experiments.

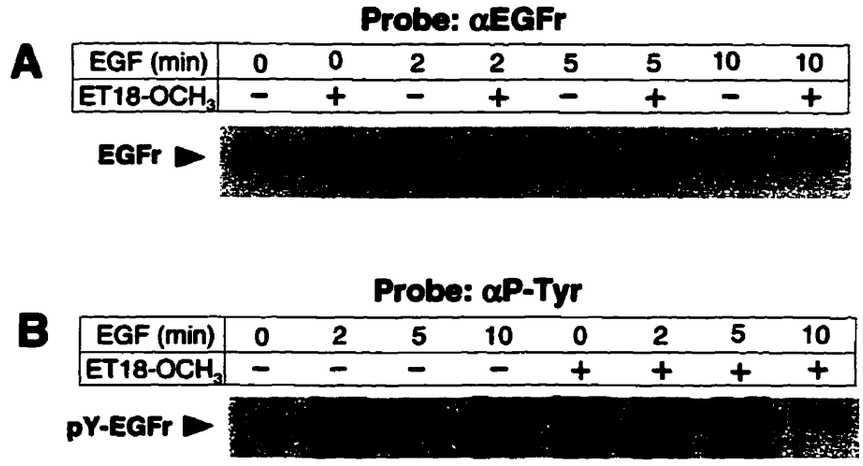

Figure 39. Effect of ET18-OCH_3 on the tyrosine phosphorylation of EGF receptors in MCF-7 cells. Quiescent MCF-7 cells were incubated with or without ET18-OCH_3 (10 μg/ml, 3 h) followed by stimulation with 10 ng/ml EGF for 2, 5, or 10 min, or left untreated as control. The cells were washed and lysed in a detergent-containing buffer. The extracts were sonicated and centrifuged. The supernatant was used for immunoprecipitation with anti-EGFr Ab (αEGFr). The immunoprecipitates were resolved on 8% SDS gels, transferred to nitrocellulose membranes, probed with αEGFr or anti-phosphotyrosine Ab (αP-Tyr), respectively. The bands of EGFr (*upper panel*) and tyrosine phosphorylated EGFr (*lower panel*) are indicated by the arrow. Two independent experiments with different cell preparations showed similar results.

analysis of the $p21^{ras}$-associated guanine nucleotides (GDP or GTP) and calculation of the ratio of GTP/(GDP + GTP) on Ras. The results displayed in **Figure 40** show preincubation of the cells with ET18-OCH_3 had no effect on the activation of $p21^{ras}$ that peaked between 2 and 4 min and declined to the resting level by 8 min.

4.3.6 ET18-OCH_3 perturbed Raf-1 association with cell membranes

Activated $p21^{ras}$ mediates the translocation of Raf-1 from the cytosol to the membrane where it is activated by an as yet unknown mechanism. To investigate the effect of ET18-OCH_3 on Raf-1 activation, we examined its effect on the translocation of Raf from the cytosol to the membrane in control cells and those preincubated with ET18-OCH_3. In cells stimulated with EGF (**Figure 41A**), densitometric analysis of the blots revealed that the membrane-associated Raf-1 in control and cells preincubated with ET18-OCH_3 increased similarly at 2 min while at 4 and 7 min, 1.8- and 3.4-fold more Raf-1, respectively, was associated with control membrane relative to membrane from ET18-OCH_3-treated cells. Results from serum-stimulated cells (**Figure 41B**) showed a similar pattern that obtained with EGF-stimulated cells, where membrane-associated Raf-1 in ET18-OCH_3-treated cells decreased as early as 5 min after serum stimulation. After 5 and 10 min the levels in membranes from ET18-OCH_3-loaded cells were 1.6- and 2.6-fold less, respectively, than those in control membranes. Western blot analysis was performed with cell lysates to investigate whether the above differential association of Raf-1 with membranes was due to differences in the Raf-1 protein content in cells treated with or without ET18-OCH_3. The results revealed that there were no differences in Raf-1 content between ET18-OCH_3-treated

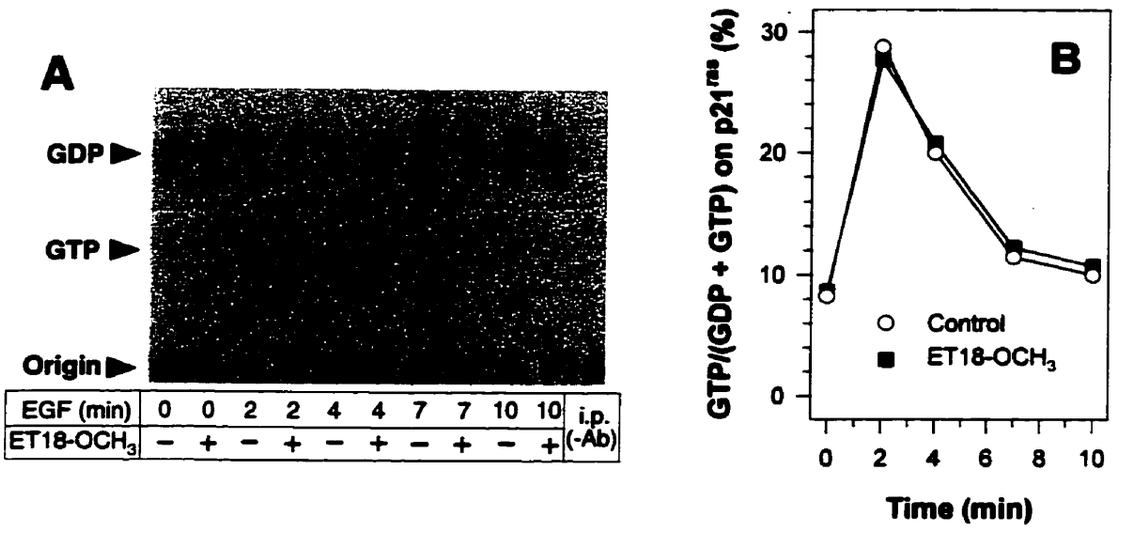

Figure 40. Effect of ET18-OCH_3 on $p21^{ras}$ activation in MCF-7 cells. Quiescent MCF-7 cells prelabeled with [^{32}P]orthophosphate were incubated with or without ET18-OCH_3 (10 μg/ml, 3 h) followed by stimulation with 10 ng/ml EGF for 2-10 min, or left untreated as control. $p21^{ras}$ was immunoprecipitated from cell lysates (500 μg protein) with anti-Ras antibody (259). Guanine nucleotides were extracted from the immunoprecipitates and separated by TLC. The amount of associated radioactivity was visualized by autoradiography (*A*). Spots were scraped from the TLC plates and the radioactivity was quantitated. The ratio of GTP/(GDP + GTP) was calculated and plotted against the time for cell stimulation (*B*). The results are from a single experiment that is representative of two independent experiments with different cell preparations.

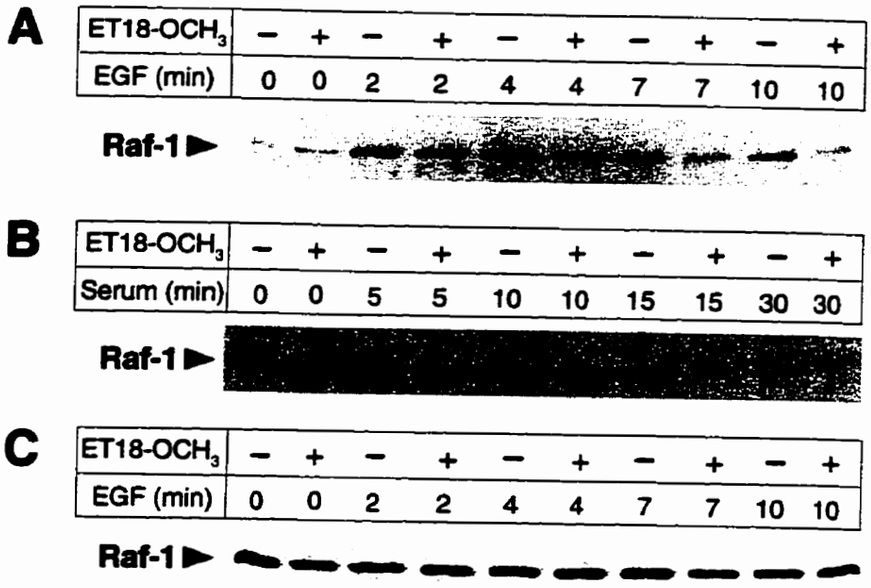

Figure 41. Effect of ET18-OCH_3 on the association of Raf-1 with membrane in MCF-7 cells. (*A*) Effect of ET18-OCH_3 on Raf-1 membrane association in EGF-stimulated cells. Quiescent cells were incubated with or without 10 μg/ml ET18-OCH_3 for 3 h, washed and subsequently stimulated with 10 ng/ml EGF for the time indicated. Membranes were prepared, solubilized and 40 μg of protein were separated on 10% SDS gels, transferred to nitrocellulose membranes and immunoblotted with anti-Raf-1 Abs. The results are from a single experiment that is representative of three with different cell preparations. (*B*) Effect of ET18-OCH_3 on Raf-1 membrane association in serum-stimulated cells. Experiments were similar to those in (*A*) except stimulation of cells with DMEM/FBS. (*C*) Effect of ET18-OCH_3 on Raf-1 content in MCF-7 cells. Experiments were conducted as described in (*A*), but the cells were lysed in detergent-containing buffer after stimulation. Each lane was loaded with 10 μg of cell lysate protein. The results are from a single experiment that is representative of two with different cell preparations.

and control cells (**Figure 41C**).

4.3.7 Preincubation of cells with ET18-OCH_3 inhibited Raf-1 kinase activity

Translocation of Raf-1 from the cytosol to the plasma membrane is required for the activation of the Raf-1 kinase activity. To investigate if the decreased membrane-association of Raf-1 caused by ET18-OCH_3 preincubation was translated into reduced Raf-1 kinase activity in the membrane, Raf-1 kinase activity was measured in Raf-1 immunoprecipitates from membranes of control and ET18-OCH_3-loaded cells. The results (**Figure 42A** and **B**) clearly showed that there was greater phosphorylation of MEK-1 and histone H1 in assays with immunoprecipitates from membranes of control EGF-treated cells than cells preincubated with ET18-OCH_3. The time course of Raf-1 kinase activity (**Figure 42**) paralleled that of Raf-1 membrane association (**Figure 41**). The ratio of the increase in phosphorylation of the substrates over blanks in controls relative to ET18-OCH_3-treated cells as assessed densitometrically ranged from 1.5 at 2 min to 12 at 10 min for MEK-1 and 1.2 to 4.3 for histone H1 from 2 to 10 min, respectively. Addition of ET18-OCH_3 to the assays did not have any effect on the kinase activity of Raf-1 immunoprecipitates from membranes of EGF-stimulated and unstimulated cells (**Figure 42C**). Thus, ET18-OCH_3 had no direct effect on Raf-1 kinase activity.

4.3.8 Correlation between ET18-OCH_3 accumulation, Raf-1 membrane association and MAPK activation

As we observed a time-dependent accumulation of ET18-OCH_3 which could account

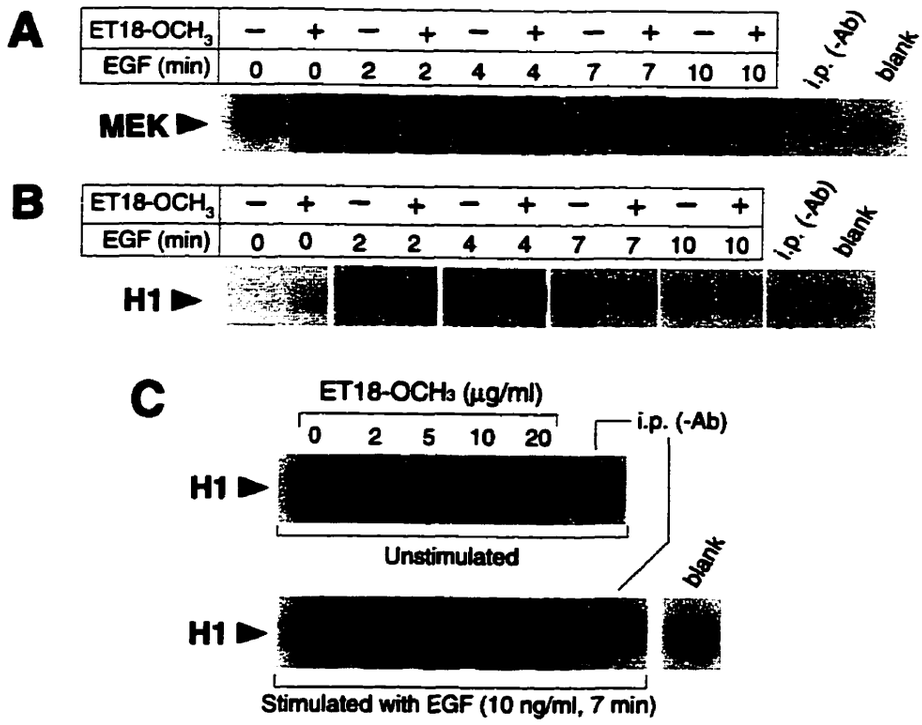

Figure 42. Effect of ET18-OCH$_3$ on Raf-1 kinase activity. (*A*) ET18-OCH$_3$ inhibited Raf-1 kinase activity toward MEK. Quiescent cells were incubated with or without 10 μg/ml ET18-OCH$_3$ for 3 h, washed and subsequently stimulated with 10 ng/ml EGF for the time indicated. Membranes were prepared and solubilized. Raf-1 was immunoprecipitated from membrane extracts of cells (300 μg protein). The immunoprecipitates were washed and used in kinase assays to measure the phosphorylation of MEK (*FL*). Controls without Abs in Raf-1 immunoprecipitation and non-specific phosphorylation of MEK-1 in assays with just buffer and [γ-^{32}P]ATP are also indicated. The results are from a single experiment that is representative of two independent experiments. (*B*) ET18-OCH$_3$ inhibited Raf-1 kinase activity toward histone H1. Experiments were similar to those in (*A*) except the use of histone H1 as substrate in assays. The results are from a single experiment that is representative of three independent experiments. (*C*) Addition of ET18-OCH$_3$ in *in vitro* Raf-1 kinase assay did not affect the kinase activity. Raf-1 was immunoprecipitated from EGF-stimulated (*lower panel*) or unstimulated (*upper panel*) cells. Histone H1 kinase activity was measured with the immunocomplex in the absence or presence of ET18-OCH$_3$ (2-20 μg/ml). The results are a single experiment that is representative of two independent experiments.

for the differential effect on cell proliferation showed in **Figure 29A**, we investigated whether this could be correlated with differences in the extent of Raf-1 membrane association and MAPK activity. Quiescent MCF-7 cells were incubated with ET18-OCH_3 for 0, 1, and 3 h before stimulation with EGF for 7 min and cellular fractions were processed for examination of Raf-1 membrane association and MAPK activity. The results (**Figure 43**) show that Raf-1 association with the membrane decreased as a function of increasing incubation time with ET18-OCH_3 and that the order of decreasing MAPK activity correlated with decreased membrane-bound Raf-1 and increasing ET18-OCH_3 accumulation.

4.3.9 ET18-OCH_3 did not affect the cellular level of cAMP and PKA activity

Since PKA activation may lead to inhibition of Raf-1 activity (Cook & McCormick, 1993), we determined the cAMP levels and PKA activity in ET18-OCH_3-treated and untreated MCF-7 cells to investigate whether the inhibitory effect of ET18-OCH_3 was mediated via activation of PKA. ET18-OCH_3 did not affect cellular levels of cAMP in control and EGF-treated cells (**Figure 44**) or PKA activity which remained unchanged from the basal level of 3.6 ± 1.7 pmol/min per mg protein.

4.3.10 Transient stimulation of quiescent MCF-7 cells with serum before ET18-OCH_3 treatment counterbalanced the cytostatic effect of the compound

If the inhibition of the MAPK cascade by ET18-OCH_3 contributes substantially to the antiproliferative effects of the compound as the above studies suggest, these effects should be minimized if the AEL is added subsequent to the transient activation of the cells. To test

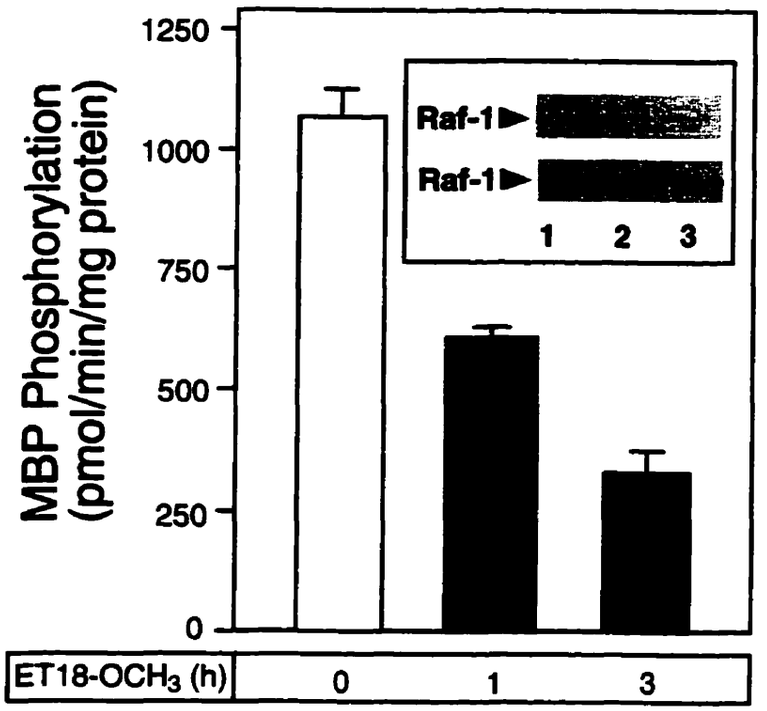

Figure 43. Effect of preincubation time with ET18-OCH_3 on Raf-1 membrane association and MAPK activity. Quiescent MCF-7 cells were incubated without (*open bar*; *insert* lane *1*) or with 10 μg/ml ET18-OCH_3 for 1 h (*grey bar*; *insert* lane *2*), or 3 h (*black bar*, *insert* lane *3*). The cells were washed and stimulated with 10 ng/ml EGF for 7 min. MAPK activity in the cytosolic fraction (*bar graph*) and Raf-1 association with the membrane (*insert*) were determined as described in **Sections 3.5.5** and **3.5.11**, respectively. Raf-1 associated with membranes from unstimulated and stimulated cells are showed in the upper and lower panels of the insert, respectively. The results are from a single experiment that is representative of two independent experiments with different cell preparations.

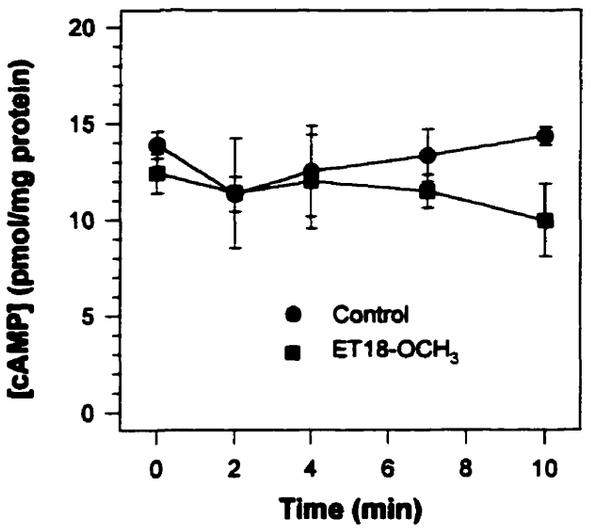

Figure 44. Effect of ET18-OCH_3 on cellular cAMP content. Cyclic AMP levels in quiescent MCF-7 cells preincubated with or without 10 μg/ml ET18-OCH_3 for 3 h followed by stimulation with 10 ng/ml EGF for 0-10 min were determined as described in **Section 3.5.14.** The results are the means ± S.D. of two separate experiments conducted in triplicates.

this idea, quiescent MCF-7 cells were therefore incubated with DMEM/FBS for 1 h to transiently activate MAPK (**Figure 36A**). The cells were washed, and incubated with ET18-OCH_3 for 3 h. At the end of this incubation the cells were washed and incubated with DMEM/FBS and subsequently processed for flow cytometric analysis. **Table 10** shows that whereas preincubation with ET18-OCH_3 before the addition of FBS completely inhibited cell cycle progression into S phase, this inhibition was significantly ($P < 0.001$) blunted when the cells were transiently activated with FBS prior to the addition of ET18-OCH_3. The above results demonstrate that inhibition of early signaling events by ET18-OCH_3 contributes concretely to the antiproliferative action of the compound. However, the observation that there was a difference of nearly one third in the percentage of the number of cells in S phase between control cells incubated without ET18-OCH_3 (FBS/BSA/FBS) and those incubated with ET18-OCH_3 after the transient activation (FBS/ET18-OCH_3/FBS) suggests that the inhibition of cellular events by the AEL after the transient activation may also contribute to the inhibition of MCF-7 cells proliferation by ET18-OCH_3.

5 DISCUSSION

5.1 No Correlation Exists Between Cell Sensitivity to ET18-OCH_3 and Their Ether Phospholipid Content or Composition in Five Epithelial Cancer Cell Lines

Ideal controls for studying the mechanism underlying the selective effects of ET18-OCH_3 on cancer cells would be the normal cells from which the cancer cells were derived.

Table 10. Transient stimulation of MCF-7 cells with serum prior to ET18-OCH_3 treatment counterbalances the cytostatic effect of the compound. Quiescent MCF-7 cells were incubated with DMEM/BSA (*A* and *B*) or DMEM/FBS (*C* and *D*) for 1 h. The cells were washed and incubated with ET18-OCH_3 (10 μg/ml) in DMEM/BSA (*B* and *D*) or DMEM/BSA alone (*A* and *C*) for 3 h, followed by washing and incubation with DMEM/FBS (*B*, *C* and *D*) or DMEM/BSA (*A*). All cells were harvested 25 h after initial treatment with DMEM/FBS or DMEM/BSA and processed for flow cytometry analysis. The results are the means ± S.D. of four independent experiments. Asterisks indicate the comparisons to the results obtained from group *A* with significant differences (* $P < 0.05$, ** $P < 0.01$, *** $P < 0.001$), while crosses indicate the comparisons to the results obtained from group *C* with significant differences († $P < 0.01$, †† $P < 0.001$). Data were analyzed by Student's *t* test.

Group	Treatment	Cell cycle distribution (% ± S.D.)		
		G_0/G_1	S	G_2/M
A	BSA/BSA/BSA	81.5 ± 3.1	10.5 ± 1.7	8.0 ± 1.8
B	BSA/ET18-OCH_3/FBS	81.7 ± 2.8	6.7 ± 1.7 *	11.5 ± 1.3 *
C	FBS/BSA/FBS	59.5 ± 1.0 ***	24.2 ± 1.0 ***	16.0 ± 1.4 ***
D	FBS/ET18-OCH_3/FBS	66.0 ± 2.9 *** †	17.2 ± 1.3 *** ††	16.2 ± 2.2 **

However, these are usually unavailable. A common approach, as a practical remedy, is to identify cells that are differentially affected by the ALP and to investigate if there is a correlation between susceptibility and various cellular parameters that may or may not be altered by the ether lipid. Using this approach, Chabot *et al.* (1989) showed that the ALP-sensitive neurophilic promyelocytic cell line HL-60 had a greater ether phospholipid content than the ALP-resistant erythroleukemic cell line, K562. This led to the hypothesis that the greater the ether phospholipid content in a cell, the more susceptible to the effect of ALP it was (Chabot *et al.*, 1989).

We applied a similar approach to investigate whether the hypothesis could be extended to other cell lines. Five epithelial cancer cell lines derived from different tissues [breast (MCF-7), lung (A427 and A549), colon (T84) and skin (Mamle 3M)] whose proliferation was differentially affected by ET18-OCH_3 were used for the studies. As shown in **Table 3**, significant differences were observed in the subclass composition of CGP and EGP fractions extracted from the different cells. The decreasing order of ether lipid content in the CGP and EGP fractions, expressed as a percentage of the total phospholipids, was T84 > A427 = Malme 3M = A549 > MCF-7 (**Table 4**). If the postulated hypothesis was applied to these cells, T84 would be the most susceptible, whereas MCF-7, with an ether lipid content which was 10-20 times less than that in other cells, would be the least susceptible. Our results showed that T84 was indeed very susceptible to the growth-inhibitory effect of ET18-OCH_3, but so was MCF-7 in spite of its low ether content (**Figure 17**). Applying the hypothesis to A427, A549 and Malme 3M, one would expect their relative sensitivity to ET18-OCH_3 to be similar, however, as shown in **Figure 17**, A549 (IC_{50} = 10.31 μg/ml) and

A427 (IC_{50} = 8.91 μg/ml) were much more resistant to the AEL than Malme 3M (IC_{50} = 4.10 μg/ml). Thus, our results did not reveal any causal link between the ether lipid content and the susceptibility of these cells to ET18-OCH_3.

We also compared the distribution of the ether phospholipid content in the CGP and EGP fractions. The orders of decreasing ether lipid content in the CGP or EGP fraction were T84 > A427 > A549 = Malme 3M > MCF-7 or A549 = T84 = Malme 3M > A427 > MCF-7, respectively (**Table 3**). Using either parameter, no correlation between the ether lipid content and susceptibility to ET18-OCH_3 was apparent.

To explain the postulated relationship between ether lipid content and susceptibility of cells, Chabot *et al.* (1989) suggested that the inhibition of cell proliferation may be due to increased production of alkylacyl glycerols from alkylacyl glycerophosphocholine (alkylacyl GPC) in the sensitive cells as the ether analogues of diacylglycerol presumably inhibit PKC activity and hence the transmission of growth signals (Daniel *et al.*, 1988). The order of decreasing alkylacyl GPC distribution, T84 > A427 > Malme 3M > A549 > MCF-7 (**Table 3**), also did not correlate with the order of sensitivity of the cells. It is worth pointing out that ether analogues of diacylglycerol have also been reported to activate protein kinase C (Ford *et al.*, 1989).

Our results lead us to conclude that the postulated relationship between the cellular ether phospholipid content and the ET18-OCH_3-susceptibility of cells may not be a general phenomenon and is definitely not applicable to the epithelial cells used in our study. Cells derived from different tissues could have inherent differences in the phospholipid composition. It was fortuitous that the phospholipid composition of the five cell lines used

in our studies was fairly similar, perhaps reflecting their epithelial pedigree. Because observations from leukemic cells were used in postulating a link between the cellular ether phospholipid content with the ALP-susceptibility, we cannot discount the possibility that the underlying factors responsible for the selectivity of ET18-OCH_3 may differ between cell types. Thus, while the ether lipid content may be related to the ALP-sensitivity in leukemic cells, it is not the case in epithelial cells. Nor is it likely to be a factor in explaining the relative resilience of normal cells to ET18-OCH_3 as there is overwhelming evidence that the process of neoplasticity is not accompanied by an increase in the ether glycerophospholipid content in cells or tissues (Gerstl *et al.*, 1965; Gray, 1963; Howard BV and Howard WJ, 1975; Nakamura *et al.*, 1980; Robert *et al.*, 1976; Van Hoeven *et al.*, 1972).

5.2 OMG Produced from ET18-OCH_3 Does Not Account for the Growth-inhibitory Effect by ET18-OCH_3 Treatment

ET18-OCH_3 has been shown to be rapidly taken up and incorporated into MCF-7, T84, A427 and A549 cells, but no correlation between the extent of uptake and incorporation was observed (Lu and Arthur, 1992a; 1992b). We have further shown that ET18-OCH_3 is very slowly, as reported in leukemic cells, metabolized into OMG in these cells (**Table 4**). Our results also confirm the observations by other investigators (Fleer *et al.*, 1987; Hoffman *et al.*, 1986; Wilcox *et al.*, 1987) that cellular metabolism of ET18-OCH_3 does not involve a cleavage of the C-1 moiety but, instead, occurs via the hydrolysis of ET18-OCH_3 to OMG by PLC hydrolysis (see **Section 4.1.4**). We did not observe any correlation between the extent of the metabolism of ET18-OCH_3 and the susceptibility to its growth-inhibitory effects

in our cell lines (**Table 5, 6,** and **Figure 19**).

ET18-OCH_3 is not a substrate of the alkyl cleavage enzyme, while OMG is (Hoffman *et al.*, 1986). Thus, the transfer of the radiolabel from the C-1 alkyl moiety to an ester moiety in phospholipids suggests that, following production of OMG, there is a cleavage of the alkyl group by a monooxygenase to release a fatty aldehyde that is subsequently oxidized to fatty acid before incorporation into phospholipids. It seems that both the fatty alcohol and fatty acid produced do not accumulate, but are very rapidly metabolized since no detectable radiolabeling was found in these two fractions. No product resulting from cleavage of the 2-*O*-methyl group of OMG was observed in MCF-7, A427, or A549 cells. In contrast, such a cleavage was reported in human polymorphonuclear neutrophils and HL-60 cells (Hoffman *et al.*, 1986; Vallari *et al.*, 1988).

Although the production of OMG from ET18-OCH_3 has been previously reported (Fleer *et al.*, 1987; Hoffman *et al.*, 1986; van Blitterswijk *et al.*, 1987; Weber and Benning, 1988; Wilcox *et al.*, 1987), there was conflicting evidence on whether the growth-inhibitory effects are mediated by the parent compound or the metabolite OMG. There is a body of opinion that ET18-OCH_3 and other AELs inhibit cell proliferation by inhibition of PKC (Powis, 1991). Fleer *et al.* (1987) proposed that the compounds inhibiting PKC activity are the apolar alcohols formed from PLC hydrolysis of the parent compound. This view is supported by evidence that OMG is a more potent inhibitor of PKC and more effective in inhibiting phorbol ester binding to its receptors than ET18-OCH_3 (van Blitterswijk *et al.*, 1987). But OMG at relatively high concentrations did not affect the growth of HL-60 cells, implying that the active compound is ET18-OCH_3.

To investigate whether the production of OMG is responsible for inhibiting the growth of epithelial cancer cell lines, the quantity of OMG in cells incubated with ET18-OCH_3 or OMG was determined and the effect of these incubations on cell proliferation was examined. Despite the much higher content of OMG in cells incubated with 1 μg/ml of OMG relative to 5 μg/ml of ET18-OCH_3 (**Table 6**), incubation with the former had little effect on cell growth (**Figure 19**). These results clearly indicate that metabolism of ET18-OCH_3 is not necessary for the growth-inhibitory action of the compound in these cells. This conclusion is also supported by previous studies from others (Hoffman *et al.*, 1986; Wilcox *et al.*, 1987). Therefore, we conclude that there is no correlation between the quantity of OMG produced from ET18-OCH_3 and the sensitivity of cells to the AEL. Furthermore, the nonphosphorus alkyl ether lipids such as 1-*O*-hexadecyl-2-*O*-methyl-3-*S*-thioglucosyl-*sn*-glycerol (Lu *et al.*, 1994) and phosphonate analogues of ether lipids (Ashagbley *et al.*, 1996) that cannot be metabolized by PLC are still effective anticancer agents (Honma *et al.*, 1991). These observations also argue against metabolism being an obligatory step in the antiproliferative effects of AEL.

Interestingly, A549, the most resilient of the three cell lines to the growth-inhibitory effects of ET18-OCH_3 (Lu and Arthur 1992b), was the most susceptible to the growth-inhibitory effects of OMG. The relatively high amounts of OMG accumulated by A549 cells may be a contributory factor, but the fact that MCF-7 cells accumulated as much OMG as the A549 cells and yet were not as susceptible argues against a strict correlation between the cell susceptibility and the amount of OMG accumulated. Whether ET18-OCH_3 and OMG inhibit cell growth through a common mechanism is presently unknown, but our results

would suggest that they may act via distinct mechanisms.

5.3 Perturbation of Phospholipid Metabolism by ET18-OCH_3 Does Not Underlie Its Antiproliferative Action

The use of [^{3}H]glycerol in studies of lipid metabolism allowed effects of ET18-OCH_3 on the *de novo* synthesis of all glycerolipids to be monitored. Such effects were found in MCF-7 and A549 cell lines. ET18-OCH_3 stimulated the incorporation of [^{3}H]glycerol into DAG in MCF-7 cells (**Table 7** and **8**). This could be due to a direct activation of PtdOH phosphatase since the activity of the enzyme was enhanced by the ALP in *in vitro* assays (**Figure 25**). Although a moderate increase in glycerol incorporation into DAG was observed in A549 cells, a similar explanation cannot be proffered as PtdOH phosphatase activity in A549 microsomes was inhibited by ET18-OCH_3. Incubation of MDCK cells with hexadecyl-phosphocholine (HePC) also resulted in an increased production of DAG (Haase *et al.*, 1991).

DAG is a key intermediate in glycerolipid synthesis. The observed increase in its synthesis caused by ET18-OCH_3, especially in MCF-7 cells (**Table 7** and **8**), would be expected to affect the synthesis of other lipids. An increase in the cellular level of DAG would stimulate the rate of PtdCho biosynthesis since DAG could serve as both a substrate for PCCT and a modulator of PCCT for its binding to endoplasmic reticulum. PtdEtn and TAG would compete for DAG as a substrate for their synthesis. It is not clear how cells control the amount of DAG channeled in each direction (see **Figure 11**). Our results clearly show that the increased production of DAG did not automatically lead to increased synthesis

of all the lipids. In both cell types the major effect of ET18-OCH_3 was a decline in the synthesis of PtdCho (**Table 7**) with concomitant increases in the synthesis of other lipids, namely PtdEtn and PtdOH in MCF-7 cells, and TAG in A549 cells as well as in MCF-7 cells (**Table 7** and **8**). The inhibition of PtdCho synthesis, in spite of increased DAG synthesis, suggests that ET18-OCH_3 has specific effects on the biosynthetic enzymes. Previous studies have reported that both ET18-OCH_3 and HePC inhibited PtdCho synthesis by interfering in the translocation of *P*Cho cytidylyltransferase (Geilen *et al.*, 1992; Haase *et al.*, 1991; Tronchere *et al.*, 1991) without any direct effect on the enzyme activity. Our results suggest that the inhibition of PtdCho synthesis may also involve direct inhibition of the PCCT enzyme by ET18-OCH_3 (**Figure 25**).

Based on the degree of inhibition of *P*Cho cytidylyltransferase in the two cell lines (**Figure 25**), a greater inhibition of PtdCho synthesis would be predicted in MCF-7 cells compared to A549 cells. This was in fact observed (**Figure 21**). MCF-7 cells take up ET18-OCH_3 at a much faster rate than A549 cells (Lu and Arthur, 1992b). Although the differential incorporation of ET18-OCH_3 into the two cell lines would obviously account for the greater inhibition of PtdCho synthesis observed in MCF-7 cells, we can still argue that ET18-OCH_3 as an inhibitor for cellular *P*Cho cytidylyltransferase would be more potent in MCF-7 cells than in A549 cells since a greater inhibition of the enzyme from MCF-7 cells was seen in the *in vitro* assays conducted with identical amounts of this AEL. It is not clear why differences between *P*Cho cytidylyltransferase activity in the preparations from the two cell lines were observed. The results may indicate inherent differences in the enzymes or possibly differences in the membrane environment of the enzymes which may modulate the effect of ET18-OCH_3.

The increase in PtdEtn synthesis observed in cells treated with ET18-OCH_3 might be due in part to the increased production of DAG in MCF-7 cells, but the large increase in CDP-Etn production observed in the [^{3}H]ethanolamine labeling studies (**Figure 23**) suggests that activation of *P*Etn cytidylyltransferase in these cells may also be a contributory factor. This speculation was supported by the observed activation of both *P*Etn cytidylyltransferase and CDP-Etn phosphotransferase by ET18-OCH_3 in *in vitro* assays; in A549 fractions, the activation of these enzymes was much lower than the effects in MCF-7 fractions (**Figure 25**). These observations are consistent with the relatively minor changes observed in the cytosolic ethanolamine metabolites and PtdEtn in A549 cells (**Figure 23** and **Table 7** and **8**). Since the *in vitro* assays were conducted with identical concentrations of ET18-OCH_3, the results again point to inherent differences in the enzymes or their environments between the two cell lines. The increased incorporation of ethanolamine or glycerol into PtdEtn in MCF-7 cells was not a compensatory response to a rapid degradation of PtdEtn because ET18-OCH_3 did not significantly affect PtdEtn degradation as monitored by the loss of [^{3}H]glycerol from PtdEtn (**Figure 28**).

Enhanced TAG synthesis in both MCF-7 and A549 cells was quite notable (**Table 7** and **8**). This increase may be a compensatory response to the decreased PtdCho synthesis. In A549 cells the loss of the label in PtdCho was virtually all channeled to TAG, perhaps revealing this route as the primary one available to prevent the build up of DAG. In MCF-7 cells, the increased production of CDP-Etn from the activation of *P*Etn cytidylyltransferase and ethanolaminephosphotransferase by ET18-OCH_3 (**Figure 25**), which results in increased PE synthesis from DAG, as well as utilization of DAG for PtdOH synthesis would compete

for the available DAG, thereby reducing the quantities available for synthesis of TAG (**Figure 11**).

One implication of the effect of ET18-OCH_3 on lipid-metabolizing enzymes and on translocation of *P*Cho cytidylyltransferase (Tronchere *et al.*, 1991) is that ET18-OCH_3 may be internalized rather than localized exclusively in the plasma membrane as previously thought (Berdel, 1991; Berdel *et al.*, 1985). *P*Etn cytidylyltransferase has recently been localized to the rough endoplasmic reticulum in rat liver (Van Hellemond *et al.*, 1994). Hence, the observed effect of ET18-OCH_3 on this activity in intact cells (increased CDP-Etn production) implies the presence of ET18-OCH_3 in this intracellular organelle. CDP-Etn and CDP-Cho phosphotransferases, and PtdOH phosphatase are all found in the endoplasmic reticulum (Vance, 1991). A direct effect of the compound on the enzymes necessitates its interaction with the endoplasmic reticulum. The perturbation of translocation of *P*Cho cytidylyltransferase between the soluble and membrane fractions (Tronchere *et al.*, 1991) would also require interaction of the compound with the enzyme in intracellular compartments. Since *P*Cho cytidylyltransferase may be an intranuclear enzyme (Wang *et al.*, 1993a, 1993b; Watkins and Kent, 1992), our results suggest that ET18-OCH_3 may also reach the nucleus. Its soluble nature and rapid redistribution during homogenization and subcellular fraction have made it difficult to establish its cellular distribution (Vallari *et al.*, 1989), but the results of our study suggest that it may be more widely distributed intracellularly than hitherto appreciated.

Under the experimental conditions used for these metabolic studies only the proliferation of MCF-7 cells was inhibited. The metabolic effect of ET18-OCH_3 on lipid

metabolism that might conceivably affect the proliferation of the cells was the decrease in PtdCho synthesis (**Table 7** and **Figure 21**). However, evidence that this decreased synthesis was not responsible for the inhibition of cell growth was obtained in studies where the induced inhibition of PtdCho synthesis was overridden by oleic acid without significant effect on the inhibition of cell growth (**Figure 27**). These results clearly dissociate the inhibition of PtdCho synthesis from the inhibition of cell growth by ET18-OCH_3. Further evidence for the lack of correlation was obtained from the analysis of cellular PtdCho content (**Figure 28**): no significant differences in the quantity of PtdCho or PtdEtn were observed in cells incubated with or without ET18-OCH_3 for 6 h, even though the MCF-7 cells had ceased proliferating. After a 12-h incubation with ET18-OCH_3, a decrease in the PtdCho content was observed in MCF-7 as well as A549 cells. Despite this decrease, the proliferation of A549 cells was still similar to that of control cells. Taken together, we conclude that the observed changes in lipid metabolism are not the primary cause for the inhibition of MCF-7 cell growth.

5.4 ET18-OCH_3 Appears to Inhibit MCF-7 Cell Proliferation by Interference in Cellular Signal Transduction

Having examined the cellular ether phospholipid content and composition, the metabolism of ET18-OCH_3, and the effect of ET18-OCH_3 on lipid metabolism in cells with differential sensitivity to the AEL, our results did not reveal any correlation between cell susceptibility to ET18-OCH_3 and any observed differences in the above metabolic parameters in the cells tested. Thus, we investigated effects of ET18-OCH_3 on cellular signal transduction via the MAPK cascade and the PKC-dependent pathway.

5.4.1 ET18-OCH_3 inhibits the PKC-dependent phosphorylation in MCF-7 cells

While there is sufficient evidence to indicate that ET18-OCH_3 inhibits PKC activity *in vitro*, its effect on the activity of the enzyme in intact cells and the severity of any such inhibition remains to be established. We have circumvented problems associated with *in vitro* assays of PKC by examining the effect of ET18-OCH_3 on the phosphorylation of endogenous proteins in intact cells in response to PKC activators. Although previous studies have used a similar approach, the relationship between conditions for ET18-OCH_3 incubation used in leukemic cells and effects of these treatments on inhibition of cell proliferation were not clarified (Kiss *et al.*, 1987). The authors also reported that although addition of ET18-OCH_3 (75 μM) for 40 min was sufficient to inhibit phosphorylation induced by 20 nM of TPA, no inhibitory effect of the AEL was observed when 200 nM of TPA was used to stimulate HL-60 or K569 cells.

In our studies, preincubation with 10 μg/ml (≈ 20 μM) of ET18-OCH_3 for 3 h inhibited the stimulatory effect of 1 μM TPA. Under these conditions, proliferation of MCF-7 cells was completely inhibited after re-addition of the growth medium, without any effect on the viability of the cells (see **Section 4.2.2**). ET18-OCH_3 effectively inhibited the phosphorylation of endogenous proteins by PKC to the degree observed with the specific PKC inhibitor Ro 31-8220 (Simpson *et al.*, 1993; Standaert *et al.*, 1996; Sullivan *et al.*, 1994), which provides evidence that the AEL acts as a potent inhibitor of PKC in intact MCF-7 cells. The complete inhibition observed in our studies (**Figure 34**) is in contrast with other studies based on *in vitro* measurements of PKC activity in cell fractions that reported only moderate inhibition of PKC activity (Berkovic *et al.*, 1994; Salari *et al.*, 1992). This

discrepancy could well be due to the approaches used. The *in vitro* assays did not discriminate between the effect of the compound on the activated PKC fraction and the total PKC fraction. However, since leukemic cells were used by Berkovic *et al* (1994), Kiss *et al* (1987), and Salari *et al* (1992) whereas an epithelial cell line was used in our studies, we cannot rule out the possibility that this may be due to differences between the two cell types. As we have noted differences in the effects of antitumor ether lipids on cellular ether lipid content between the two cell types, the results once again suggest that the mechanism underlying the inhibition of cell growth by ET18-OCH_3 could well differ between leukemic and epithelial cell types.

One of the novel and unexpected findings of our studies was the observation that ET18-OCH_3 stimulates the enhanced incorporation of ^{32}P into selected proteins in MCF-7 cells (**Figure 33** and **34**). In contrast, no effect on basal phosphorylation was observed in similar studies with HL-60 or K562 leukemic cell lines (Kiss *et al.*, 1987). We do not know if the observed enhanced phosphorylation in MCF-7 cells is due to inhibition of phosphatases or activation of kinase(s) by ET18-OCH_3. If it is the latter, the inability of Ro 31-8220 to inhibit the enhanced phosphorylation (**Figure 34G**) suggests that it is a PKC-independent phenomenon. We were also unable to observe an increase in PKA activity in cells pre-treated with ET18-OCH_3 (see **Section 4.3.9**). The enhanced phosphorylation of proteins by ET18-OCH_3 leaves open the possibility that the inappropriate phosphorylation of proteins could contribute to the antiproliferative effects of the compound.

Both Salari *et al* (1992) and Berkovic *et al* (1994) reported that the AELs had no effect on the translocation of PKC. Our studies on the translocation of selected isotopes of

PKC, on the whole, tends to support this view. What effects ET18-OCH_3 had on PKC translocation were minimal (**Figure 35A** and **35B**) and unlikely to be the basis for the complete inhibition of the PKC-dependent phosphorylation of endogenous proteins by the AEL. At present, we do not know how ET18-OCH_3 acts as a PKC inhibitor in MCF-7 cells. It may compete with phosphatidylserine (Shoji *et al.*, 1991; Zheng *et al.*, 1990) or irreversibly inhibit PKC activity directly (Berkovic *et al.*, 1994) as other investigators have suggested.

Whether the inhibition of PKC by ET18-OCH_3 in MCF-7 cells is a prerequisite for the antiproliferative action of the compound still remains to be established. In leukemic cells inhibition of PKC activity does not appear to be required for the antiproliferative action of antitumor ether lipids (Berkovic *et al.*, 1994). The most convincing evidence was obtained from a study using anomers of an ether lipid with differential effects on cell proliferation but identical effects on PKC activity (Salari *et al.*, 1992). Unfortunately, the differential effects seen with leukemic cells were not observed with a number of epithelial cells including MCF-7 cells (Lu *et al.*, 1994) and, therefore, we are unable to use this approach to determine whether inhibition of PKC activation is a prerequisite to the growth-inhibitory action of the compounds in MCF-7 cells.

In view of our results that ET18-OCH_3 effectively inhibits PKC activity in intact MCF-7 cells under conditions where cell proliferation is inhibited, we believe the relevant issue in these cells hinges on whether PKC activation is essential for the proliferation of these cells. Evidence that the specific PKC inhibitor Ro 31-8220 inhibits MCF-7 cell proliferation in a dose-dependent fashion and in a range of concentrations at which the

compound completely inhibits PKC activity in intact cells (**Figure 32**) strongly supports a view that inhibition of PKC by ET18-OCH_3 would account, at least in part, for its antiproliferative action in MCF-7 cells.

5.4.2 ET18-OCH_3 inhibits MAPK activation by disrupting Raf-1 association with membrane

Activation of the MAPK cascade may be sufficient to initiate cell proliferation (Kolch *et al.*, 1993). Our results demonstrate that in an ET18-OCH_3-sensitive cell line (MCF-7), uptake of the drug inhibits the sustained phosphorylation and activation of MAPK as a consequence of its effect on Raf-1. This is based on the following: [1] ET18-OCH_3 had no effect on the binding of EGF to its receptors (**Figure 38A**). Although EGFr internalization was inhibited as previously reported (Kosano *et al.*, 1989), it occurred after the decrease of MAPK activity to near-resting levels (**Figure 38B** and **36A**) ; [2] ET18-OCH_3 did not affect the extent and kinetics of tyrosine phosphorylation of EGF receptors (**Figure 39**), suggesting that the drug had no effect on EGFr kinase activity; [3] ET18-OCH_3 did not affect the activation of $p21^{ras}$ in the cells (**Figure 40**); [4] Preincubation of cells with ET18-OCH_3 did not reduce the Raf-1 content of the cells but significantly decreased the duration of Raf-1 association with membranes within 4 min of stimulation (**Figure 41**). This reduced association correlated with a decrease in the membrane-associated Raf-1 kinase activity (**Figure 42**); [5] Since ET18-OCH_3 had no effect on the cellular cAMP levels (**Figure 44**) and PKA activity (**Section 4.3.9**), the inhibition of Raf-1 activity was not caused by a direct or indirect increase of PKA activity by this compound; and [6] The decrease in

MAPK activity (**Figure 36**) paralleled that of Raf-1 kinase activity (**Figure 42**), and resulted from decreased phosphorylation of MEK (**Figure 37B**), and subsequently of MAPK rather than a direct effect of ET18-OCH_3 on MAPK activity (**Figure 37A**). Furthermore, the reduction in magnitude and duration of MAPK activation and the decreased association of Raf-1 with membranes after EGF or serum stimulation in MCF-7 cells preincubated with ET18-OCH_3 have also been observed in insulin-stimulated cells (Richard and Arthur, unpublished observations).

The mechanism by which ET18-OCH_3 interferes in the association of Raf-1 with the membrane is not known. Since Ras activation, which localizes Raf-1 to the plasma membrane (Leevers *et al.*, 1994; Stokoe *et al.*, 1994), is unaffected by ET18-OCH_3 (**Figure 40**), it is not surprising that even though ET18-OCH_3 was already present in the membrane before stimulation of the cells with growth factors, it was unable to prevent the initial increase in Raf-1 association with membranes (**Figure 41**). We believe the initial activation of MAPK after cell stimulation is due to the Ras-mediated translocation and the subsequent activation of Raf-1, but the presence of ET18-OCH_3 in the membranes appears to activate or enhance an opposing process that results in the dissociation of membrane-associated Raf-1 much earlier than its occurrence in the control cells (**Figure 41**). However, we cannot yet categorically rule out an effect of ET18-OCH_3 on the translocation process. Our results lead us to postulate that the accelerated dissociation of Raf-1 results in the truncation of the sustained activation of MAPK. Since growth-inhibitory conditions with ET18-OCH_3 used in our studies did not completely block MAPK activation, we can surmise that the magnitude and duration of activation of the kinase were insufficient for the phosphorylation and activation of downstream molecules to levels required to initiate proliferation. This

interpretation is consistent with the postulation that the magnitude and duration of MAPK activation is crucial in determining cellular response to stimulation (Marshall, 1995). These results do not rule out the possibility that the effect of ET18-OCH_3 on parallel growth-requiring signal transduction pathways such as the PKC-dependent pathway (see **Section 5.4.1**) also contribute to inhibition of cell proliferation by this AEL.

We do not know whether the ET18-OCH_3-induced inhibition of Raf-1 activation is due to a direct interaction of the compound with Raf-1, or whether this is achieved indirectly via its effects on unknown intermediary molecules required for the activation and/or attachment of Raf-1 to the membrane. It has been suggested that lipids may play a role in Raf-1 activation (Cai *et al.*, 1993; Dent *et al.*, 1995; Ghosh *et al.*, 1994; 1996). Irrespective of the exact mode of action of ET18-OCH_3 on Raf-1, its ability to interfere in the activation of this key signaling molecule in a dose-dependent fashion should make it useful in assessing the effects of differential activation of the MAPK cascade on cellular responses.

The correlation between the accumulation of ET18-OCH_3, the extent of growth inhibition, the Raf-membrane association and the MAPK activation (**Figure 29** and **43**) suggests that the inhibition of the MAPK pathway by ET18-OCH_3 is likely to contribute significantly to its antiproliferative effects. This view is supported by recent studies in our laboratory demonstrating that *R* and *S* enantiomers of a double bond phosphonocholine ALP analogue had differential effects on MCF-7 cell growth which correlated with their ability or inability to inhibit MAPK activation (Samadder, Bittman, Byun and Arthur, unpublished observations). The differential effects of the phosphonocholine enantiomers on cell proliferation also provide support for the widely held view that the inhibitory effects of AELs

are not due to nonspecific perturbation of membranes (Houlihan *et al.*, 1995; Lohmeyer and Bittman, 1994).

The results shown in **Table 10** clearly indicate that the transient stimulation of MCF-7 cells with serum which would result in activation of MAPK cascade is essential for the G_1-S transition. Thus, we extrapolate that inhibition of the early events in cell activation by ET18-OCH_3 such as inhibition of the MAPK cascade could significantly contribute to its antiproliferative effects and therefore underlie the mechanism of action of the compound. However, as other signaling molecules such as PKC, PI-3K, and PLC that may be activated within this period could be inhibited by AELs, this cautions against attributing the inhibition of growth by ET18-OCH_3 solely to its ability to inhibit the MAPK cascade. An assessment of whether these enymes are inhibited under ET18-OCH_3 preincubation conditions that inhibit Raf-1 activation and whether their activation is essential for growth will be required before such a conclusion can be made. As discussed in **Section 5.4.1**, under the identical conditions for ET18-OCH_3 preincubation, the PKC-dependent phosphorylation of cellular proteins was potently inhibited by the AEL. Furthermore, PKC activities appear to be essential for MCF-7 cell growth (**Figure 32**). These suggest that the inhibition of PKC activation by ET18-OCH_3 would at least partially contribute to the growth-inhibitory action of the compound. It is worth noting that PKC has been reported to activate Raf-1 in some cells (Buchner, 1995; Carroll *et al.*, 1994; Kolch *et al.*, 1993). Studies on the role of PKC in regulation of Raf-1 activation in MCF-7 cells should provide an insight into the mechanism of growth-inhibitory action by ET18-OCH_3.

Based on our results, we propose a model for the antiproliferative action of ET18-

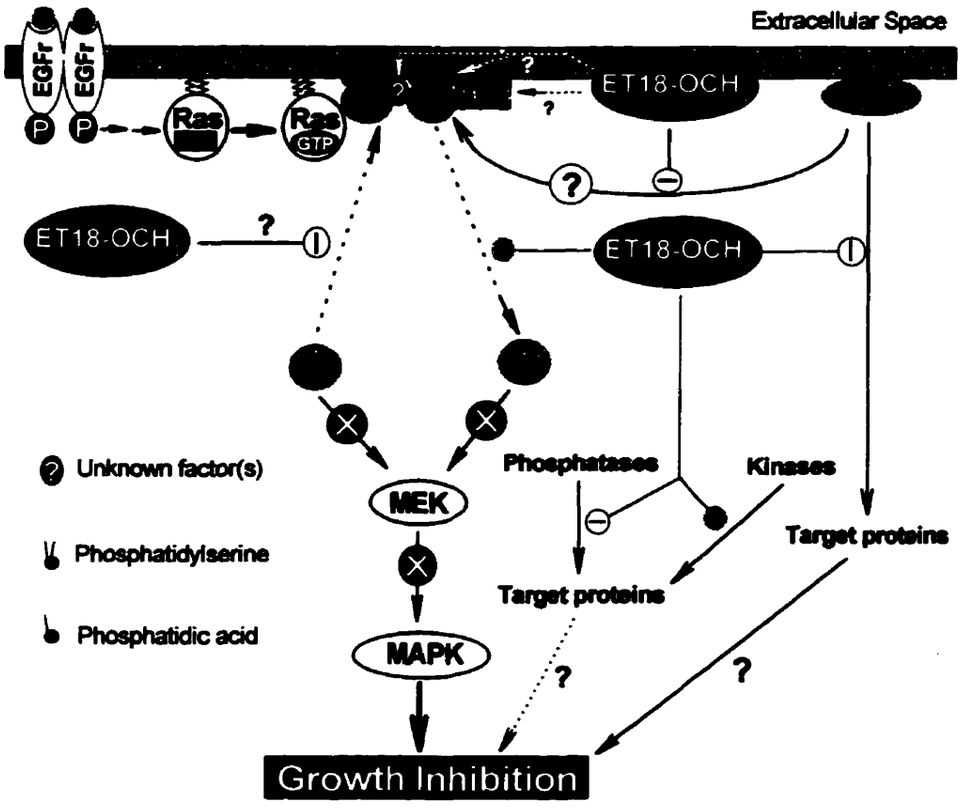

Figure 45. The proposed model of the antiproliferative action by ET18-OCH_3.

ET18-OCH_3 is widely distributed in intracellular compartments. It blocks the transduction of growth signals most likely via inhibition of the activation of the MAPK cascade and of the PKC pathway. Inhibition of the MAPK cascade is achieved by interference with the Raf-membrane association while the target(s) for inhibition of the PKC pathway are currently unknown. The possible mechanisms underlying the decrease in Raf-membrane association are shown in the figure. ⊕ indicates a positive effect, ⊖ a negative effect, ⊗ a blockage, and ? an uncertain or unknown event.

OCH_3 in MCF-7 cells (**Figure 45**). In this model, although there are still many gaps, conjectures and unknowns, ET18-OCH_3 blocks the growth signal transduction via interference in the Raf-membrane association leading to an abrogation of MAPK activation and by inhibition of the PKC-dependent signaling pathway as well.

6 CONCLUSION

The antiproliferative activities of AELs have been established firmly by studies from many laboratories. A number of hypotheses have been proposed to address the question as to the mechanisms underlying the action of AELs. In these studies, we have explored the mechanism of action of AELs using ET18-OCH_3, the archetype of AELs, and epithelial cancer cell lines with differential sensitivity to the compound. The conclusions that can be drawn from our studies are:

[1] The postulated relationship between cellular ether phospholipid content and ET18-OCH_3-sensitivity based on studies with leukemic cell lines does not exist in epithelial cancer cell lines used in our studies.

[2] ET18-OCH_3, rather than its major metabolite OMG, is the principal active compound responsible for its antiproliferative action in MCF-7, a sensitive cell line.

[3] ET18-OCH_3 affects cellular lipid metabolism. It reduces PtdCho synthesis and stimulates PtdEtn, PtdOH, DAG and TAG in either MCF-7 or A549 cells. The inhibition of PtdCho synthesis by ET18-OCH_3 does not underlie its antiproliferative activity in MCF-7 cells.

[4] ET18-OCH_3 inhibits the PKC-dependent phosphorylation, but stimulates the PKC-independent phosphorylation in intact MCF-7 cells. The significance of these effects in its antitumor activities has yet to be explored.

[5] ET18-OCH_3 disrupts the association of Raf-1 with the membrane, which results in an abortive activation of MAP kinase, namely reduction in the magnitude and duration of MAPK activation. A correlation between the accumulation of ET18-OCH_3, the extent of growth inhibition, the Raf-membrane association and MAPK activation exists in MCF-7 cells.

Although ET18-OCH_3 affects a number of other cellular events (Berdel, 1991; Houlihan *et al.*, 1995; Lohmeyer and Bittman, 1994), as far as we are aware the studies in this thesis are the first to demonstrate its inhibition of a signal transduction pathway, the MAPK cascade, which is directly linked to initiation of cell growth. The localization of an inhibitory effect of ET18-OCH_3 downstream of Ras, implies that ET18-OCH_3 and related compounds should be effective against activating Ras mutations which have been observed in at least one-third of human cancers (Lowy and Willumsen, 1993, Marshall, 1993). Precisely how ET18-OCH_3 interferes in Raf-membrane association remains to be elucidated, but such studies should provide insight on the mechanisms that regulate Raf-1 activation. Another implication of our studies is that the apparent cell selective effects of ET18-OCH_3 may be due to fundamental differences in the regulation of Raf-membrane associations between the AEL-sensitive and -insensitive cells or differences in the signal transduction pathways (Raf-dependent or -independent pathway) that mediate cell proliferation in different cell types. Future studies to resolve the basis of the selective effects should lead to the rational use of these compounds in cancer therapy.

7. REFERENCES

Abdel-Hafiz HAM, Heasley LE, Kyriakis JM, Avruch J, Kroll DJ, Johnson GL, Hoeffler JP **(1992)** Activating transcription factor-2 DNA-binding activity is stimulated by phosphorylation catalyzed by p42 and p54 microtubule-associated protein kinases. *Mol. Endocrinol.* **6,** 2079-89

Adler V, Pincus MR, Brandt-Rauf PW, Ronai Z **(1995)** Complexes of $p21^{RAS}$ with JUN N-terminal kinase and JUN proteins. *Proc. Natl. Acad. Sci. USA.* **92,** 10585-9

Ahn NG, Krebs EG **(1990)** Evidence for an epidermal growth factor-stimulated protein kinase cascade in Swiss 3T3 cells. *J. Biol. Chem.* **256,** 11495-501

Ahn NG, Seger R, Bratlien RL, Ditz CD, Tonks NK, Krebs EG **(1991)** Multiple components in an epidermal growth factor-stimulated protein kinase cascade. In vitro activation of a myelin basic protein/microtubule-associated protein 2 kinase. *J. Biol. Chem.* **266,** 4220-7

Ahn NG, Weiel JE, Chan CP, Krebs EG **(1990)** Identification of multiple epidermal growth factor-stimulated protein serine/threonine kinases from Swiss 3T3 cells. *J. Biol. Chem.* **265,** 11487-94

Aitken A (1995) 14-3-3 proteins on the MAP. *Trends Biochem. Sci.* **20,** 95-7

Aitken A, Howell S, Jones D, Madrazo J, Petel Y **(1995)** 14-3-3 α and δ are the phosphorylated forms of Raf-activating 14-3-3 β and ζ: *In vivo* stoichiometric phosphorylation in brain at a Ser-Pro-Glu-Lys Motif. *J. Biol. Chem.* **270,** 5706-9

Alberts B, Bray D, Lewis J, Raff M, Roberts K, Watson JD **(1994)** Molecular Biology of the Cell. (3rd ed.), pp. 477-506, 599-651, 1255-94, Garland Publishing, Inc. New York.

Alblas J, van Corven EJ, Hordijk PL, Milligan G, Moolenaar WH **(1993)** G_i-mediated

activation of the $p21^{ras}$-mitogen-activated protein kinase pathway by α_2-adrenergic receptors expressed in fibroblasts. *J. Biol. Chem.* **268,** 22235-8

Alessandrini A, Crews CM, Erikson RL **(1992)** Phorbol ester stimulates a protein-tyrosine/threonine kinase that phosphorylates and activates the *Erk-1* gene product. *Proc. Natl. Acad. Sci. USA* **89,** 8200-4

Alessi DR, Saito Y, Campbell DG, Cohen P, Sithanandam G, Rapp UR, Ashworth A, Marshall CJ, Cowley S **(1994)** Identification of the sites in MAP kinase kinase-1 phosphorylated by p74raf-1. *EMBO J.* **13,** 1610-9

Altschuler DL, Peterson SN, Ostrowski MC, Lapetina EG **(1995)** Cyclic AMP-dependent activation of Rap1b *J. Biol. Chem.* 10373-6

Alvarez E, Northwood IC, Gonzalez FA, Latour DA, Seth A, Abate C, Curran T, Davis RJ **(1991)** Pro-Leu-Ser/Thr-Pro is a consensus primary sequence for substrate protein phosphorylation. *J. Biol. Chem.* **266,** 15277-85

Ammerer G (1994) Sex, stress and integrity: the importance of MAP kinases in yeast. *Curr. Opin. Genet. Dev.* **4,** 90-5

Anderson NG, Li P, Marsden LA, Williams N, Robert TM, Sturgill TW **(1991)** Raf-1 is a potential substrate for mitogen-activated protein kinase *in vivo*. *Biochem. J.* **277,** 573-6

Anderson NG, Maller JL, Tonks NK, Sturgill TW **(1990)** Requirement for integration of signals from two distinct phosphorylation pathways for activation of MAP kinase. *Nature* **343,** 651-3

Andreesen R, Modolell M, Weltzien HU, Eibl H, Common HH, Löhr GW, Munder PG **(1978)** Selective destruction of human leukemic cell by alkyl-lysophospholipids. *Cancer Res.*

38, 3894-9

Arnold D, Weltzien HU, Westphal O **(1967)** Uber die Synthese von Lysolecithinen und ihren Atheranaloga. *Liebigs Ann. Chem.* **709,** 234-9

Aronheim A, Engelberg D, Li N, Al-Alawi N, Schlessinger J, Karin M **(1994)** Membrane targeting of the nucleotide exchange factor Sos is sufficient for activating the Ras signaling pathway. *Cell* **78,** 949-61

Arthur G, Choy PC **(1984)** Acyl specificity of hamster heart CDP-choline 1,2-diacylglyderol phosphocholine transferase in phosphatidylcholine biosynthesis. *Biochim. Biophys. Acta* **795,** 221-9

Arthur G, Mock T, Zaborniak C, Choy PC **(1985)** The distribution and acyl composition of plasmalogens in guinea pig heart. *Lipids* **20,** 693-8

Arthur G, Page L **(1991)** Synthesis of phosphatidylethanolamine and ethanolamine plasmalogen by the CDP-ethanolamine and decarboxylase pathways in rat heart, kidney and liver. *Biochem. J.* **273,** 121-5

Arvidson GAE (1968) Structural and metabolic heterogeneity of rat liver glycerophosphatides. *Eur. J. Biochem.* **4,** 478-86

Asaoka Y, Nakamura S, Yoshida K, Nishizuka Y **(1992)** Protein kinase C, calcium and phospholipid degradation. *Trends Biochem. Sci.* **17,** 414-7

Ashagbley A, Samadder P, Bittman R, Erukulla RK, Byun H-S, Arthur G **(1996)** Synthesis of ether-linked analogues of lysophosphatidate and their effect on the proliferation of human epithelial cancer cells *in vitro*. *J. Med. Chem.* **39,** 1545-8

Ashwell JD, Berger NA, Cidlowski JA, Lane DP, Korsmeyer SJ **(1994)** Coming to terms

with death: apoptosis in cancer and immune development. *Immunol. Today* **15,** 147-51

Avruch J, Zhang X, Kyriakis JM **(1994)** Raf meets Ras: completing the framework of a signal transduction pathway. *Trends Biochem. Sci.* **19,** 279-83

Baeuerle PA, Baltimore D **(1988)** Activation of DNA-binding activity in an apparently cytoplasmic precursor of the NF-κB transcriptin factor. *Cell* **53,** 211-7

Bansal VS, Majerus PW **(1990)** Phosphatidylinositol-derived precursors and signals. *Annu. Rev. Cell Biol.* **6,** 41-67

Barbacid M (1987) *ras* genes. *Annu. Rev. Biochem.* **56,** 779-827

Barone MV, Crozat A, Tabaee A, Philipson L, Ron D **(1994)** CHOP (GADD153) and its oncogentic variant, TLC-CHOP, have opposing effects on the induction of G1/S arrest. *Genes Dev.* **8,** 453-64

Batchvarova N, Wang XZ, Ran D **(1995)** Inhibition of adipogenesis by the stress-induced protein CHOP (Gadd153). *EMBO J.* **14,** 4654-61

Bauchinger M, Dresp J, Schmid E, Berdel WE **(1983)** Cytogenetic effects of an alkyl-lysophospholipid derivative in human peripheral lymphocytes exposed *in vitro* and *in vivo*. *Mutat. Res.* **121,** 225-31

Bennett AM, Tang TL, Sugimoto S, Walsh CT, Neel BG **(1994)** Protein-tyrosine-phosphatase SHPTP2 couples platelet-derived growth factor receptor β to Ras. *Proc. Natl. Acad. Sci.* **91,** 7335-9

Benbrook DM, Jones NC **(1990)** Heterodimer formation between CREB and JUN proteins. *Oncogene* **5,** 295-302

Beranger F, Goud B, Tavitian A, de Gunzburg J **(1991)** Association of the Ras-antagonistic

Rap1/Krev-a proteins with the Goligi complex. *Proc. Natl. Acad. Sci. USA* **88,** 1606-10

Berdel WE (1991) Membrane-interactive lipids as experimental anticancer drugs. *Br. J. Cancer* **64,** 208-11

Berdel WE, Andreesen R, Munder PG **(1985)** Synthetic alkylphospholipid analogs; a new class of antitumor agents. In: *Phospholipids and cellular regulation*, vol. II (Kuo, JF ed.) pp. 41-73, CRC Press, Boca Raton FL.

Berdel WE, Korth R, Reichert A, Houlihan WJ, Bicker U, Nomura H, Vogler WR, Beneviste J, Rastetter J **(1987)** Lack of correlation between cytotoxicity of agonists and antagonists of platelet activating factor (PAF-acether) in neoplastic cells and modulation of [^{3}H]-PAF-acether binding to platelets from numans *in vitro*. *Anticancer Res.* **7,** 1181-7

Berggren MI, Gallegos A, Dressler LA, Modest EJ, Powis G **(1993)** Inhibition of the signalling enzyme phosphatidylinositol-3-kinase by antitumor ether lipid analogues. *Cancer Res.* **53,** 4297-302

Berkovic D, Fleer EAM, Eibl H, Unger C **(1992)** Effects of hexadecylphosphocholine on cellular function. *Prog. Exp. Tumor Res.* **34,** 59-68

Berkovic D, Berkovic K, Fleer EA, Eibl H, Unger C **(1994)** Inhibition of calcium-dependent protein kinase C by hexadecylphosphocholine and 1-*O*-octadecyl-2-*O*-methyl-*rac*-glycero-3-phosphocholine do not correlate with the inhibition of proliferation of HL60 and K562 cell lines. *Eur. J. Cancer* **30A,** 509-15

Berra E, Diaz-Meco MT, Dominguez I, Municio MM, Sanz L, Lozano J, Chapkin RS,

Moscat J **(1993)** Protein kinase C ζ isoform is critical for mitogenic signal transduction. *Cell* **74,** 555-63

Berridg MJ (1993) Inositol triphosphate and calcium signalling. *Nature* **361,** 315-25

Binetruy B, Smeal T, Karin M **(1991)** Ha-Ras augments c-Jun activity and stimulates phosphorylation of its activation domain. *Nature* **351,** 122-7

Bjørkøy G, Øvervatn A, Diaz-Meco MT, Moscat J, Johansen T **(1995)** Evidence for a bifurcation of the mitogenic signaling pathway activated by Ras and phosphatidylcholine-hydrolyzing phospholipase C. *J. Biol. Chem.* **270,** 21299-306

Blank JL, Gerwisn P, Elliott EM, Sather S, Johnson GL **(1996)** Molecular cloning of mitogen-activated protein/ERK kinase kinases (MEKK) 2 and 3. *J. Biol. Chem.* **271,** 5361-8

Blenis J (1993) Signal transduction via the MAP kinases: proceed at your own RSK. *Proc. Natl. Acad. Sci. USA* **90,** 5889-92

Block C, Janknecht R, Herrmann C, Nassar N, Wittinghofer A **(1996)** Quantitative structure-activity analysis correlating Ras/Raf interaction *in vitro* to Raf activation *in vivo*. *Nat. Struct. Biol.* **3,** 244-51

Blumer KJ, Johnson GL **(1994)** Diversity in function and regulation of MAK kinase pathway. *Trends Biochem. Sci.* **19,** 236-40

Boguski M, McCormick F **(1993)** Proteins regulating Ras and its relatives. *Nature* **366,** 643-54

Bokemeyer D, Sorokin A, Yan M, Ahn NG, Templeton DJ, Dunn MJ **(1996)** Induction of mitogen-activated protein kinase phosphatase 1 by the stress-activated protein kinase signaling pathway but not by extracellular signal-regulated kinase in fibroblasts. *J. Biol.*

Chem. **271,** 639-642

Bokoch GM (1993) Biology of the Rap proteins, members of the *ras* superfamily of GTP-binding protein. *Biochem. J.* **289,** 17-24

Bonni A, Ginty DD, Dudek H, Greenberg ME **(1995)** Serine 133-phosphorylated CREB induces transcription via a cooperative mechanism that may confer specificity to neurotrophin signals. *Mol. Cell. Neurosci.* **6,** 168-83

Boucher L-M, Wiegmann K, Futterer A, Pfeffer K, Mak TW, Kronke M **(1995)** CD28 signals through acidic sphingomyelinase. *J. Exp. Med.* **181,** 2059-68

Bourne H, Sanders DA, McCormick F **(1990)** The GTPase superfamily: a conserved switch for diverse cell functions. *Nature* **348,** 125-32

Bourne H, Sanders DA, McCormick F **(1991)** The GTPase superfamily: conserved structure and molecular mechanism. *Nature* **349,** 117-27

Bowtell D, Fu P, Simon M, Senior P **(1992)** Identification of murine homologues of the Drosophila son of sevenless gene: potential activators of ras. *Proc. Natl. Acad. Sci. USA* **89,** 6511-5

Braselmann S, McCormick F **(1995)** BCR and RAF form a complex *in vivo* via 14-3-3 proteins. *EMBO J.* **14,** 4839-48

Brtva TR, Drugan JK, Ghosh S, Terrell RS, Campbell-Burk S, Bell RM, Der CJ **(1995)** Two distinct Raf domains mediate interaction with Ras. *J. Biol. Chem.* **270,** 9809-12

Bruder JT, Heidecker G, Rapp UR **(1992)** Serum-, TPA-, and Ras-induced expression from Ap-1/Ets-driven promoters requires Raf-1 kinase. *Genes Dev.* **6,** 545-56

Brunet A, Pouyssegur J **(1996)** Identification of MAP kinase domains by redirecting stress

signals into growth factor responses. *Science* **272,** 1652-5

Brunner D, Oellers N, Szabad J, Biggs WH 3rd, Zipursky SL, Hafen E **(1994)** A gain-of-function mutation in Drosophila MAP kinase activates multiple receptor tyrosine kinase signaling pathways. *Cell* **76,** 875-88

Buchner K (1995) Protein kinase C in the transduction of signals toward and within the cell nucleus. *Eur. J. Biochem.* **228,** 211-21

Buday L, Downward J **(1993)** Epidermal growth factor regulates $p21^{ras}$ through the formation of a complex of receptor, Grb2 adapter protein, and Sos nucleotide exchange factor. *Cell* **73,** 611-20

Burdzy K, Munder PG, Fischer HZ, Westphal O **(1964)** Increase of the phagocytosis of peritoneal macrophages by lysolecithin. *Z. Naturforsch.* **19b,** 1118-20

Burgering BMT, Bos JL **(1995)** Regulation of Ras-mediated signalling: more than one way to skin a cat. *Trends Biochem. Sci.* **20,** 18-22

Burgering BMT, Coffer PJ **(1995)** Protein kinase B (c-Akt) in phosphatidylinositol-3-OH kinase signal transduction. *Nature* **376,** 599-602

Burgering BMT, Pronk GJ, van Weeren PC, Chardin P, Bos JL **(1993)** cAMP antagonizes $p21^{ras}$-directed activation of extracellular signal-regulated kinase 2 and phosphorylation of mSos nucleotide exchange factor. *EMBO J.* **12,** 4211-20

Cai H, Erhardt P, Troppmair J, Diaz-Meco MT, Sithanandam G, Rapp UR, Moscat J, Cooper GM **(1993)** Hydrolysis of phosphatidylcholine couples Ras to activation of Raf protein kinase during mitogenic signal transduction. *Mol. Cell. Biol.* **13,** 7645-51

Campa MJ, Chang K-J, Molina-y-Vedia L, Reep BR, Lapetina EG **(1991)** Inhibition of

ras-induced germinal vesicle breakdown in Xenopus oocytes by rap-1B. *Biochem. Biophys. Res. Commun.* **174,** 1-5

Cano E, Mahadevan LC **(1995)** Parallel signal processing among mammalian MAPKs. *Trends Biochem. Sci.* **20,** 117-22

Carroll MP, May WS **(1994)** Protein kinase C-mediated serine phosphorylation directly activates Raf-1 in murine hematopoietic cells. *J. Biol. Chem.* **269,** 1249-56

Casey PJ (1995) Protein lipidation in cell signaling. *Science* **268,** 221-5

Catling AD, Schaeffer HJ, Reuter CWM, Reddy GR, Weber MJ **(1995)** A proline-rich sequence unique to MEK1 and MEK2 is required for Raf binding and regulates MEK function. *Mol. Cell Biol.* **15,** 5214-25

Chabot MC, Wykle RL, Modest EJ, Daniel IW **(1989)** Correlation of ether lipid content of human leukemia cell lines and their susceptibility to 1-*O*-octadecyl-2-*O*-methyl-*rac*-glycero-3-phosphocholine. *Cancer Res.* **49,** 4441-5

Chao T-SO, Byron KL, Lee K-M, Villereal M, Rosner MR **(1992)** Activation of MAP kinases by calcium-dependent and calcium-independent pathways. Stimulation by thapsigargin and epidermal growth factor. *J. Biol. Chem.* **267,** 19876-83

Chardin P, Camonis JH, Gale NW, van Aelst L, Schlessinger J, Wigler MH, Bar-Sagi D **(1993)** Human Sos1: a guanine nucleotide exchange factor for Ras that binds to GRB2. *Science* **260,** 1338-43

Cheatham B, Vlahos, CJ, Cheatham L, Wang L, Blenis J, Kahn CR **(1994)** Phosphatidylinositol 3-kinase activation is required for insulin stimulation of pp70 S6 kinase, DNA synthesis, and glucose transporter translocation. *Mol. Cell. Biol.* **14,** 4902-11

Chen R-H, Abate C, Blenis J **(1993)** Phosphorylation of the c-Fos transrepression domain by mitogen-activated protein kinase and 90-kDa ribosomal S6 kinase. *Proc. Natl. Acad. Sci. USA* **90,** 10952-6

Cheng M, Boulton TG, Cobb MH **(1996a)** ERK3 is a constitutively nuclear protein kinase. *J. Biol. Chem.* **271,** 8951-8

Cheng M, Zhen E, Robinson MJ, Ebert D, Goldsmith E, Cobb MH **(1996b)** Characterization of a protein kinase that phosphorylates serine 189 of the mitogen-activated protein kinase homolog ERK3. *J. Biol. Chem.* **271,** 12057-62

Chrivia JC, Kwok RP, Lamb N, Hagiwara M, Montminy MR, Goodman RH **(1993)** Phosphorylated CREB binds specifically to the nuclear protein CBP. *Nature* **365,** 855-9

Chuang E, Barnard D, Hettich L, Zhang X, Avruch J, Marshall MS **(1994)** Critical binding and regulatory interations between Ras and Raf occur through a small, stable N-terminal domain of Raf and specific Ras effector residues. *Mol. Cell. Biol.* **14,** 5318-25

Chung J, Pelech SL, Blenis J **(1991)** Mitogen-activated Swiss mouse 3T3 RSK kinases I and II are related to $pp44^{mpk}$ from sea star oocytes and participate in the regulation of $pp90^{rsk}$ activity. *Proc. Natl. Acad. Sci. USA* **88,** 4981-5

Ciapa B, Pesando D, Wilding M, Whitaker M **(1994)** Cell-cycle calcium transients driven by cyclic changes in insoitol trisphosphate levels. *Nature* **368,** 875-8

Cockcroft S, Thomas GMH **(1992)** Inositol-lipid-specific phospholipase C isoenzymes and their differential regulation by receptors. *Biochem. J.* **288,** 1-14

Cohen GB, Ren R, Baltimore **(1995)** Modular binding domains in signal transduction proteins. *Cell* **80,** 237-48

Comfurius P, Zwaal RFA **(1977)** The enzymatic synthesis of phosphatidylserine and purification by CM-cellulose column chromatography. *Biochim. Biophys. Acta* **488,** 36-42

Conklin DS, Galaktionov K, Beach D **(1995)** 14-3-3 proteins associate with cdc25 phosphatases. *Proc. Natl. Acad. Sci. USA* **92,** 7892-6

Cook SJ, McCormick F **(1993)** Inhibition by cAMP of Ras-dependent activation of Raf. *Science* **262,** 1069-72

Cook SJ, Rubinfeld B, Albert I, McCormick F **(1993)** RapV12 antagonizes Ras-dependent activation of ERK1 and ERK2 by LPA and EGF in Rat-1 fibroblasts. *EMBO J.* **12,** 3475-85

Cook SJ, Wakelam MJO **(1992)** Epidermal growth factor increases *sn*-1,2-diacylglycerol levels and activates phospholipase D-catalysed phosphatidylcholine breakdown in Swiss 3T3 cells in the absence of inositol-lipid hydrolysis. *Biochem. J.* **285,** 247-53

Cornell R (1989) Cholinephosphotransferase. In: *Phosphatidylcholine Metabolism.* (Vance DE, ed.) pp. 47-64, CRC Press, Boca Raton, FL.

Crews CM, Erikson RL **(1993)** Extracellular signals and reversible protein phosphorylation: what to Mek of it all. *Cell* **74,** 215-7

Crompton T, Gilmour KC **(1996)** The MAP kinase pathway controls differentiation from double-negative to double-positive thymocyte. *Cell* **86,** 243-51

Cuadrado A, Molloy CJ **(1990)** Overexpression of phospholipase C-γ in NIH 3T3 fibroblasts results in increased phosphatidylinositol hydrolysis in response to platelet-derived growth factor and basic fibroblast growth factor. *Mol. Cell. Biol.* **10,** 6069-72

Cummings R, Soderquist A, Carpenter G **(1985)** The oligosaccharide moities of the epidermal growth factor receptor in A431 cells. *J. Biol. Chem.* **260,** 11944-52

Daniel LW, Small GW, Schmitt JD, Marnso C, Ishag K, Plantadosi C **(1988)** Alkyl-linked diglycerides inhibit protein kinase C activation by diacylglycerols. *Biochem. Biophys. Res. Commun.* **151,** 291-7

Daum G, Eisenmann-Tappe I, Fries H-W, Troppmair J, Rapp UR **(1994)** The ins and outs of Raf kinases. *Trends Biochem. Sci.* **19,** 474-80

Davis RJ (1993) The mitogen-activated protein kinase signal transduction pathway. *J. Biol. Chem.* **268,** 14553-6

Davis RJ (1995) Transcriptional regulation by MAP kinases. *Mol. Reprod. Dev.* **42,** 459-67

Dekker LV, Parker PJ **(1994)** Protein kinase C - a question of specificity. *Trends Biochem. Sci.* **19,** 73-7

den Hertog J, Tracy S, Hunter T **(1994)** Phosphorylation of receptor protein-tyrosine phosphatase α on Tyr789, a binding site for the SH3-SH2-SH3 adaptor protein GRB-2 *in vivo*. *EMBO J.* **13,** 3020-32

Dennis EA, Rhee SG, Billah MM, Hannun YA **(1991)** Role of phospholipases in generating lipid second messengers in signal transduction. *FASEB J.* **5,** 2068-77

Dent P, Haser W, Haystead TAJ, Vincent LA, Robers TM, Sturgill TW **(1992)** Activation of mitogen-activated protein kinase kinase by v-Raf in NIH 3T3 cells and in vitro. *Science* **257,** 1404-7

Dent P, Jelinek T, Morrison DK, Weber MJ, Sturgill TW **(1995)** Reversal of Raf-1 activation by purified and membrane-associated protein phosphatases. *Science* **268,** 1902-6

Dent P, Reardon DB, Morrison DK, Sturgill TW **(1995)** Regulation of Raf-1 and Raf-1 mutants by Ras-dependent and Ras-independent mechanisms in vitro. *Mol. Cell. Biol.* **15,**

4125-35

Dérijard B, Hibi M, Wu IH, Barrett T, Su B, Deng T, Karin M, Davis-RJ **(1994)** JNK1: a protein kinase stimulated by UV light and Ha-Ras that binds and phosphorylates the c-Jun activation domain. *Cell* **76,** 1025-37

Dérijard B, Raingeaud J, Barrett T, Wu, I-H, Han J, Ulevitch RJ, Davis RJ **(1995)** Independent human MAP kinase signal transduction pathways defined by MEK and MEKK isoforms. *Science* **267,** 682-5

Dhand R, Hiles I, Panayotou G, Roche S, Fry MJ, Gout I, Totty NF, Truong O, Vicendo P, Yonezawa K, Kasuga M, Courtneidge SA, Waterfield MD **(1994)** PI 3-kinase is a dual specificity enzyme: autoregulation by an intrinsic protein-serine kinase activity. *EMBO J.* **13,** 522-33

Didichenko SA, Tilton B, Hemmings BA, Ballmer-Hofer K, Thelen M **(1996)** Constitutive activation of protein kinase B and phosphorylation of $p47^{phox}$ by a membrane-targeted phosphoinositide 3-kinase. *Curr. Biol.* **6,** 1271-8

Diomede L, Colotta F, Piovani B, Re F, Modest EJ, Salmona M **(1993)** Induction of apoptosis in human leukemic cells by the ether lipid 1-octadecyl-2-methyl-*rac*-glycero-3-phosphocholine. A possible basis for its selective action. *Int. J. Cancer* **53,** 124-30

Diomede L, Piovani B, Modest EJ, Noseda A, Salmona M **(1991)** Increased ether lipid cytotoxicity by reducing membrane cholesterol content. *Int. J. Cancer* **49,** 409-13

Diomede L; Piovani B; Re F; Principe P; Colotta F; Modest EJ; Salmona M **(1994)** The induction of apoptosis is a common feature of the cytotoxic action of ether-linked glycerophospholipids in human leukemic cells. *Int. J. Cancer* **57,** 645-9

Dive C, Watson JV, Workman P **(1991)** Multiparametric flow cytometry of the modulation of tumor cell membrane permeability by developmental antitumor ether lipid SRI 62-834 in EMT6 mouse mammary tumor and HL-60 human promyelocytic leukemia cells. *Cancer Res.* **51,** 799-806

Divecha N, Banfić H, Irvine RF **(1993)** Inositides and the nucleus and inositides in the nucleus. *Cell* **74,** 405-7

Divecha N, Irvine R **(1995)** Phospholipid signaling. *Cell* **80,** 269-78

Dobrowsky RT, Hannun YA **(1992)** Ceramide stimulates a cytosolic protein phosphatase. *J. Biol. Chem.* **267,** 5048-51

Dominguez I, Diaz-Meco MT, Municio MM, Berra E, Garcia de Herreros A, Cornet ME, Sanz L, Moscat J **(1992)** Evidence for a role of protein kinase C ζ subspecies in maturation of *Xenopus laevis* oocytes. *Mol. Cell. Biol.* **12,** 3776-83

Downes CP, Carter AN **(1991)** Phosphoinositides 3-kinase: a new effector in signal transduction? *Cell. Signalling* **3,** 501-13

Downes CP, Macphee CH **(1990)** *myo*-Inositol metabolites as cellular signals. *Eur. J. Biochem.* **193,** 1-18

Downward J (1992) Regulatory mechanisms for *ras* proteins. *BioEssays* **14,** 177-84

Downward J (1995a) KSR: a novel player in the RAS pathway. *Cell* **83,** 831-4

Downward J (1995b) A target for PI(3) kinase. *Nature* **376,** 553-4

Downward J, Graves JD, Warne PH, Rayter S, Cantrell DA **(1990)** Stimulation of $p21^{ras}$ upon T-cell activation. *Nature* **346,** 719-23

Drugan JK, Khosravi-Far R, White MA, Der CJ, Sung Y, Hwang Y, Campbell S **(1996)** Ras

interaction with two distinct binding domains in Raf-1 may be required for Ras transformation. *J. Biol. Chem.* **271,** 233-7

Dryja TP, Rapaport JM, Joyce JM, Petersen RA **(1986)** Molecular detection of deletions involving band q14 of chromosome 13 in retinoblastomas. *Proc. Natl. Acad. Sci. USA* **83,** 7391-4

Dubois M-F, Nguyen VT, Dahmus ME, Pagès G, Pouysségur J, Bensaude O **(1994)** Enhanced phosphorylation of the C-terminal domain of RNA polymerase II upon serum stimulation of quiescent cells: possible involvement of MAP kinases. *EMBO J.* **13,** 4787-97

Duchesne M, Schweighoffer F, Parker F, Clerc F, Frobert Y, Thang MN, Tocqué B **(1993)** Identification of the SH3 domain of GAP as an essential sequence for Ras-GAP-mediated signaling. *Science* **259,** 525-8

Edelmann HML, Kuhne C, Petritsch C, Ballou LM **(1996)** Cell cycle regulation of p70 S6 kinase and p42/p44 mitogen-activated protein kinases in Swiss mouse 3T3 fibroblasts. *J. Biol. Chem.* **271,** 963-71

Egan SE, Giddings BW, Brooks MW, Buday L, Sizeland AM, Weinberg RA **(1993)** Association of Sos Ras exchange protein with Grb2 is implicated in tyrosine kinase signal transduction and transformation. *Nature* **363,** 45-51

Ellis RW, DeFeo D, Shih TY, Gonda MA, Young HA, Tsuchida N, Lowy DR, Scolnick EM **(1981)** The p21 *src* genes of Harvey and Kirsten sarcoma viruses originate from divergent members of a family of normal vertebrate genes. *Nature* **292,** 506-11

Exton JH (1990) Signaling through phosphatidylcholine breakdown. *J. Biol. Chem.* **265,** 1-4

Exton JH (1994) Phosphatidylcholine breakdown.and signal transduction *Biochim. Biophys.*

Acta **1212,** 26-42

Fabian JR, Daar IO, Morrison DK **(1993)** Critical tyrosine residues regulate the enzymatic and biological acitvity of Raf-1 kinase. *Mol. Cell Biol.* **13,** 7170-9

Fantl WJ, Muslin AJ, Kikuchi A, Martin JA, MacNicol AM, Gross RW, Williams LT **(1994)** Activation of Raf-1 by 14-3-3 proteins. *Nature* **371,** 612-4

Farrar MA, Alberola-Ila J, Perlmutter RM **(1996)** Activation of the Raf-1 kinase cascade by coumermycin-induced dimerization. *Nature* 178-81

Fath I, Schweighoffer F, Rey I, Multon M-C, Boiziau J, Duchesne M, Tocqué B **(1994)** Cloning of a Grb2 isoform with apoptotic properties. *Science* **264,** 971-4

Faure M, Voyno-Yasenetskaya TA, Bourne HR **(1994)** cAMP and $\beta\gamma$ subunites of heterotrimeric G proteins stimulate the mitogen-activated protein kinase pathway in COS-7 cells. *J. Biol. Chem.* **269,** 7851-4

Feig LA, Schaffhausen B **(1994)** The hunt for Ras targets. *Nature* **370,** 508-9

Ferrell Jr JE (1996) MAP kinases in mitogenesis and development. *Curr. Topics Dev. Biol.* **33,** 1-60

Fidler IJ, Balch CM **(1987)** The biology of cancer metastasis and implications for therapy. *Curr. Probl. Surg.* **24,** 129-209

Fischer H (1964) Lysolecithin and the action of complement. *Ann. N. Y. Acad. Sci.* **116,** 1063-9

Fleer EAM, Berkovic D, Unger C, Eibl H **(1992)** Cellular uptake and metabolic fate of hexadecylphosphocholine. *Prog. Exp. Tumor Res.* **34,** 33-46

Fleer EAM, Unger C, Kim D-J, Eibl H **(1987)** Metabolism of ether phospholipids and analogs in neoplastic cells. *Lipids* **22,** 856-61

Ford DA, Miyaka R, Glaser PE, Gross RW **(1989)** Activation of protein kinase C by naturally occurring ether-linked diglycerides. *J. Biol. Chem.* **264,** 13818-24

Franke TF, Yang SI, Chan TD, Datta K, Kazlauskas A, Morrison DK, Kaplan DR, Tsichlis PN **(1995)** The protein kinase encoded by the Akt proto-oncogene is a target of the PDGF-activated phosphatidylinositol 3-kinase. *Cell* **81,** 727-36

Freed E, Symons M, Macdonald SG, McCormick F, Ruggieri R **(1994)** Binding of 14-3-3 proteins to the protein kinase Raf and effects on its activation. *Science* **265,** 1713-6

Fridman M, Tikoo A, Varga M, Murphy A, Nur-E-Kamal MSA, Maruta H **(1994)** The minimal fragments of c-Raf-1 and NF1 that can suppress v-Ha-Ras-induced malignant phenotype. *J. Biol. Chem.* **269,** 30105-8

Friend SH, Bernards R, Rogelj S, Weinberg RA, Rapaport JM, Albert DM, Dryja TP **(1986)** A human DNA segment with properties of the gene that predisposes to retinoblastoma and osteosarcoma. *Nature* **323,** 643-6

Frödin M, Peraldi P, Van Obberghen E **(1994)** Cyclic AMP activates the mitogen-activated protein kinase cascade in PC12 cells. *J. Biol. Chem.* **269,** 6207-14

Fu H, Xia K, Pallas DC, Cui C, Conroy K, Narsimhan RP, Mamon H, Collier RJ, Roberts TM **(1994)** Interaction of the protein kinase Raf-1 with 14-3-3 proteins. *Science* **266,** 126-9

Fujiwara K, Mohri H, Shirafuji H, Kohno I, Anne C, Wallen CA, Modest EJ **(1992)** The increase of nuclear protein in hypodipoid fraction of ovarian cancer cells induced by ET-18-OCH_3. *Proc. Am. Assoc. Cancer Res.* **33,** Abstract No. 2476

Fujiwara K, Ohishi Y, Sawada S, Shirafuji H, Kohno I, Modest EJ **(1993)** Difference in the lethal effect on ovarian cancer cells of ET18-OCH_3 and the DNA-interacting agent, etoposide. *Proc. Am. Assoc. Cancer Res.* **34,** Abstract No. 1988

Galaktionov K, Jessus C, Beach D **(1995)** Raf1 interaction with Cdc25 phosphatase ties mitogenic signal transduction to cell cycle activation. *Genes Dev.* **9,** 1046-58

Galcheva-Gargova Z, Dérijard B, Wu I-H, Davis RJ **(1994)** An osmosensing signal transduction pathway in mammalian cells. *Science* **265,** 806-8

Geilen CC, Wieder T, Reutter W **(1992)** Hexadecylphosphocholine inhibits translocation of CTP:choline phosphate cytidyltransferase in Madin-Darby canine kidney cells. *J. Biol. Chem.* **267,** 6719-24

Gerstl B, Hayman RB, Ramorino P, Tavastsjerna MG, Smith JK **(1965)** Lipids of malignant tumors. *Am. J. Clin. Pathol.* **43,** 314-8

Ghosh S, Bell RM **(1994)** Identification of discrete segments of human Raf-1 kinase critical for high affinity binding to Ha-Ras. *J. Biol. Chem.* **269,** 30785-8

Ghosh S, Strum JC, Sciorra VA, Daniel L, Bell RM **(1996)** Raf-1 kinase possesses distinct binding domains for phosphatidylserine and phosphatidic acid. Phosphatidic acid regulates the translocation of Raf-1 in 12-*O*-tetradecanoylphorbol-13-acetate-stimulated Madin-Darby canine kidney cells. *J. Biol. Chem.* **271,** 8472-80.

Ghosh S, Xie WQ, Quest AFG, Mabrouk GM, Strum JC, Bell RM **(1994)** The cysteine-rich region of raf-1 kinase contains zinc, translocates to liposomes, and is adjacent to a segment that binds GTP-ras. *J. Biol. Chem.* **269,** 10000-7

Gibbs JB, Oliff A, Kohl NE **(1994)** Farnesyltransferase inhibitors: Ras research yields a

potential cancer therapeutic. *Cell* **77,** 175-8

Ginty DD, Bonni A, Greenberg ME **(1994)** Nerve growth factor activates a Ras-dependent protein protein kinase that stimulates c-*fos* transcription via phosphorylation of CREB. *Cell* **77,** 713-25

Gray GM (1963) The lipid composition of tumor cells. *Biochem. J.* **86,** 350-7

Grove JR, Price DJ, Banerjee P, Balasubramanyam A, Ahmad MF, Avruch J **(1993)** Regulation of an epitope-tagged recombinant Rsk-1 S6 kinase by phorbol ester and erk/MAP kinase. *Biochemistry* **32,** 7727-38

Grunicke H, Hofmann J, Maly K, Überall F, Posch L, Oberhuber H, Fiebig H **(1989)** The phospholipid- and calcium-dependent protein kinase as a target in tumor chemotherapy. *Adv. Enzyme Regulation* **28,** 201-6

Gulbins E, Bissonnette R, Mahboubi A, Martin S, Nishioka W, Brunner T, Baler G, Baier-Bitterlich G, Byrd C, Lang F, Kolesnick R, Altman A, Green D **(1995)** FAS-induced apoptosis is mediated via a ceramide-initiated RAS signaling pathway. *Immunity* **2,** 341-51

Gupta S, Campbell D, Dérijard B, Davis RJ **(1995)** Transcription factor AFT2 regulation by the JNK signal transduction pathway. *Science* **267,** 389-93

Guse AH, Greiner E, Emmrich F, Brand K **(1993)** Mass changes of inositol 1,3,4,5,6-pentakisphosphate and inositol hexakisphosphate during cell cycle progression in Rat thymocytes. *J. Biol. Chem.* **268,** 7129-33

Haase R, Wieder T, Geilen CC, Reutter W **(1991)** The phospholipid analogue hexadecylphosphocholine inhibits phosphatidylcholine biosynthesis in Madin-Darby canine kidney cells. *FEBS Lett.* **288,** 129-32

Hafner S, Adler HS, Mischak H, Janosch P, Heidecker G, Wolfman A, Pippig S, Lohse M, Ueffing M, Kolck W **(1994)** Mechanism of inhibition of Raf-1 by protein kinase A. *Mol. Cell Biol.* **14,** 6696-703

Hai T, Curran T **(1991)** Cross-family dimerization of transcription factors Fos/Jun and ATF/CREB alters DNA binding specificity. *Proc. Natl. Acad. Sci. USA* **88,** 3720-4

Hall A (1994) A biochemical function for Ras—at last. *Science* **264,** 1413-4

Hallberg B, Rayter SI, Downward J **(1994)** Interaction of Ras and Raf in intact mammalian cells upon extracellular stimulation. *J. Biol. Chem.* **269,** 3913-6

Hamel PA, Gallie BL, Phillips RA **(1992)** The retinoblastoma protein and cell cycle regulation. *Trends Genetics* **8,** 180-5

Han J, Lee JD, Bibbs L, Ulevitch RJ **(1994)** A MAP kinase targeted by endotoxin and hyperosmolarity in mammalian cells. *Science* **265,** 808-11

Han J, Lee JD, Jiang Y, Li Z, Feng L, Ulevitch RJ **(1996)** Characterization of the structure and function of novel MAP kinase kinase (MKK6). *J. Biol. Chem.* **271,** 2886-91

Han M, Golden A, Han Y, Sternberg PW **(1993)** *C. elegans* lin-45 raf gene participates in let-60 ras-stimulated vulval differentiation. *Nature* **363,** 133-40

Hanahan DJ, Munder PG, Satouchi K, McManus L, Pinckard RN **(1981)** Potent platelet stimulating activity of anantiomers of acetyl glyceryl ether phosphorylcholine and its methoxy analogues. *Biochem. Biophys. Res. Commun.* **99,** 183-8

Hanks SK, Hunter T **(1995)** The eukaryotic protein kinase superfamily: kinase (catalytic) domain structure and classification. *FASEB J.* **9,** 576-96

Hannun YA (1994) The sphingomyelin cycle and the second messenger function of

ceramide. *J. Biol. Chem.* **269,** 3125-8

Hannun YA, Obeid LM **(1995)** Ceramide: an intracellular signal for apoptosis. *Trends Biochem. Sci.* **20,** 73-7

Hariharan IK, Carthew RW, Rubin GM **(1991)** The *Drosophila* roughened mutation: activation of a rap homolog disrupts eye development and interferes with cell determination. *Cell* **67,** 717-22

Hartwell LH, Kastan MB **(1994)** Cell cycle control and cancer. *Science* **266,** 1821-8

Harwood AE, Cambier J **(1993)** B cell antigen receptor crosslinking triggers rapid protein kinase C independent activation of $p21^{ras}$. *J. Immunol.* **151,** 4513-22

Haystead TAJ, Haystead CMM, Hu C, Lin T-A, Lawrence Jr. JC **(1994)** Phosphorylation of PHAS-I by mitogen-activated protein (MAP) kinase. Identification of a site phosphorylated by MAP kinase *in vitro* and response to insulin in rat adipocytes. *J. Biol. Chem.* **269,** 23185-91

Heesbeen EC, Verdonck LF, Hermans SWG, Van Heugten HG, Staal GEL, Rijksen G **(1991)** Alkyllysophospholipid ET-18-OCH_3 acts as an activator of protein kinase C in HL-60 cells. *FEBS Lett.* **290,** 231-4

Heidecker G, Huleihel M, Cleveland JL, Kölch W, Beck TW, Lloyd P, Pawson T, Rapp UR **(1990)** Mutational activation of c-raf-1 and definition of the minimal transforming sequence. *Mol. Cell. Biol.* **10,** 2503-12

Heidecker G, Kölch W, Morrison DK, Rapp UR **(1992)** The role of Raf-1 phosphorylation in signal transduction. *Adv. Cancer Res.* **58,** 53-73

Helfman DM, Barnes KC, Kinkade JM, Jr. Vogler WR, Shoji M, Kuo JF **(1983)**

Phospholipid-sensitive Ca^{2+}-dependent protein phosphorylation system in various types of leukemic cells from human patients and in human leukemic cell lines HL60 and K562, and its inhibition by alkl-lysophospholipid. *Cancer Res.* **43,** 2955-61

Hepler PK (1992) Calcium and mitosis. *Int. Rev. Cytol.* **138,** 239-68

Herrmann DBJ (1985) Changes in cellular lipid synthesis of normal and neoplastic cells during cytolysis induced by alkyllysophospholipid analogues. *J. Natl. Cancer Inst.* **75,** 423-30

Herrmann DBJ, Neumann HA **(1986)** Cytotoxic ether phospholipids. Different affinities to lysophosphocholine acyltransferase in sensitive and resistant cells. *J. Biol. Chem.* **261,** 7742-7

Hibi M, Lin A, Smeal T, Minden A, Karin-M **(1993)** Identification of an oncoprotein- and UV-responsive protein kinase that binds and potentiates the c-Jun activation domain. *Genes Dev.* **7,** 2135-48

Hill CS, Treisman R **(1995)** Transcriptional regulation by extracellular signals: mechanisms and specificity. *Cell* **80,** 199-211

Hipskind RA, Büscher D, Nordheim A, Baccarini M **(1994)** Ras/MAP kinase-dependent and -independent signaling pathways target distinct ternary complex factors. *Gene & Dev.* **8,** 1803-16

Hoffman DR, Hoffman LH, Snyder F **(1986)** Cytotoxicity and metabolism of alkyl phospholipid analogs in neoplastic cells. *Cancer Res.* **46,** 5803-9

Hoffman DR, Thomas VL, Snyder F **(1992)** Inhibition of cellular transport systems by alkyl phospholipid analogs in HL-60 human leukemia cells. *Biochim. Biophys. Acta* **1127,** 74-80

Honma Y, Kasukabe T, Hozumi M, Tsushima S, Nomura H **(1981)** Induction of differentiation of cultured human and mouse myeloid leukemia cells by alkyl-lysophospholipids. *Cancer Res.* **41,** 3211-6

Honma Y, Kasukabe T, Hozumi M, Akimoto H, Momura H **(1991)** Induction of differentiation of human myeloid leukemia HL-60 cells by novel nonphosphorus alkyl ether lipids. *Lipids* **26,** 1445-9

Horrocks LA (1972) Content, composition and metabolism of mammalian and avian lipids that contain ether groups. In: *Ether Lipids: Chemistry and Biology.* (Snyder F, ed), pp. 177-272, Academic Press, New York.

Hordijik PL, Verlaan I, Jalink K, van Corven EJ, Moolenaar WH **(1994)** cAMP abrogates the $p21^{ras}$-mitogen-activated protein kinase pathway in fibroblasts. *J. Biol. Chem.* **269,** 3534-8

Hordijik PL, Verlaan I, Jalink K, van Corven EJ, Moolenaar WH **(1994a)** Protein tyrosine phsophorylation induced by lysophosphatidic acid in rat-1 fibroblasts. Evidence that phosphorylation of MAP kinase is mediated by the G_i-$p21^{ras}$ pathway. *J. Biol. Chem.* **269,** 645-51

Houlihan WJ, Lohmeyer M, Workman P, Cheon SH **(1995)** Phospholipid antitumor agents. *Med. Res. Rev.* **15,** 157-223

Howard BV, Howard WJ **(1975)** Lipids in normal and tumor cells in culture. *Progr. Biochem. Pharmacol.* **10,** 135-66

Howard BV, Morris HP, Bailey M **(1972)** Ether-lipids, α-glycerol phosphate dehydrogenase, and growth rate in tumors and cultured cells. *Cancer Res.* **32,** 1533-8

Howe LR, Leevers SJ, Gomez N, Nakielny S, Cohen P, Marshall CJ **(1992)** Activation of the MAP kinase pathway by the protein kinase raf. *Cell* **71,** 335-42

Hu C-D, Kariya K, Tamada M, Akasaka K, Shirouzu M, Yokoyama S, Kataoka T **(1995)** Cysteine-rich region of Raf-1 interacts with activator domain of post-translationally modified Ha-Ras. *J. Biol. Chem.* **270,** 30274-7

Hu Q, Klippel A, Muslin AJ, Fantl WJ, Williams LT **(1995)** Ras-dependent induction of cellular responses by constitutively active phosphatidylinositol-3 kinase. *Science* **268,** 100-2

Huang DCS, Marshall CJ, Hancock JF **(1993)** Plasma membrane-targeted *ras*GTPase-activating protein is a potent suppressor of $p21^{ras}$ function. *Mol. Cell. Biol.* **13,** 2420-31

Hug H, Sarre TF **(1993)** Protein kinase C isoenzymes: divergence in signal transduction? *Bioehm. J.* **291,** 329-43

Huleihel M, Goldsborough M, Cleveland JL, Gunnell M, Bonner T, Rapp UR **(1986)** Characterization of murine A-raf, a new oncogene related to the v-raf oncogene. *Mol. Cell. Biol.* **6,** 2655-62

Hunter T (1995) Protein kinases and phosphatases: the ying and yang of protein phosphorylation and signaling. *Cell* **80,** 225-36

Huwlier A, Brunner J, Hummel R, Vervoordeldonk M, Stabel S, Van Den Bosch H, Pfeilschifter J **(1996)** Ceramide-binding and activation defines protein kinase c-Raf as a ceramide-activated protein kinase. *Proc. Natl. Acad. Sci. USA* **93,** 9659-63

Hynes RO (1994) The impact of molecular biology on models for cell adhesion. *BioEssays* **16,** 663-9

Ichijo H, Nishida E, Irie K, ten Dijke P, Saitoh M, Moriguchi T, Takagi M, Matsumoto K,

Miyazono K, Gotoh Y **(1997)** Induction of apoptosis by ASK1, a mammalian MAPKKK that activates SAPK/JNK and p38 signaling pathway. *Science* **275,** 90-4

Inglese J, Koch WJ, Touhara K, Lefkowtiz RJ **(1995)** $G_{\beta\gamma}$ interactions with PH domains and Ras-MAPK signalling pathway. *Trends Biochem. Sci.* **20,** 151-6

Irie K, Gotoh Y, Yashar BM, Errede B, Nishida E, Matsumoto K **(1994)** Stimulatory effects of yeast and mammalian 14-3-3 proteins on the Raf protein kinase. *Science* **265,** 1716-9

Irvine RF (1991) Inositol tetrakisphosphate as a second messenger: confusions, contradictions, and a potential resolution. *BioEssays* **13,** 419-27

Irvine RF, Cullen PJ **(1993)** Will the real IP_4 receptor please stand up? *Curr. Biol.* **3,** 540-3

Ishidate K (1989) Choline transport and choline kinase. In: *Phosphatidylcholine Metabolism.* (Vance DE, ed.) pp. 9-32, CRC Press, Boca Raton, FL.

Ivashkiv LB, Liou HC, Kara CJ, Lamph WW, Verma IM, Glimcher LH **(1990)** mXBP/CRE-BP2 and c-Jun form a complex which binds to the cyclic AMP, but not to the 12-*O*-tetradecanoylphorbol-13-acetate, response element. *Mol. Cell. Biol.* **10,** 1609-21

Jackowski S (1994) Coordination of membrane phospholipid synthesis with the cell cycle. *J. Biol. Chem.* **269,** 3858-67

Janknecht R, Ernst WH, Pingoud V, Nordheim A **(1993)** Activation of ternary complex factor Elk-1 by MAP kinases. *EMBO J.* **12,** 5097-104

Jayadev S, Liu B, Bielawsha AE, Lee JY, Nazaire F, Pushkareva MY, Obeid LM, Hannun YA **(1995)** Role for ceramide in cell cycle arrest. *J. Biol. Chem.* **270,** 2047-52

Jiang Y, Chen C, Li Z, Guo W, Gegner JA, Shengcai L, Han J **(1996)** Characterization of the structure and function of a new mitogen-activated protein kinase (p38β). *J. Biol. Chem.*

271, 17920-6

John J, Sohmen R, Feuerstein J, Linke R, Wittinghofer A, Goody RS **(1990)** Kinetics of interaction of nucleotides with nucleotide-free H-ras p21. *Biochemistry* **29,** 6058-65

Johnson MR, DeClue JE, Felzmann S, Vass W, Xu G, White R, Lowy DR **(1994)** Neurofibromin can inhibit Ras-dependent growth by a mechanism independent of its GTPase-accelerating function. *Mol. Cell. Biol.* **14,** 641-5

Kamb A (1995) Cell-cycle regulation and cancer. *Trends Genetics* **11,** 136-40

Kato S, Endoh H, Masuhiro Y, Kitamoto T, Uchiyama S, Sasaki H, Masushigo S, Gotoh Y, Nishida E, Kawashima H, Metzger D, Chambon P **(1995)** Activation of the estrogen receptor through phosphorylation by mitogen-activated protein kinase. *Science* **270,** 1491-4

Kennedy EP (1989) Discovery of the pathways for the biosyntheis of phosphatidylcholine. In: *Phosphatidylcholine Metabolism* (Vance DE, ed.) pp. 1-9, CRC press, Boca Raton, FL.

Kharbanda S, Saleem A, Emoto Y, Stone R, Rapp U, Kufe D **(1994)** Activation of Raf-1 and mitogen-activated protein kinases during monocytic differentiation of human myeloid leukemia cells. *J. Biol. Chem.* **269,** 872-8.

Kikuchi A, Williams LT **(1996)** Regulation of interaction of *ras* p21 with RalGDS and Raf-1 by cyclic AMP-dependent protein kinase. *J. Biol. Chem.* **271,** 588-94

King M-T, Eckhardt K, Gocke E, Wild D, Berdel WE, Munder PG **(1981)** Failure to detect mutagenic effects of anti-tumor alkyl-lysophospholipids. *Cancer Lett.* **12,** 217-22

Kiss Z, Anderson WB **(1989)** Phorbol ester stimulates the hydrolysis of phosphatidylethanolamine in leukemic HL-60, NIH 3T3, and baby hamster kidney cells. *J. Biol. Chem.* **264,** 1483-7

Kiss Z, Anderson WB **(1990)** ATP stimulates the hydrolysis of phosphatidylethanolamine in NIH 3T3 cells. Potentiating effects of guanosine triphosphates and sphingosine. *J. Biol. Chem.* **265,** 7345-50

Kiss Z, Deli E, Vogler WR, Kuo JF **(1987)** Antileukemic agent alkyllysophospholipid regulates phosphorylation of distinct proteins in HL60 and K562 cells and differentiation of HL60 cells promoted by phorbol ester. *Biochem. Biophys. Res. Commun.* **142,** 661-6

Kitayama H, Sugimoto Y, Matsuzaki T, Ikawa Y, Noda M **(1989)** A ras-related gene with transformation suppressor activity. *Cell* **56,** 77-84

Koide H, Satoh Y, Nakafuku M, Kaziro Y **(1993)** GTP-dependent association of Raf-1 with Ha-Ras: identification of Raf as a target downstream of Ras in mammalian cells. *Proc. Natl. Acad. Sci USA* **90,** 8683-6

Kolch W, Heidecker G, Kochs G, Hummel R, Vahidi H, Mischak H, Finkenzeller G, Marmé D, Rapp UR **(1993)** Protein kinase Cα activates RAF-1 by direct phosphorylation. *Nature* **364,** 249-52

Kolesnick RN (1991) Sphingomyelin and derivatives as cellular signals. *Prog. Lipid Res.* **30,** 1-38

Kolesnick RN, Golde DW **(1994)** The sphingomyelin pathway in tumor necrosis factor and interleukin-1 signaling. *Cell* **77,** 325-8

Kornfeld K, Hom DB, Horvitz HR **(1995)** The *ksr-1* gene encodes a novel protein kinase involved in Ras-mediated signaling in C. elegans. *Cell* **83,** 903-13

Kortenjann M, Thomae O, Shaw PE **(1994)** Inhibition of v-*raf*-dependent c-*fos* expression and transformation by kinase-defective mutant of the mitogen-activated protein kinase Erk

2. *Mol. Cell. Biol.* **14,** 4815-24

Kosano H, Takatani O **(1988)** Reduction of epidermal growth factor binding in human breast cancer cell lines by an alkyl-lysophospholipid. *Cancer Res.* **48,** 6033-6

Kosano H, Takatani O **(1989)** Inhibition by an alkyl-lysophospholipid of the uptake of epidermal growth factor in human breast cancer cell lines in relation to epidermal growth factor internalization. *Cancer Res.* **49,** 2868-70

Kramer RM, Roberts EF, Strifler BA, Johnstone EM **(1995)** Thrombin induces activation of p38 MAP kinase in human platelets. *J. Biol. Chem.* **270,** 27395-8

Krontiris TG, Cooper GM **(1981)** Transforming activity of human tumour DNAs. *Proc. Natl. Acad. Sci. USA* **78,** 1181-4

Kudo I, Nojima S, Chang HW, Yanoshita R, Hayashi H, Kondo E, Nomura H, Inoue K **(1987)** Antitumor activity of synthetic alkylphospholipids with or without PAF activity. *Lipids* **22,** 862-7

Kwok RPS, Lundblad JR, Chrivia JC, Richards JP, Bachinger HP, Brennan RG, Roberts SG, Green MR, Goodman RH **(1994)** Nuclear protein CBP is a coactivator for the transcription factor CREB. *Nature* **370,** 223-6

Kyriakis JM, App H, Zhang X-F, Banerjee P, Brautigan DL, Rapp UR, Avruch J **(1992)** Raf-1 activates MAP kinase-kinase. *Nature* **358,** 417-21

Kyriakis JM, Banerjee P, Nikolakaki E, Dai T, Rubie EA, Ahmad MF, Avruch J, Woodgett JR **(1994)** The stress-activated protein kinase subfamily of c-Jun kinases. *Nature* **369,** 156-60

Laemmli UK (1970) Cleavage of structural proteins during the assembly of the head of bacteriophase T4. *Nature* **227,** 680-5

Lam K, Carpenter CL, Ruderman NB, Friel JC, Kelly KL **(1994)** The phosphatidylinositol 3-kinase serine kinase phosphorylates IRS-1. Stimulation by insulin and inhibition by wortmannin. *J. Biol. Chem.* **269,** 20648-52

Lamb P, Crawford LV **(1986)** Characterization of the human p53 gene. *Mol. Cell. Biol.* **6,** 1379-85

Lange-Carter CA, Pleiman CM, Gardner AM, Blumer KJ, Johnson GL **(1993)** A divergence in the MAP kinase regulatory network defined by MEK kinase and Raf. *Science* **260,** 315-9

Langlois WJ, Sasaoka T, Saltiel AR, Olefsky JM **(1995)** Negative feedback regulation and desensitization of insulin- and epidermal growth factor-stimulated $p21^{ras}$ activation. J. Biol. Chem. **270,** 25320-3

Lavoie JN, L'Allemain G, Brunet A, Müller R, Pouyssegur J **(1996)** Cyclin D1 expression is regulated positively by the $p42/44^{MAPK}$ and negatively by the $p38/HOG^{MAPK}$ pathway. *J. Biol. Chem.* **271,** 20608-16

Lavoinne A, Erikson E, Maller JL, Price DJ, Avruch J, Cohen P **(1991)** Purification and characterisation of the insulin-stimulated protein kinase from rabbit skeletal muscle; close similarity to S6 kinase II. *Eur. J. Biochem.* **199,** 723-8

Lazenby CM, Thompson MG, Hickman JA **(1990)** Elevation of leukemic cell intracellular calcium by the ether lipid SRI 62-834. *Cancer Res.* **50,** 3327-30

Lechner C, Zahalka MA, Giot JF, Moller NPH, Ullrich A **(1996)** ERK6, a mitogen-activated protein kinase involved in C2C12 myoblast differentiation. *Proc. Natl. Acad. Sci. USA* **93,** 4355-9

Lee MS, Ogg S, Xu M, Parker LL, Donoghue DJ Maller JL, Piwnica-Worms H **(1992)** cdc25^{-} encodes a protein phosphatase that dephosphorylates p34^{cdc2}. *Mol. Biol. Cell* **3,** 73-84

Lee RM, Cobb MH, Blackshear PJ **(1992)** Evidence that extracellular signal-regulated kinases are the insulin-activated Raf-1 kinase kinases. *J. Biol. Chem.* **267,** 1088-92

Leevers SJ, Paterson HF, Marshall CJ **(1994)** Requirement for Ras in Raf activation is overcome by targeting Raf to the plasma membrane. *Nature* **369,** 411-4

Li B-Q, Kaplan D, Kung H, Kamata T **(1992)** Nerve growth factor stimulation of the Ras-guanine nucleotide exchange factor and GAP activities. *Science* **256,** 1456-9

Li N, Bastzer A, Daly R, Yajnik V, Skolnik E, Chardin P, Bar-Sagi D, Morgolis B, Schlessinger J **(1993)** Guanine-nucleotide-releasing factor hSos1 binds to Grb2 and links receptor tyrosine kinases to Ras signalling. *Nature* **363,** 85-8

Li W, Nishimura R, Kashishian A, Batzer AG, Kim WJH, Cooper JA, Schlessinger J **(1994)** A new function for a phosphotyrosine phosphatase: linking GRB2-Sos to a receptor tyrosine kinase. *Mol. Cell. Biol.* **14,** 509-17

Lin A, Minden A, Martinetto H, Claret F-X, Lange-Carter C, Mercurio F, Johnson GL, Karin M **(1995)** Identification of a dual specificity kinase that activates the Jun kinases and p38-Mpk2. *Science* **268,** 286-90

Lin LL, Wartmann M, Lin AY, Knopf JL, Seth A, Davis RJ **(1993)** cPLA$_2$ is phosphorylated and activated by MAP kinase *Cell* **72,** 269-78

Liou H-C, Baltimore D **(1993)** Regulation of the NFκB/rel transcription factor and IκB inhibitor system. *curr. Opin. Cell Biol.* **5,** 477-87

Liscovitch M (1992) Crosstalk among multiple signal-activated phospholipases. *Trends*

Biochem. Sci. **17,** 393-9

Liscovitch M, Cantley LC **(1994)** Lipid second messengers. **77,** 329-34

Lohmeyer M, Bittman R **(1994)** Antitumor ether lipids and alkylphosphocholines. *Drugs Future* **19,** 1021-37

Lohmeyer M, Workman P **(1992)** Antitumour ether lipids and platelet-activating factor analogues have different cytotoxic profiles and calcium mobilizing effects - a structure-activity study. In: *Eicosanoids and Other Bioactive Lipids in Cancer, Inflammation and Radiation Injury.* (Nigam S, Honn KV, Marnett LJ, Walden TL, eds.)pp. 699-702, Kluwer Academic Publishers, Boston, USA

Lohmeyer M, Workman P **(1993)** The role of intracellular free calcium mobilization in the mechanism of action of antitumour ether lipids SRI 62-834 and ET18-OMe. *Biochem. Pharmacol.* **45,** 77-86

Lopez-llasaca M, Crespo P, Pellici PG, Gutkind JS, Wetzker R **(1997)** Linkage of G protein-coupled receptors to the MAPK signaling pathway through PI 3-kinase γ. *Science* **275,** 394-7

Lowry OH, Rosebrough NJ, Farr AL, Randall RJ **(1951)** Protein measurement with the Folin phenol reagent. *J. Biol. Chem.* **193,** 265-75

Lowy DR, Willumsen BM **(1993)** Function and regulation of Ras. *Annu. Rev. Biochem.* **62,** 851-91

Lozano J, Berra E, Municio MM, Diaz-Meco MT, Domiguez I, Sanz L, Moscat J **(1994)** Protein kinase C ζ isoform is critical for κB-dependent promoter activation by sphingomyelinase. *J. Biol. Chem.* 19200-2

Lu X, Arthur G **(1992a)** Perturbations of cellular acylation processes by the synthetic alkylysophopholipid 1-*O*-octadecyl-2-*O*-methylglycero-3-phosphocholine do not correlate with inhibition of proliferation of MCF7 and T84 cell lines. *Cancer Res.* **52,** 2806-12

Lu X, Arthur G **(1992b)** The differential susceptibility of A427 and A549 cell lines to the growth-inhibitory effects of ET-18-OCH_3 does not correlate with the relative effects of the alkyl-lysophopholipid on the incorporation of fatty acids into cellular phospholipids. *Cancer Res.* **52,** 2813-7

Lu X, Rengan K, Bittman R, Arthur G **(1994)** The α and β anomers of 1-*O*-headecyl-2-*O*-methyl-3-*S*-thioglucosyl-*sn*-glycerol inhibit the proliferation of epithelial cancer cell lines. *Oncology Reports* **1,** 933-6

Ludwig S, Engel K, Hoffmeyer A, Sithanandam G, Neufeld B, Palm D, Gaestel M, Rapp UR **(1996)** 3pK, a novel mitogen-activated protein (MAP) kinase-activated protein kinase, is targeted by three MAP kinase pathways. *Mol. Cell. Biol.* **16,** 6687-97

Luo Z, Tzivion G, Belshaw PJ, Vavvas D, Marshall M, Avruch J **(1996)** Oligomerization activates c-Raf-1 through a Ras-dependent mechanism. *Nature* **383,** 181-5

Macgregor PF, Abate C, Curran T **(1990)** Direct cloning of leucine zipper proteins: Jun binds cooperatively to the CRE with CRE-BP1. *Oncogene* **5,** 451-8

Malarkey K, Belham CM, Paul A, Graham A, McLees A, Scott P, Plevin R **(1995)** The regulation of tyrosine kinase signalling pathways by growth factor and G-protein-coupled receptors. *Biochem. J.* **309,** 361-75

Marais R, Light Y, Paterson HF, Marshall CJ **(1995)** Ras recruits Raf-1 to the plasma membrane for activation by tyrosine phosphorylation. *EMBO J.* **14,** 3136-45

Marais R, Wynne J, Treisman R **(1993)** The SRF accessory protein Elk-1 contains a growth factor-regulated transcriptional activition domain. *Cell* **73,** 381-93

Margolis B, Franks ZC, Felder S, Kremer S, Ullrich A, Rhee SG, Skorecki K, Schlessinger J **(1990)** Effect of phospholipase C-γ overexpression on PDGF-induced second messengers and mitogenesis. *Science* **248,** 607-10

Martin GA, Viskochil D, Bollag G, McCabe PC, Crosier WJ, Haubruck H, Conroy L, Clark R, O'Connell P, Cawthon RM, Innis MA, McCormick F **(1990)** The gap-related domain of the neurofibromatosis type I gene product interacts with ras p21. *Cell* **63,** 843-9

Marshall CJ (1994) MAP kinase kinase kinase, MAP kinase kinase and MAP kinase. *Curr. Opin. Genet. Dev.* **4,** 82-9

Marshall CJ (1995) Specificity of receptor tyrosine kinase signaling: transient versus sustained extracellular signal-regulated kinase activation. *Cell* **80,** 179-85

Marshall CJ (1996) Raf gets it together. *Nature* **383,** 127-8

Marshall MS (1993) The effector interaction of $p21^{ras}$. *Trends Biochem. Sci.* **18,** 250-4

Martelli AM, Gilmour RS, Bertagnoto V, Neri LM, Manzoli L, Cocco L **(1992)** Nuclear localization and signalling activity of phosphoinositidase C_β in Swiss 3T3 cells. *Nature* **358,** 242-5

Marx J (1993) Two major signal pathways linked. *Science* **262,** 988-90

Matsuda S, Gotoh Y, Nishida E **(1993)** Phosphorylation of Xenopus mitogen-activated protein (MAP) kinase kinase by MAP kinase kinase kinase and MAP kinase. *J. Biol. Chem.* **268,** 3277-81

Matsudaira PT, Burgess DR **(1978)** SDS microslab linear gradient polyacrylamide gel

electrophoresis. *Anal. Biochem.* **87,** 386-96

Maurer HR, Hilgard P **(1992)** Induction of tumor cell differentiation by alkylphosphocholines: a new approach for *in vitro* screening. *Prog. Exp. Tumor Res.* **34,** 90-7

McLaughlin S, Aderem A **(1995)** The myristoyl-electrostatic switch: a modulator of reversible protein-membrane interactions. *Trends Biochem. Sci.* **20,** 272-6

Melchior DL, Carruthers A, Makriyannis A, Duclos Jr RI, Abdel-Mageed OH **(1990)** Alterations in red blood cell sugar transport by nanomolar concentrations of alkyl lysophospholipid. *Biochim. Biophys. Acta* **1028,** 1-8

Menniti FS, Oliver KG, Putney Jr JW, Shears SB **(1993)** Inositol phosphates and cell signaling: new views of InsP_5 and InsP_6. *Trends Biochem. Sci.* **18,** 53-6

Mertens S, Craxton M, Goedert M **(1996)** SAP kinase-3, a new member of the family of mammalian stree-activated protein kinases. *FEBS Lett.* **383,** 273-6

Michaud NR, Fabian JR, Mathes KD, Morrison DK **(1995)** 14-3-3 is not essential for Raf-1 function: identification of Raf-1 proteins that are biologically activated in a 14-3-3- and Ras-independent manner. *Mol. Cell. Biol.* **15,** 3390-7

Michell RH (1992a) Inositol lipids in cellular signalling mechanisms. *Trends Biochem. Sci.* **17,** 274-6

Michell RH (1992b) Nuclear PIPs. *Curr. Biol.* **2,** 200-2

Milligan G, Parenti M, Magee AI **(1995)** The dynamic role of palmitoylation in signal transduction. *Trends Biochem. Sci.* **20,** 181-6

Minden A, Lin A, McMahon M, Lange-Carter C, Dérijard B, Davis RJ, Johnson GL, Karin M **(1994)** Differential activation of ERK and JNK mitogen-activated protein kinases by Raf-

1 and MEKK. *Science* **266,** 1719-23

Mischak H, Pierce JH, Goodnight J, Kazanietz MG, Blumberg PM, Mushinski JF **(1993)** Phorbol ester-induced myeloid differentiation is mediated by protein kinase C-α and -δ and not by protein kinase C-βII, -ϵ, -ζ, and -η. *J. Biol. Chem.* **268,** 20110-5

Mittal R, Ahmadian MR, Goody RS, Wittinghofer A **(1996)** Formation of a transition-state analog of the Ras GTPase reaction by Ras-GDP, tetrafluoroaluminate, and GTPase-activating proteins. *Science* **273,** 115-7

Modollel M, Andreesen R, Pahlke W, Brugger U, Mender PG **(1979)** Disturbance of phospholipid metabolism during the selective destruction of tumor cells induced by alkyllysophospholipids. *Cancer Res.* **39,** 4681-6

Mohammadi M, Dionne CA, Li W, Li N, Spivak T, Honegger AM, Jaye M, Schlessinger J **(1992)** Point mutation in FGF receptor eliminates phosphatidylinositol hydrolysis without affecting mitogenesis. *Nature* **358,** 681-4

Mollinedo F, Martinez-Dalmau R, Modolell M **(1993)** Early and selective induction of apoptosis in human leukemic cells by the alkyl-lysophopholipid ET-18-OCH_3. *Biochem. Biophys. Res. Commun.* **192,** 603-9

Moolenaar WH (1995) Lysophosphatidic acid, a multifunctional phospholipid messenger. *J. Biol. Chem.* **270,** 12949-52

Moriboto H, Broquet C, Principe P, Mencia-Huerta JM, Barquet P, Bonavida B **(1991)** Cytotoxic activity of synthetic aza alkyl lysophospholipids against drug sensitive and drug resistant human tumor cell lines. *Anticancer Res.* **11,** 2223-30

Morrison DK, Cutler Jr RE **(1997)** The complexity of Raf-1 regulation. *Curr. Opin. Cell Biol.* **9,** 174-9

Morrison DK, Heidecker G, Rapp UR, Copeland TD **(1993)** Identification of the major phosphorylation sites of the Raf-1 kinase. *J. Biol. Chem.* **268,** 17309-16

Mosior M, Epand RM **(1993)** Mechanism of activation of protein kinase C: roles of diolein and phosphatidylserine. *Biochemistry* **32,** 66-75

Mott HR, Carpenter JW, Zhong S, Ghosh S, Bell RM, Campbell SL **(1996)** The solution structure of the Raf-1 cysteine-rich domain: a novel Ras and phospholipid binding site. *Proc. Natl. Acad. Sci USA* **93,** 8312-7

Munder PG, Modolell M, Bausert W, Oettgen HE, Westphal O **(1981)** Alkyllysophospholipids in cancer therapy. In: *Augmenting Agents in Cancer Therapy* (Hersh EM, ed.) pp. 441-58, Raven Press, New York

Munder PG, Modolell M, Ferber E, Fischer H **(1966)** Phospholipoide in quarzgeschädigten Makrophagen. *Biochem. Z.* **344,** 310-3

Munder PG, Weltzien HU, Modolell M **(1977)** Lysolecithin analogs: a new class of immunopotentiators. *Immunopathology* **7,** 411-24

Murray NR, Baumgardner GP, Burns DJ, Fields AP **(1993)** Protein kinase C isotypes in human erythroleukemia (K562) cell proliferation and differentiation: evidence that β_{II} protein kinase C is required for proliferation. *J. Biol. Chem.* **268,** 15847-53

Muslin AJ, Tanner JW, Allen PM, Shaw AS **(1996)** Interaction of 14-3-3 with signaling proteins is mediated by the recognition of phosphoserine. *Cell* **84,** 889-97

Nakajima T, Kinoshita S, Sasagawa T, Sasaki K, Naruto M, Kishimoto T, Akira S **(1993)** Phosphorylation at threonine-235 by a ras-dependent mitogen-activated protein kinase cascade is essential for transcription factor NF-IL6. *Proc. Natl. Acad. Sci. USA* **90,** 2207-11

Nakamura M, Onodera T and Akino T **(1980)** Characteristics of phospholipids in human lungcarcinoma. *Lipids* **15,** 616-23

Nakanishi H, Brewer KA, Exton JH **(1993)** Activation of the ζ isozyme of protein kinase C by phosphatidylinositol 3,4,5-trisphosphate. *J. Biol. Chem.* **268,** 13-6

Nassar N, Horn G, Herrmann C, Scherer A, McCormick F, Wittinghofer A **(1995)** The 2.2 Å crystal structure of the Ras-binding domain of the serine/threonine kinase c-Raf1 in complex with Rap1A and a GTP analogue. *Nature* **375,** 554-60

Nebreda AR (1994) Inactivation of MAP kinases. *Trends Biochem. Sci.* **19,** 1-2

Nemenoff RA, Winitz S, Qian N-X, Van Putten V, Johnson GL, Heasley LE **(1993)** Phosphorylation and activation of a high molecular weight form of phospholipase A_2 by p42 microtubule-associated protein 2 kinase and protein kinase C. *J. Biol. Chem.* **268,** 1960-4

Nesterov A, Kurten RC, Gill GN **(1995)** Association of epidermal growth factor receptors with coated pit adaptins via a tyrosine phosphorylation-regulated mechanism. *J. Biol. Chem.* **270,** 6320-7

Newton AC (1995) Protein kinase C: structure, function, and regulation. *J. Biol. Chem.* **270,** 28495-8

Newton AC (1997) Regulation of protein kinase C. *Curr. Opin. Cell Biol.* **9,** 161-7

Nicholson NB, Chen S, Blanck G, Pollack R **(1984)** SV40 transformation of Swiss 3T3 cells can cause a stable reduction in the calcium requirement for growth. *J. Cell Biol.* **99,** 2314-21

Nigg EA (1992) Assembly and cell cycle dynamics of the nuclear lamina. *Semin. Cell Biol.* **3,** 245-53

Nishida E, Gotoh Y **(1992)** Mitogen-activated protein kinase and cytoskeleton in mitogenic signal transduction. *Int. Rev. Cytol.* **138,** 211-38

Nishida E, Gotoh Y **(1993)** The MAP kinase cascade is essential for diverse signal transduction pathways. *Trends Biochem. Sci.* **18,** 128-31

Nishizuka Y (1995) Protien kinase C and lipid signaling for sustained cellular responses. *FASEB J.* **9,** 484-96

Nishizuka Y (1992) Intracellular signaling by hydrolysis of phospholipids and activation of protein kinase C. *Science* **258,** 607-14

Noda M (1993) Structures and functions of the K rev-1 transformation suppressor gene and its relatives. *Biochim. Biophys. Acta* **1155,** 97-109

Northwood IC, Gonzalez FA, Wartmann M, Raden DL, Davis RJ **(1991)** Isolation and characterization of two growth factor-stimulated protein kinases that phosphorylate the epidermal growth factor receptor at threonine 669. *J. Biol. Chem.* **266,** 15266-76

Noseda A, Berens ME, Piantadosi C, Modest E **(1987)** Neoplastic cell inhibition with new ether lipid analogues. *Lipids* **22,** 878-83

Noseda A, White JG, Godwin PL, Jerome WG, Modest EJ **(1989)** Membrane damage in leukemic cells induced by ether and ester lipids: an electron microscopic study. *Exp. Mol. Pathol.* **50,** 69-83

Obeid LM, Hannun YA **(1995)** Ceramide: a stress signal and mediator of growth suppression and apoptosis. *J. Cell. Biochem.* **58,** 191-8

Okabayashi Y, Kido Y, Okutani T, Sugimoto Y, Sakaguchi K, Kasuga M **(1994)** Tyrosines 1148 and 1173 of activated human epidermal growth factor receptors are binding sites of Shc in intact cells. *J. Biol. Chem.* **269,** 18674-8

Okutani T, Okabayashi Y, Kido Y, Sugimoto Y, Sakaguchi K, Matuoka K, Takenawa T, Kasuga M **(1994)** Grb2/Ash binds directly to tyrosines 1068 and 1086 and indirectly to tyrosine 1148 of activated human epidermal growth factor receptors in intact cells. *J. Biol. Chem.* **269,** 31310-4

Orr JW, Newton AC **(1992a)** Interaction of protein kinase C with phosphatidylserine. 1. Cooperativity in lipid binding. *Biochemistry* **31,** 4661-7

Orr JW, Newton AC **(1992b)** Interaction of protein kinase C with phosphatidylserine. 2. Specificity and regulation. *Biochemistry* **31,** 4667-73

Pagès G, Lenormand P, L'Allemain G, Chambard JC, Meloche S, Pouyssegur J **(1993)** Mitogen-activated protein kinases $p42^{mapk}$ and $p44^{mapk}$ are required for fibroblast proliferation. *Proc. Natl. Acad. Sci. USA* **90,** 8319-23

Pan M-G, Wang Y-H, Hirsch DD, Labudda K, Stork PJS **(1995)** The Wnt- proto-oncogene regulates MAP kinase activation by multiple growth factors in PC12 cells. *Oncogene* **11,** 2005-12

Panayotou G, Waterfield MD **(1993)** The assembly of signalling complexes by receptor tyrosine kinases. *BioEssays* **15,** 171-7

Pandey A, Duan H, Fiore PPD, Dixit VM **(1995)** The Ret receptor protein tyrosine kinase associates with the SH2-containing adapter protein Grb10. *J. Biol. Chem.* **270,** 21461-3

Park RK, Liu Y, Durden DL **(1996)** A role for Shc, Grb2, and Raf-1 in FcγRI signal relay.

J. Biol. Chem. **271,** 13342-8

Parker PJ, Waterfield MD **(1992)** Phosphatidylinositol 3-kinase: a novel effector. *Cell Growth & Differ.* **3,** 747-52

Pawelczyk T, Lowenstein JM **(1993)** Inhibition of phospholipase C delta by hexadecylphosphorylcholine and lysophospholipids with antitumor activity. *Biochem. Pharmacol.* **45,** 493-7

Pawson T (1995) Protein modules and signalling networks. *Nature* **373,** 573-80

Pelech SL, Sanghera JS **(1992)** Mitogen-activated protein kinases: versatile transducers for cell signaling. *Trends Biochem. Sci.* **17,** 233-8

Pelech SL, Vance DE **(1989)** Signal transduction via phosphatidylcholine cycles. *Trends Biochem. Sci.* **14,** 28-30

Peters KG, Marie J, Wilson E, Ives HE, Escobedo J, Rosario MD, Mirda D, Williams LT **(1992)** Point mutation of an FGF receptor abolishes phosphatidylinositol turnover and Ca^{2+} flux but not mitogenesis. *Nature* **358,** 678-81

Peter M, Sanghera JS, Pelech SL, Nigg EA **(1992)** Mitogen-activated protein kinases phosphorylate nuclear lamins and display sequence specificity overlapping that of mitotic protein kinase $p34^{cdc2}$. *Eur. J. Biochem.* **205,** 287-94

Piazza GA, Ritter JL, Baracka CA **(1995)** Lysophosphatidic acid induction of transforming growth factor α and β: modulation of proliferation and differentiation in cultured human keratinocytes and mouse skin. *Exp. Cell Res.* **216,** 51-64

Plotzke KP, Haradahira T, Stancato L, Olken NM, Skinner S, Gross MD, Wahl RL, Counsell RE **(1992)** Selective localization of radioiodinated alkylphosphocholine derivatives

in tumors. *Int. J. Radiat. Appl. Instrument. Part B, Nucl. Med. Biol.* **19,** 765-73

Polakis PT, McCormick F **(1993)** Structural requirements for the interaction of $p21^{ras}$ with GAP, exchange factors, and its biological effector target. *J. Biol. Chem.* **268,** 9157-60

Porter TJ, Kent C **(1992)** Choline/ethanolamine kinase from rat liver. *Methods Enzymol.* **209,** 134-46

Posada J, Cooper JA **(1992)** Requirements for phosphorylation of MAP kinase during meiosis in Xenopus oocytes. *Science* **255,** 212-5

Posada J, Cooper JA **(1992a)** Molecular signal integration. Interplay between serine, threonine, and tyrosine phosphorylation. *Mol. Biol. Cell* **3,** 583-92

Posada J, Yew N, Ahn NG, Vande Woude GF, Cooper JA **(1993)** Mos stimulates MAP kinase in *Xenopus* oocytes and activates a MAP kinase kinase in vitro. *Mol. Cell. Biol.* **13,** 2546-53

Powis G (1991) Signalling targets for anticancer drug development. *Trends Pharmacol. Sci.* **12,** 188-94

Powis G, Seewald MJ, Gratas C, Melder D, Riebow J, Modest EJ **(1992a)** Selective inhibition of phosphatidylinositol phospholipase C by cytotoxic ether lipid analogues. *Cancer Res.* **52,** 2835-40

Powis G, Seewald MJ, Riebow J, Gratas C, Modest E **(1992b)** Ether lipid antitumor agents inhibit phosphatidylinositol phospholipase C. In: *Eicosanoids and Other Bioactive Lipids in Cancer, Inflammation and Radiation Injury.* (Nigam S, Honn KV, Marnett LJ, Walden TL, eds.), pp 699-702, Kluwer Academic Publishers, Boston, MA

Principe P, Braquet P **(1995)** Advances in ether phospholipids treatment of cancer. *Crit.*

Rev. Oncol. Hematol. **18,** 155-78

Pulverer BJ, Kyriakis JM, Avruch J, Nikolakaki E, Woodgett JR **(1991)** Phosphorylation of c-jun mediated by MAP kinases. *Nature* **353,** 670-4

Ralph RK, Darkin-Rattray S, Schofield P **(1990)** Growth related protein kinases. *BioEssays* **12,** 121-4

Rao VN, Reddy SP **(1994)** elk-1 proteins interact with MAP kinases. *Oncogene* **9,** 1855-60

Rapp UR, Heidecker G, Huleihel M, Cleveland JL, Choi WC, Pawson T, Ihle JN, Anderson WB **(1988)** *raf* family serine/threonine protein kinases in mitogen signal transduction. *Cold Spring Harbor Symp. Quant. Biol.* **53,** 173-84

Reszka AA, Seger R, Diltz CD, Krebs EG, Fischer EH **(1995)** Association of mitogen-activated protein kinase with the microtubule cytoskeleton. *Proc. Natl. Acad. Sci. USA* **92,** 8881-5

Rhee SG, Choi KD **(1992)** Regulation of inositol phospholipid-specific phospholipase C isozymes. *J. Biol. Chem.* **267,** 12393-6

Ridgway ND (1989) Phosphatidylethanolamine *N*-methyltransferase. In: *Phosphatidylcholine Metabolism* (Vance DE, ed.) pp. 103-20, CRC Press, Boca Raton, FL.

Ridley AJ, Hall A **(1992)** The small GTP-binding protein rho regulates the assembly of focal adhesions and actin stress fibers in response to growth factors. *Cell* **70,** 389-99

Rivera VM, Miranti CK, Misra RP, Ginty DD, Chen RH, Blenis J, Greenberg ME **(1993)** A growth factor-induced kinase phosphorylates the serum response factor at a site that regulates its DNA-binding activity. *Mol. Cell. Biol.* **13,** 6260-73

Robert JM, Mandel P, Rebel G **(1976)** Neutral lipids and phospholipid from cultured

astroblasts. *J. Neurochem.* **26,** 771-7

Robertson LM, Kerppola TK, Vendrell M, Luk D, Smeyne RJ, Bocchiaro C, Morgan JI, Curran T **(1995)** Regulation of c-fos expression in transgenic mice requires multiple interdependent transcription control elements. *Neuron* **14,** 241-52

Robinson MJ, Cheng M, Khokhlatchev A, Ebert D, Ahn N, Guan KL, Stein B, Goldsmith E, Cobb MH **(1996)** Contributions of the mitogen-activated protein (MAP) kinase backbone and phosphorylation loop to MEK specificity. *J. Biol. Chem.* **271,** 29734-40

Robinson MJ, Cobb MH **(1997)** Mitogen-activated protein kinase pathways. *Curr. Opin. Cell Biol.* **9,** 180-6

Rodriguez-Viciana P, Warne PH, Dhand R, Vanhaesebroeck B, Gout I, Fry MJ, Waterfield MD, Downward J **(1994)** Phosphatidylinositol-3-OH kinase as a direct target of Ras. *Nature* **370,** 527-32

Ron D, Habener JF **(1992)** CHOP, a novel developmentally regulated nuclear protein that dimerizes with transcription factors C/EBP and LAP and functions as a dominant-negative inhibitor of gene transcription. *Genes Dev.* **6,** 439-53

Rotin D, Margolis B, Mohammadi M, Daly RJ, Daum G, Li N, fischer EH, Burgess WH, Ullrich A, Schlessinger J **(1992)** SH2 domains prevent tyrosine dephosphorylation of the EGF receptor: identification of Tyr992 as the high-affinity binding site for SH2 domains of phospholipase Cγ. *EMBO J.* **11,** 559-67

Rouse J, Cohen P, Trigon S, Morange M, Alonso-Llamazares A, Zamanillo D, Hunt T, Nebreda AR **(1994)** A novel kinase cascade triggered by stress and heat shock that stimulates MAPKAP kinase-2 and phosphorylation of the small heat shock proteins. *Cell* **78,** 1027-37

Rozengurt E (1986) Early signals in the mitogenic response. *Science* **234,** 161-6

Rubin E, Farber JL **(1994)** Neoplasia. In: *Pathology* (Rubin E, Farber JL, eds), pp. 143-98, J. B. Lippincott Company, Philadephia

Ruta M, Wolford R, Dhar R, DeFeo-Jones D, Ellis RW, Scolnick EM **(1986)** Nucleotide sequence of the two rat cellular rasH genes. *Mol. Cell. Biol.* **6,** 1706-10

Salari H, Dryden P, Davenport R, Howard S, Jones K, Bittman R **(1992)** Inhibition of protein kinase C by ether-linked lipids is not correlated with their antineoplastic activity on WEH1-3B and R6X-B15 cells. *Biochim. Biophys. Acta* **1134,** 81-8

Sánchez I, Hughes RT, Mayer BJ, Yee K, Woodgett JR, Avruch J, Kyriakis JM, Zon LI **(1994)** Role of SAPK/ERK kinase-1 in the stress-activated pathway regulating transcription factor c-Jun. *Nature* **372,** 794-8

Satoh T, Endo M, Nakafuku M, Akiyama T, Yamamoto T, Kaziro Y **(1990a)** Accumulation of $p21^{ras}$-GTP in response to stimulation with epidermal growth factor and oncogene products with tyrosine kinase activity. *Proc. Natl. Acad. Sci. USA* **87,** 7926-9

Satoh T, Endo M, Nakafuku M, Nakamura S, Kaziro Y **(1990b)** Platelet-derived growth factor stimulates formation of active $p21^{ras}$-GTP complex in Swiss mouse 3T3 cells. *Proc. Natl. Acad. Sci. USA* **87,** 5993-7

Schaap D, de Widt J, van der Wal J, Vandekerkhove J, van Damme J, Gussow D, Ploegh HL, van Blitterswijk WJ, van der Bend RL **(1990)** Purification, cDNA-cloning and expression of human diacylglycerol kinase. *FEBS Lett.* **275,** 151-8

Schlessinger J, Ullrich A **(1992)** Growth factor signaling by receptor tyrosine kinases. *Neuron* **9,** 383-91

Schulte TW, Blagosklonny MV, Ingui C, Neckers L **(1995)** Disruption of the Raf-1-Hsp90 molecular complex results in destabilization of Raf-1 and loss of Raf-1-Ras association. *J. Biol. Chem.* **270,** 24585-8

Schulte TW, Blagosklonny MV, Romanova L, Mushinski JF, Monia BP, Johnston JF, Nguyen P, Trepel J, Neckers LM **(1996)** Destabilization of Raf-1 by geldanamycin leads to distruption of the Raf-1-MEK-mitogen-activated protein kinase signalling pathway. *Mol. Cell Biol.* **16,** 5839-45

Seewald MJ, Olsen RA, Sehgal I, Melder DC, Modest EJ, Powis G **(1990)** Inhibition of growth factor-dependent inositol phosphate Ca^{2+} signaling by antitumor ether lipid analogues. *Cancer Res.* **50,** 4458-63

Seth A, Alvarez E, Gupta S, Davis RJ **(1991)** A phosphorylation site located in the NH2-terminal domain of c-Myc increases transactivation of gene expression. *J. Biol. Cehm.* **266,** 23521-4

Seuwen K, Pouysségur J **(1992)** G protein-controlled signal transduction pathways and the regulation of cell proliferation. *Adv. Cancer Res.* **58,** 75-94

Sherr CJ (1996) Cancer cell cycles. *Science* **274,** 1672-7

Shibuya H, Yamaguchi K, Shirakabe K, Tonegawa A, Gotoh Y, Ueno N, Irie K, Nishida E, Matsumoto K **(1996)** TAB1: an activator of the TAK1 MAPKKK in TGF-β signal transduction. *Science* **272,** 1179-82

Shih C, Padhy LC, Murray M, Weinberg RA **(1981)** Transforming genes of carcinomas and neuroblastomas introduced into mouse fibroblasts. *Nature* **290,** 261-4

Shimizu K, Goldfarb M, Suard Y, Perucho M, Li Y, Kamata T, Feramisco J, Stavnezer E,

Fogh J, Wigler MH **(1983)** Three human transforming genes are related to the viral *ras* oncogenes. *Proc. Natl. Acad. Sci. USA* **80,** 2112-6

Shimizu K, Kuroda S, Yamamori B, Matsuda S, Kaibuchi K, Yamauchi T, Isobe T, Irie K, Matsumoto K, Takai Y **(1994)** Synergistic activation by Ras and 14-3-3 protein of a mitogen-activated protein kinase kinase kinase named Ras-dependent extracellular signal-regulated kinase kinase stimulator. *J. Biol. Chem.* **269,** 22917-20

Shoji M, Raynor RL, Fleer EA, Eibl H, Vogler WR, Kuo JF **(1991)** Effects of hexadecylphosphocholine on protein kinase C and TPA-induced differentiation of HL60 cells. *Lipids* **26,** 145-9

Simpson J, Johnson MS, Mitchell R **(1993)** H7-resistant protein kinase C substrates in two-dimensional gels of proestrous rat anterior pituitary gland. *Biochim. Biophys. Acta* **1220,** 69-75

Singh GK, Mathews TJ, Clarke SC, Yannicos T, Smith BL **(1995)** Annual summary of births, marriages, divorces and deaths: United State, 1994. *Monthly Vital Statistics Report* **43,** 1-41

Sithanandam G, Dean M, Brennscheidt U, Beck T, Gazdar A, Minna JD, Brauch H, Zbar B, Rapp UR **(1989)** Loss of heterozygosity at the c-raf locus in small cell lung carcinoma. *Oncogene* **4,** 451-5

Sithanandam G, Kölch W, Duh F-M, Rapp UR **(1990)** Complete coding sequence of a human *B-raf* cDNA and detection of B-raf protein kinase with isozyme specific antibodies. *Oncogene* **5,** 1775-80

Sithanandam G, Latif F, Duh FM, Bernal R, Smola U, Li H, Kuzmin I, Wixler V, Geil L,

Shrestha S, Lloyd PA, Bader S, Sekido Y, Tartof KD, Kashuba VI, Zabarovsky ER, Dean M, Klein G, Lerman MI, Minna JD, Rapp UR, Allikmets R **(1996)** 3pK, a new mitogen-activated protein kinase-activated protein kinase located in the small cell lung cancer tumor suppressor gene region. *Mol. Cell. Biol.* **16,** 868-76

Sleight R, Kent C **(1980)** Regulation of phosphatidylcholine biosynthesis in cultured chick embryonic muscle treated with phospholipase C. *J. Biol. Chem.* **255,** 10644-50

Snyder F (1991) Metabolism, regulation, and function of ether-linked glycerolipids and their bioactive species. In: *Biochemistry of Lipids, Lipoproteins and Membranes.* (Vance DE, Vance J, eds.), pp. 241-67 Elsevier Science Publisher, Amsterdam, The Netherlands

Snyder F, Blank ML, Wykle RL **(1971)** The enzymatic synthesis of ethanolamine plasmalogens. *J. Biol. Chem.* **246,** 3639-45

Snyder R, Wood R **(1968)** The occurrence and metabolism of alkyl and alk-1-enyl ethers of glycerol in transplantable rat and mouse tumors. *Cancer Res.* **28,** 972-8

Snyder R, Wood R **(1969)** Alkyl and alk-1-enyl ethers of glycerol in lipids from normal and neoplastic human tissues. *Cancer Res.* **29,** 251-5

Söling U, Eibl H, Nagel GF, Ungers C **(1987)** Effect of synthetic phospholipids on platelet aggregation and serotonin release. *Lipids* **22,** 868-70

Songyang Z, Shoelson SE, Chaudhuri M, Gish G, Pawson T, Haser WG, King F, Roberts T, Ratnofsky S, Lechleider RJ, Neel BG, Brige RB, Fajardo JE, Chou MM, Hanafusa H, Schaffausen B, Cantley LC **(1993)** SH2 domains recognize specific phosphopeptide sequences. *Cell* **72,** 767-78

Sontag E, Fedorov S, Kamibayashi C, Rabbins D, Cobb M, Mumby M **(1993)** The

interaction of SV40 small tumor antigen with protein phosphatase 2A stimulates the Map kinase pathway and induces cell proliferation. *Cell* **75,** 887-97

Sorkin A, Carpenter G **(1993)** Interaction of activated EGF receptors with coated pit adaptins. *Science* **261,** 612-5

Sorkin A, Waters CM **(1993)** Endocytosis of growth factor receptors. *BioEssays* **15,** 375-82

Sözeri O, Vollmer K, Liyanage M, Frith D, Kour G, Mark III GE, Stabel S **(1992)** Activation of the c-Raf protein kinase by protein kinase C phosphorylation. *Oncogene* **7,** 2259-62

Sprague Jr GF (1992) Kinase cascade conserved. *Curr. Biol.* **2,** 587-9

Stancato LF, Chow YH, Hutchison KA, Perdew GH, Jove R, Pratt WB **(1993)** Raf exists in a native heterocomplex with hsp90 and p50 that can be reconstituted in a cell-free system. *J. Biol. Chem.* **268,** 21711-6

Standaert ML, Avignon A, Yamada K, Bandyopadhyay G, Farese RV **(1996)** The phosphatidylinositol 3-kinase inhibitor, wortmannin, inhibits insulin-induced activation of phosphatidylcholine hydrolysis and associated protein kinase C translocation in rat adipocytes. *Biochem J.* **313,** 1039-46

Stein D, Wu J, Fuqua SA, Roonprapunt C, Yajnik V, D'Eustachio P, Moskow JJ, Buchberg AM, Osborne CK, Margolis B **(1994)** The SH2 domain protein GRB-7 is co-amplified, overexpressed and in a tight complex with HER2 in breast cancer. *EMBO J.* **13,** 1331-40

Stephens L, Eguinoa A, Corey S, Jackson T, Hawkins PT **(1993)** Receptor stimulated accumulation phosphatidylinositol(3,4,5)-trisphosphate by G-protein mediated pathways in human myeloid derived cells. *EMBO J.* **12,** 2265-73

Stephens L, Smrcka A, Cooke FT, Jackson TR, Sternweis PC, Hawkins PT **(1994)** A novel

phosphoinositide 3 kinase activity in myeloid-derived cells is activated by G protein βγ subunits. *Cell* **77,** 83-93

Stoker M, O'Neill C, Berryman S, Waxman V **(1968)** Anchorage and growth regulation in normal and virus-transformed cells. *Int. J. Cancer* **3,** 683-693

Stokoe D, Campbell DG, Nakielny S, Hidaka H, Leevers SJ, Marshall C, Cohen P **(1992)** MAPKAP kinase-2; a novel protein kinase activated by mitogen-activated protein kinase. *EMBO J.* **11,** 3985-94

Stokoe D, Macdonald SG, Cadwallader K, Symons M, Hancock JF **(1994)** Activation of Raf as a result of recruitment to the plasma membrane. *Science* **264,** 1463-7

Storm SM, Brennscheidt U, Sithanandam G, Rapp UR **(1990a)** *raf* oncogenes in carcinogenesis. *CRC Rev. Cancer* **2,** 1-8

Storm SM, Cleveland JL, Rapp UR **(1990b)** Expression of raf family proto-oncogenes in normal mouse tissues. *Oncogene* **5,** 345-51

Stoyanov B, Volinia S, Hanck T, Rubio I, Loubtchenkov M, Malek D, Stoyanova S, Vanhaesebroeck B, Dhand R, Nürnberg B, Gierschik P, Seedorf K, Hsuan JJ, Waterfield MD, Wetzker R **(1995)** Cloning and characterization of a G protein-activated human phosphoinositide-3 kinase. *Science* **269,** 690-3

Stricker SA, Centonze VE, Paddock SW, Schatten G **(1992)** Confocal microscopy of fertilization-induced calcium dynamics in sea urchin eggs. *Devl. Biol.* **149,** 370-80

Sturgill TW, Ray LB, Erikson E, Maller JL **(1988)** Insulin-stimulated MAP-2 kinase phosphorylates and activates ribosomal protein S6 kinase II. *Nature* **334,** 715-8

Sullivan JA, Merrit JE, Budd JM, Booth RFG, Hallam TJ **(1994)** Effect of a selective

protein kinase C inhibitor, Ro 31-8425, on Mac-1 expression and adhesion of human neutrophils. *Eur. J. Immunol.* **24,** 621-6

Sun H, Charles CH, Lau LF, Tonks NK **(1993)** MKP-1 (3CH134), an immediate early gene product, is a dual specificity phosphatase that dephosphorylates MAP kinase in vivo. *Cell* **75,** 487-93

Sun H, Tonks NK **(1994)** The coordinated action of protein tyrosine phosphatases and kinases in cell signaling. *Trends Biochem. Sci.* **19,** 480-5

Sundaram M, Han M **(1995)** The C. elegans *ksr-1* gene encodes a novel Raf-related kinase involved in Ras-mediated signal transduction. *Cell* **83,** 889-901

Sundler R (1973) Biosynthesis of rat liver phosphatidylethanolamines from intraportally injected ethanolamine. *Biochim. Biophys. Acta* **306,** 218-26

Sundler R (1975) Ethanolaminephosphate cytidylyltransferase. Purification and characterization of the enzyme from rat liver. *J. Biol. Chem.* **250,** 8585-90

Sundler R, Åkesson B **(1975)** Regulation of phospholipid biosynthesis in isolated rat hepatocytes. Effects of different substrates. *J. Biol. Chem.* **250,** 3359-67

Sutherland C, Campbell DG, Cohen P **(1993)** Identification of insulin-stimulated protein kinase-1 as the rabbit equivalent of rskmo-2. Identification of two threonines phosphorylated during activation by mitogen-activated protein kinase. *Eur. J. Biochem.* **212,** 581-8

Szeles A, Bajalica-Lagercrantz S, Lindblom A, Lushnikova T, Kashuba VI, Imreh S, Nordenskjold M, Klein G, Zabarovsky ER **(1996)** Mapping of a new MAP kinase activated protein kinase gene (3PK) to human chromosome band 3p21.2 and ordering of 3PK and two cosmid markers in the 3p22-p21 tumour-suppressor region by two-colour fluorescence in situ

hybridization. *Chromosome Res.* **4,** 310-3

Takishima K, Griswold-Prenner I, Ingebritsen T, Rosner MR **(1991)** Epidermal growth factor (EGF) receptor T669 peptide kinase from 3T3-L1 cells is an EGF-stimulated "MAP" kinase. *Proc. Natl. Acad. Sci. USA* **88,** 2520-4

Takuwa N, Zhou W, Kumada M, Takuwa Y **(1992)** Activation of protein kinase C induce $p34^{cdc2}$ histone H1 kinase stimulation in Swiss 3T3 fibroblasts. *Biochem. Biophys. Res. Commun.* **188,** 1084-9

Tarnowski GS, Mountain JM, Stock CC, Munder PG, Weltzien HU, Westphal O **(1978)** Effect of lysolecithin and analogs on mouse ascites tumors. *Cancer Res.* **38,** 339-44

Tercé F, Record M, Ribbes G, Chap H, Douste-Blasy L **(1988)** Intracellular processing of cytidylyltransferase in Krebs II cells during stimulation of phophatidylcholine synthesis. *J. Biol. Chem.* **263,** 3142-9

Thanos D, Maniatis T **(1995)** NF-κB: a lesson in family values. *Cell* **80,** 529-32

Therrien M, Chang HC, Solomon NM, Karim FD, Wassarman DA, Rubin GM **(1995)** KSR, a novel protein kinase required for RAS signal transduction. *Cell* **83,** 879-88

Therrien M, Michaud NR, Rubin GM, Morrison DK **(1996)** KSR modulates signal propagation within the MAPK cascade. *Genes Dev.* **10,** 2684-95

Thomas G (1992) MAP kinase by any other name smells just as sweet. *Cell* **68,** 3-6

Thompson NT, Garland LG, Bonser RW **(1993)** Phospholipase D: regulation and functional significance. *Adv. Pharmacol.* **24,** 199-238

Tijburg LBM, Houweling M, Geelen MJH, van Golde LMG **(1988)** Effects of dietary conditions on the pool sizes of precursors of phosphatidylcholine and

phosphatidylethanolamine synthesis in rat liver. *Biochim. Biophys. Acta* **959,** 1-8

Trahey M, McCormick F **(1987)** A cytoplasmic protein stimulates normal N-ras p21 GTPase, but does not affect oncogenic mutants. *Science* **238,** 542-5

Tronchere H, Tercé F, Record M, Ribbes G, Chap H **(1991)** Modulation of CTP:phosphocholine cytidylyltransferase translocation by oleic acid the antitumoral alkylphospholipid in HL-60 cells. *Biochem. Biophys. Res. Commun.* **176,** 157-65

Troppmair J, Bruder JT, Munoz H, Lloyd PA, Kyriakis J, Banerjee P, Avruch J, Rapp UR **(1994)** Mitogen-activated protein kinase/extracellular signal-regulated protein kinase activation by oncogenes, serum, and 12-O-tetradecanoylphorbol-13-acetate requires Raf and is necessary for transformation. *J. Biol. Chem.* **269,** 7030-5

Ubeda M, Wang XZ, Zinszner H, Wu I, Habener JF, Ron D **(1996)** Stress-induced binding of the transcriptional factor CHOP to a novel DNA control element. *Mol. Cell. Biol.* **16,** 1479-89

Überall F, Oberhuber H, Maly K, Zaknun J, Demuth L, Grunicke HH **(1991)** Hexadecylphosphocholine inhibits inositol phosphate formation and protein kinase C activity. *Cancer Res.* **51,** 807-12

Ueda T, Imamura S, Kawai Y, Wano Y, Kamiya K, Tsutani H, Nakamura T **(1990)** Successful treatment of myelodysplastic syndrome with 1-beta-D-arabinofuranosylcytosine 5'-stearylphosphate [letter] *Leuk. Res.* **14,** 1067-8

Ueda Y, Hirai S, Osada S, Suzuki A, Mizuno K, Ohno S **(1996)** Protein kinase Cδ activates the MEK-ERK pathway in a manner independent of Ras and dependent on Raf. *J. Biol. Chem.* **271,** 23512-9

Ullrich SJ, Anderson CW, Mercer WE, Appella E **(1992)** The p53 tumor suppressor protein, a modulator of cell proliferation. *J. Biol. Chem.* **267,** 15259-62

Unger C, Eibl H **(1991)** Hexadecylphosphocholine: preclinical and the first clinical results of a new antitumor drug. *Lipids* **26,** 1412-7

Uno I, Fukami K, Kato H, Takenawa T, Ishikawa T **(1988)** Essential role for phosphatidylinositol 4,5-bisphosphate in yeast cell proliferation. *Nature* **333,** 188-90

Vagnetti D, Mamcini A, Santarella B, Binaglia L **(1990)** Effect of alkyl-lysophospholipid analogs on the morphology of a murine lymphoma cell line. *J. Submicrosc. Cytol. Pathol.* **22,** 415-24

Vallari DS, Smith ZL, Snyder F **(1988)** HL-60 cells become resistant towards antitumor ether-linked phospholipids following differentiation into granulocytic form. *Biochem. Biophys. Res. Commun.* **156,** 1-8

Vallari DS, Record M, Smith ZL, Snyder F **(1989)** *O*-Alkyl-*O*-methylglycerophosphocholine, an antineoplastic lipid, undergoes spontaneous redistribution between biological membranes prepared from HL-60. *Biochim. Biophys. Acta* **1006,** 250-4

Vallee RB, Herskovits JS, Aghajanian JG, Burgess CC, Shpetner HS **(1993)** Dynamin, a GTPase involved in the initial stages of endocytosis. In: *The GTPase Superfamily* (Marsh J, Goode J, eds), pp.185-93, John Wiley & Sons, Chichester

van Biesen T, Hawes BE, Raymond JR, Luttrell LM, Koch WJ, Lefkowitz RJ **(1996)** G_o-protein α-subunits activate mitogen-activated protein kinase via a novel protein kinase C-dependent mechanism. *J. Biol. Chem.* **271,** 1266-9

van Blitterswijk WJ, van der Bend RL, Kramer IM, Verhoeven AJ, Hilkmann H, de Widt

J **(1987)** A metabolite of an antineoplastic ether phospholipid may inhibit transmembrane signalling via protein kinase C. *Lipids* **22,** 842-6

van Corven EJ, Groenink A, Jalink K, Eichholtz T, Moolenaar WH **(1989)** Lysophosphatidate-induced cell proliferation: identification and dissection of signaling pathways mediated by G proteins. *Cell* **59,** 45-54

van der Bend R, Brunner J, Jalink K, van Corven EJ, Moolenaar WH, van Blitterswijk WJ **(1992)** Identification of a putative membrane receptor for the bioactive phospholipid, lysophosphatidic acid. *EMBO J.* **11,** 2495-501

Van Hellemond JJ, Slot WJ, Geelen MJH, van Golde MG, Vermenlen PS **(1994)** Ultrastructural localization of CTP:phosphoethanolamine cytidylyltransferase in rat liver. *J. Biol. Chem.* **269,** 15415-8

Van Hoeven RP, Emmelot P **(1972)** Studies on plasma membranes: XVII lipid class composition of plasma membranes isolated from rat and mouse liver and hepatomas. *J. Membrane Biol.* **9,** 105-26

Vance DE (1989) Regulatory and functional aspects of phosphatidylcholine metabolism. In: *Phosphatidylcholine Metabolism.* (Vance DE, ed.), pp. 225-39, CRC Press, Boca Raton, FL.

Vance DE (1990) Phosphatidylcholine metabolism: masochistic enzymology, metabolic regulation, and lipoprotein assembly. *Biochem. Cell Biol.* **68,** 1151-65

Vance DE (1991) Phospholipid metabolism and cell signalling in eucaryotes. In: *New Comprehensive Biochemistry (Vol. 20). Biochemistry of Lipids, Lipoproteins and Membranes* (Vance DE, Vance JE, eds.), pp. 205-40, Elsevier Science Publishers B. V., Amsterdam

Van Hellemond JJ, Slot WJ, Geelen MJH, van Golde MG, Vermenlen PS **(1994)**

Ultrastructural localization of CPT:phosphoethanolamine cytidylyltransferase in rat liver. *J. Biol. Chem.* **269,** 15415-8

Verheij M, Bose R, Lin XH, Yao B, Jarvis WD, Grant S, Birrer MJ, Szabo E, Zon LI, Kyriakis JM, Haimovitz-Friedman A, Fuks Z, Kolesnick RN **(1996)** Requirement for ceramide-initiated SAPK/JNK signalling in stress-induced apoptosis. *Nature* **380,** 75-9

Vieira AV, Lamaze C, Schmid SL **(1997)** Control of EGF receptor signaling by clathrin-mediated endocytosis. *Science* **274,** 2086-9

Vincenz C, Dixit V **(1996)** 14-3-3 proteins associate with A20 in an isoform-specific manner and function both as chaperone and adaptor molecules. *J. Biol. Chem.* **271,** 20029-34

Vogler WR, Olson AC, Berdel WE, OKamoto S, Glasser L **(1990)** Purging leukemia remission marrows with alkyllysophospholipids, preclinical and clinical results. *Bone Marrow Purging Processing* pp.1-20, Alan R. Liss, Inc.

Vogler WR, Whigham E, Bennet WD, Olsen AC **(1985)** Effect of alkyl-lysophospholipids on phosphatidylcholine biosynthesis in leukaemic cell lines. *Exp. Hematol.* **13,** 629-33

Vossler MR, Yao H, York RD, Pan M-G, Rim CS, Stork PJS **(1997)** cAMP activates MAP kinase and Elk-1 through a B-Raf- and Rap-1dependent pathway. *Cell* **89,** 73-82

Wahl M, Gruenstein E **(1993)** Intracellular free Ca^{2+} in the cell cycle in human fibroblasts: transitions between G_1 and G_0 and progression into S phase. *Mol. Biol. Cell* **4,** 293-302

Walter G, Mumby M **(1993)** Protein serine/threonine phosphatases and cell transformation. *Biochim. Biophys. Acta* **1155,** 207-26

Wang X, Ron D **(1996)** Stress-induced phosphorylation and activation of the transcription factor CHOP (GADD153) by p38 MAP kinase. *Science* **272,** 1347-9

Wang Z, Moran MF **(1996)** Requirement for the adapter protein GRB2 in EGF receptor endocytosis. *Science* **272,** 1935-9

Ward Y, Gupta S, Jensen P, Wartmann M, Davis RJ, Kelly K **(1994)** Control of MAP kinase activation by the mitogen-induced threonine/tyrosine phosphatase PAC1. *Nature* **367,** 651-4

Warnock DE, Schmid SL **(1996)** Dynamin GTPase, a force-generating molecular switch. *BioEssays* **18,** 885-93

Wartmann M, Davis RJ **(1994)** The native structure of the activated Raf protein kinase is a membrane-bound multi-subunit complex. *J. Biol. Chem.* **269,** 6695-701

Waskiewicz AJ, Cooper JA **(1995)** Mitogen and stress response pathways: MAP kinase cascades and phosphatase regulation in mammals and yeast. *Curr. Opin. Cell Biol.* **7,** 798-805

Waters SB, Holt KH, Ross SE, Syu LJ, Guan KL, Saltiel AR, Koretzky GA, Pessin JE **(1995)** Desensitization of Ras activation by a feedback disassociation of the SOS-Grb2 complex. *J. Biol. Chem.* **270,** 20883-6

Watson JV, Workman P, Thompson MG, Hickman JA, Dive C **(1990)** Antitumour ether lipid SRI 62-834 modulates calcium flux and membrane permeability: analysis by multiparameter flow cytometry. *Cytometry* **Suppl. 4,** Abstract No. 402A

Weber N, Benning H **(1988)** Metabolism of ether glycolipids with potentially antineoplastic activity by Ehrlich ascites tumor cells. *Biochim. Biophys. Acta* **959,** 91-4

Weinhold PA, Charles L, Rounsifer ME, Feldman DA **(1991)** Control of phosphatidylcholine synthesis in Hep G2 cells. Effect of fatty acids on the activity and immunoreactive content of choline phosphate cytidylyltransferase. *J. Biol. Chem.* **266,** 6093-

Wella MA, Dittmer JC **(1966)** A microanalytical techinque for the quantitative determination of twenty-four classes of brain lipids. *Biochemistry* **5,** 3405-18

Weltzien HU (1979) Cytolytic and membrane-perturbing properties of lysophosphatidylcholine. *Biochim. Biophys. Acta* **559,** 259-287

Westphal O (1987) Ether lipids in oncology—welcoming address. *Lipids* **22,** 787-8

Westwick JK, Bielawska AE, Dbaibo G, Hannun YA, Brenner DA **(1995)** Ceramide activates the stress-activated protein kinases. *J. Biol. Chem.* **270,** 22689-92

Whitmarsh AJ, Shore P, Sharrocks AD, Davis RJ **(1995)** Integration of MAP kinase signal transduction pathways at the serum response element. *Science* **269,** 403-7

Wilcox RW, Wykle RL, Schmitt JD, Daniel LW **(1987)** The degradation of platelet-activation factor and related lipids: susceptibility to phospholipase C and D. *Lipids* **22,** 800-7

Wiley HS, Cunningham DD **(1981)** A steady state model for analyzing the cellular binding, internalization and degradation of polypeptide ligands. *Cell* **25,** 433-40

Winitz S, Russell M, Qian N-X, Gardner A, Dwyer L, Johnson GL **(1993)** Involvement of Ras and Raf in the Gi-coupled acetycholine muscarinic m2 receptor activation of mitogen-activated protein (MAP) kinase kinase and MAP kinase. *J. Biol. Chem.* **268,** 19196-9

Winkelmann M, Ebeling K, Strohmeyer G, Hottenrott G, Mechl Z, Berges W, Scholten T, Westerhausen M, Schlimok G, Sterz R **(1992)** Treatment results of the thioether lipid ilmofosine in patients with malignant tumours. *J. Cancer Res. Clin. Oncol.* **118,** 405-7

Wolff RA, Dobrowsky RT, Bielawska A, Obeid LM, Hannun YA **(1994)** Role of ceramide-activated protein phosphatase in ceramide-mediated signal transduction. *J. Biol. Chem.* **269,**

19605-9

Workman P (1990) The cell membrane and cell signals: new targets for novel anticancer drugs. *Annals of Oncology* **1,** 100-11

Wright-SD, Kolesnick RN **(1995)** Does endotoxin stimulate cells by mimicking ceramide? *Immunol. Today* **16,** 297-302

Wu J, Dent P, Jelinek T, Wolfman A, Weber MJ, Sturgill TW **(1993)** Inhibition of the EGF-activated MAP kinase signaling pathway by adenosine 3',5'-monophosphate. *Science* **262,** 1065-9

Xia K, Mukhopadhyay NK, Inhorn RC, Barber DL, Rose PE, Lee RS, Narsimhan RP, Dandrea AD, Griffin JD, Roberts TM **(1996)** The cytokine-activated tyrosine kinase JAK2 activates Raf-1 in a p21ras-dependent manner. *Proc. Natl. Acad. Sci. USA* **93,** 11681-6

Xing J, Ginty DD, Greenberg ME **(1996)** Coupling of the Ras-MAPK pathway to gene activation by RSK2, a growth factor-regulated CREB kinase. *Science* **273,** 959-63

Xu S, Robbins DJ, Christerson LB, English JM, Vanderbilt CA, Cobb MH **(1996)** Cloning of rat MEK kinase 1 cDNA reveals an endogenous membrane-associated 195 kDa protein with a large regulatory domain. *Proc. Natl. Acad. Sci. USA* **93,** 5291-5

Yamada H, Mizuguchi J, Nakanishi M **(1991)** Antigen receptor-mediated calcium signals in B cells as revealed by confocal fluorescence micorscopy. *FEBS Lett.* **284,** 249-51

Yamaguchi K, Shirakabe K, Shibuya H, Irie K, Oishi I, Ueno N, Taniguchi T, Nishida E, Matsumoto K **(1995)** Identification of a member of the MAPKKK family as a potential mediator of TGF-β signal transduction. *Science* **270,** 2008-11

Yamashita S, Hosaka K, Miki Y, Numa S **(1981a)** Glycerolipid acyltransferase from rat

liver: 1-acylglycerophosphate acyltransferase, 1-acylglycerophosphorylcholine acyltransferase, and diacylglycerol acyltransferase. *Methods Enzymol.* **71,** 528-36

Yamashita S, Numa S **(1981b)** Glycerophosphate acyltransferase from rat liver. *Methods Enzymol.* **71,** 550-4

Yamauchi K, Holt K, Pessin JE **(1993)** Phosphatidylinositol 3-kinase functions upstream of Ras and Raf in mediating insulin stimulation of c-*foc* transcription. *J. Biol. Chem.* **268,** 14597-600

Yan M, Dai T, Deak JC, Kyriakis JM, Zon LI, Woodgett JR, Templeton DJ **(1994)** Activation of stress-activated protein kinase by MEKK1 phosphorylation of its activator SEK1. *Nature* **372,** 798-800

Yan M, Templeton DJ **(1994)** *J. Biol. Chem.* **269,** 10967-73

Yang S, Van Aelst L, Bar-Sagi D **(1995)** Differential interactions of human Sos1 and Sos2 with Grb2. *J. Biol. Chem.* **270,** 18212-5

Yao B, Zhang Y, Delikat S, Mathias S, Basu S, Kolesnick R **(1995)** Phosphorylation of Raf by ceramide-activated protein kinase. *Nature* **378,** 307-10

Yoker A, Meyer M, Reddy KK, Falck JR, Aneja R, Aneja S, Parra A, Burns DJ, Ballas LM, Cantley LC **(1994)** Activation of protein kinase C family members by the novel polyphosphoinositides PtdIns-3,4-P_2 and PtdIns-3,4,5-P_3. *J. Biol. Chem.* **269,** 32358-67

York JD, Majerus PW **(1994)** Nuclear phosphatidylinositols decrease during S-phase of the cell cycle in HeLa cells. *J. Biol. Chem.* **269,** 7847-50

Young SW, Dickens M, Tavaré JM **(1994)** Differentiation of PC12 cells in response to a cAMP analogue is accompanied by sustained activation of mitogen-activated protein kinase.

Comparison with the effects of insulin, growth factors and phorbol ester. *FEBS Lett.* **338,** 212-6

Zervos AS, Faccio L, Gatto JP, Kyriakis JM, Brent R **(1995)** Mxi2, a mitogen-activated protein kinase that recognizes and phosphorylates Max protein. *Proc. Natl. Acad. Sci. USA* **92,** 10531-4

Zhang X, Settleman J, Kyriakis JM, Takeuchi-Suzuki E, Elledge SJ, Marshall MS, Bruder JT, Rapp UR, Avruch J **(1993)** Normal and oncogenic $p21^{ras}$ proteins bind to the amino-terminal regulatory domain of c-Raf-1. *Nature* **364,** 308-13

Zhang Y, Yao B, Delikat S, Bayoumy S, Lin X-H, Basu S, McGinley M, Chan-Hui P-Y, Lichenstein H, Kolesnick R **(1997)** Kinase suppressor of Ras is ceramide-activated protein kinase. *Cell* **89,** 63-72

Zheng B, Oishi K, Shoji M, Eibl H, Berdel WE, Hadju J, Vogler WR, Kuo JF **(1990)** *Cancer Res.* **50,** 3025-31

Zheng C-F, Guan K-L **(1993)** Properties of MEKs, the kinases that phosphorylate and activate the extracellular signal-regulated kinases. *J. Biol. Chem.* **268,** 23933-9

Zhou G, Qin Bao Z, Dixon JE **(1995)** Components of a new human protein kinase signal transduction pathway. *J. Biol. Chem.* **270,** 12665-9

Zhou X, Arthur G **(1992a)** Improved procedures for the determination of lipid phosphorus by malachite green. *J. Lipid Res.* **33,** 1233-6

Zhou X, Lu X, Arthur G **(1992b)** The relationship between cellular ether glycerophospholipid content and sensitivity of cancer cells to 1-O-octadecyl-2-O-methyl-glycerophosphocholine. *Anticancer Res.* **12,** 1659-62

Zinck R, Hipskind RA, Pingoud V, Nordheim A **(1993)** c-*fos* transcriptional activation and repression correlate temporally with the phosphorylation status of TCF. *EMBO J.* **12,** 2377-87